Studies on the Green Synthesis of Silver Nanoparticles and their Utilization on the Development of Polymer Nanocomposites for Water Disinfection and Wound Healing Applications

A Thesis Dissertation

Submitted in Partial Fulfillment for the Award of the Degree of

DOCTOR OF PHILOSOPHY

by

ANUPAMA BORA

(Roll No. 156152007)

CENTER FOR THE ENVIROMENT

INDIAN INSTITUTE OF TECHNOLOGY GUWAHATI

GUWAHATI-781039, ASSAM, INDIA

MAY 2022

Dedicated to

God, my Parents, Sisters

and

everyone who has helped me in this journey.

INDIAN INSTITUTE OF TECHNOLOGY, GUWAHATI

Center for the Environment

Guwahati-781039

DECLARATION

I do hereby declare that the research work embodied in this thesis entitled "***Studies on the Green Synthesis of Silver Nanoparticles and their Utilization on the Development of Polymer Nanocomposites for Water Disinfection and Wound Healing Applications***" has been carried out by me under the Guidance of **Prof. Subhendu Sekhar Bag** as the Supervisor **Prof. Animes Kr. Golder** as Co-supervisor from the Center for the Environment, Indian Institute of Technology Guwahati, India.

In keeping with the general practice of reporting scientific observations, due acknowledgements have been made wherever the work described is based on the findings of other investigators.

IIT Guwahati
May, 2022

Anupama Bora

INDIAN INSTITUTE OF TECHNOLOGY, GUWAHATI

Center for the Environment

Guwahati-781039

CERTIFICATE

This is to certify that the research work presented in this thesis entitled "***Studies on the Green Synthesis of Silver Nanoparticles and their Utilization on the Development of Polymer Nanocomposites for Water Disinfection and Wound Healing Applications***" is an authentic record of the results obtained from the research work carried out by **Ms. Anupama Bora** under our supervision at the Center for the Environment, Indian Institute of Technology Guwahati, India. This work is original and has not been submitted elsewhere for a degree or award.

Prof. Subhendu Sekhar Bag
(*Thesis Supervisor*)
Professor,
Department of Chemistry and Centre for the Environment
IIT Guwahati
Ph: +91-361-258-2324(O)
Fax: +91-361-258-2349
Email: ssbag75@iitg.ac.in
Place: Guwahati, Assam

Prof Animes Kr. Golder
(*Thesis Co-Supervisor*)
Professor,
Department of Chemical Engineering and Centre for the Environment
IIT Guwahati
Ph: +91-361-258-2269(O)
Fax: +91-361-258-2291
Email: animes@iitg.ac.in
Place: Guwahati, Assam

ACKNOWLEDGMENT

Firstly, I express my sincere gratitude to my supervisor **Prof. Subhendu Sekhar Bag,** for his guidance, valuable suggestions and support during my research work. I thank my co-supervisor **Prof. Animes Kr. Golder** and my Doctoral Committee members, **Prof. Mohammad Qureshi** (chairman), **Prof. Vishal Trivedi** (member) and **Prof. Kaustubha Mohanty** (member), for their intellectual input, valuable suggestions and comments during my course of entire research work. I would also like to thank **Dr. Rajkumar P. Thummer** for allowing me to access his stem cell laboratory and **Dr. Uttam Manna** for contributing in my research.

I thank my batch mates from the center for the environment Dr. Himali, Dr. Jayakrishnan, Dr. Arnab, Dr. Sayanti, Dr. Tanushree, Dr. Jinat and Dr. Poulami, for their cooperation, support and pleasant company throughout my research work. I thank my friends from other departments Dr. Susmita, Dr. Madonna, Dr. Ankur, Dr. Sounak, Kunal, Dr. Indu, Dr. Ranjan, Apurba, Shashi, Jon, Dr. Jyotish and Gyanendra, they have contributed in a very supportive and motivational way. Thanks to a few of my other lab mates from other departments, they are Sourav, Angana, Khyati, Krishna and Angshuman, who have helped me in my research work.

I want to express my heartiest regards to my lab seniors, Dr. Hiranya, Dr. Afsana, Dr. Narendra, Dr. Gopi, Dr. Paulomi, Dr. Kamalesh, Dr. Smruti, Rajneesh and Anirudha for enlightening me with valuable advice. I also acknowledge my lab juniors Sayantan, Shilpa, Samir, Sourav, Aniket, Suravi, Sinchini, Hirak and Sujata for their help, support and pleasant company in the laboratory. Thanks to my trainees Sampada and Upasana, whom I met during my research life, they have helped me mold my work in a better direction. Also, thanks to few other juniors Ankit, Sudeshna, Himadri, Prabhat, Dharitri, Pulak and Gaurav, for making my moments at the center laboratory very joyful.

My sincere regards to all the technical and official staffs, including Dr. Deepmoni, Partha Sir, Dr. Babulal and Kaustubh Sir from the Center for the Environment, Chemistry and Chemical Engineering department, for their help and guidance in collecting various experimental data and other official works. Thanks to all Central library staff for their support. I acknowledge the Center for the Environment, Department of Chemistry and Chemical Engineering Department, IIT Guwahati for allowing me to carry out my research work using the various facilities available in the laboratories. I am also thankful to the Central Instrument Facility(CIF) IIT Guwahati for providing all the instrument facilities for my research work. I am incredibly grateful for the support from all the staff and operators of the CIF, especially Mr. Sujit and Ms. Rumi.

Special thanks to the medical facility of IIT Guwahati for their tireless efforts. Also, I would like to thank the indoor and outdoor sports facilities for providing us a lively environment for more productivity and better physical and mental health. Thanks to the counselors of IIT Guwahati, Namrata Mam and Pallabita Mam for being there when I needed guidance and support.

Lastly, but not least I owe the success to my family, including my parents, Mr. Ananda Kr. Bora and Mrs. Kanchan Saud Bora and my sisters Ruplekha and Sagarika, they have always believed in me and my dreams. They have been a constant source of inspiration and supported me to carry out my career. Finally, I want to express my heartfelt gratitude to God for keeping me safe, helping me work with all my dedication and passion towards my goals and making me a better human being with each passing day.

(Anupama Bora)

CURRICULUM VITAE

ANUPAMA BORA

Present Address:

C/O: Prof. Subhendu Sekhar Bag
Department of Chemistry/
Center for the Environment
Indian Institute of Technology Guwahati
Guwahati – 781039, Assam, India
Phone: +91-361-258-3046(RL-2)
Email: anupama.bora@iitg.ac.in

Permanent Address:

Satyam Apartments,
Lankeshwar, Jalukbari
Guwahati-781014
Assam, India
Ph: 9678314877

Area of Interest:

Development of nanocomposites and nanomaterials using polymers for various applications.

Education:

2021 **Doctor of Philosophy (Ph.D)** *(thesis submitted)*
Title: "Studies on the Green Synthesis of Silver Nanoparticles and their Utilization on the Development of Polymer Nanocomposites for Water Disinfection and Wound Healing Applications"

2015 **Master of Technology** (*Food Engineering and Technology*)
Tezpur University, Assam, India

2013 **Bachelor of Technology** *(Biotechnology)*
Gauhati University Institute of Science and Technology(GUIST), Gauhati University, Assam, India

Honors/Awards:

- Qualified Graduate Aptitude Test (**GATE**) in Biotechnology in 2013 which was awarded by MHRD, Government of India.
- Awarded with Engineering Merit Scholarship in Biotechnology from 2009-2013 by AICTE, Government of Assam, India.
- Anundoram Borooah Award, 2006 awarded by Government of Assam, India.

List of Publications:

1. Bag, S. S.*, **Bora, A** and Golder, A. (2021) 'Turning Wastes into Value-Added Materials: Polystyrene Nanocomposites (PS-AgNPs) from Waste Thermocol and

Green Synthesized Silver Nanoparticles for Water Disinfection Application', *Polymer Composites*. https://doi.org/10.1002/pc.26287

2. Bag, S. S.*, **Bora, A.** and Golder, A. (2020) 'Biomimetic Synthesis of Silver Nanoparticles Using Bhimkol *(Musa balbisiana*) Peel Extract as Biological Waste: Its Antibacterial Activity and Role of Ripen Stage of the Peel', *Current Nanomaterials*, 05, 01. 47-65. doi: 10.2174/2405461505666200228121003.
3. Bag, S. S.*, Banerjee, A., Singh, A., Golder, A. and **Bora, A.** (2018) 'Green Synthesis of Silver Nanoparticle using *Sechium edule* Aqueous Extract and Study of Antimicrobial and Catalytic Activity', *Current Nanomaterials*, 03, 03. 140-146. doi: 10.2174/2405461503666181002115659
4. Bag, S. S.*, **Bora, A** and Golder, A. (2022) Biomacromolecule Gelatin-PVA-AgNPs Triad Composite as Wound Healing Hydrogel with Wounded Skin Surface Protective Efficiency (*Communicated*).

List of Conferences/Workshops

1. **Oral Presentation** at International Conference on Functional Materials (**ICFM 2020)** held on 6-8 January 2020 at Material Science Center, IIT Kharagpur, West Bengal, India.
2. **Oral presentation** at Issues and challenges in water treatment and allied research for sustainable environment **(WATER 2020)** held on 23-25 January 2020 at Center of the Environment, IIT Guwahati.
3. **Poster presentation** at **DST-UKIERI** supported Workshop cum Symposium – Bio-inspired Nanomaterials for Environmental Applications held on 12-13 Feb, 2020 at Indian Institute of Technology Guwahati.
4. **Poster presentation** at Indo-Japan Bilateral symposium on Future perspective of Bioresource Utilization in North-East India **(IJBS17)** held on 1-4 Feb, 2018 by IIT Guwahati and Gifu University at IIT Guwahati.
5. **Poster Presentation** at Research Conclave 2017 and 2019 held at IIT Guwahati.
6. Attended one-day workshop on "Thermal analysis (DSC and TGA) of materials" conducted by the Department of Chemical Engineering, IIT Guwahati in association with the Indian Institute of Chemical Engineers - Guwahati Regional Centre and the Central Instruments Facility, IIT Guwahati on May 31, 2019 at CIF, IIT Guwahati.
7. Attended one-day workshop on **Intellectual Property Rights** conducted by IPR Cell, R& D section on Nov 30-Dec 1, 2016 held at IIT Guwahati.

ABSTRACT

Silver nanoparticles(AgNPs) have gained major interest due to their distinctive electrical, physical, optical, antimicrobial properties, and broad applications. They illustrate lower toxicity to human health whereas higher toxicity to various micro-organisms. For this cause, there is a broad scope of AgNPs to be applied for antimicrobial application, medical instruments, and products for health care such as burn dressing, scaffolds, water purification, and also in agricultural uses. AgNPs can easily be synthesized by using various methods, primarily classified into two types. Physical methods include laser ablation, evaporation, condensation etc. The second method of the synthesis of AgNPs is the chemical method which includes sodium borohydride, hydrazine etc. mediated reduction of silver salts and Green synthesis. While the reduction with chemical reagents is not environmentally friendly, the green synthesis is a non-toxic, eco-friendly and cost-effective method among all these processes. The alteration of energy level from continuous band to discrete band of AgNPs with a decrease in particle size offers to achieve strong size-dependent chemical and physical properties useable for various applications.

Therefore, this thesis entitled **"Studies on the Green Synthesis of Silver Nanoparticles and their Utilization on the Development of Polymer Nanocomposites for Water Disinfection and Wound Healing Applications"** contains embodiment of research aimed towards (a) Synthesis, optimization and characterization of silver nanoparticles (AgNPs) via the green route using 'Bhimkol' (*Musa balbisiana Colla*) peel extracts; (b) Study of the phytochemical properties of Bhimkol *(Musa balbisiana Colla)* peels and the antibacterial activities of both bhimkol peel extract and green synthesized AgNPs; (c) Synthesis and characterization of Silver Nanoparticle via green route using *Sechium edule* Aqueous Extract, study of their antimicrobial as well as catalytic activity; (d) Characterization and development of polystyrene nanocomposites (PS-AgNPs) from waste thermocol and green synthesized AgNPs for water disinfection application and (e) Characterization and development of PVA/gelatin/AgNPs based polymer nanocomposite hydrogel for wound dressing application.

The thesis contains a total of 5 chapters, including one Introduction Chapter (Chapter 1). Each chapter has its individual introduction, objectives, results and discussion and reference sections. The chapters are discussed briefly within the subsequent sections.

CHAPTER 1: STATE-OF-THE-ART IN THE SYNTHESIS AND APPLICATIONS OF SILVER NANOPARTICLES

In the field of nanotechnology, AgNPs has gained much recent interests because of their exceptional properties such as superior conductivity, chemical stability, catalytic activity,

antimicrobial and anti-inflammatory property. Thus, AgNPs can be used to prepare composite fibres, cryogenic superconducting materials, electronic components, cosmetic products, and in the food industry. Because of the antimicrobial property AgNPs are used in various biomedical applications, such as wound healing bandages, topical creams and antiseptic sprays. Silver shows antiseptic property and displays a broad biocidal effect against microorganisms through the disruption of the unicellular membrane, thus distressing their enzymatic activities. The AgNPs are synthesized by various chemical and physical methods, which are quite expensive and potentially hazardous to the environment involving the use of toxic and hazardous chemicals responsible for various biological risks. The advancement of biologically inspired processes for the syntheses of nanoparticles and AgNPs is growing into an important branch of nanotechnology.

To avoid the discharge or use of hazardous chemicals during the synthesis of nanoparticles it is an urgent need for environmentally friendly synthetic methods. Thus, the biosynthesis or green synthesis of nanoparticles received extensive attention currently. In biosynthetic methods, eco-friendly reducing and capping agents are mainly used, which include protein, carbohydrate, bacteria, peptides, fungi, algae, yeast and plants. In biological synthesis, toxic reagents and organic solvents are not used as the stabilizers. Production of AgNPs via the biological/green route is much better as it avoids the use of toxic reagents and organic solvents. Thus synthesized nanoparticles are more stable for a longer time than the chemically produced nanoparticles. Green chemistry-based synthesis, which is included under green synthesis methods, are known as environment-friendly synthesis methods.

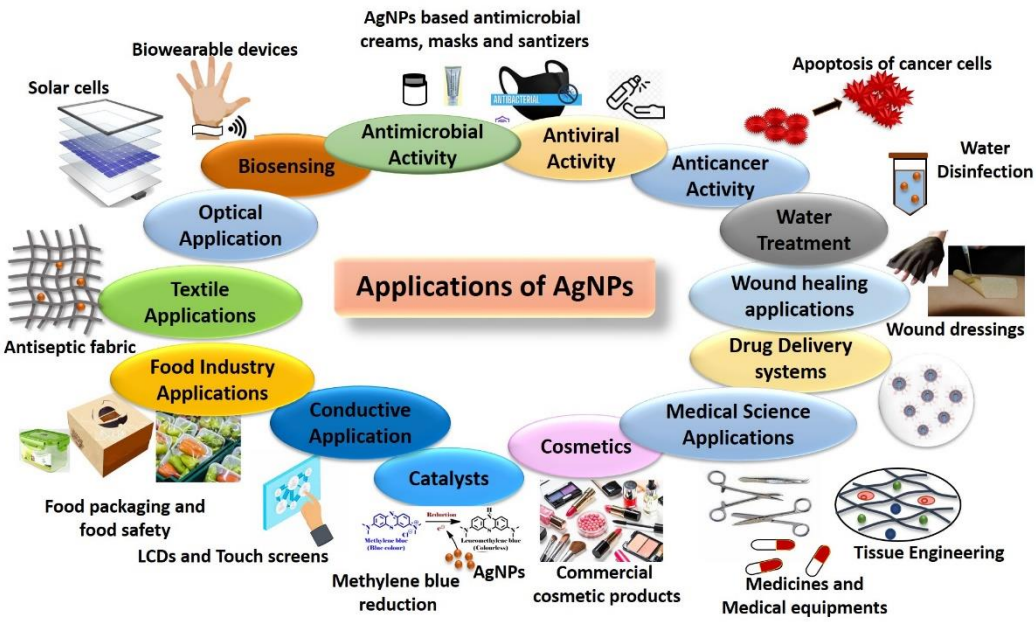

Figure A1. Various applications of AgNPs.

Silver nanoparticles are one of the most attractive nanomaterials for their wide properties and applications. The applications ranges from Chemistry, Biology, optoelectronic, environment and Medical. Some of the applications includes (a) Microbial Resistant Applications: Antibacterial, Antifungal, Anticancer, Antiviral, Anti-Inflammatory and Anti-Angiogenic applications; (b) Diagnostic, Biosensor, and Gene Therapy Applications; (c) Water Treatment; (d) Catalysis; (e) Protective Dressings: Bandages; (f) optical devices. The **Figure A1** shows a schematic presentation of various applications of AgNPs

CHAPTER 2: SYNTHESIS OF SILVER NANOPARTICLES USING BHIMKOL (*Musa Balbisiana*) PEEL EXTRACT AS BIOLOGICAL WASTE: ANTIBACTERIAL ACTIVITY AND ROLE OF RIPEN STAGE OF THE PEELS

This chapter describes a cost-effective and environment-friendly synthesis of silver nanoparticles using Bhimkal (*Musa balbisiana*) peel aqueous extract as biological waste. The Bhimkal (*Musa balbisiana*) peel aqueous extract acts as reducing as well as stabilizing agent for the preparation of AgNPs from $AgNO_3$. The formation of silver nanoparticles by various spectroscopic techniques. All the particles are almost spherical in morphology and the diameter of the mostly monodispersed AgNPs is in the range of 30-70 nm with an average size of 44.24 nm. Among the three stages of development (unripe, ripe, and blacken), we have found the ripening stage as most efficient in the highest yielding of AgNPs because of maximum presence of phenol containing biological macromolecules. The synthesized AgNPs showed moderate antibacterial activity against both gram negative bacteria as well as gram positive bacteria.

The attractive phytochemicals present and the availability of 'Bhimkol' (*Musa balbisiana*) peel waste, we framed our objective as below:

- Synthesis of AgNPs via the green route using 'Bhimkol' (*Musa balbisiana*) peel extracts as bioreductant and stabilizing agent.
- Optimization and characterization of these AgNPs by X-ray diffraction (XRD) method, TEM and SEM.
- Study of the phytochemical properties of Bhimkol *(Musa balbisiana*) peels at all its three stages of development.
- Study of the effect of pH on the synthesis of AgNPs with the help of UV-visible spectroscopy.
- Study of the antibacterial activities of both bhimkol peel extract and green synthesized AgNPs.

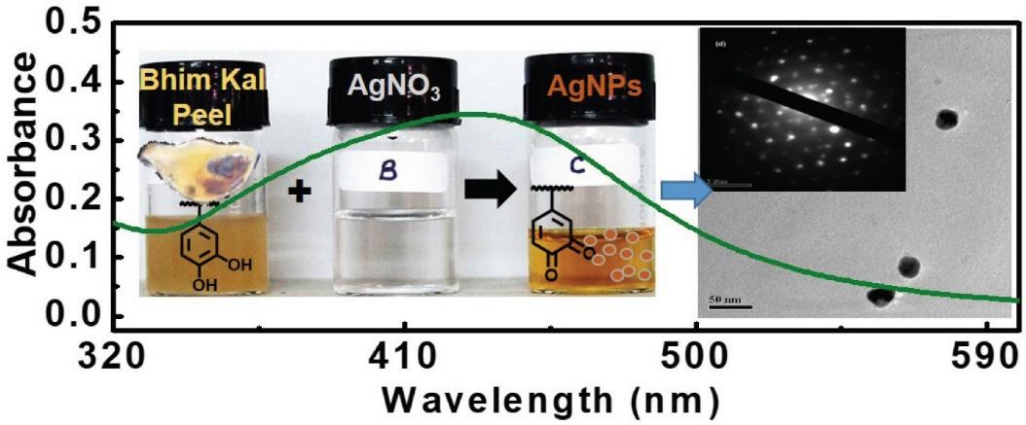

Figure A2. Synthesis of AgNPs using Bhimkol Peel Extract, its UV-visible spectra and TEM image.

Thus, we wanted to study the phytochemical properties of three stages of development of Bhimkol (*Musa balbisiana*) peels and to compare the efficiency of synthesis of silver nanoparticles using the three stages of development of bhimkol peels (**Figure A2**).

A qualitative and quantitative analysis of phytochemical composition was also carried out for the three different stages of development of the peels for the first time. Synthesis of silver nanoparticles was also carried out using all three stages (ripe, unripe and blacken) of the development of peels. We observed that the ripe peels were best for consideration of the efficient synthesis of silver nanoparticles in high yield due to its presence of the highest amount of phenolic components. The characterization was done using various spectroscopic and imaging techniques. The average size of the nanoparticles formed was around 44 nm, as indicated by TEM and FESEM images. The synthesized AgNPs showed moderate antibacterial activity against both gram-negative bacteria as well as gram-positive bacteria. The advantage of our method lies in the fact that we utilized waste peels material both for the generation and stabilization of silver nanoparticles. Currently, we are interested in the preparation of wound healing gel out of AgNPs and banana peel composite.

CHAPTER 3: GREEN SYNTHESIS OF SILVER NANOPARTICLE USING *Sechium Edule* AQUEOUS EXTRACT AND STUDY OF ANTIMICROBIAL AND CATALYTIC ACTIVITY

In this chapter, a cost effective and environment friendly biomimetic green synthesis of silver nanoparticles from the aqueous extract of Chayote squash is demonstrated. In north eastern region of India chayote is known as Squash and used for benefit for stomach.

Therefore, we have used, for the first time, the Squash vegetable extract which is widely available, cheap and has antioxidant properties for the synthesis of stable silver nanoparticles. The advantage of our method lies on the fact that squash acts both as a reducing agent and a stabilizer of silver nanoparticles. The carbohydrate and the fiber part are most probably acts as stabilizers. The synthesized nanoparticles are found to show antimicrobial activity and catalytic activity toward the reduction of methylene blue. The reduction of methylene blue by Ag-NPs in presence of sechium edule aqueous extract is attributed to the electron relay effect.

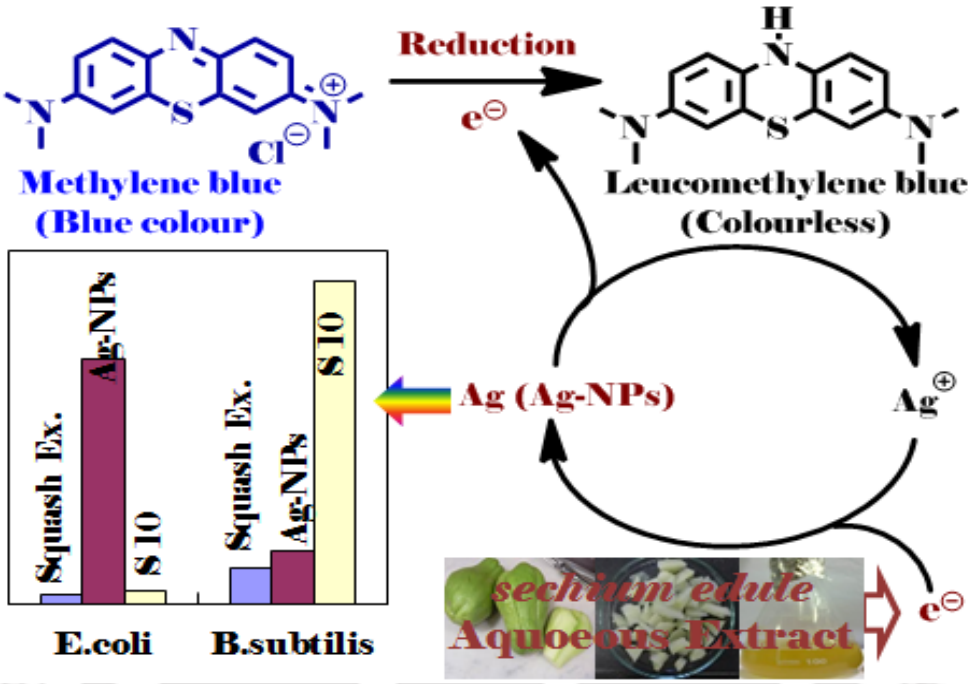

Figure A3. Chayote Squash (*Sechium edule)* fruits, pulp pieces, aqueous extract and the synthesis of AgNPs via reduction of Ag^{+} to Ag^{0} by *sechium edule* aqueous extract. The comparison of antibacterial activity of squash aqueous extract and Ag-NPs with control S10 and the catalytic action of AgNPs on methylene blue.

Following the background literature, we have concentrated ourselves for the first time to use a vegetable, Chayote (*Sechium edule*) known as 'Squash' which is widely available, cheap and has antioxidant properties for framing the following research objectives for this chapter.

- Synthesis of stable silver nanoparticles(AgNPs) with the bioreduction method using chayote squash, or *Sechium edule* aqueous extract (**Figure A3**).
- Characterization and determination of the crystalline phase of synthesized AgNPs from X-ray diffraction (XRD) method.
- Evaluation of the antimicrobial effect of biologically synthesized Ag-NPs by disc diffusion method against gram positive and gram negative bacteria.

- Study of the catalytic activity of synthesized Ag-NPs toward the reduction of methylene blue using UV–visible spectrophotometer (**Figure A3**).

The ability of *Sechium edule* fruit aqueous extract to synthesize silver nanoparticles has been demonstrated. The phytoconstituents such as polyphenols, the amide groups and COOH groups might act as a ligand for the synthesis and stabilizing the Ag-NPs as is evident from FT-IR studies. Synthesized silver nanoparticles were characterized by UV-Visible, FTIR, and XRD. The antimicrobial results state that the silver nanoparticles have strong antibacterial effect on gram negative bacteria. Moreover, the synthesized AgNPs show catalytic activity which influences the reduction of methylene blue in presence of *Sechium edule* aqueous extract which is attributed to the electron relay effect. Currently, we are exploring the catalytic effect of AgNPs in organic transformations under reducing environment.

CHAPTER 4: SYNTHESIS OF POLYSTYRENE NANOCOMPOSITES (PS-AGNPS) FROM WASTE THERMOCOL AND GREEN SYNTHESIZED SILVER NANOPARTICLES FOR WATER DISINFECTION APPLICATION

This chapter reports the development of PS-AgNPs composite using green synthesized AgNPs and waste thermocol. Firstly, the green synthesized AgNPs were prepared in different concentrations and embedded accordingly into the PS matrix. The morphology of PS-AgNPs nanocomposites was studied using FESEM and FETEM. Fourier transform infrared spectroscopy (FTIR) was used to evaluate the surface chemical bonding and surface composition of the prepared nanocomposites. The thermal property of the nanocomposites was investigated by thermogravimetric analysis (TGA). The tensile strength of the composites was also estimated. These PS-AgNPs nanocomposites showed an antibacterial effect against *E. coli*, a disease-causing gram-negative bacteria commonly found in water. Among them, the PS-AgNPs cup encapsulating 10% AgNPs showed optimum tensile strength and bacteria disinfection property. These nanocomposites have been utilized to prepare cups as a model of water tank for water storage having disinfection properties.

Scientists worldwide are keen to develop cost-effective, non-toxic and eco-friendly water disinfection systems to suffice the scarcity of clean water. Achieving proper disinfection without creating harmful byproducts for removing or inactivating waterborne pathogens is the main challenge. In this respect, polystyrene (PS) nanocomposites find wide applications in water storage, food packaging material, transportation, medicine, etc. The addition of

nanoparticles such as silver nanoparticles(AgNPs) into PS enhances its mechanical properties, gas barrier properties, thermal stability, etc. This study reports the development of PS-AgNPs composite using green synthesized AgNPs and waste thermocol.

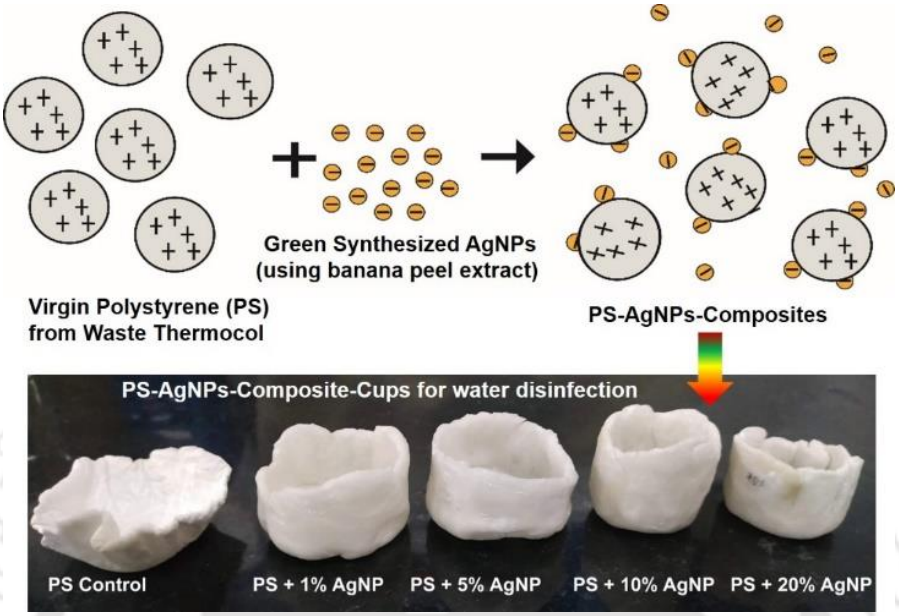

Figure A4. AgNPs-PS nanocomposite and the cups for water disinfection study.

Motivated by the environmental issue related to the waste management and with an aim turning wastes into value-added materials, and following the background literatures, we have concentrated ourselves to use our already synthesized AgNPs via green route for making composite with waste thermocol for water disinfection study. Thus we framed our objectives as below:

- Green synthesis of AgNPs using Bhimkol (*Musa balbisiana*) peel extract.
- Development of PS nanocomposites by directly mixing waste thermocol in acetone with the addition of different amount of AgNPs.
- Characterization of PS nanocomposites using UV-Vis spectrophotometry, Fourier transformation infrared(FT-IR) spectrometry, Energy-dispersive X-ray(EDX), Field Emission Transmission Electron Microscope(FESEM), Field Emission Transmission Electron Microscope(FETEM) and Thermogravimetric analysis(TGA) performed in nitrogen gas.
- Water disinfection application of the nanocomposite.

Waste thermocols and green synthesized AgNPs were used to develop low-cost, functional PS-AgNPs nanocomposites for water disinfection purpose. AgNPs were green synthesized

using bhimkol (*Musa balbisiana*) peels which act as reducing as well as a stabilizing agent. Different percentage of the green synthesized AgNPs were embedded in the PS matrix to produce PS-AgNPs nanocomposite materials. FESEM and EDX results confirm the quantitative and qualitative presence of AgNPs in the PS matrix, and from FETEM imaging, the size and shape of PS and AgNPs in the nanocomposites were examined. Good dispersion of the AgNPs observed in the polymer matrix. Due to the encapsulation of the AgNPs into the polymer matrix, undesirable polymer degradation was prevented, which ultimately increases the durability of the PS-AgNPs composites. The introduction of a small amount of AgNPs in the PS matrix considerably increases the thermal stability of the PS nanocomposites. The mechanical strength and the antibacterial activity of the PS nanocomposite cups are superior to the pure PS cup. 10% AgNPs content was found to be optimum as it has good mechanical strength and water disinfection property against *E. coli*. This study may shed light on the development of PS-based functional materials as a part of turning wastes into value-added materials and, thus, to find a solution to the disposal problem and make an effort to save the environment from plastic pollution.

CHAPTER 5: DEVELOPMENT OF PVA-GELATIN-AgNPs BASED POLYMER HYDROGEL NANOCOMPOSITE FILMS FOR WOUND DRESSING APPLICATION

This chapter focuses on the development of a low-cost composite polymer hydrogel composed of triads materials - polyvinyl alcohol(PVA), gelatin, and green-synthesized silver nanoparticles (AgNPs) for wound dressing application. Thus, the AgNPs were synthesized using peels of *Musa balbisiana* (Bhimkol) and incorporated into the PVA-Gelatin blend. The hydrogel films showed no toxicity against the BJ normal human foreskin fibroblasts cells. Our triad polymeric nanocomposite hydrogel was found to accelerate wound healing, efficiently protect the wounded skin surface against exudate accumulation/dehydration, and prevent bacterial growth and infection. All the properties made our PVA-gelatin-AgNPs triad nanocomposite hydrogel ideal for wound dressing applications.

The effective wound-healing hydrogels should have the property to create a moist environment for wound healing, prevent the wound surface from microbial penetration and provide higher water vapour permeability. Toward this end, as a part of our ongoing research on the synthesis of antibacterial AgNPs-based composite materials, we thought that it would be worthwhile to utilize the green-synthesized AgNPs for developing low-cost composite polymer hydrogel for wound dressing application. Literature study suggested that a material

formulation based on PVE-gelatin-blend mixed with silver nanoparticles in lower concentrations would provide promising hydrogel with potent antibacterial activity and wound dressing property. We, thus, thought to utilize our previously reported green-synthesized AgNPs for the preparation of triad composite polymeric hydrogel with wound healing/dressing property.

Thus, we framed out objectives as below:

- Green synthesis of AgNPs by reducing silver nitrate($AgNO_3$) using Bhimkol (*Musa balbisiana*) peel extract.
- Development of polymer based hydrogel nanocomposite films by adding PVA, gelatin and AgNPs by the casting method.
- Swelling kinetics, mechanical strength, water transmission rate(WVTR) analysis, contact angle measurements analysis was performed.
- Characterization of the PVA/gelatin/AgNPs hydrogel nanocomposite films using Fourier transformation infrared(FT-IR) spectrometry, Energy-dispersive X-ray(EDX), Field Emission Transmission Electron Microscope(FESEM), Field Emission Transmission Electron Microscope(FETEM) and Thermogravimetric analysis(TGA) performed in nitrogen gas and X-Ray Diffraction(XRD) Analysis
- Cell viability assay and *in vitro* scratch wound healing assay performed to observed the cell toxicity and the wound healing efficacy of the hydrogel films.

In summary, a very cost effective and easily usable functional wound dressing hydrogel was developed by combining polyvinyl alcohol(PVA) and gelatin and silver nanoparticles (AgNPs). The polymeric hydrogels showed superior crosslinking. Incorporation of AgNPs within the matrix provided better swelling behaviour, mechanical strength and thermal stability to the prepared polymer hydrogel films. The synthesized and optimized polymeric hydrogel nanocomposite showed antibacterial activities against *E. coli* and *S. aureus*, respectively, with 70% of bacterial cell death. Cellular toxicity studies demonstrated that the prepared PVA-Gelatin-AgNP hydrogels are non-cytotoxic. The cell viability was more than 60% after 24 and 48 hours for the PVA-Gelatin-AgNP hydrogel. Thus, the material was used to study its wound healing property. Wound closure was reported to be more than 90% in both control and AgNPs incorporated hydrogel films after 24 hours of exposure when evaluated by the scratch assay. Overall our synthesized material is biocompatible and can be utilized in wound healing bandages as it can accelerate the wound healing process and also protect the wound site from possible bacterial infections.

List of Symbols/Abbreviations

Symbols/ Abbreviations	Brief Description
°	Degree
Å	Angstrom
Λ	Lambda
mM	Millimolar
Nm	nanometer
cm^{-1}	Wave number
pH	Potential of Hydrogen
AgNPs	Silver Nanoparticles
BPE	Banana Peel Extract
$AgNO_3$	Silver Nitrate
PVA	Poly(vinyl) Alcohol
PS	Polystyrene
OD	Optical Density
CFU	Colony Forming Unit
Na_2HPO_4	Disodium Hydrogen Phosphate
NaH_2PO_4	Monosodium Phosphate
HCL	Hydrochloric acid
$FeCl_3$	Ferric chloride
$K_4Fe(CN)_6$	Potassium ferrocyanide
MB	Methylene Blue
LB broth	Luria-Bertini Broth
PDA	Potato Dextrose Agar
UTM	Universal Testing Machine
EDX	Energy-Dispersive X-Ray Spectroscopy
FTIR	Fourier Transform Infrared Sepctroscopy
FESEM	Field Emission Scanning Electron Microscopy
FETEM	Field Emission Transmission Electron Microscopy
TGA	Thermogravimetric Analysis
DSC	Differential Scanning Calorimetry Analysis
DLS	Dynamic Light Scattering
WVTR	Water Vapour Transmission Rate
H	Hour
Mins	Minutes
RT	Room Temperature
AE	Antibacterial Effect
SD	Standard Deviation
HR-TEM	High Resolution-Transmission Electron Microscopy
SAED	Selected Area Diffraction
UV-Vis	Ultra violet visible
XRD	X-Ray Diffraction Analysis

CONTENTS	Page No.
CHAPTER 1: State-of-the-Art in the Synthesis and Applications of Silver Nanoparticles	1-47
1.1. Nanotechnology	1-2
1.2. Silver nanoparticles	2-3
1.2.1. Various Approaches for the Synthesis of Silver Nanoparticles (AgNPs)	4-6
1.2.2. Various Methods for the Synthesis of Silver Nanoparticles (AgNPs)	6-15
1.2.2.1. Chemical Synthesis of Silver Nanoparticles (AgNPs)	6-9
1.2.2.2. Physical Synthesis of Silver Nanoparticles (AgNPs)	10-11
1.2.2.3. Biological Synthesis of Silver Nanoparticles (AgNPs)	11-13
1.2.2.4. Green Synthesis of Silver Nanoparticles (AgNPs)	13-15
1.3. Applications of AgNPs	15-24
1.3.1. Antimicrobial AgNPs	15-17
1.3.2. Antiviral AgNPs	17-18
1.3.3. Antifungal AgNPs	18-18
1.3.4. Anticancer AgNPs	18-19
1.3.5. Bacterial Disinfection of Water by AgNPs	19-19
1.3.6. Applications of AgNPs in Medical Science	19-20
1.3.7. AgNPs in Wound Dressings Materials	20-21
1.3.8. AgNPs in Catalysis	21-22
1.3.9. AgNPs in Solar Cell/Photovoltaic Devices	22-22
1.3.10. AgNPs in Fabrication of Biosensor	22-23
1.3.11. AgNPs in Ink-Jet Printing	23-23
1.3.12. AgNPs in Food Packaging Materials	23-23
1.3.13. Other Applications of AgNPs	24-24
1.4. Importance and Future Scopes	24-25
1.5. References	25-47

CONTENTS	Page No.
CHAPTER 2: Synthesis of Silver Nanoparticles using Bhimkol (*Musa Balbisiana*) Peel Extract as Biological Waste: Antibacterial Activity and Role of Ripen Stage of the Peels	48-83
2.1. Introduction	48-48
2.2. Green Synthesis of Silver Nanoparticles (AgNPs)	48-49
2.3. Green synthesis using Agricultural Waste	50-54
2.4. Background: Banana Peels as Agricultural waste	54-55
2.5. Aim and Objectives	55-55
2.6. Results and Discussion	55-68
2.6.1. Study of the Qualitative and Quantitative Phytochemical Compositions of Bhimkol (*Musa balbisiana*) Peels	55-57
2.6.2. Comparative Efficiency of Three Stages of Development of Bhimkol Peels for the Green Synthesis of AgNPs	57-58
2.6.3. Green Synthesis of AgNPs	58-62
2.6.3.1. Effect of Concentration of BPE	59-60
2.6.3.2. Effect of pH	60-60
2.6.3.3. Effect of $AgNO_3$ Concentration	60-61
2.6.3.4. Effect of Reaction Time	61-62
2.6.4. Characterisation of AgNPs	62-66
2.6.4.1. Fourier Transform Infrared (FTIR) Analysis	62-63
2.6.4.2. Field Emission Electron Scanning Microscopy (FESEM) Analysis	63-63
2.6.4.3. Transmission Electron Microscopy (TEM) Analysis	64-64
2.6.4.4. X-ray Diffraction Analysis	64-65
2.6.4.5. Particle Size Distribution	65-65
2.6.4.6. Energy Dispersive X-ray (EDX) Analysis	65-66
2.6.4.7. Zeta Potential (ZP) Measurement	66-66
2.6.5. Study of the Antibacterial Activity of Both Bhimkol Peel Extract and AgNPs Synthesized by using Bhimkol Peels	66-68
2.6.5.1. Zone of Inhibition Assay	66-68
2.7. Conclusion	68-68
2.8. Experimental Section	69-77
2.8.1. Materials and Methods	69-70
2.8.2. Characterizations of AgNPs	70-73
2.8.3. Qualitative and Quantitative Phytochemical Analysis of Bhimkol (*Musa balbisiana*) Peels	73-77
2.9. References	78-83

CONTENTS	Page No.
CHAPTER 3: Green Synthesis of Silver Nanoparticle using *Sechium Edule* Aqueous Extract and Study of Antimicrobial and Catalytic Activity	84-102
3.1. Introduction	84-84
3.2. Green synthesis of AgNPs using Plant Extracts	84-88
3.3. Aim and Objectives	88-88
3.4. Results and Discussion	88-94
3.4.1. Preparation of the Chayote Squash Aqueous Extract	88-89
3.4.2. Study of the Qualitative Phytochemical Compositions of the Chayote(Sechium edule) Squash	89-90
3.4.3. Synthesis of Silver nanoparticles(AgNPs)	90-91
3.4.4. Characterisation of AgNPs	91-92
3.4.5. Study of Antibacterial/Antifungal Activity	92-94
3.4.6. Study of Catalytic Activity	94-94
3.5. Conclusion	94-95
3.6. Experimental Section	95-97
3.6.1. Materials and Methods	95-95
3.6.2. Characterization of AgNPs	96-97
2.6.3. Application of AgNPs	97-97
3.7. References	97-102

CONTENTS	Page No.
CHAPTER 4: Synthesis of Polystyrene Nanocomposites (PS-AgNPs) from Waste Thermocol and Green Synthesized Silver Nanoparticles for Water Disinfection Application	103-130
4.1. Introduction	103-104
4.2. Nanocomposites	104-109
4.2.1. Types of Nanocomposites	104-106
4.2.2. Polymer Nanocomposites	106-108
4.2.3. Polystyrene-Ag-Nanocomposites	109-109
4.3. Aim and Objectives	110-110
4.4. Results and Discussion	110-124
4.4.1. Synthesis of AgNPs	110-111
4.4.2. Development of Functional PS-Ag Nancomposites	111-112
4.4.3. Characterization of the PS-Ag Nanocomposites	112-117
4.4.3.1. UV-Vis Spectroscopy of the PS nanocomposites	112-113
4.4.3.2. FTIR Analysis	113-113
4.4.3.3. Field Emission Scanning Electron Microscope (FESEM) Study	114-115
4.4.3.4. Energy-dispersive X-ray analysis(EDX) Analysis	115-116
4.4.3.5. Field Emission Transmission Electron Microscopy (FETEM) study	116-117
4.4.4. Study of Thermal Stability of the PS-Ag Nanocomposites by Thermogravimetric Analysis(TGA)	117-119
4.4.5. Study of Mechanical Properties of the PS-Ag Nanocomposites	119-121
4.4.6. Study of Water Disinfection Activity of the PS-Ag Nanocomposites	121-123
4.5. Conclusion	123-123
4.6. Experimental Section	123-126
4.6.1. Materials and Methods	123-124
4.6.2. Characterization of the PS Nanocomposites	124-125
4.6.3. Water Disinfection Activity	125-126
4.7. References	126-130

CONTENTS	Page No.
CHAPTER 5: Development and Characterization of PVA/Gelatin/AgNPs Based Polymer Hydrogel Nanocomposite for Wound Dressing Application	131-174
5.1. Introduction	131-132
5.2. Nanocomposite Hydrogels	132-133
5.3. Applications of Nanocomposite Hydrogels	133-134
5.4. Silver Nanoparticle(AgNP)-Hydrogel Composites	134-135
5.4.1. Application of AgNPs Based Wound Dressings	136-137
5.4.2. Application of polymer-Ag based Hydrogel Wound Dressings	137-139
5.5. Aim and Objectives	139-139
5.6. Results and Discussion	140-161
5.6.1. Preparation of the Polymer Nanocomposites Hydrogel	140-141
5.6.2. Study of Swelling Properties of The NC Hydrogel Films	141-143
5.6.3. Study of Mechanical Properties of The NC Hydrogel Films	143-145
5.6.4. Study of Fourier Transform Infrared (FT-IR) Spectroscopic Character of the NC Hydrogel Films	145-146
5.6.5. Study of Water Vapour Transmission Rate (WVTR)	147-148
5.6.6. Study of Hydrophilicity and Wettability by Contact Angle Measurement	149-150
5.6.7. Study of Morphology of NC Hydrogel Films by FESEM	150-151
5.6.8. Study of Morphology of NC Hydrogel Films by Field Emission Transmission Electron Microscopy (FETEM) Analysis	151-152
5.6.9. Study of X-Ray Diffraction of the NC Hydrogel	152-153
5.6.10. Study of Elemental Analysis of the NC Hydrogel via EDX	154-154
5.6.11. Study of Thermal Property of NC Hydrogel Films	154-156
5.6.12. Applications of NC Hydrogel Films	156-161
5.6.12.1. Study of Antibacterial Activity of NC Hydrogel Films	156-159
5.6.12.2. Study of Cell Viability of NC Hydrogel Films	158-160
5.6.12.3. Study of Wound Healing Property of NC Hydrogel Films via In vitro Scratch Wound Healing Analysis	160-161
5.7. Conclusion	161-162
5.8. Experimental Section	162-167
5.8.1. Materials and Methods	162-163
5.8.2. Characterizations of the NC Hydrogel Films	163-166
5.8.3. Applications of the NC Hydrogel Films	166-167
5.9. References	168-174
Summary and Thesis Outlook	175-177

CHAPTER 1:

State-of-the-Art in the Synthesis and Applications of Silver Nanoparticles

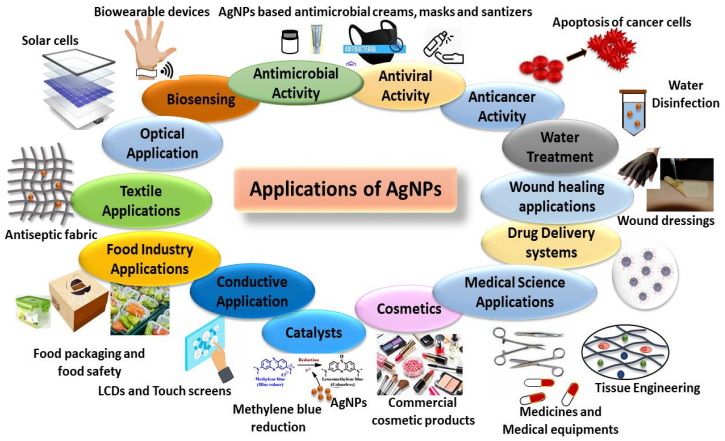

1.1. Nanotechnology

Nanotechnology is a field of science and engineering involved in the fabrication of nanoscale materials and their various applications in imaging, electronics, medicine, cosmetics, agriculture, food, environment etc. These materials and devices are the smallest functional organization that can be referred to as at least one dimension in the nanometer scale range or one billionth of a meter.[1] At the nanoscale level (size range of 1 to 100 nm), the properties, such as physiochemical, structural, and electronic properties of the nanoparticles (NPs)/ nanomaterials, become different from that of the bulk materials.[2] The flexible physicochemical characteristics of nanomaterials, such as melting point, thermal and electrical conductivity, light absorption, catalytic activity, wettability and scattering, have made them efficient to show improved performance over their bulk counterparts.[3] Therefore, the field of nanotechnology has attracted the interest of scientists across the globe. The current research trend focuses on discovering and developing nanomaterials with novel properties that would help to advance the field of nanoscience and nanotechnology.[4]

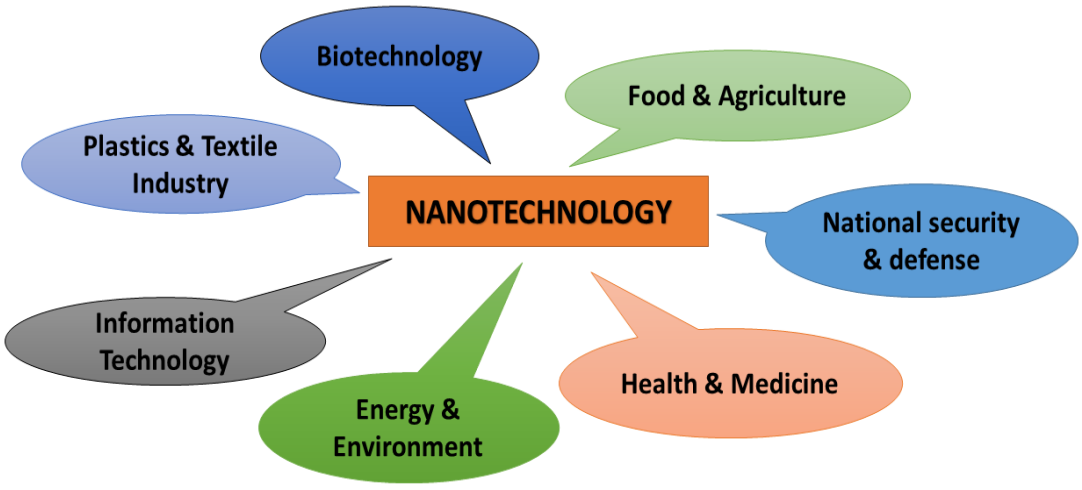

Figure 1.1: Applications of nanotechnology in various research fields.

Figure 1.1 depicts the multiple applications of nanotechnology in different areas of research. The areas in which nanotechnology plays a significant role are national security and defense, agriculture and food, information technology, energy and environment, biotechnology, plastics and textile industry, health and medicine, cosmetics, aerospace engineering, etc.

Among all nanomaterials, metallic nanoparticles are considered the most promising as they turn out to be an alternative route for stopping the spread of antimicrobial resistance, often

resulting from growing microbial resistance against metal ions and antibiotics.[5] These nanoparticles consist of significant antibacterial properties resulting from (a) generation of Reactive Oxygen Species (ROS), (b) surface charge of NPs, and (c) Inter-molecular interaction of the NPs with the active site of pathogenic protein/enzyme.

In this respect, silver is considered a distinguished antimicrobial agent effective against a broad range of microorganisms, including various gram-positive and gram-negative bacteria, viruses, and fungi. Silver has been depicted as a therapeutic agent for many diseases in the ancient Indian medical system to deter microbial growth. Further, it is the least toxic to animal cells out of all the metals with antimicrobial properties.[6] Silver is generally used in nitrate form to induce an antimicrobial effect. $AgNO_3$ is known to bind to the thiol groups of the bacterial protein resulting in denaturation.[7]

Therefore, nanomaterials made up of silver (AgNPs) have gained significant interest due to their distinctive electrical, physical, optical, antimicrobial properties and a broad range of applications. The alteration of energy level from a continuous band to a discrete band of AgNPs with a decrease in particle size offers strong size-dependent chemical and physical properties useful for various applications.[8] The AgNPs illustrate lower toxicity to human health whereas higher toxicity to various micro-organisms. Hence, there is a broad scope of AgNPs for utilization in various applications, such as antimicrobial applications, medical instruments, and products for health care such as burn wound dressing, scaffolds, water purification, and agricultural uses. AgNPs can easily be synthesized by using various methods, primarily classified into two types. Physical methods include laser ablation, evaporation, condensation, etc. The second method of synthesizing AgNPs is the chemical method which includes sodium borohydride, hydrazine, etc. mediated reduction of silver salts and the Green synthesis. While the reduction with chemical reagents is not environmentally friendly, green synthesis is a non-toxic, eco-friendly, and cost-effective method among all these processes.

1.2. Silver Nanoparticles

For centuries, elemental silver and silver salts have been well-known agents in remedial and preventive health care.[9] Remarkably, silver possesses both an oligodynamic effect and a bactericidal impact concerning its action against microbes. Silver has been depicted as a therapeutic agent for many diseases in the ancient Indian medical system. To avoid transmission of Neisseria gonorrhea, aqueous silver nitrate drops, in general, were administered to the newborn's eyes during childbirth. Silver nitrate is not harmful to mammals but it can be

toxic to fish and aquatic organisms. If the registrered product is used and disposed following the instructions, there can be no environmental risk. Silver wares were used in daily household activities due to their antimicrobial properties.[10] It was also known that the colloidal nano-silver is comparatively safe for humans, plants, and all multicellular living matter. However, in some reports, it has also been observed that AgNPs in higher concentrations/doses can result in toxicity which is due to the oxidation of surface ions by biological macromolecules resulting in silver cations that can affect basic cellular functions in mammalian cells[11] and cellular transportation. Additionally, the AgNPs are electronically stable compared to the silver cation salts and complexes and hence are robust and can be conjugated or modified/engineered easily and also can be applied across various environmental/reaction conditions. The immobilization of silver on polymer substrates seems advantageous since it will not allow the direct uptake of the particles from mammalian cells. Silver-containing agents like silver sulfadiazine are regularly used in clinical wound dressings, and silver-impregnated catheters are used in the coatings of biomedical materials.[12–14]

Nanoparticles have a wide range of potential applications in cosmetics, energy and environmental remediation, medicine, and biomedical research and devices due to their enhanced and diverse properties.[15] Among all other types of nanoparticles, silver nanoparticles (AgNPs) attained more interest because of their distinctive properties, such as their chemical, physical, physicochemical, thermal/electrical conductivity, Raman scattering (surface improved), and biological properties.[16] It shows broad-spectrum bactericidal and fungicidal activity.[17] In consumer products, nanosilver is utilized mainly in products like disinfecting medical devices, water treatment equipment, and home appliances. Nanosilver is used in liquid form or colloid form in shampoos, coatings and sprays. Nanosilver is also integrated into fibres in textile industries as well as in water purification systems in filtration membranes. Among all other nanotechnology-enabled products, nanosilver is one of the most significant. Nanosilver-based products are also effectively used in health and fitness, according to an article published in 2008 by the silver nanotechnology commercial inventory. The records were compared with other categories, including medical applications, electronics, and computers.[18] AgNPs have a wide range of applications; as such, the industry and the scientific community are interested in the various development in the research of AgNPs.[19]

1.2.1. Various Approaches for the Synthesis of Silver Nanoparticles (AgNPs)

Synthesis of stable AgNPs provides an unconventional perception for environmental disinfection and sterilization. There are various methods to synthesize AgNPs. However, the three prominent routes are: (a) solid-phase route, (b) liquid-phase route, and (c) aerosol or gas-phase route are discussed in this chapter and represented in figure 1.2.[20]

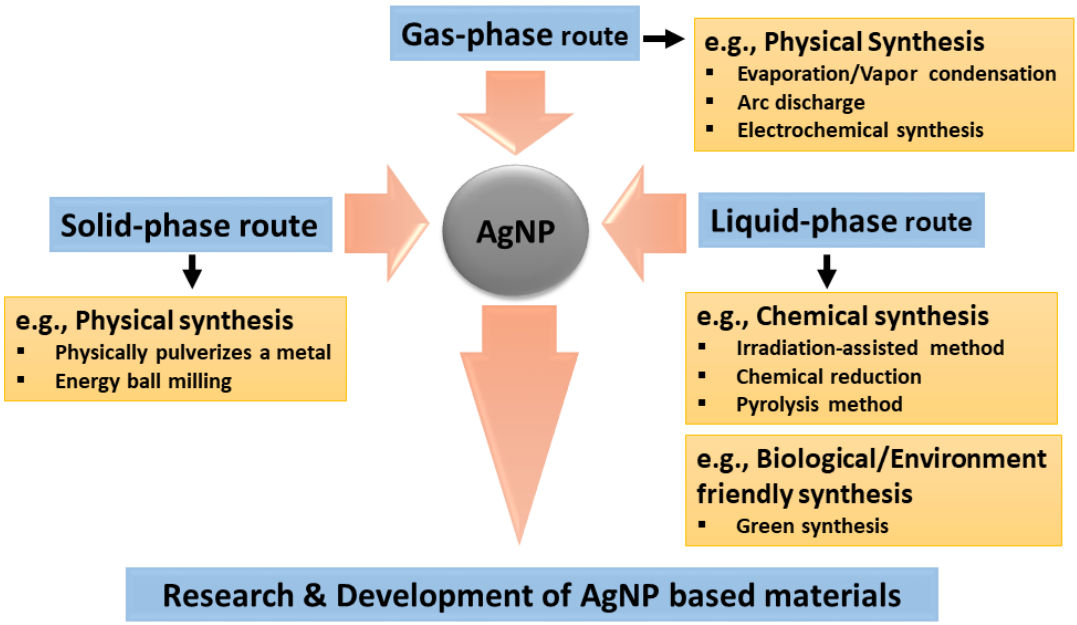

Figure 1.2: Various routes for AgNPs synthesis are classified into three-phase routes: solid, liquid, and gas-phases routes for research and development of silver nanoparticle-based materials(Image adapted from Nakamura *et al.*, 2019).

Nanoparticles are synthesized by various chemical and physical methods that are quite expensive and potentially hazardous to the environment and involve toxic and hazardous chemicals responsible for multiple biological risks. The advancement of biologically inspired tentative processes for the synthesis of nanoparticles is growing into an essential branch of nanotechnology. Two approaches are involved in the synthesis of AgNPs. They are top to bottom approach and bottom to Top approach. Figure 1.3 represents the two major approaches for the synthesis of nanoparticles.

Top to Bottom Approach: Appropriate bulk material breaks down into fine particles by size reduction with various lithographic procedures such as sputtering, grinding, milling, and thermal or laser ablation in top to bottom approach.

Bottom to Top Approach: Nanoparticles can be synthesized using chemical, biological methods by self-assemble atoms to new nuclei that grow into a nanoscale particle in the bottom-to-top approach. Here, the most standard way to synthesize AgNP is chemical reduction.[21,22]

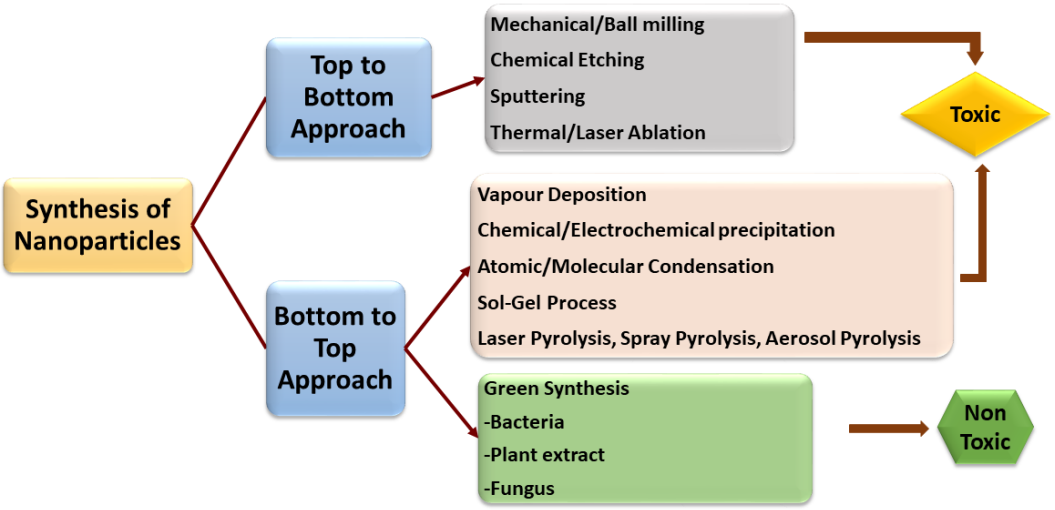

Figure 1.3: Two main types of approaches for the synthesis of nanoparticles i.e., top to bottom and bottom to top(Graphical flowchart adapted from Ahmed *et al.*, 2016).

Figure 1.4 represents the two major pathways for nanoparticle synthesis- (a) bottom to top in which atoms/molecules coverts to nuclei and then to nanoparticles, and (b) top to bottom approach where bulk materials convert to finer particles.

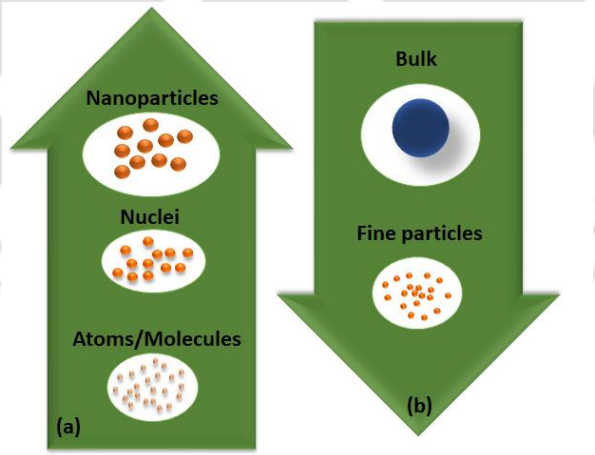

Figure 1.4: The two major pathways for nanoparticle synthesis-(a) bottom to top, and (b) top to bottom approaches.

In the case of the other approach (top to bottom), nanoparticles are generally synthesized by evaporation, condensation using a tube furnace at atmospheric pressure. In this method, the foundation material is placed centred at the furnace and is vaporized into a carrier gas. Ag, Au,

PbS, and fullerene nanoparticles have previously been produced using the evaporation/condensation technique. The production of AgNPs using a tube furnace has several drawbacks as it occupies ample space and requires a great deal of energy while raising the environmental temperature around the source material. It also requires a lot of time to enhance thermal stability.[23–27] One of the most significant limitations in this process is the imperfections in the surface structure of the product, and the other physical properties of nanoparticles are highly dependent on the surface structure in reference to surface chemistry. Some of the most frequently used methods for the synthesis of AgNPs are discussed herein.

1.2.2. Various Methods for the Synthesis of Silver Nanoparticles (AgNPs)

Below is the pictorial representation of various common methods for the synthesis of silver nanoparticles (AgNPs).

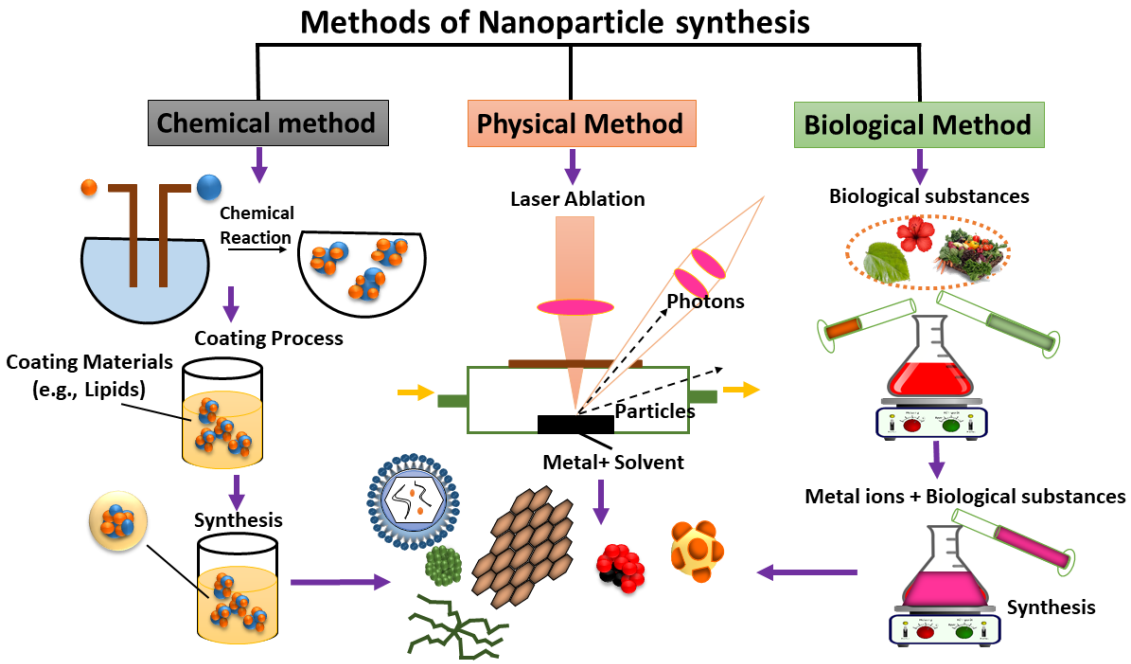

Figure 1.5. Various frequently used methods for synthesis of nanoparticles (graphical abstract adapted from Jeyaraj *et al.*, 2019).

1.2.2.1. Chemical Synthesis of Silver Nanoparticles (AgNPs)

Out of several methods, the chemical reduction method is one of the most applied methodologies for the synthesis of AgNPs in colloidal dispersions. There are mainly three components involved in the process of chemical synthesis of the AgNPs, namely (i) organic/inorganic reducing agents, (ii)metal precursors, and (iii) capping or stabilizing

agents.[28] Two stages involved in the reduction of silver salts to colloidal solutions are nucleation and subsequent growth. Ag^+ ion gets reduced into metallic (Ag^0) silver, which undergoes nucleation. The newly formed particles attaining the Kelvin diameter gain thermodynamic stability and crystalize to attain the required quantum confinement.[39] For the production of AgNPs few of the common reductants used are citrate, borohydride, ascorbate and compounds with hydroxyl and carboxyl groups.[29–31] The most frequently used precursors for chemical reductions are silver nitrate,[32–35] silver acetate,[36,37] silver chlorate,[37,38] and silver citrate.[37,39] Uniformly distributed monodispersed AgNPs can also be synthesized if all the nuclei form at the same time. If they have a similar size, they will have a subsequent growing pattern. The primary nucleation and the growth of nuclei can be optimized mainly by controlling the reaction parameters such as reaction temperature, reducing agents, pH, stabilizing agents, and precursors.[19]

Synthesis of AgNPs is straightforward and convenient in the liquid phase via various chemical methods. Polyol process is the process in which a large number of monodisperse silver nanocubes can be synthesized via the reduction of silver nitrate using polyethylene glycol (PEG) and polyvinyl pyrrolidone (PVP). Varying the experimental parameters the size of the silver nanocubes can be also controlled. While the polyethylene glycol works as solvent as well as reductant,[40] the presence of PVP and the molar ratio of PVP with respect to silver nitrate determines the size as well as the geometric shape of the final product. Other polymeric systems reported to be effective as capping agents for stabilization, are polymethacrylic acid (PMAA) and polymethylmethacrylate (PMMA).[28,41] For synthesizing AgNPs, some of the popular chemical methods were chemical reduction, electrochemical synthesis pyrolysis and irradiation assisted methodologies. Some of these chemical methodologies for silver nanoparticle synthesis are represented in Table 1.1 which discusses the various reducing agent, cathode, anode, gases, or type of irradiation used for AgNP synthesis.[20]

Table 1.1. Different chemical methods for synthesizing silver nanoparticles.

Various chemical Methodologies	Size of the nanoparticles(nm)	Various reducing agent used
Chemical reduction	<50	Hydrogen peroxide[42]
	7,29,89	Gallic acid[43]
	<30	Sodium citrate[44]
	7.6-13.11	Sodium borohydride[45]

	5,7,10,15,20,30,50,63,85,100	Sodium borohydride, trisodium citrate[46]
	9,11,24,30	Hydrazine hydrate, sodium citrate[47]
	~5	Sodium borohydride, citrate[48]
		Solvents/cathode/anode used
Electrochemical reduction	4.8	Under argon atmosphere, dry oxygen-free solvents used
	1-18	Ion exchange of film(cathode) to Ag in $AgNO_3$ solutions
	30,46	Platinum(cathode/anode)
		Gases used
Pyrolysis methodology	3-150	Oxygen
	20-300	Argon under oxygen-free environment
		Types of irradiation used
Irradiation assisted method	2-8	UV irradiation(266nm)
	3-30	Radiation crosslinking and reduction
	50	Microwave irradiation
	30-120	Dual beam illumination system(546/440nm)

Chemical Reduction: The most significant method among all the chemical methodologies is the chemical reduction method that consists of a silver source and reducing agent. Among the various reducing agents, borohydride proved to be very strong and widely used. Silver nanoparticles were also synthesized by a co-reduction technique in which the sodium borohydride was used as primary reductant; trisodium citrate was used as a secondary reductant and protective agent.[46] During the synthesis, growth kinetics and nucleation are generally controlled precisely to afford monodispersed silver nanoparticles with a good yield. Silver nitrate is mainly used to supply silver ions to the synthesis process.[49] Transition metal colloids in the nanometer range can also be made in an electrochemical process in which AgNPs synthesized can be of ≤ 20 nm size.[50]

Electrochemical Method (Electrolysis): In this method, various nanoparticles can be synthesized through electrochemical reduction of the metal sol at the liquid/liquid interface. The size and homogeneity of the NPs can be controlled by changing the composition of the electrolytic solutions. A plate is used as an anode and a rotating disk electrode is used as a cathode. It results in the formation of electro-deposited Ag^0 nanoparticles. Particles are

obtained by anodically dissolving metal sheet and at the cathode, intermediate metal salts are reduced. By adjusting the current density, precise size-controlled and high purity particles are obtained.[50] Following the method the production of AgNPs (2-7nm) having silver plasmon band at 370 nm have been reported via the dissolution of the metallic anode in an aprotic solvent.[51] Methyl viologen-mediated electroreduction of AgCl for the efficient synthesis of AgNPs has also been reported. Thus, the produced AgNPs are stabilized by CTA+ surface-active cations on carbon electrode.[52]

Photochemical Methods: In this methodology, photo-irradiation processes are used for the successful synthesis of AgNPs. Thus, photo-assisted irradiation of a reaction mixture with a light source(lamp or laser) without using surfactants or stabilizers in the presence of photo reducing agents has been utilized to produce stable and well dispersed AgNPs.[53–55] The irradiation-assisted method has also been exploited for the synthesis of silver nanocrystals (triangular, monodisperse) of 30-120 nm edge length and 2-8 nm length.[56,57] By simultaneous radiation crosslinking and reduction, nano-silver with gelatin and chitosan hydrogels synthesis has been reported. This hydrogel shows high stability with uniform distribution of silver nanoparticles into the hydrogel matrix.[58] The pulse radiolysis method is used to produce nanoparticles by silver perchlorate salt. Instead of chemical materials, UV light mediated photo reduction of Ag^{+} to Ag^{0} has been reported for the synthesis of nanomaterials and used in a natural rubber matrix for preparing composites. Microwave irradiation method has also been used for the synthesis of nanomaterials.[59] In this method, it has been observed that the time required for preparation and the size of the formed nanoparticles is directly proportional to the irradiation power of the light source.[60] The microwave irradiation method exhibits features like rapid reaction and the generation of high concentration of AgNPs at the same exposure and temperature.[59,61,62]

Ultrasonic Spray Pyrolysis: This is a convenient and pioneering tool for AgNP synthesis, which facilitates controlled and uniformed particle size.[63–65] In this technique, a metal-containing solution is atomized under reduced temperature forming aerosol, enabling easy control of nanopowder morphology and convenience in obtaining cost-effective precursors. This method generates an aerosol from the dilute aqueous metal salt solution that produces narrow-sized particles. AgNPs(<20nm) have been synthesized by pyrolysis of an ultrasonically atomized spray of dilute silver nitrate solution at more than 650°C which is below the melting point of silver.[66]

1.2.2.2. Physical Synthesis of Silver Nanoparticles (AgNPs)

Synthesis of nanoparticles by physically pulverizing a metal is usually carried out by using physical methods.[67] Some commonly used physical methods for AgNPs synthesis in liquid solutions are evaporation, dispersion/condensation, ball milling and laser ablation.[68]

Vapor Condensation Method: Mainly, two steps are involved in this process; evaporation and condensation. These processes are carried out under atmospheric pressure in a tube furnace. The source material is vaporized in carrier gas inside the furnace.[69–73] Without solvent contamination, uniform nanoparticles and thin films can be prepared by vaporizing the target materials with the heat source and then rapidly condensing them. However, there are few disadvantages involved in using this process: high energy consumption raises the temperature of the environment, large space consumption of the furnace, and more time required for achieving thermal stability.[41,74]

Arc Discharge Method: It is an efficient method for the synthesis of nanoparticles using a direct current arc voltage applying across two graphite electrodes immersed in inert gases like He, Ne or Ar. Nanosilver is prepared in water suspensions without using any surfactants and stabilizers. The surface layer of Ag wires evaporates and then condenses into the water layer, turning the colourless solution into coloured colloidal suspension.[28] Silver nanoparticles have been synthesized in powder form by a thermal decomposition technique where Ag^{+1} and oleate form a complex when reacted with sodium oleate and $AgNO_3$ and decompose, leading to AgNPs synthesis. Without the addition of any surfactants or stabilizers, 20-30 nm diameter AgNPs have been synthesized by the arc discharge method. When silver rods are consumed at a rate of 100 mg/mins, metallic AgNPs and ionic Ag are produced at a concentration of 11 ppm and 19 ppm, respectively.[75]

Laser Ablation Method: A rapid and simple irradiation technique has been developed for the synthesis of nanoparticles by laser irradiation of an aqueous solution of inorganic ions. As for an example the synthesis of AgNPs has been demonstrated via illuminating silver plates immersed in liquid phases with laser beam of high energy.[76–78] Thus, this method allows one-pot fabrication. AgNPs contained in calcium phosphate sub microspheres were applicable for the control of infection and dental healthcare.[79] In laser ablation method has the advantage compared to the other conventional methods for metal colloid synthesis. In these systems, metal laser ablation in solution can cause pure nanosilver colloids synthesis without chemical reagents. Laser fluence and laser shot numbers influence nanosilver size, morphology and

concentration.[80–84] The physical deposition method is unique in which well-dispersed AgNPs are synthesized with uniform geometry and particle size (<5 nm).

1.2.2.3. Biological Synthesis of Silver Nanoparticles (AgNPs)

Due to the need for environmentally friendly synthesis methods to avoid the discharge or use of hazardous chemicals during the synthesis of nanoparticles, the biosynthesis or green synthesis of nanoparticles received extensive attention. The mainly used eco-friendly reducing and capping agents for biosynthesis methods are protein,[85] carbohydrate,[86] bacteria,[87] peptides,[88] fungi,[89] algae, yeast[90] and plants.[91,92] In biological synthesis, toxic reagents and organic solvents are not used as stabilizers. The reducing agents are the reactive functional groups in the phytoconstituent molecules produced or present in carbohydrate, bacteria, yeasts, protein, plants or fungi. The biological synthesis includes enzymatic and non-enzymatic reduction. In enzymatic reduction, nicotinamide ADP-dependent reductase produces AgNPs; its rate is between 24-120 hours which is quite slow.[93] But in non-enzymatic reduction of Ag, plants and the microorganisms are the reducing and stabilizing agents. Non-enzymatic reduction is faster and reasonably comparable to chemical reduction; these can handle extreme factors for the quicker synthesis process.[87]

Microbial synthesis: The use of microbes as environmentally sustainable precursors for AgNPs production has achieved a significant research interest. Bacteria and fungi play a major role in the remediation of toxic metals by reducing metal ions. Bacteria mainly help in the fabrication of an ecological method for the synthesis of AgNPs. During the synthesis of biogenic AgNPs, *Lactobacillus fermentum* reduces the growth of *P. aeruginosa* and controls biofilm formation.[94] Thus, an optimized culture of *Bacillus* sp. has been reported for fabrication for rapid synthesis of AgNPs. AgNPs synthesized using *Bacillus cereus* needed an incubation period of 3-5 days at room temperature.[95] Again, *Bacillus subtilis* showed that AgNPs were in the range of 5-50 nm. The extracellular synthesis can produce monodispersed particles.[96] The extracellular synthesis is advantageous over intracellular as nanoparticles are formed inside the biomass deposited in the desired areas. Synthesized AgNP's stability depends on the cell-free culture supernatants of psychrophilic bacteria.[97] Specific parameters such as pH, temperature and concentration of $AgNO_3$ mainly control the AgNPs size during the synthesis via certain bacteria like *Klebsiella pneumonia*, *Enterobacter cloacae*, and *Escherichia coli*.[98,99] The interaction of silver ions with bacteria determines the shape and size of the synthesized AgNPs

when microbes are used.[100,101] Prokaryotes are also highly focused for metallic nanoparticle synthesis due to their abundance and adaptation to extreme conditions.

Metallic nanoparticles can also be synthesized by using fungi because they produce a high amount of protein, which mainly intensifies nanoparticle production, scale-up, and thus, downstream becomes easier. *Aspergillus terreus* aids in synthesizing AgNPs at room temperature.[102] *Spirulina platensis* cell extracts are used to reduce aqueous silver ions; this method is non-toxic, cost-effective, has economic viability, and is environmentally benign.[103] Polydispersed and spherical AgNPs of 17-33 nm has been synthesized using *Helminthosporium tetramera* cell-free filtrates that showed good antibacterial activity.[104] *Humicola* sp. forms extracellular nanoparticles by reducing silver ions.[105] Again, *Aspergillus niger* aids in AgNPs synthesis at ideal conditions such as 37°C, 2.0 mM substrate concentration, and 6.0 pH.[106] In table 1.2 few other fungae that aid in the process of AgNPs synthesis are represented. The enzymes present in the microbes are mainly responsible for the reduction of silver ions and the formation of AgNPs. Thus the microbial-assisted synthesis of AgNPs has developed a biomimetic conduit towards the plant species.

Production of AgNPs via the biological route is better as it avoids the use of toxic reagents and organic solvents. Thus synthesised nanoparticles are more stable for a longer time than the chemically produced nanoparticles.[96] The biological synthesis of AgNPs using some microorganisms are listed below in table 1.2.

Table 1.2: Biological synthesis of AgNPs using some important microorganisms.

Biological material	AgNPs Size (nm)	Microorganism/plant variety used for AgNPs synthesis(scientific name)	References
Bacteria	10-15	*Rhodococcus spp.*	107
	28-122	*E.coli*	108
	38-85	*Ochrobactrum anhtropi*	109
	41-68	*Bacillus brevis*	110
	5-50	*Bacillus subtilis*	96
	44–143	*Bacillus thuringiensis*	111
	8.1–91	*Pantoea ananatis*	112
	105	*Bacillus mojavensis*	113
	12-61	*Bacillus flexus*	114

Fungi	1-20	*Aspergillus terreus*	102
	8-50	*Pleurotus ostreatus*	115
	10,50	*Penicillium fellutanum*	116
	14,25	*Penicillium expansum*	117
	25-50	*Bryophilous rhizoctoni*	118
	1-2	*Spirulina platensis*	103
	17-33	*Helminthosporium tetramera*	104
	5-50	*Trichoderma reesei*	119
	10-60	*Bipolaris nodulosa*	120
	10-60	*Fusarium semitectum*	121
	5-40	*Fusarium acuminatum*	122
	5-25	*Asperigullus fumigates*	123
	27-79	*Alternaria alternata*	124

1.2.2.4. Green synthesis of Silver Nanoparticles (AgNPs)

The green synthesis represents itself as a critical process and proving its potential at the top. The green synthesis of nanoparticles is advantageous over chemical and physical methods because green synthesis is cost-effective, environment friendly and can be easily scaled up for large-scale synthesis. Moreover, there is no need to use high temperature, energy, pressure and toxic chemicals.[125] It is the best for the synthesis of nanoparticles, being free from toxic chemicals as well as providing natural capping agents for the stabilization of silver nanoparticles. The green synthesis of nanoparticles using plant extracts and agricultural wastes is also advantageous over the biological synthesis using microorganisms. Because, it reduces the cost of microorganisms isolation and their culture media and hence green synthesis of nanoparticles increases the cost-competitive feasibility over the synthesis by microbes.[2,126] Thus, the advancement of green synthesis of nanoparticles is succeeding as a key branch of nanotechnology, where the use of biological entities like microorganisms, plant extract or plant biomass for the production of nanoparticles could be an alternative to chemical and physical methods in an eco-friendly manner.[127] Thus, green synthesis methods are also known as environment-friendly synthesis as it does not pollute the environment with hazardous chemicals.

A natural reducing agent and silver nitrate are the basic requirements for the green synthesis of AgNPs.[128] In the green synthesis, the need for any external agents as stabilizers or capping

agents is minimized.[129] Natural resources, especially the plant resources are considered as more susceptible and efficient for the synthesis of AgNPs compared to that using microorganisms. Green synthesis is devoid of steps of cell culture and are less bio-threatening.[130] Therefore, the rich biodiversity of plants and their various parts with potential secondary metabolites are used in recent times widely to synthesize varieties of nanoparticles.[131] Plant extracts contain abundant phytochemicals such as alkaloids, flavonoids, saponins, steroids, tannins, phenols and other nutritional compounds. They act as bioreductant in the synthesis process as well as they stabilize the produced nanomaterials. Table 1.3 represents some of the plant varieties that are used for the AgNPs synthesis. These plants are eco-friendly, readily available and also give a high yield of nanoparticles. These plants consist of a wide variety of metabolites that helps in the reduction of silver ions and are also less time consuming for the synthesis of AgNP.

Table 1.3: Green synthesis of silver nanoparticles using various plant species/Microorganism.

Microorganism/plant variety used for AgNPs synthesis(scientific name)	**AgNPs Size (nm)**	**References**
Wild kund flower (*Jasminum nervosum*)	9	132
Japanese mugwort (*Artemisia princeps*)	10–40	133
Arabian coffee (*Coffea Arabica*)	20, 30	134
Mature Tea Tree (*Cassia auriculata*)	20	135
Coral vine (*Antigonon leptopus*)	10-60	136
European ash (*Fraxinus excelsior*)	25-40	137
False daisy (*Eclipta prostrata*)	34	138
Sarang semut (*Myrmecodia pendans*)	10-20	139
Teak (*Tectona grandis*)	30-40	140
Java plum (*Syzygium cumini*)	10-15	141
Ja-Kharia (*Rhynchotechum ellipticum*)	51-73	142
Pummelo (*Citrus maxima*)	2.5-5.7	143
Salparni (*Desmodium gangeticum*)	18-39	144
Yellow oleander (*Thevetia peruviana*)	10-30	145
Tomato (*Lycopersicon esculentum Mill*)	30-40	146
Pepper vines (*Piper pedicellatum*)	2-3	147
Indian pennywort (*Centella asiatica L.*)	30-50	148
Indian frankincense (*Boswellia serrata*)	40	149
Neem leaf (*Azadirachta indica) and triphala*	43-59	150

Krishna tulsi leaf (*Ocimum sanctum*)	40-50	151
Peppermint (*Mentha piperita*)	90	152
Curry leaf (*Murraya koenigii*)	10-25	153
Madras Leaf flower (*Phyllanthus maderaspatensis*)	59	154

1.3. Applications of AgNPs

AgNPs are one of the most attractive nanomaterials for various industrial and commercial applications. AgNPs exhibit advantageous property over other metallic nanoparticles due to their catalytic effects, chemical stability and their antibacterial, antiviral, antifungal, anticancer and anti-inflammatory activities. AgNPs also find industrial applications in electronic products and as antimicrobial agents. Figure 1.6 represents the various applications of AgNPs.

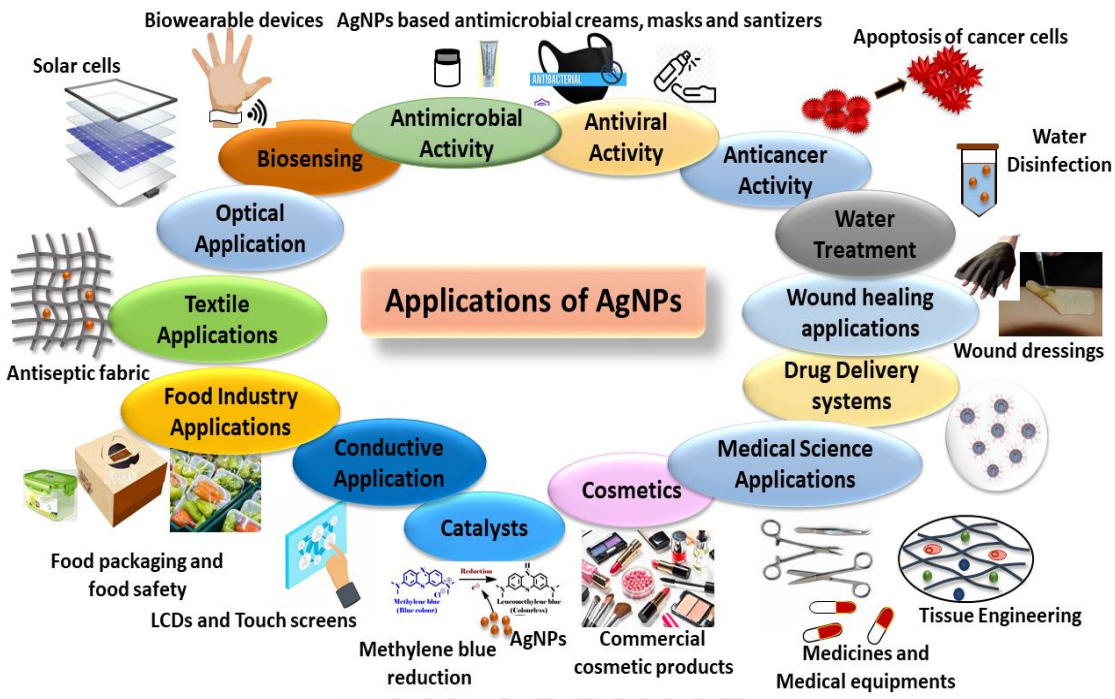

Figure 1.6: Various applications of AgNPs.

1.3.1. Antimicrobial AgNPs

The size of nanoparticle, concentration and shape determine the antimicrobial efficacy. AgNPs show broad antibacterial effect on a wide range of gram-positive and gram-negative bacteria and on antibiotic-resistant bacterial strains. The antibacterial effect of AgNPs is mainly due to the formation of free radical on the surface that penetrates the bacterial cell membrane, thus, perturb the intracellular processes in bacteris.[155] The study of bactericidal ability of

AgNPs against *E.coli* revealed that the AgNPs accumulated in the bacterial cell wall forming pits generate free radicals which damages the bacterial cell and results in the death of the bacteria.[156] It is also reported that the damage of the bacteria may be due to the release of silver ions from the AgNPs which react with the thiol group of cysteine in the bacterial proteins/crucial enzymes inhibiting the metabolic enzymes within the bacteria. This event occurs either by replacing the silver ions with other metal ions that bind with the cysteine or via bond formation between the silver ions and cysteine residues in the peptide, resulting in bacterial death. It is also known that the smaller-sized AgNPs have a higher bactericidal effect compared to their larger counter parts. This is due to the fact that the smaller AgNPs can release silver ions from their surface easily and hence shows much higher antibacterial activity.[157,158] Although silver ions showed a strong microbicidal activity against prokaryotic cells, the activity against gram-positive bacteria is poor due to the thicker cell wall. Silver ions do not reach the cell membrane as they get trapped in the cell wall due to their stronger affinity with the peptidoglycan layer present in the cell wall of the gram-positive bacteria.[159]

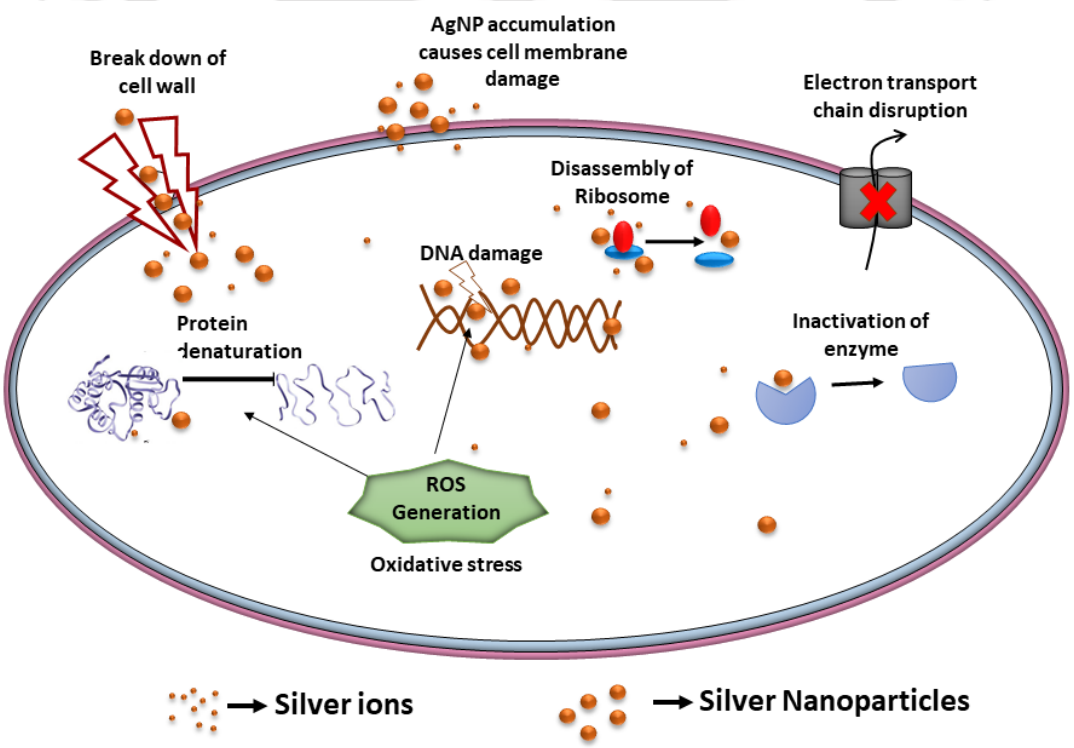

Figure: 1.7: The various antimicrobial mode of action of AgNPs(Diagram adapted from Roy *et al.*, 2019).

The different environmental factors like high temperatures, thiol groups, proteins carrying oxygen, and the presence of chlorine influence the presence of silver ions' and finally influence

the microbial activity of AgNPs.[156] Shape dependent antimicrobial activity of different nanosilver such as silver nanorods, silver nanoparticles, and silver nanoplates against *S. aureus* and *E. coli* has also been reported. Among these, silver nanoplates had the best antimicrobial activity.[160] In figure 1.7, the various modes of antibacterial action of AgNPs is described which include the various distinct mechanisms such as- (i) cell wall and cell membrane damage, (ii) penetration of AgNPs inside the cell and intracellular structures and biomolecules damage, e.g., DNA, protein, ribosomes damage, etc., and (iii) cellular toxicity and generation of Reactive Oxygen Species(ROS) causing oxidative stress. AgNPs also modulate the human cell's immune system by creating an inflammatory response, resulting in microorganism inhibition.[161,162]

1.3.2. Antiviral AgNPs

When a virus's nucleic acids enter into a host and replication occurs, viral infection is established. AgNPs can act on the surface of the virus and inhibit interaction with the host cells physically.[163,164] Studies show that AgNPs are vital for causing antiviral effects similar to their antibacterial activities. AgNPs of ≤ 25nm in size are effective against arenavirus[165] and 7-20 nm sized AgNPs have antiviral activities against herpes simplex virus(HSV)types ½ as well as for human parainfluenza virus type-3.[166] AgNPs are also observed to adhere to the envelope of the human immunodeficiency virus(HIV) and inhibit cell infection.[167] AgNPs with a size ≤ 10 nm are effective against influenza virus.[168,169] Further, AgNPs with 10 nm size is known to prevents Monkey pox virus(MPV).[170] In general, with increasing nanoparticle diameter, the antiviral effect decreases and larger AgNPs encourage the increase of the plaque-forming unit(PFU) mean number of MPV compared to controls samples. This may be due to the nanoparticle agglomeration, which helps the interaction of virus particles with the host cells, resulting in PFU increases. So the AgNPs particle size is a significant factor that influences the nanoparticles' antiviral properties.[20] Due to the limited antifungal arsenal, researchers have sought to improve treatment via different approaches, as such nanoparticles aids as antifungal activity carriers. If the reducing agent has antifungal activity, it serves as a capping agent as it deposits over the nanoparticle surface; this leads to synergistic antifungal activities. Biogenic silver can be used for the preparation of antifungal drug delivery systems.[162] Spherical AgNPs of 9.8 nm sized were synthesized by using Delftia sp. strain KCM-006. Then, the antifungal miconazole drug was conjugated to the biogenic AgNPs surface. This conjugation revealed a substantial fungicidal effect, ROS level increase causing inhibition of biofilm and ergosterol biosynthesis.[171] Green synthesized AgNPs are also effective against plant pathogenic fungi *Magnaporthe grisea* and *Biopolaris sorokiniana* by applying ionic silver and nanosilver in

vitro.[172] Hyphae and conidia of *Botrytis cinerea* and *Alternaria alternata* fungi are damaged when green synthesized AgNPs are applied.[173] Other plant pathogenic fungi such as *Fusarium oxysporum, Penicillium expansum, Fusarium graminearum* and *Fusarium solani* also get damaged due to AgNP's strong synergistic activity. There are more antifungal activities of AgNPs which are reported by several researchers.[174–176]

1.3.3. Antifungal AgNPs

Numerous studies have reported on the antifungal activities of AgNPs, along with their antibacterial activities. AgNPs exhibit good antifungal characteristics against many fungal species and thus can be effectively used as an antifungal agent.[69] In case of fungi, silver ions and AgNPs has a significant inhibition effect on the microbial colony formation, mycelium growth, spore germination, germ tube development and mycotoxin production. Antifungal activity is attributed by the smaller size to large surface ratio of AgNPs. Smaller sized AgNPs can easily penetrate through the cell boundaries. The toxicity of AgNPs is partially due to the reactive oxygen species(ROS) production which finally leads to apoptosis. As for examples, AgNPs shows good antifungal activity against certain fungal strains like *Candida albicans, Trichophyton mentagrophytes, Aspergillus* and *Saccharomyces*[177,178]. A Tollens process of evaluation has shown the antifungal activity of the AgNPs against Candida sp., which is a common pathogen, by determining its minimum inhibitory concentration(MIC), minimum fungicidal concentration (MFC) and also yeast growth inhibition (time-dependent). AgNPs inhibit the growth of the specific yeasts at lower concentrations (below the cytotoxic limit) against specific human fibroblasts on AgNPs concentration of 30mg/L.[179] Yeast isolated from bovine mastitis are also inhibited by AgNPs of diameter around 13.5 nm.[180]

1.3.4. Anticancer AgNPs

AgNPs have many biomedical applications as they have shown good potential as an antitumor agent by numerous mechanisms. These mechanisms involve oxidative stress, DNA damage, cell cycle arrest, necrosis or apoptosis.[181] Autophagy inhibition enhances the anticancer activity of AgNPs, which revealed a novel biological activity of AgNPs in the production of cytoprotective autophagy. Also, autophagy inhibition may increase AgNP's efficacy in antitumor therapy.[182] AgNPs synthesized from *Acalypha indica* showed 40% cell inhibition against human breast cancer cells(MDA-MB-231).[183] AgNPs produced by *Dendrophthoe falcate* cause loss of 50% viability of MCF-7 cells.[184] Again, AgNPs prepared using *Sterculia foetida* seed extracts showed cellular DNA fragmentation against HeLa cancer

cell lines.[185] *Datura inoxia*-AgNPs inhibited about 50% proliferation of human breast cancer cell line MCF7 by suppressing its growth and reducing the DNA synthesis to cause apoptosis.[186] Again, AgNPs synthesized using *Origanum vulgare* showed a dose-dependent response when tested against lung cancer cell line A549.[187] Thus, 95% apoptosis was reported for prostate cancer cells (PC3) and 99% growth inhibition for breast cancer cells(MCF-7) by the AgNPs using 25 µl/mL doses of *Alternanthera sessilis*.[188] AgNPs synthesized using 100 µg of *Morinda citrifolia* roots showed 100% cell death when treated with the HeLa cell line.[189] AgNPs produced using *Aloe*, *Eucalyptus* and *Magnolia* Leaf extracts(2-4 ppm concentration) are found to be non-cytotoxic to human embryonic kidney 293 cells.[190] Cytotoxic activity was sensitive to the nanoparticle sizes, and the cell viability was dependent on the dosages.[191,192] Further, AgNPs also act as a biocompatible vehicle for the nanosilver transportation to the human lung carcinoma cells (A549).[193] Aloe vera conjugated-AgNPs, when treated with human dermal fibroblasts(HDF) cells, showed no cytotoxicity; but possessed excellent antibacterial activity on E.Coli even at low concentrations.[194]

1.3.5. Bacterial Disinfection of Water by AgNPs

Compared to bulk silver, AgNPs have a long-lasting and cost-effective approach with a controlled release rate of silver ions. AgNPs play a vital role in water disinfection, in food industry, and other disinfection-related applications. Ordinary tap water consists of a hazardous level of minerals, microbes or pesticides. So water purification is necessary for drinking or any other purposes. In this respect, AgNPs incorporated in water filtration systems find wide applications for purifying drinking water.[195] AgNPs are generally incorporated into water filtrations to prevent membrane filter's bacterial fouling.[196–198] Again, AgNPs have been utilized for impregnation with paper for testing bacteria(*Escherichia coli* and *Enterococcus faecalis*) inactivation and silver leaching for point-of-use water treatment. AgNPs showed antibacterial properties against bacterial suspensions.[199] AgNPs synthesized using fresh leaf bud extract of *Anacardium occidentale* at 80°C have been utilized for sensing Chromium ions[Cr(VI)] contamination in tap water.[200] The bacterial disinfection of sewage by AgNPs is also reported. Thus, the AgNPs synthesized using leaf extract of *Prosopis juliflora* when treated with sewage, a decrease of the bacterial population was observed, which again was more prominent as the concentration and incubation time increased.[201] Thus, contaminated water can be disinfected by effective green synthesized AgNPs and AgNPs incorporated filters or composites.

1.3.6. Applications of AgNPs in Medical Science

The applications of AgNPs in the medical sector is divided into two types; diagnostic and therapeutic applications. AgNPs based Surface Enhanced Raman Spectroscopy(SERS) can help in non-invasive cancer detection.[202] Some of the significant applications of AgNPs in medical sciences are in wound dressing, eye treatment, dental hygiene,[203] scaffolds and biomaterials for bone substitutes.[8] Some of the crucial applications of AgNPs recently studied are diagnostic imaging, cancer therapy and diagnosis, biosensing and drug delivery vehicles.[204,205] The plasmonic nature of AgNPs can destroy unwanted cells by absorbing light leading to thermal ablation of the targeted cells.[206] Disinfectant products based on AgNPs are beneficial as a cure for environmental or disease-causing pathogens.[204]

The strong and broad-spectrum microbial activity of AgNPs help protects the health care workers from contact infection and various infectious diseases. To prevent contact infection, the health workers wear protective clothing. These protective clothing can be developed using AgNPs-chitin sheet conjugate embedded with a fibre-like surface structure of clothing.[207,208] These chitin nanofiber sheets (CNFS) exhibit anti-infectious activity and biochemical activities for angiogenesis or wound repair and stabilizes or activates the growth factors.[209,210] AgNPs incorporated with central venous catheters (CVC) surgical meshes are found less infective in bloodstream.[211] The development of devices with antibacterial properties and improvement of catheters coated with AgNPs mainly to reduce toxicity to microorganisms are advancing rapidly.[212–214] Urinary catheters coated with AgNPs are very much effective to suppress bacterial infections. These catheters exhibit hydrophilic properties and prevent the accumulation of protein and electrolytes results in a reduction in biofilm formation.[215]

1.3.7. AgNPs in Wound Dressings Materials

The human body skin is susceptible to numerous injuries and stimuli and produces wounds. Dressing of such wounds needs antimicrobial wound dressing materials. Such wound dressings are mainly used to prevent the wound area from bacterial infection and keep a moist environment around the wound. Thus, the development of wound dressings with antibacterial activity has been recently studied primarily regarding the resistant bacteria due to recurrent use of antibiotics.[216] The AgNPs release silver ions, which is the primary origin of the antibacterial property of AgNPs. This property is exploited for the preparation of AgNPs-coated wound dressings materials.[217] AgNPs also improves collagen alignment after wound healing. One example of commercial wound dressing is Acticoat made up of polyamide ester membrane

coated with AgNPs.[218] Incorporating AgNPs at the surface of wound dressings increases antibacterial properties and provides superior biocompatibility and better efficacy after wound healing.[219] Thus, *in vitro* analysis of an AgNPs based dressing, Acticoat Flex 3, showed reduced mitochondrial activity when applied to a 3D fibroblast cell culture and a burn wound.[220] During skin wound healing, wound inflammation reduces with modulation in kidney and liver functions mainly due to the antimicrobial properties of AgNPs.[221] AgNPs incorporated on cotton fabric, and dressings lead to a significant decrease in wound healing within 3-4 days, and bacterial clearance increased from the infected wounds without any adverse effects.[222]

In wound dressing material research, hydrogels are proven as excellent wound dressing materials that offer a moist environment to the wound and absorb the excess exudates of the injury. They are prepared using synthetic and natural polymers or composites helpful in controlled drug and protein delivery, regenerative medicine, and tissue engineering.[223] As such, polymer-based hydrogel dressings with antimicrobial properties are of much importance in medicine.[224,225] Especially with improved sterility and longevity of the wound dressing materials reduce the frequent change of dressings in the wound sites.[226] When AgNPs are incorporated into polymer blends, it increases stability and functionality.[101,226] AgNPs helps in faster healing of the wound, reduces scars and cause no inflammation when used in a dose-dependent manner; it reduces infections caused by bacteria. Hydrogels conjugated with AgNPs derived using *Arnebia nobilis* root extract reported exhibiting wound healing activity in the excision animal model providing a novel therapeutic direction for wound treatment in the healthcare sector.[41]

1.3.8. AgNPs in Catalysis

Nanocatalysis is a domain at the interface between heterogeneous and homogenous catalysis, offering distinctive solutions for improvement in catalysis processes.[227] Metallic nanoparticles have high catalytic activities for many chemical reactions; during catalytic processes, AgNPs would congregate. Due to the activation of the nanosized metal particles in the solution, they are prone to merge for the weak van der Waals forces and high surface energy. Metal catalysts are stabilized by surface modifications using polymers, surfactants and complex ligands.[228] The sodium borohydride mediated synthesis of highly monodispersed and spherical AgNPs coated with sodium citrate has been reported to demonstrate the efficient catalytic reduction of Rhodamine B.[229] The sodium borohydride mediated reduction of

Methylene blue(MB) is enhanced in the presence of AgNPs.[230] The AgNPs synthesized using a pod of *Acacia nilotica* with a modified glassy carbon electrode showed higher catalytic activity in the benzyl chloride reduction. *Ulva lactuca* mediated synthesized AgNPs helped in the photocatalytic degradation of methyl orange unpon visible light illumination.[231] AgNPs produced using Triticum aestivum extract aided in the reduction of hydrogen peroxide with excellent catalytic activity.[232] AgNPs find wide industrial applications for catalysis.[233]

1.3.9. AgNPs in Solar Cell/Photovoltaic Devices

The solar cell fabrication industry uses nanoscale properties of AgNPs, which improves the light trapping activities of the silicon solar cells. When AgNPs are composed of a dielectric material, surface plasmon excitation occurs with a combined surface charge and electromagnetic wave character. This is because AgNPs scatter lights, and then that light is collected between the AgNPs and dielectric thin films.[234] Another study reported that reflectance reduction of 11-13% was observed when two different thicknesses of silver thin films made of AgNPs were annealed at different temperatures for a specific period under vacuum conditions.This is mainly due to the plasmonic effect and the solar cell conversion efficiency enhancement.[235] The use of thin polymer films for enhancing the light trapping and environment coupling efficiency in organic photovoltaic devices is a great challenge. But, the surface plasmon resonance effect of AgNPs, mechanical flexibility and the high surface area of the nanofibers enhance energy harvesting. Hence, using the thin layer of the hybrid material of AgNPs and PVP nanofibers in organic solar cells, power conversion efficiency increases by 18.9%(PCE).[234,236]

1.3.10. AgNPs in Fabrication of Biosensor

AgNPs are highly feasible and efficient for numerous biosensor fabrication research. A nanoenzymatic glucose biosensor is developed by the in situ chemical reduction method by depositing AgNPs on TiO_2 nanotubes synthesized by an anodic oxidation process. AgNPs of length and diameter about 1.2 µm and 120 nm was attached inside and outside the TiO_2 nanotubes. Its composition was mainly fabricated as an electrode of a nonenzymatic biosensor for glucose oxidation. Due to the excellent selectivity, repeatability and stability of the nanoenzymatic glucose biosensors, they have potential application in sensor areas and catalysis.[237] Oligonucleotide- AgNPs composite conjugated with magnetic beads have also been reported as a biosensor for *E.coli* detection. It detects the presence of DNA targets with high efficiency, and the best detection signal achieved was up to 1.3ng/µl.[238] AgNPs

synthesized via the chemical reduction method could be used in SPR biosensors as an active ingredient.[239] Again, an enzymatic biosensor using AgNPs was developed for selective detection of penicillin.[240] Also, protein sensing studies could use AgNPs labelling by liquid electrode plasma-atomic emission spectrometry. On-site portable analysis was suitable with this technique; this detection method could have a considerable variety with favourable applications in nanoparticle-labelled biomolecule detection.[241]

1.3.11. AgNPs in Ink-Jet Printing

AgNPs are also found applications in ink-jet printing. As an example, AgNPs synthesised via the chemical reduction method using trimethylamine was utilised for the preparation of thin film which. After that, the film was treated with UVO-100 UV ozone for about 30 mins. Spin coating of the AgNPs suspensions (500 rpm, 15s) was carried out on the polyimide substrate and dried at room temperature for removing the solvent. The synthesized AgNPs was used to fabricate flexible electronics for developing ink-jet printing.[242]

1.3.12. AgNPs in Food Packaging Materials

For extension of food shelf life and reduction of the risk of pathogens, AgNPs coated antimicrobial packing seems to be a promising as active food packaging material.[243] The addition of AgNPs into polymeric matrics significantly influences the film permeability, ultimately influencing the product quality. Some of the common non-degradable polymers used to host AgNPs for food packaging are polyethylene (PE),[244] ethylene vinyl alcohol (EVOH) and polyvinyl chloride (PVC). The packaging materials based on low-density polyethylene (LDPE) incorporated with ZnO nanoparticles/AgNPs are used to preserve and extend the shelf life of orange juice.[245] Biodegradable polymeric films are a better alternative currently in food packaging sectors as they can be obtained from renewable sources at a low cost without contributing to environmental pollution. Mostly used edible biodegradable polymer in packaging is polysaccharides. The most commonly used polysaccharides in food packaging are cellulose,[246,247] pullulan,[248] starch,[249] chitosan[243] and agarose.[250] Moreover, AgNPs are incorporated into a hydroxypropyl methylcellulose (HPMC) matrix for food packaging applications. Such materials showed good antibacterial properties against *S. aureus* and *E.coli*.[251] When incorporated with AgNPs and essential oils, edible pullulan films aided in meat preservation and showed good antimicrobial activity.[248,252] When AgNPs were combined with the edible packaging materials and stabilizing agents like sodium alginate, it created biopolymer matrix films for food packaging. AgNPs incorporated sodium alginate films

reported in reduction of fruit and vegetable decay rate.[253] Along with the food packaging studies, the migration of silver from different types of nanocomposites into food simulants was also reported.[254]

1.3.13. Other Applications of AgNPs

AgNPs also find applications in agriculture, marine, plant nutrition and defence against diseases.[255] Plant productivity can be enhanced by the use of intelligent plant sensors with actuating electronic devices. These nanosensors optimize and automate agrochemical and water allocation; it also enables plant chemical phenotyping.[10] AgNPs can be delivered with pesticides to the crops to increase crop production.[255] AgNPs also have effective larvicidal and antifouling properties, which can be effectively used in agriculture and marine pest control.[256]

AgNPs, when synthesized in a polymer solution by a one-step method, produces AgNP/polymer nano paint. This AgNPs embedded drying oil acts as a suitable coating material for wood, polystyrene, and glass.[257] AgNPs are used as a silver paste in electrodes due to their high conductivity. In electronically conductive adhesives (ECAs), AgNPs are used as conductive fillers.[258] Unlike pigments and dyes, AgNPs are efficient at absorbing and scattering light. It also has a colour that mainly depends on the shape and size of the particles. AgNPs are popularly used as functional components in various optical sensors and products.[28]

1.4. IMPORTANCE AND FUTURE SCOPES

This chapter provides an overview of all the different resources for the synthesis of AgNPs. Reducing agents such as borohydride or hydrazine can be hazardous and may lead to the formation of toxic by-products and finally deteriorate the environment. Thus, the traditional techniques for synthesizing AgNPs require a massive amount of energy and chemicals that are pretty hazardous. Out of various available methods and processes for synthesizing AgNPs, green synthesis is preferred over conventional methodologies due to environmental concerns. Thus, using various components such as polyphenols from plant extracts, polymers, enzymes, bacteria, and agricultural wastes under favourable conditions might lead to the sustainable synthesis of uniform-sized AgNPs. When plants and their excerpts are used instead of other sources such as fungi and bacteria, the AgNPs synthesis becomes more accessible, faster and cost-effective. The green methodology for AgNPs synthesis using renewable materials is quite a promising method as it involves non-toxic chemicals for silver salt reduction. Metallic nanoparticles act as a novel bioactive functional agent due to their high surface area to volume

ratio and numerous optical, magnetic, chemical, and physical properties. AgNPs with these unique properties has proven to be a better alternative for developing new antimicrobial agents. AgNPs have the most diversified applications includes antibacterial, antifungal, anticancer, antiviral activities, etc. Due to their various characteristics, AgNPs are highly feasible for use in water treatment, biosensor fabrication, development of catalysis and optical devices, drug delivery systems, biomedicine and medical care, food packaging industries, etc. Currently, nanotechnology has opened new possibilities in all sectors, especially in medicine and for the treatment of various diseases. Considering the environmental issues and vast potential applications, the research of AgNPs should be towards greener synthesis and development of size and shape-controlled nanoparticles. Also, AgNPs would be utilized towards the development of anticancer and antimicrobial nanomedicine, wearable intelligent equipment, and other novel nanocomposites/nanodevices for a wide scope of applications. Therefore, AgNPs can be a lead nanoparticle of the future with a wide range of applications.

1.5. REFERENCES

(1) Saini, R.; Saini, S.; Sharma, S. Nanotechnology: The Future Medicine. *J. Cutan. Aesthet. Surg.* **2010**, *3* (1), 32.

(2) Ahmed, T.; Bhatti, Z. A.; Maqbool, F.; Mahmood, Q.; Faridullah; Qayyum, S.; Mushtaq, N. A Comparative Study of Synthetic and Natural Coagulants for Silver Nanoparticles Removal from Wastewater. *Desalin. Water Treat.* **2016**, *57* (40), 18718–18723.

(3) Jeevanandam, J.; Barhoum, A.; Chan, Y. S.; Dufresne, A.; Danquah, M. K. Review on Nanoparticles and Nanostructured Materials: History, Sources, Toxicity and Regulations. *Beilstein J. Nanotechnol.* **2018**, *9* (1), 1050–1074.

(4) Joob, B.; Wiwanitkit, V. Nanotechnology for Health: A New Useful Technology in Medicine. *J Med J DY Patil Univ* **2017**, *10*, 401–405.

(5) Khalil, K. A.; Fouad, H.; Elsarnagawy, T.; Almajhdi, F. N. Preparation and Characterization of Electrospun PLGA / Silver Composite Nanofibers for Biomedical Applications. *Int. J. Electrochem. Sci.* **2013**, *8*, 3483–3493.

(6) Ankanna, S.; Prasad, T. N. V. K. V.; Elumalai, E. K.; Savithramma, N. Production of Biogenic Silver Nanoparticles Using Boswellia Ovalifoliolata Stem Bark. *Dig. J. Nanomater. Biostructures* **2010**, *5* (2), 369–372.

(7) Prabhu, S.; Poulose, E. K. Silver Nanoparticles: Mechanism of Antimicrobial Action, Synthesis, Medical Applications, and Toxicity Effects. *Int. Nano Lett.* **2012**, *2* (32), 2228–5326.

(8) Nurani, S. J.; Saha, K. C.; Rahman Khan, M. A.; Sunny, S. M. H. Silver Nanoparticles Synthesis, Properties, Applications and Future Perspectives: A Short Review. *IOSR J. Electr. Electron. Eng. Ver. I* **2015**, *10* (6), 117–126.

(9) Searle, A. B. *The Use of Metal Colloids in Health and Disease*; Constable & Company Ltd: London, 1920.

(10) Tarannum, N.; Divya; Gautam, Y. K. Facile Green Synthesis and Applications of Silver Nanoparticles: A State-of-the-Art Review. *RSC Adv.* **2019**, *9* (60), 34926–34948.

(11) Grunlan JC, C. J. Antimicrobial Behavior of Polyelectrolyte Multilayer Films Containing Cetrimide and Silver. *Biomacromolecules* **2005**, *6*, 1149.

(12) Dastjerdi, R.; Montazer, M. A Review on the Application of Inorganic Nano-Structured Materials in the Modification of Textiles: Focus on Anti-Microbial Properties. *Colloids Surf. B. Biointerfaces* **2010**, *79* (1), 5–18.

(13) Harrasser, N.; Jüssen, S.; Obermeir, A.; Kmeth, R.; Stritzker, B.; Gollwitzer, H.; Burgkart, R. Antibacterial Potency of Different Deposition Methods of Silver and Copper Containing Diamond-like Carbon Coated Polyethylene. *Biomater. Res.* **2016**, *20*, 17.

(14) Jain, J.; Arora, S.; Rajwade, J. M.; Omray, P.; Khandelwal, S.; Paknikar, K. M. Silver Nanoparticles in Therapeutics: Development of an Antimicrobial Gel Formulation for Topical Use. *Mol. Pharm.* **2009**, *6* (5), 1388–1401.

(15) De, M.; Ghosh, P. S.; Rotello, V. M. Applications of Nanoparticles in Biology. *Adv. Mater.* **2008**, *20* (22), 4225–4241.

(16) Sharma, V. K.; Yngard, R. A.; Lin, Y. Silver Nanoparticles: Green Synthesis and Their Antimicrobial Activities. *Advances in Colloid and Interface Science*. Netherlands January 2009, pp 83–96.

(17) Ahamed, M.; Alsalhi, M. S.; Siddiqui, M. K. J. Silver Nanoparticle Applications and Human Health. *Clin. Chim. Acta.* **2010**, *411* (23–24), 1841–1848.

(18) Kim, D.; Jeong, S.; Moon, J. Synthesis of Silver Nanoparticles Using the Polyol Process and the Influence of Precursor Injection. *Nanotechnology* **2006**, *17* (16), 4019–4024.

(19) Tran, Q. H.; Nguyen, V. Q.; Le, A.-T. Silver Nanoparticles: Synthesis, Properties, Toxicology, Applications and Perspectives. *Adv. Nat. Sci. Nanosci. Nanotechnol.* **2013**, *4* (3), 33001.

(20) Nakamura, S.; Sato, M.; Sato, Y.; Ando, N.; Takayama, T.; Fujita, M.; Ishihara, M. Synthesis and Application of Silver Nanoparticles (AgNPs) for the Prevention of Infection in Healthcare Workers. *Int. J. Mol. Sci.* **2019**, *20* (15), 3620.

(21) Elghanian, R.; Storhoff, J. J.; Mucic, R. C.; Letsinger, R. L.; Mirkin, C. A. Selective Colorimetric Detection of Polynucleotides Based on the Distance-Dependent Optical Properties of Gold Nanoparticles. *Science* **1997**, *277* (5329), 1078–1081.

(22) Hurst, S. J.; Lytton-Jean, A. K. R.; Mirkin, C. A. Maximizing DNA Loading on a Range of Gold Nanoparticle Sizes. *Anal. Chem.* **2006**, *78* (24), 8313–8318.

(23) Daniel, M.-C.; Astruc, D. Gold Nanoparticles: Assembly, Supramolecular Chemistry, Quantum-Size-Related Properties, and Applications toward Biology, Catalysis, and Nanotechnology. *Chem. Rev.* **2004**, *104* (1), 293–346.

(24) Prathna, T. C.; Chandrasekaran, N.; Raichur, A. M.; Mukherjee, A. Kinetic Evolution Studies of Silver Nanoparticles in a Bio-Based Green Synthesis Process. *Colloids Surfaces A Physicochem. Eng. Asp.* **2011**, *377* (1), 212–216.

(25) Samberg, M. E.; Oldenburg, S. J.; Monteiro-Riviere, N. A. Evaluation of Silver Nanoparticle Toxicity in Skin in Vivo and Keratinocytes in Vitro. *Environ. Health Perspect.* **2010**, *118* (3), 407–413.

(26) Sintubin, L.; De Gusseme, B.; Van der Meeren, P.; Pycke, B. F. G.; Verstraete, W.; Boon, N. The Antibacterial Activity of Biogenic Silver and Its Mode of Action. *Appl. Microbiol. Biotechnol.* **2011**, *91* (1), 153–162.

(27) Vijay Kumar, P. P. N.; Satyanarayana, K. V. V; Kollu, P.; Pammi, S. V. N.; Shameem, U. Green Synthesis and Characterization of Silver Nanoparticles Using *Boerhaavia diffusa* Plant Extract and Their Anti Bacterial Activity. *Ind. Crop. Prod.* **2014**, *52*, 562–566.

(28) Yusuf, M. Silver Nanoparticles: Synthesis and Applications. In *Handbook of Ecomaterials*; 2019; pp 2343–2356.

(29) Chou, K. Sen; Lai, Y. S. Effect of Polyvinyl Pyrrolidone Molecular Weights on the Formation of Nanosized Silver Colloids. *Mater. Chem. Phys.* **2004**, *83* (1), 82–88.

(30) Chou, K.-S.; Lu, Y.-C.; Lee, H.-H. Effect of Alkaline Ion on the Mechanism and Kinetics of Chemical Reduction of Silver. *Mater. Chem. Phys.* **2005**, *94* (2), 429–433.

(31) Yoosaf, K.; Ipe, B. I.; Suresh, C. H.; Thomas, K. G. In Situ Synthesis of Metal Nanoparticles and Selective Naked-Eye Detection of Lead Ions from Aqueous Media. *J. Phys. Chem. C* **2007**, *111* (34), 12839–12847.

(32) Tolaymat, T. M.; El Badawy, A. M.; Genaidy, A.; Scheckel, K. G.; Luxton, T. P.; Suidan, M. An Evidence-Based Environmental Perspective of Manufactured Silver Nanoparticle in Syntheses and Applications: A Systematic Review and Critical Appraisal of Peer-Reviewed Scientific Papers. *Sci. Total Environ.* **2010**, *408* (5), 999–

1006.

(33) Creighton, J. A.; Blatchford, C. G.; Albrecht, M. G. Plasma Resonance Enhancement of Raman Scattering by Pyridine Adsorbed on Silver or Gold Sol Particles of Size Comparable to the Excitation Wavelength. *J. Chem. Soc. Faraday Trans. 2 Mol. Chem. Phys.* **1979**, *75* (0), 790–798.

(34) Shi, Y.; Lv, L.; Wang, H. A Facile Approach to Synthesize Silver Nanorods Capped with Sodium Tripolyphosphate. *Mater. Lett.* **2009**, *63* (30), 2698–2700.

(35) Sui, Z.; Chen, X.; Wang, L.; Chai, Y.; Yang, C.; Zhao, J. An Improved Approach for Synthesis of Positively Charged Silver Nanoparticles. *Chem. Lett.* **2004**, *34* (1), 100–101.

(36) Horiuchi, Y.; Shimada, M.; Kamegawa, T.; Mori, K.; Yamashita, H. Size-Controlled Synthesis of Silver Nanoparticles on Ti-Containing Mesoporous Silica Thin Film and Photoluminescence Enhancement of Rhodamine 6G Dyes by Surface Plasmon Resonance. *J. Mater. Chem.* **2009**, *19* (37), 6745–6749.

(37) Zielińska, A.; Skwarek, E.; Zaleska, A.; Gazda, M.; Hupka, J. Preparation of Silver Nanoparticles with Controlled Particle Size. *Procedia Chem.* **2009**, *1* (2), 1560–1566.

(38) Henglein, A.; Giersig, M. Formation of Colloidal Silver Nanoparticles: Capping Action of Citrate. *J. Phys. Chem. B* **1999**, *103* (44), 9533–9539.

(39) Pietrobon, B.; Kitaev, V. Photochemical Synthesis of Monodisperse Size-Controlled Silver Decahedral Nanoparticles and Their Remarkable Optical Properties. *Chem. Mater.* **2008**, *20* (16), 5186–5190.

(40) Sun, Y.; Xia, Y. Shape-Controlled Synthesis of Gold and Silver Nanoparticles. *Science (80).* **2002**, *298* (5601), 2176–2179.

(41) Zhang, S.; Tang, Y.; Vlahovic, B. A Review on Preparation and Applications of Silver-Containing Nanofibers. *Nanoscale Res. Lett.* **2016**, *11* (1), 1–8.

(42) Zhang, Q.; Li, N.; Goebl, J.; Lu, Z.; Yin, Y. A Systematic Study of the Synthesis of Silver Nanoplates: Is Citrate a "Magic" Reagent? *J. Am. Chem. Soc.* **2011**, *133* (46), 18931–18939.

(43) Martínez-Castañón, G. A.; Niño-Martínez, N.; Martínez-Gutierrez, F.; Martínez-Mendoza, J. R.; Ruiz, F. Synthesis and Antibacterial Activity of Silver Nanoparticles with Different Sizes. *J. Nanoparticle Res.* **2008**, *10* (8), 1343–1348.

(44) Matteis, V. De; Malvindi, M. A.; Galeone, A.; Brunetti, V.; Luca, E. De; Kote, S.; Kshirsagar, P.; Sabella, S.; Bardi, G.; Pompa, P. P. Negligible Particle-Specific Toxicity Mechanism of Silver Nanoparticles : The Role of Ag^{+} Ion Release in the Cytosol.

Nanomedicine Nanotechnology, Biol. Med. **2015**, *11* (3), 731–739.

(45) Shameli, K; Ahmad, M. B.; Yunis, W. Z.; Ibrahim, N. A.; Darroudi, M. Synthesis and Characterization of Silver/Talc Nanocomposites Using the Wet Chemical Reduction Method. *Int J Nanomedicine* **2010**, *5*, 743–751.

(46) Agnihotri, S.; Mukherji, S.; Mukherji, S. Size-Controlled Silver Nanoparticles Synthesized over the Range 5–100 nm Using the Same Protocol and Their Antibacterial Efficacy. *RSC Adv.* **2014**, *4* (8), 3974–3983.

(47) Guzmán, M. G.; Dille, J.; Godet, S. Synthesis of Silver Nanoparticles by Chemical Reduction Method and Their Antibacterial Activity. **2009**, 104–111.

(48) Pinto, V. V; José, M.; Silva, R.; Santos, H. A.; Silva, F.; Pereira, C. M. Physicochemical and Engineering Aspects Long Time Effect on the Stability of Silver Nanoparticles in Aqueous Medium : Effect of the Synthesis and Storage Conditions. *Colloids Surfaces A Physicochem. Eng. Asp.* **2010**, *364* (1–3), 19–25.

(49) Khan, S. U.; Saleh, T. A.; Wahab, A.; Khan, M. H. U.; Khan, D.; Khan, W. U.; Rahim, A.; Kamal, S.; Khan, F. U.; Fahad, S. Nanosilver: New Ageless and Versatile Biomedical Therapeutic Scaffold. *Int. J. Nanomedicine* **2018**, *13*, 733–762.

(50) Reetz, M. T.; Helbig, W. Size-Selective Synthesis of Nanostructured Transition Metal Clusters. *J. Am. Chem. Soc.* **1994**, *116* (16), 7401–7402.

(51) Rodriguez-Sanchez, L.; MC, B.; MA, L.-Q. Electrochemical Synthesis of Silver Nanoparticles. *J. Phys. Chem. B* **2000**, *104* (41), 9683–9688.

(52) Nasretdinova, G. R.; Fazleeva, R. R.; Osin, Y. N.; Gubaidullin, A. T.; Yanilkin, V. V. Methylviologen-Mediated Electrochemical Synthesis of Silver Nanoparticles via the Reduction of AgCl Nanospheres Stabilized by Cetyltrimethyl ammonium Chloride. *Russ. J. Electrochem.* **2017**, *53* (1), 25–38.

(53) Huiying, J.; Jiangbo, Z.; Wei, S.; Jing, A.; Bing, Z. Preparation of Silver Nanoparticles by Photo-Reduction for Surface-Enhanced Raman Scattering. *Thin Solid Films* **2006**, *496* (2), 281–287.

(54) Tsuji, T.; Okazaki, Y.; Tsuji, M. Photo-Induced Morphological Conversions of Silver Nanoparticles Prepared Using Laser Ablation in Water—Enhanced Morphological Conversions Using Halogen Etching. *J. Photochem. Photobiol. A Chem.* **2008**, *194* (2–3), 247–253.

(55) Kshirsagar, P.; Sangaru, S. S.; Malvindi, M. A.; Martiradonna, L.; Cingolani, R.; Pompa, P. P. Synthesis of Highly Stable Silver Nanoparticles by Photoreduction and Their Size Fractionation by Phase Transfer Method. *Colloids Surfaces A Physicochem. Eng. Asp.*

2011, *392* (1), 264–270.

(56) Jin, R.; Charles Cao, Y.; Hao, E.; Métraux, G. S.; Schatz, G. C.; Mirkin, C. A. Controlling Anisotropic Nanoparticle Growth through Plasmon Excitation. *Nature* **2003**, *425* (6957), 487–490.

(57) Huang, L.; Zhai, M. L.; Long, D. W.; Peng, J.; Xu, L.; Wu, G. Z.; Li, J. Q.; Wei, G. S. UV-Induced Synthesis, Characterization and Formation Mechanism of Silver Nanoparticles in Alkalic Carboxymethylated Chitosan Solution. *J. Nanoparticle Res.* **2008**, *10* (7), 1193–1202.

(58) Zhou, Y.; Zhao, Y.; Wang, L.; Xu, L.; Zhai, M.; Wei, S. Radiation Synthesis and Characterization of Nanosilver / Gelatin / Carboxymethyl Chitosan Hydrogel. *Radiat. Phys. Chem.* **2012**, *81* (5), 553–560.

(59) Veerasamy, R.; Xin, T. Z.; Gunasagaran, S.; Xiang, T. F. W.; Yang, E. F. C.; Jeyakumar, N.; Dhanaraj, S. A. Biosynthesis of Silver Nanoparticles Using Mangosteen Leaf Extract and Evaluation of Their Antimicrobial Activities. *J. Saudi Chem. Soc.* **2011**, *15* (2), 113–120.

(60) Zaarour, M.; El Roz, M.; Dong, B.; Retoux, R.; Aad, R.; Cardin, J.; Dufour, C.; Gourbilleau, F.; Gilson, J.-P.; Mintova, S. Photochemical Preparation of Silver Nanoparticles Supported on Zeolite Crystals. *Langmuir* **2014**, *30* (21), 6250–6256.

(61) Al-Mubaddel, F. S.; Haider, S.; Al-Masry, W. A.; Al-Zeghayer, Y.; Imran, M.; Haider, A.; Ullah, Z. Engineered Nanostructures: A Review of Their Synthesis, Characterization and Toxic Hazard Considerations. *Arab. J. Chem.* **2017**, *10*, S376–S388.

(62) Prabhu, S.; Poulose, E. K. Silver Nanoparticles: Mechanism of Antimicrobial Action, Synthesis, Medical Applications, and Toxicity Effects. *Int. Nano Lett.* **2012**, *2* (1), 32.

(63) Jokanović, V.; Spasić, A. M.; Uskoković, D. Designing of Nanostructured Hollow TiO_2 Spheres Obtained by Ultrasonic Spray Pyrolysis. *J. Colloid Interface Sci.* **2004**, *278* (2), 342–352.

(64) Emil Kaya, E.; Kaya, O.; Alkan, G.; Gürmen, S.; Stopic, S.; Friedrich, B. New Proposal for Size and Size-Distribution Evaluation of Nanoparticles Synthesized via Ultrasonic Spray Pyrolysis Using Search Algorithm Based on Image-Processing Technique. *Materials (Basel).* **2020**, *13* (1), 38.

(65) Ueda, M.; Yokota, T.; Honda, M.; Lim, P. N.; Osaka, N.; Makita, M.; Nishikawa, Y.; Kasuga, T.; Aizawa, M. Regulating Size of Silver Nanoparticles on Calcium Carbonate via Ultrasonic Spray for Effective Antibacterial Efficacy and Sustained Release. *Mater. Sci. Eng. C* **2021**, *125*, 112083.

(66) Pingali, K. C.; Rockstraw, D. A.; Deng, S. Silver Nanoparticles from Ultrasonic Spray Pyrolysis of Aqueous Silver Nitrate. *Aerosol Sci. Technol.* **2005**, *39* (10), 1010–1014.

(67) Wei, L.; Lu, J.; Xu, H.; Patel, A.; Chen, Z.-S.; Chen, G. Silver Nanoparticles: Synthesis, Properties, and Therapeutic Applications. *Drug Discov. Today* **2015**, *20* (5), 595–601.

(68) Iravani, S.; Korbekandi, H.; Mirmohammadi, S. V; Zolfaghari, B. Synthesis of Silver Nanoparticles: Chemical, Physical and Biological Methods. *Res. Pharm. Sci.* **2014**, *9* (6), 385–406.

(69) Abou El-Nour, K. M. M.; Eftaiha, A.; Al-Warthan, A.; Ammar, R. A. A. Synthesis and Applications of Silver Nanoparticles. *Arab. J. Chem.* **2010**, *3* (3), 135–140.

(70) Maisels, A.; Kruis, F. E.; Fissan, H.; Rellinghaus, B.; Zähres, H. Synthesis of Tailored Composite Nanoparticles in the Gas Phase. *Appl. Phys. Lett.* **2000**, *77* (26), 4431–4433.

(71) Magnusson, M. H.; Deppert, K.; Malm, J.-O.; Bovin, J.-O.; Samuelson, L. Gold Nanoparticles: Production, Reshaping, and Thermal Charging. *J. Nanoparticle Res.* **1999**, *1* (2), 243–251.

(72) Schmidt-Ott, A. New Approaches to in Situ Characterization of Ultrafine Agglomerates. *J. Aerosol Sci.* **1988**, *19* (5), 553–563.

(73) Jung, J. H.; Cheol Oh, H.; Soo Noh, H.; Ji, J. H.; Soo Kim, S. Metal Nanoparticle Generation Using a Small Ceramic Heater with a Local Heating Area. *J. Aerosol Sci.* **2006**, *37* (12), 1662–1670.

(74) Ge, L.; Li, Q.; Wang, M.; Ouyang, J.; Li, X.; Xing, M. M. Q. Nanosilver Particles in Medical Applications: Synthesis, Performance, and Toxicity. *Int. J. Nanomedicine* **2014**, *9* (1), 2399–2407.

(75) Tien, D.-C.; Tseng, K.-H.; Liao, C.-Y.; Huang, J.-C.; Tsung, T.-T. Discovery of Ionic Silver in Silver Nanoparticle Suspension Fabricated by Arc Discharge Method. *J. Alloys Compd.* **2008**, *463* (1), 408–411.

(76) Fojtik, A.; Giersig, M.; Henglein, A. Formation of Nanometer-Size Silicon Particles in a Laser Induced Plasma in SiH_4. *Berichte der Bunsengesellschaft für Phys. Chemie* **1993**, *97* (11), 1493–1496.

(77) Mafuné, F.; Kohno, J.; Takeda, Y.; Kondow, T.; Sawabe, H. Formation and Size Control of Silver Nanoparticles by Laser Ablation in Aqueous Solution. *J. Phys. Chem. B* **2000**, *104* (39), 9111–9117.

(78) González-Castillo, J. R.; Rodriguez, E.; Jimenez-Villar, E.; Rodríguez, D.; Salomon-García, I.; de Sá, G. F.; García-Fernández, T.; Almeida, D. B.; Cesar, C. L.; Johnes, R.; Ibarra, J. C. Synthesis of Ag@Silica Nanoparticles by Assisted Laser Ablation.

Nanoscale Res. Lett. **2015**, *10* (1), 399.

(79) Nakamura, M.; Oyane, A.; Shimizu, Y.; Miyata, S.; Saeki, A.; Miyaji, H. Physicochemical Fabrication of Antibacterial Calcium Phosphate Submicrospheres with Dispersed Silver Nanoparticles via Coprecipitation and Photoreduction under Laser Irradiation. *Acta Biomater.* **2016**, *46*, 299–307.

(80) Tsuji, T.; Iryo, K.; Watanabe, N.; Tsuji, M. Preparation of Silver Nanoparticles by Laser Ablation in Solution: Influence of Laser Wavelength on Particle Size. *Appl. Surf. Sci.* **2002**, *202* (1), 80–85.

(81) Neddersen, J.; Chumanov, G.; Cotton, T. M. Laser Ablation of Metals: A New Method for Preparing SERS Active Colloids. *Appl. Spectrosc.* **1993**, *47* (12), 1959–1964.

(82) Pyatenko, A.; Shimokawa, K.; Yamaguchi, M.; Nishimura, O.; Suzuki, M. Synthesis of Silver Nanoparticles by Laser Ablation in Pure Water. *Appl. Phys. A* **2004**, *79* (4), 803–806.

(83) Procházka, M.; Mojzeš, P.; Štěpánek, J.; Vlčková, B.; Turpin, P.-Y. Probing Applications of Laser-Ablated Ag Colloids in SERS Spectroscopy: Improvement of Ablation Procedure and SERS Spectral Testing. *Anal. Chem.* **1997**, *69* (24), 5103–5108.

(84) Pyatenko, A. Synthesis of Silver Nanoparticles with Laser Assistance. In *Silver Nanoparticles*; 2010; pp 121–144.

(85) Naik, R. R.; Stringer, S. J.; Agarwal, G.; Jones, S. E.; Stone, M. O. Biomimetic Synthesis and Patterning of Silver Nanoparticles. *Nat. Mater.* **2002**, *1* (3), 169–172.

(86) Anisha, B. S.; Biswas, R.; Chennazhi, K. P.; Jayakumar, R. Chitosan-Hyaluronic Acid/Nano Silver Composite Sponges for Drug Resistant Bacteria Infected Diabetic Wounds. *Int. J. Biol. Macromol.* **2013**, *62*, 310–320.

(87) Sintubin, L.; De Windt, W.; Dick, J.; Mast, J.; van der Ha, D.; Verstraete, W.; Boon, N. Lactic Acid Bacteria as Reducing and Capping Agent for the Fast and Efficient Production of Silver Nanoparticles. *Appl. Microbiol. Biotechnol.* **2009**, *84* (4), 741–749.

(88) Nam, K. T.; Lee, Y. J.; Krauland, E. M.; Kottmann, S. T.; Belcher, A. M. Peptide-Mediated Reduction of Silver Ions on Engineered Biological Scaffolds. *ACS Nano* **2008**, *2* (7), 1480–1486.

(89) Balaji, D. S.; Basavaraja, S.; Deshpande, R.; Mahesh, D. B.; Prabhakar, B. K.; Venkataraman, A. Extracellular Biosynthesis of Functionalized Silver Nanoparticles by Strains of *Cladosporium cladosporioides* Fungus. *Colloids Surf. B. Biointerfaces* **2009**, *68* (1), 88–92.

(90) Sintubin, L.; Verstraete, W.; Boon, N. Biologically Produced Nanosilver: Current State

and Future Perspectives. *Biotechnol. Bioeng.* **2012**, *109* (10), 2422–2436.

(91) Shankar, S.; Jaiswal, L.; Aparna, R. S. L.; Vara Prasad, R. G. S.; Kumar, G. P.; Manohara, C. M. Wound Healing Potential of Green Synthesized Silver Nanoparticles Prepared from *Lansium domesticum* Fruit Peel Extract. *Mater. Express* **2015**, *5* (2), 159–164.

(92) Shankar, S. S.; Ahmad, A.; Sastry, M. Geranium Leaf Assisted Biosynthesis of Silver Nanoparticles. *Biotechnol. Prog.* **2003**, *19* (6), 1627–1631.

(93) Anil Kumar, S.; Abyaneh, M. K.; Gosavi, S. W.; Kulkarni, S. K.; Pasricha, R.; Ahmad, A.; Khan, M. I. Nitrate Reductase-Mediated Synthesis of Silver Nanoparticles from $AgNO_3$. *Biotechnol. Lett.* **2007**, *29* (3), 439–445.

(94) Zhang, M.; Zhang, K.; De Gusseme, B.; Verstraete, W.; Field, R. The Antibacterial and Anti-Biofouling Performance of Biogenic Silver Nanoparticles by *Lactobacillus fermentum*. *Biofouling* **2014**, *30* (3), 347–357.

(95) Sunkar, S.; Nachiyar, C. V. Biogenesis of Antibacterial Silver Nanoparticles Using the Endophytic Bacterium *Bacillus cereus* Isolated from *Garcinia xanthochymus*. *Asian Pac. J. Trop. Biomed.* **2012**, *2* (12), 953–959.

(96) Saifuddin, N.; Wong, C. W.; Yasumira, A. A. N. Rapid Biosynthesis of Silver Nanoparticles Using Culture Supernatant of Bacteria with Microwave Irradiation. *E-Journal Chem.* **2009**, *6*, 734264.

(97) Shivaji, S.; Madhu, S.; Singh, S. Extracellular Synthesis of Antibacterial Silver Nanoparticles Using Psychrophilic Bacteria. *Process Biochem.* **2011**, *46* (9), 1800–1807.

(98) Gurunathan, S.; Kalishwaralal, K.; Vaidyanathan, R.; Venkataraman, D.; Pandian, S. R. K.; Muniyandi, J.; Hariharan, N.; Eom, S. H. Biosynthesis, Purification and Characterization of Silver Nanoparticles Using *Escherichia coli*. *Colloids Surf. B. Biointerfaces* **2009**, *74* (1), 328–335.

(99) Minaeian, S.; Shahverdi, A. R.; Nohi, A. S.; Shahverdi, H. R. Extracellular Biosynthesis of Silver Nanoparticles by Some Bacteria. *Jundishapur J. Nat. Pharm. Prod.* **2008**, *17* (66), 1–4.

(100) Panacek, A.; Kvítek, L.; Prucek, R.; Kolar, M.; Vecerova, R.; Pizúrova, N.; Sharma, V. K.; Nevecna, T.; Zboril, R. Silver Colloid Nanoparticles: Synthesis, Characterization, and Their Antibacterial Activity. *J. Phys. Chem. B* **2006**, *110* (33), 16248–16253.

(101) Morones, J. R.; Elechiguerra, J. L.; Camacho, A.; Ramirez, J. T. The Bactericidal Effect of Silver Nanoparticles. *Nanotechnology* **2005**, *16* (2346), 53.

(102) Li, G.; He, D.; Qian, Y.; Guan, B.; Gao, S.; Cui, Y.; Yokoyama, K.; Wang, L. Fungus-Mediated Green Synthesis of Silver Nanoparticles Using *Aspergillus terreus*. *Int. J. Mol. Sci.* **2012**, *13* (1), 466–476.

(103) Sharma, G.; Jasuja, N. D.; Kumar, M.; Ali, M. I. Biological Synthesis of Silver Nanoparticles by Cell-Free Extract of *Spirulina platensis*. *J. Nanotechnol.* **2015**, 132675.

(104) Shelar, G. B.; Chavan, A. M. Fungus–Mediated Biosynthesis of Silver Nanoparticles and Its Antibacterial Activity. *Arch. Appl. Sci. Res.* **2014**, *6* (2), 111–114.

(105) Syed, A.; Saraswati, S.; Kundu, G. C.; Ahmad, A. Biological Synthesis of Silver Nanoparticles Using the *Fungus humicola Sp*. and Evaluation of Their Cytoxicity Using Normal and Cancer Cell Lines. *Spectrochim. Acta. A. Mol. Biomol. Spectrosc.* **2013**, *114*, 144–147.

(106) Sangappa, M.; Thiagarajan, P. Mycobiosynthesis and Characterization of Silver Nanoparticles From *Aspergillus niger* : A Soil Fungal Isolate. *Int. J. Life Sci. Biotechnol. Pharma Res.* **2012**, *1* (2), 282–289.

(107) Otari, S. V; Patil, R. M.; Nadaf, N. H.; Ghosh, S. J.; Pawar, S. H. Green Synthesis of Silver Nanoparticles by Microorganism Using Organic Pollutant: Its Antimicrobial and Catalytic Application. *Environ. Sci. Pollut. Res.* **2014**, *21* (2), 1503–1513.

(108) El-Shanshoury, A. E.-R. R.; ElSilk, S. E.; Ebeid, M. E. Extracellular Biosynthesis of Silver Nanoparticles Using *Escherichia coli* ATCC 8739, *Bacillus subtilis* ATCC 6633, and S*treptococcus thermophilus* ESh1 and Their Antimicrobial Activities. *ISRN Nanotechnol.* **2011**, 385480.

(109) Thomas, R.; Janardhanan, A.; Varghese, R. T.; Soniya, E. V; Mathew, J.; Radhakrishnan, E. K. Antibacterial Properties of Silver Nanoparticles Synthesized by *Marine ochrobactrum Sp*. *Brazilian J. Microbiol. [publication Brazilian Soc. Microbiol.* **2014**, *45* (4), 1221–1227.

(110) Saravanan, M.; Barik, S. K.; MubarakAli, D.; Prakash, P.; Pugazhendhi, A. Synthesis of Silver Nanoparticles from *Bacillus brevis* (NCIM 2533) and Their Antibacterial Activity against Pathogenic Bacteria. *Microb. Pathog.* **2018**, *116*, 221–226.

(111) Najitha Banu, A.; Balasubramanian, C.; Moorthi, P. V. Biosynthesis of Silver Nanoparticles Using *Bacillus thuringiensis* against Dengue Vector, *Aedes aegypti* (Diptera: Culicidae). *Parasitol. Res.* **2014**, *113* (1), 311–316.

(112) Monowar, T.; Rahman, M. S.; Bhore, S. J.; Raju, G.; Sathasivam, K. V. Silver Nanoparticles Synthesized by Using the Endophytic Bacterium *Pantoea ananatis* Are

Promising Antimicrobial Agents against Multidrug Resistant Bacteria. *Molecules* **2018**, *23* (12), 3220.

(113) Iqtedar, M.; Aslam, M.; Akhyar, M.; Shehzaad, A.; Abdullah, R.; Kaleem, A. Extracellular Biosynthesis, Characterization, Optimization of Silver Nanoparticles (AgNPs) Using *Bacillus mojavensis* BTCB15 and Its Antimicrobial Activity against Multidrug Resistant Pathogens. *Prep. Biochem. Biotechnol.* **2019**, *49* (2), 136–142.

(114) Priyadarshini, S.; Gopinath, V.; Meera Priyadharsshini, N.; MubarakAli, D.; Velusamy, P. Synthesis of Anisotropic Silver Nanoparticles Using Novel Strain, *Bacillus flexus* and Its Biomedical Application. *Colloids Surf. B. Biointerfaces* **2013**, *102*, 232–237.

(115) Devika, R.; Elumalai, S.; Manikandan, E.; Eswaramoorthy, D. Biosynthesis of Silver Nanoparticles Using the Fungus *Pleurotus ostreatus* and Their Antibacterial Activity. *Open Access Sci. Reports* **2012**, *1* (12), 1–5.

(116) Bhangale, H.; Sarode, K.; Patil, A.; Patil, D. Microbial Synthesis of Silver Nanoparticles Using *Aspergillus flavus* and Their Characterization. In *ICATSA 2016:Techno-Societal 2016*; 2018; pp 463–470.

(117) Ammar, H. A. M.; El-Desouky, T. A. Green Synthesis of Nanosilver Particles by *Aspergillus terreus* HA1N and *Penicillium expansum* HA2N and Its Antifungal Activity against Mycotoxigenic Fungi. *J. Appl. Microbiol.* **2016**, *121* (1), 89–100.

(118) Raudabaugh, D. B.; Tzolov, M. B.; Calabrese, J. P.; Overton, B. E. Synthesis of Silver Nanoparticles by a *Bryophilous rhizoctonia* Species. *Nanomater. Nanotechnol.* **2013**, *3*, 2.

(119) Vahabi, K.; Mansoori, G. A.; Karimi, S. Biosynthesis of Silver Nanoparticles by Fungus Trichoderma Reesei (A Route for Large-Scale Production of AgNPs). *Insciences J.* **2011**, *1* (1), 65–79.

(120) Saha, S.; Sarkar, J.; Chattopadhyay, D.; Patra, S.; Chakraborty, A.; Acharya, K. Production Of Silver Nanoparticles By A Phytopathogenic Fungus *Bipolaris nodulosa* And Its Antimicrobial Activity. *Dig. J. Nanomater. Biostructures* **2010**, *5* (4), 887–895.

(121) Basavaraja, S.; Balaji, S. D.; Lagashetty, A.; Rajasab, A. H.; Venkataraman, A. Extracellular Biosynthesis of Silver Nanoparticles Using the Fungus *Fusarium semitectum*. *Mater. Res. Bull.* **2008**, *43* (5), 1164–1170.

(122) Ingle, A.; Gade, A.; Pierrat, S.; Sonnichsen, C.; Rai, M. Mycosynthesis of Silver Nanoparticles Using the Fungus *Fusarium acuminatum* and Its Activity Against Some Human Pathogenic Bacteria. *Curr. Nanosci.* **2008**, *4* (2), 141–144.

(123) Bhainsa, K. C.; D'Souza, S. F. Extracellular Biosynthesis of Silver Nanoparticles Using

the Fungus *Aspergillus fumigatus*. *Colloids Surf. B. Biointerfaces* **2006**, *47* (2), 160–164.

(124) Baharvandi, A.; Soleimani, M. J.; Zamani, P. Mycosynthesis of Nanosilver Particles Using Extract of *Alternaria alternata*. *Arch. Phytopathol. Plant Prot.* **2015**, *48* (4), 313–318.

(125) Dhuper S, Panda D, N. P. Green Synthesis and Characterization of Zero Valent Iron Nanoparticles from the Leaf Extract of *Mangifera indica*. Nano Trends. *J Nanotech App.* **2012**, *13* (2), 16–22.

(126) Kharissova, O. V; Dias, H. V. R.; Kharisov, B. I.; Pérez, B. O.; Pérez, V. M. J. The Greener Synthesis of Nanoparticles. *Trends Biotechnol.* **2013**, *31* (4), 240–248.

(127) Reddy, G.; Joy, J. M.; Mitra, T.; Sabnam, S.; Silpa, T. Nano Silver – a Review. *Int J Adv Pharm* **2012**, *2* (1), 09–15.

(128) Naidu, K. S. B.; Govender, P.; Adam, J. K. Nano Silver Particles in Biomedical and Clinical Applications: Review. *J. Pure Appl. Microbiol.* **2015**, *9* (Special Edition 2), 103–112.

(129) Srikar, S. K.; Giri, D. D.; Pal, D. B.; Mishra, P. K.; Upadhyay, S. N. Green Synthesis of Silver Nanoparticles: A Review. Green and Sustainable Chemistry. *Green Sustain. Chem.* **2016**, *6* (February), 34–56.

(130) Ghaffari-Moghaddam, M.; Hadi-Dabanlou, R.; Khajeh, M.; Rakhshanipour, M.; Shameli, K. Green Synthesis of Silver Nanoparticles Using Plant Extracts. *Korean J. Chem. Eng.* **2014**, *31* (4), 548–557.

(131) Madhumitha, G.; Roopan, S. M. Devastated Crops: Multifunctional Efficacy for the Production of Nanoparticles. *J. Nanomater.* **2013**, *2013*, 1–12.

(132) Lallawmawma, H.; Sathishkumar, G.; Sarathbabu, S.; Ghatak, S.; Sivaramakrishnan, S.; Gurusubramanian, G.; Kumar, N. S. Synthesis of Silver and Gold Nanoparticles Using *Jasminum nervosum* Leaf Extract and Its Larvicidal Activity against Filarial and Arboviral Vector *Culex quinquefasciatus* Say (Diptera: Culicidae). *Environ. Sci. Pollut. Res.* **2015**, *22* (22), 17753–17768.

(133) Gurunathan, S.; Jeong, J.-K.; Han, J. W.; Zhang, X.-F.; Park, J. H.; Kim, J.-H. Multidimensional Effects of Biologically Synthesized Silver Nanoparticles in *Helicobacter Pylori*, *Helicobacter Felis*, and Human Lung (L132) and Lung Carcinoma A549 Cells. *Nanoscale Res. Lett.* **2015**, *10* (1), 35.

(134) Dhand, V.; Soumya, L.; Bharadwaj, S.; Chakra, S.; Bhatt, D.; Sreedhar, B. Green Synthesis of Silver Nanoparticles Using *Coffea arabica* Seed Extract and Its

Antibacterial Activity. *Mater. Sci. Eng. C* **2016**, *58*, 36–43.

(135) Parveen, A.; Rao, S. Cytotoxicity and Genotoxicity of Biosynthesized Gold and Silver Nanoparticles on Human Cancer Cell Lines. *J. Clust. Sci.* **2015**, *26* (3), 775–788.

(136) Ganaie, S. U.; Abbasi, T.; Abbasi, S. A. Rapid and Green Synthesis of Bimetallic Au–Ag Nanoparticles Using an Otherwise Worthless Weed *Antigonon leptopus*. *J. Exp. Nanosci.* **2016**, *11* (6), 395–417.

(137) Parveen, M.; Ahmad, F.; Malla, A. M.; Azaz, S. Microwave-Assisted Green Synthesis of Silver Nanoparticles from *Fraxinus excelsior* Leaf Extract and Its Antioxidant Assay. *Appl. Nanosci.* **2016**, *6* (2), 267–276.

(138) Peddi, S. P.; Sadeh, B. A. Structural Studies of Silver Nanoparticles Obtained Through Single-Step Green Synthesis. *IOP Conf. Ser. Mater. Sci. Eng.* **2015**, *92*, 12004.

(139) Zuas, O.; Hamim, N.; Sampora, Y. Bio-Synthesis of Silver Nanoparticles Using Water Extract of *Myrmecodia pendan* (Sarang Semut Plant). *Mater. Lett.* **2014**, *123*, 156–159.

(140) Nalvothula, R.; Nagati, V. B.; Koyyati, R.; Merugu, R.; Padigya, P. R. M. Biogenic Synthesis of Silver Nanoparticles Using *Tectona grandis* Leaf Extract and Evaluation of Their Antibacterial Potential. *Int. J. ChemTech Res.* **2014**, *6* (1), 293–298.

(141) Mittal, A. K.; Bhaumik, J.; Kumar, S.; Banerjee, U. C. Biosynthesis of Silver Nanoparticles: Elucidation of Prospective Mechanism and Therapeutic Potential. *J. Colloid Interface Sci.* **2014**, *415*, 39–47.

(142) Hazarika, D.; Phukan, A.; Saikia, E.; Chetia, B. Phytochemical Screening and Synthesis of Silver Nanoparticles Using Leaf Extract of *Rhynchotechum ellipticum*. *Int. J. Pharm. Pharm. Sci.* **2014**, *6* (1), 672–674.

(143) Sarvamangala, D.; Kondala, K.; Murthy, U. S. N.; Rao, B. N.; Sharma, G. V. R.; Satyanarayana, R. Biogenic Synthesis of AgNP's Using Pomelo Fruit – Characterization and Antimicrobial Activity against Gram +ve and Gram –ve Bacteria. *Int. J. Pharm. Sci. Rev. Res.* **2013**, *19* (2), 30–35.

(144) Thirunavoukkarasu, M.; Balaji, U.; Behera, S.; Panda, P. K.; Mishra, B. K. Biosynthesis of Silver Nanoparticle from Leaf Extract of *Desmodium gangeticum (L.)* DC. and Its Biomedical Potential. *Spectrochim. Acta Part A Mol. Biomol. Spectrosc.* **2013**, *116*, 424–427.

(145) Rupiasih, N. N.; Aher, A.; Gosavi, S.; Vidyasagar, P. B. Green Synthesis of Silver Nanoparticles Using Latex Extract of *Thevetia peruviana*: A Novel Approach towards Poisonous Plant Utilization. In *Journal of Physics: Conference Series*; IOP Publishing, 2013; Vol. 423, p 12032.

(146) Asmathunisha, N.; Kathiresan, K. Rapid Biosynthesis of Antimicrobial Silver and Gold Nanoparticles by *in Vitro* Callus and Leaf Extracts from *Lycopersicon esculentum* Mill. *Int. J. Pharma Bio Sci.* **2013**, *4* (1), 334–344.

(147) Tamuly, C.; Hazarika, M.; Borah, S. C.; Das, M. R.; Boruah, M. P. In Situ Biosynthesis of Ag, Au and Bimetallic Nanoparticles Using *Piper Pedicellatum* C.DC: Green Chemistry Approach. *Colloids Surf. B. Biointerfaces* **2013**, *102*, 627–634.

(148) Rout, A.; Jena, P.; Parida, U.; Bindhani, B. K. Green Synthesis of Silver Nanoparticles Using Leaves Extract of *Centella asiatica L*. for Studies against Human Pathogens. *Int. J. Pharma Bio Sci.* **2013**, *4* (4), 661–674.

(149) Kora, A. J.; Sashidhar, R. B.; Arunachalam, J. Aqueous Extract of Gum Olibanum (*Boswellia serrata*): A Reductant and Stabilizer for the Biosynthesis of Antibacterial Silver Nanoparticles. *Process Biochem.* **2012**, *47* (10), 1516–1520.

(150) Gavhane, A. J.; Padmanabhan, P.; Jangle, S. N. Synthesis Of Silver Nanoparticles Using Extract Of Neem Leaf And Triphala And Evaluation Of Their Antimicrobial Activities. *Int. J. Pharma Bio Sci.* **2012**, *3* (3), 88–100.

(151) Philip, D.; Unni, C. Extracellular Biosynthesis of Gold and Silver Nanoparticles Using Krishna Tulsi (*Ocimum sanctum*) Leaf. *Phys. E Low-dimensional Syst. Nanostructures* **2011**, *43* (7), 1318–1322.

(152) MubarakAli, D.; Thajuddin, N.; Jeganathan, K.; Gunasekaran, M. Plant Extract Mediated Synthesis of Silver and Gold Nanoparticles and Its Antibacterial Activity against Clinically Isolated Pathogens. *Colloids Surf. B. Biointerfaces* **2011**, *85* (2), 360–365.

(153) Christensen, L.; Vivekanandhan, S.; Misra, M.; Mohanty, A. K. Biosynthesis of Silver Nanoparticles Using *Murraya koenigii* (Curry Leaf): An Investigation on the Effect of Broth Concentration in Reduction Mechanism and Particle Size. *Adv. Mater. Lett.* **2011**, *2* (6), 429–434.

(154) Annamalai, A.; Christina, V. L. P.; Christina, V.; Lakshmi, P. T. V. Green Synthesis and Characterisation of Ag NPs Using Aqueous Extract of *Phyllanthus maderaspatensis L*. *J. Exp. Nanosci.* **2014**, *9* (2), 113–119..

(155) Kim, J. S.; Kuk, E.; Yu, K. N.; Kim, J.-H.; Park, S. J.; Lee, H. J.; Kim, S. H.; Park, Y. K.; Park, Y. H.; Hwang, C.-Y.; Kim, Y.-K.; Lee, Y.-S.; Jeong, D. H.; Cho, M.-H. Antimicrobial Effects of Silver Nanoparticles. *Nanomedicine* **2007**, *3* (1), 95–101.

(156) Sondi, I.; Salopek-Sondi, B. Silver Nanoparticles as Antimicrobial Agent: A Case Study on *E. coli* as a Model for Gram-Negative Bacteria. *J. Colloid Interface Sci.* **2004**, *275*

(1), 177–182.

(157) Sotiriou, G. A.; Pratsinis, S. E. Antibacterial Activity of Nanosilver Ions and Particles. *Environ. Sci. Technol.* **2010**, *44* (14), 5649–5654.

(158) Nguyen, V. Q.; Ishihara, M.; Nakamura, S.; Hattori, H.; Ono, T.; Miyahira, Y.; Matsui, T. Interaction of Silver Nanoparticles and Chitin Powder with Different Sizes and Surface Structures: The Correlation with Antimicrobial Activities. *J. Nanomater.* **2013**, 467534.

(159) Velusamy, P.; Su, C.-H.; Venkat Kumar, G.; Adhikary, S.; Pandian, K.; Gopinath, S. C. B.; Chen, Y.; Anbu, P. Biopolymers Regulate Silver Nanoparticle under Microwave Irradiation for Effective Antibacterial and Antibiofilm Activities. *PLoS One* **2016**, *11* (6), e0157612.

(160) Sadeghi, B.; Garmaroudi, F. S.; Hashemi, M.; Nezhad, H. R.; Nasrollahi, A.; Ardalan, S.; Ardalan, S. Comparison of the Anti-Bacterial Activity on the Nanosilver Shapes: Nanoparticles, Nanorods and Nanoplates. *Adv. Powder Technol.* **2012**, *23* (1), 22–26.

(161) Tian, J.; Wong, K. K. Y.; Ho, C. M.; Lok, C. N.; Yu, W. Y.; Che, C. M.; Chiu, J. F.; Tam, P. K. H. Topical Delivery of Silver Nanoparticles Promotes Wound Healing. *ChemMedChem* **2007**, *2* (1), 129–136.

(162) Roy, A.; Bulut, O.; Some, S.; Mandal, A. K.; Yilmaz, M. D. Green Synthesis of Silver Nanoparticles: Biomolecule-Nanoparticle Organizations Targeting Antimicrobial Activity. *RSC Adv.* **2019**, *9* (5), 2673–2702.

(163) Devi, L. S.; Joshi, S. R. Antimicrobial and Synergistic Effects of Silver Nanoparticles Synthesized Using Soil Fungi of High Altitudes of Eastern Himalaya. *Mycobiology* **2012**, *40* (1), 27–34.

(164) Karmali, M. A. Factors in the Emergence of Serious Human Infections Associated with Highly Pathogenic Strains of Shiga Toxin-Producing *Escherichia coli*. *Int. J. Med. Microbiol.* **2018**, *308* (8), 1067–1072.

(165) Speshock, J. L.; Murdock, R. C.; Braydich-Stolle, L. K.; Schrand, A. M.; Hussain, S. M. Interaction of Silver Nanoparticles with Tacaribe Virus. *J. Nanobiotechnology* **2010**, *8* (1), 19.

(166) Gaikwad, S.; Ingle, A.; Gade, A.; Rai, M.; Falanga, A.; Incoronato, N.; Russo, L.; Galdiero, S.; Galdiero, M. Antiviral Activity of Mycosynthesized Silver Nanoparticles against Herpes Simplex Virus and Human Parainfluenza Virus Type 3. *Int. J. Nanomedicine* **2013**, *8*, 4303–4314.

(167) Elechiguerra, J. L.; Burt, J. L.; Morones, J. R.; Camacho-Bragado, A.; Gao, X.; Lara, H.

H.; Yacaman, M. J. Interaction of Silver Nanoparticles with HIV-1. *J. Nanobiotechnology* **2005**, *3* (1), 6.

(168) Mori, Y.; Ono, T.; Miyahira, Y.; Nguyen, V. Q.; Matsui, T.; Ishihara, M. Antiviral Activity of Silver Nanoparticle/Chitosan Composites against H1N1 Influenza A Virus. *Nanoscale Res. Lett.* **2013**, *8* (1), 93.

(169) Mori, Y.; Tagawa, T.; Fujita, M.; Kuno, T.; Suzuki, S.; Matsui, T.; Ishihara, M. Simple and Environmentally Friendly Preparation and Size Control of Silver Nanoparticles Using an Inhomogeneous System with Silver-Containing Glass Powder. *J. Nanoparticle Res.* **2011**, *13* (7), 2799–2806.

(170) Rogers, J. V; Parkinson, C. V; Choi, Y. W.; Speshock, J. L.; Hussain, S. M. A Preliminary Assessment of Silver Nanoparticle Inhibition of Monkeypox Virus Plaque Formation. *Nanoscale Res. Lett.* **2008**, *3* (4), 129.

(171) Kumar, C. G.; Poornachandra, Y. Biodirected Synthesis of Miconazole-Conjugated Bacterial Silver Nanoparticles and Their Application as Antifungal Agents and Drug Delivery Vehicles. *Colloids Surf. B. Biointerfaces* **2015**, *125*, 110–119.

(172) Jo, Y. K.; Kim, B. H.; Jung, G. Antifungal Activity of Silver Ions and Nanoparticles on Phytopathogenic Fungi. *Plant Dis.* **2009**, *93* (10), 1037–1043.

(173) Ouda, S. M. Antifungal Activity of Silver and Copper Nanoparticles on Two Plant Pathogens, *Alternaria alternata* and *Botrytis cinerea*. *Res. J. Microbiol.* **2014**, *9* (1), 34–42.

(174) Ali, S. M.; Yousef, N. M. H.; Nafady, N. A. Application of Biosynthesized Silver Nanoparticles for the Control of Land Snail *Eobania vermiculata* and Some Plant Pathogenic Fungi. *J. Nanomater.* **2015**, 218904.

(175) Elgorban, A. M.; El-Samawaty, A. E.-R. M.; Yassin, M. A.; Sayed, S. R.; Adil, S. F.; Elhindi, K. M.; Bakri, M.; Khan, M. Antifungal Silver Nanoparticles: Synthesis, Characterization and Biological Evaluation. *Biotechnol. Biotechnol. Equip.* **2016**, *30* (1), 56–62.

(176) Narayanan, K. B.; Park, H. H. Antifungal Activity of Silver Nanoparticles Synthesized Using Turnip Leaf Extract (*Brassica rapa L.*) against Wood Rotting Pathogens. *Eur. J. Plant Pathol.* **2014**, *140* (2), 185–192.

(177) Kim, K.-J.; Sung, W. S.; Moon, S.-K.; Choi, J.-S.; Kim, J. G.; Lee, D. G. Antifungal Effect of Silver Nanoparticles on Dermatophytes. *J. Microbiol. Biotechnol.* **2008**, *18* (8), 1482–1484.

(178) Hua, L.; Chen, J.; Ge, L.; Tan, S. N. Silver Nanoparticles as Matrix for Laser

Desorption/Ionization Mass Spectrometry of Peptides. *J. Nanoparticle Res.* **2007**, *9* (6), 1133–1138.

(179) Panácek, A.; Kolár, M.; Vecerová, R.; Prucek, R.; Soukupová, J.; Krystof, V.; Hamal, P.; Zboril, R.; Kvítek, L. Antifungal Activity of Silver Nanoparticles against *Candida Spp*. *Biomaterials* **2009**, *30* (31), 6333–6340.

(180) Jacob, J. A.; Mahal, H. S.; Biswas, N.; Mukherjee, T.; Kapoor, S. Role of Phenol Derivatives in the Formation of Silver Nanoparticles. *Langmuir* **2008**, *24* (2), 528–533.

(181) Foldbjerg, R.; Dang, D. A.; Autrup, H. Cytotoxicity and Genotoxicity of Silver Nanoparticles in the Human Lung Cancer Cell Line, A549. *Arch. Toxicol.* **2011**, *85* (7), 743–750.

(182) Lin, J.; Huang, Z.; Wu, H.; Zhou, W.; Jin, P.; Wei, P.; Zhang, Y.; Zheng, F.; Zhang, J.; Xu, J.; Hu, Y.; Wang, Y.; Li, Y.; Gu, N.; Wen, L. Inhibition of Autophagy Enhances the Anticancer Activity of Silver Nanoparticles. *Autophagy* **2014**, *10* (11), 2006–2020.

(183) Krishnaraj, C.; Muthukumaran, P.; Ramachandran, R.; Balakumaran, M. D.; Kalaichelvan, P. T. *Acalypha indica* Linn: Biogenic Synthesis of Silver and Gold Nanoparticles and Their Cytotoxic Effects against MDA-MB-231, Human Breast Cancer Cells. *Biotechnol. Reports* **2014**, *4*, 42–49.

(184) Sathishkumar, G.; Gobinath, C.; Wilson, A.; Sivaramakrishnan, S. *Dendrophthoe falcata* (L.f) Ettingsh (*Neem mistletoe*): A Potent Bioresource to Fabricate Silver Nanoparticles for Anticancer Effect against Human Breast Cancer Cells (MCF-7). *Spectrochim. Acta. A. Mol. Biomol. Spectrosc.* **2014**, *128*, 285–290.

(185) Rajasekharreddy, P.; Rani, P. U. Biofabrication of Ag Nanoparticles Using *Sterculia foetida L*. Seed Extract and Their Toxic Potential against Mosquito Vectors and HeLa Cancer Cells. *Mater. Sci. Eng. C. Mater. Biol. Appl.* **2014**, *39*, 203–212.

(186) Gajendran, B.; Chinnasamy, A.; Durai, P.; Raman, J.; Ramar, M. Biosynthesis and Characterization of Silver Nanoparticles from *Datura inoxia* and Its Apoptotic Effect on Human Breast Cancer Cell Line MCF7. *Mater. Lett.* **2014**, *122*, 98–102.

(187) Sankar, R.; Karthik, A.; Prabu, A.; Karthik, S.; Shivashangari, K. S.; Ravikumar, V. *Origanum vulgare* Mediated Biosynthesis of Silver Nanoparticles for Its Antibacterial and Anticancer Activity. *Colloids Surf. B. Biointerfaces* **2013**, *108*, 80–84.

(188) Firdhouse, M. J.; Lalitha, P. Biosynthesis of Silver Nanoparticles and Its Applications. *J. Nanotechnol.* **2015**, 829526.

(189) Suman, T. Y.; Radhika Rajasree, S. R.; Kanchana, A.; Elizabeth, S. B. Biosynthesis, Characterization and Cytotoxic Effect of Plant Mediated Silver Nanoparticles Using

Morinda citrifolia Root Extract. *Colloids Surf. B. Biointerfaces* **2013**, *106*, 74–78.

(190) Okafor, F.; Janen, A.; Kukhtareva, T.; Edwards, V.; Curley, M. Green Synthesis of Silver Nanoparticles, Their Characterization, Application and Antibacterial Activity. *Int. J. Environ. Res. Public Health* **2013**, *10* (10), 5221–5238.

(191) Dipankar, C.; Murugan, S. The Green Synthesis, Characterization and Evaluation of the Biological Activities of Silver Nanoparticles Synthesized from *Iresine herbstii* Leaf Aqueous Extracts. *Colloids Surf. B. Biointerfaces* **2012**, *98*, 112–119.

(192) Jacob, S. J. P.; Finub, J. S.; Narayanan, A. Synthesis of Silver Nanoparticles Using *Piper longum* Leaf Extracts and Its Cytotoxic Activity against Hep-2 Cell Line. *Colloids Surf. B. Biointerfaces* **2012**, *91*, 212–214.

(193) Valodkar, M.; Jadeja, R. N.; Thounaojam, M. C.; Devkar, R. V; Thakore, S. In Vitro Toxicity Study of Plant Latex Capped Silver Nanoparticles in Human Lung Carcinoma Cells. *Mater. Sci. Eng. C* **2011**, *31* (8), 1723–1728.

(194) Zhang, Y.; Yang, D.-P.; Kong, Y.; Wang, X.; Pandoli, O.; Gao, G. Synergetic Antibacterial Effects of Silver Nanoparticles@*Aloe vera* Prepared via a Green Method. *Nano Biomed. Eng.* **2010**, *2* (4), 252–257.

(195) Jain, P.; Pradeep, T. Potential of Silver Nanoparticle-Coated Polyurethane Foam as an Antibacterial Water Filter. *Biotechnol. Bioeng.* **2005**, *90* (1), 59–63.

(196) Yoon, K. Y.; Byeon, J. H.; Park, C. W.; Hwang, J. Antimicrobial Effect of Silver Particles on Bacterial Contamination of Activated Carbon Fibers. *Environ. Sci. Technol.* **2008**, *42* (4), 1251–1255.

(197) Zodrow, K.; Brunet, L.; Mahendra, S.; Li, D.; Zhang, A.; Li, Q.; Alvarez, P. J. J. Polysulfone Ultrafiltration Membranes Impregnated with Silver Nanoparticles Show Improved Biofouling Resistance and Virus Removal. *Water Res.* **2009**, *43* (3), 715–723.

(198) Li, Q.; Mahendra, S.; Lyon, D. Y.; Brunet, L.; Liga, M. V; Li, D.; Alvarez, P. J. J. Antimicrobial Nanomaterials for Water Disinfection and Microbial Control: Potential Applications and Implications. *Water Res.* **2008**, *42* (18), 4591–4602.

(199) Dankovich, T. A.; Gray, D. G. Bactericidal Paper Impregnated with Silver Nanoparticles for Point-of-Use Water Treatment. *Environ. Sci. Technol.* **2011**, *45* (5), 1992–1998.

(200) Balavigneswaran, C. K.; Sujin Jeba Kumar, T.; Moses Packiaraj, R.; Prakash, S. Rapid Detection of Cr(VI) by AgNPs Probe Produced by *Anacardium occidentale* Fresh Leaf Extracts. *Appl. Nanosci.* **2014**, *4* (3), 367–378

(201) Raja, K.; Saravanakumar, A.; Vijayakumar, R. Efficient Synthesis of Silver Nanoparticles from *Prosopis juliflora* Leaf Extract and Its Antimicrobial Activity Using

Sewage. *Spectrochim. Acta Part A Mol. Biomol. Spectrosc.* **2012**, *97*, 490–494.

(202) Lin, J.; Chen, R.; Feng, S.; Pan, J.; Li, Y.; Chen, G.; Cheng, M.; Huang, Z.; Yu, Y.; Zeng, H. A Novel Blood Plasma Analysis Technique Combining Membrane Electrophoresis with Silver Nanoparticle-Based SERS Spectroscopy for Potential Applications in Noninvasive Cancer Detection. *Nanomedicine* **2011**, *7* (5), 655–663.

(203) Cao, H.; Liu, X. Silver Nanoparticles-Modified Films versus Biomedical Device-Associated Infections. *Wiley Interdiscip. Rev. Nanomed. Nanobiotechnol.* **2010**, *2* (6), 670–684.

(204) Majdalawieh, A.; Kanan, M. C.; El-Kadri, O.; Kanan, S. M. Recent Advances in Gold and Silver Nanoparticles: Synthesis and Applications. *J. Nanosci. Nanotechnol.* **2014**, *14* (7), 4757–4780.

(205) Shin, S.-H.; Ye, M.-K.; Kim, H.-S.; Kang, H.-S. The Effects of Nano-Silver on the Proliferation and Cytokine Expression by Peripheral Blood Mononuclear Cells. *Int. Immunopharmacol.* **2007**, *7* (13), 1813–1818.

(206) Loo, C.; Lowery, A.; Halas, N.; West, J.; Drezek, R. Immunotargeted Nanoshells for Integrated Cancer Imaging and Therapy. *Nano Lett.* **2005**, *5* (4), 709–711.

(207) Nguyen, V. Q.; Ishihara, M.; Kinoda, J.; Hattori, H.; Nakamura, S.; Ono, T.; Miyahira, Y.; Matsui, T. Development of Antimicrobial Biomaterials Produced from Chitin-Nanofiber Sheet/Silver Nanoparticle Composites. *J. Nanobiotechnology* **2014**, *12* (1), 49.

(208) Ishihara, M.; Nguyen, V. Q.; Mori, Y.; Nakamura, S.; Hattori, H. Adsorption of Silver Nanoparticles onto Different Surface Structures of Chitin/Chitosan and Correlations with Antimicrobial Activities. *Int. J. Mol. Sci.* **2015**, *16* (6), 13973–13988.

(209) Ishihara, M.; Nakanishi, K.; Ono, K.; Sato, M.; Kikuchi, M.; Saito, Y.; Yura, H.; Matsui, T.; Hattori, H.; Uenoyama, M.; Kurita, A. Photocrosslinkable Chitosan as a Dressing for Wound Occlusion and Accelerator in Healing Process. *Biomaterials* **2002**, *23* (3), 833–840.

(210) Nakamura, S.; Nambu, M.; Ishizuka, T.; Hattori, H.; Kanatani, Y.; Takase, B.; Kishimoto, S.; Amano, Y.; Aoki, H.; Kiyosawa, T.; Ishihara, M.; Maehara, T. Effect of Controlled Release of Fibroblast Growth Factor-2 from Chitosan/Fucoidan Micro Complex-Hydrogel on in Vitro and in Vivo Vascularization. *J. Biomed. Mater. Res. A* **2008**, *85* (3), 619–627.

(211) Wong, K. K. Y.; Liu, X. Silver Nanoparticles—the Real "Silver Bullet" in Clinical Medicine? *Medchemcomm* **2010**, *1* (2), 125–131.

(212) Thomas, R.; Soumya, K. R.; Mathew, J.; Radhakrishnan, E. K. Inhibitory Effect of Silver Nanoparticle Fabricated Urinary Catheter on Colonization Efficiency of Coagulase Negative Staphylococci. *J. Photochem. Photobiol. B.* **2015**, *149*, 68–77.

(213) Wu, K.; Yang, Y.; Zhang, Y.; Deng, J.; Lin, C. Antimicrobial Activity and Cytocompatibility of Silver Nanoparticles Coated Catheters via a Biomimetic Surface Functionalization Strategy. *Int. J. Nanomedicine* **2015**, *10*, 7241–7252.

(214) Mala, R.; Annie Aglin, A.; Ruby Celsia, A. S.; Geerthika, S.; Kiruthika, N.; VazagaPriya, C.; Srinivasa Kumar, K. Foley Catheters Functionalised with a Synergistic Combination of Antibiotics and Silver Nanoparticles Resist Biofilm Formation. *IET nanobiotechnology* **2017**, *11* (5), 612–620.

(215) Lu, H.; Liu, Y.; Guo, J.; Wu, H.; Wang, J.; Wu, G. Biomaterials with Antibacterial and Osteoinductive Properties to Repair Infected Bone Defects. *Int. J. Mol. Sci.* **2016**, *17* (3), 334.

(216) Negut, I.; Grumezescu, V.; Grumezescu, A. M. Treatment Strategies for Infected Wounds. *Molecules* **2018**, *23* (9), 1–23.

(217) Yang, Y.; Hu, H. A Review on Antimicrobial Silver Absorbent Wound Dressings Applied to Exuding Wounds. *J. Microb. Biochem. Technol.* **2015**, *07* (04), 228–233.

(218) Trop, M.; Novak, M.; Rodl, S.; Hellbom, B.; Kroell, W.; Goessler, W. Silver-Coated Dressing Acticoat Caused Raised Liver Enzymes and Argyria-like Symptoms in Burn Patient. *J. Trauma* **2006**, *60* (3), 648–652.

(219) Xing, Z.-C.; Chae, W.-P.; Baek, J.-Y.; Choi, M.-J.; Jung, Y.; Kang, I.-K. In Vitro Assessment of Antibacterial Activity and Cytocompatibility of Silver-Containing PHBV Nanofibrous Scaffolds for Tissue Engineering. *Biomacromolecules* **2010**, *11* (5), 1248–1253.

(220) Rigo, C.; Ferroni, L.; Tocco, I.; Roman, M.; Munivrana, I.; Gardin, C.; Cairns, W. R. L.; Vindigni, V.; Azzena, B.; Barbante, C.; Zavan, B. Active Silver Nanoparticles for Wound Healing. *Int. J. Mol. Sci.* **2013**, *14* (3), 4817–4840.

(221) Hendi, A. Silver Nanoparticles Mediate Differential Responses in Some of Liver and Kidney Functions during Skin Wound Healing. *J. King Saud Univ. Sci.* **2011**, *23* (1), 47–52.

(222) Yamanaka, M.; Hara, K.; Kudo, J. Bactericidal Actions of a Silver Ion Solution on *Escherichia coli*, Studied by Energy-Filtering Transmission Electron Microscopy and Proteomic Analysis. *Appl. Environ. Microbiol.* **2005**, *71* (11), 7589–7593.

(223) Koehler, J.; Brandl, F. P.; Goepferich, A. M. Hydrogel Wound Dressings for Bioactive

Treatment of Acute and Chronic Wounds. *Eur. Polym. J.* **2018**, *100* (January), 1–11.

(224) Pal, K.; Banthia, A.; Majumdar, D. K. Preparation and Characterization of Polyvinyl Alcohol–Gelatin Hydrogel Membranes for Biomedical Applications. *AAPS PharmSciTech* **2007**, *8* (1), 142–146.

(225) Pawde, S. M.; Deshmukh, K.; Parab, S. Preparation and Characterization of Poly(Vinyl Alcohol) and Gelatin Blend Films. *J. Appl. Polym. Sci.* **2008**, *109*, 1328–1337.

(226) Nešović, K.; Janković, A.; Kojić, V.; Vukašinović-Sekulić, M.; Perić-Grujić, A.; Rhee, K. Y.; Mišković-Stanković, V. Silver/Poly(Vinyl Alcohol)/Chitosan/Graphene Hydrogels – Synthesis, Biological and Physicochemical Properties and Silver Release Kinetics. *Compos. Part B Eng.* **2018**, *154* (July), 175–185.

(227) Philippot, K.; Serp, P. Concepts in Nanocatalysis. In *Nanomaterials in Catalysis: First Edition*; 2012; pp 1–54.

(228) Jiang, Z.-J.; Liu, C.-Y.; Sun, L.-W. Catalytic Properties of Silver Nanoparticles Supported on Silica Spheres. *J. Phys. Chem. B* **2005**, *109* (5), 1730–1735.

(229) Bastús, N. G.; Merkoçi, F.; Piella, J.; Puntes, V. Synthesis of Highly Monodisperse Citrate-Stabilized Silver Nanoparticles of up to 200 nm: Kinetic Control and Catalytic Properties. *Chem. Mater.* **2014**, *26* (9), 2836–2846.

(230) Suvith, V. S.; Philip, D. Catalytic Degradation of Methylene Blue Using Biosynthesized Gold and Silver Nanoparticles. *Spectrochim. Acta. A. Mol. Biomol. Spectrosc.* **2014**, *118*, 526–532.

(231) Kumar, P.; Govindaraju, M.; Senthamilselvi, S.; Premkumar, K. Photocatalytic Degradation of Methyl Orange Dye Using Silver (Ag) Nanoparticles Synthesized from *Ulva lactuca*. *Colloids Surf. B. Biointerfaces* **2013**, *103*, 658–661.

(232) Waghmode, S.; Chavan, P.; Kalyankar, V.; Dagade, S. Synthesis of Silver Nanoparticles Using *Triticum Aestivum* and Its Effect on Peroxide Catalytic Activity and Toxicology. *J. Chem.* **2013**, *2013*, 265864.

(233) Dong, X.-Y.; Gao, Z.-W.; Yang, K.-F.; Zhang, W.-Q.; Xu, L.-W. Nanosilver as a New Generation of Silver Catalysts in Organic Transformations for Efficient Synthesis of Fine Chemicals. *Catal. Sci. Technol.* **2015**, *5* (5), 2554–2574.

(234) Barnes, W. L.; Dereux, A.; Ebbesen, T. W. Surface Plasmon Subwavelength Optics. *Nature* **2003**, *424* (6950), 824–830.

(235) Sangno, R.; Maity, S.; Mehta, R. K. Plasmonic Effect Due to Silver Nanoparticles on Silicon Solar Cell. *Procedia Comput. Sci.* **2016**, *92*, 549–553.

(236) Tang, Y.; Vlahovic, B.; Brady, D. J. Metallic Nano-Structures for Polarization-

Independent Multi-Spectral Filters. *Nanoscale Res. Lett.* **2011**, *6* (1), 394.

(237) Li, Z.; Zhang, Y.; Ye, J.; Guo, M.; Chen, J.; Chen, W. Nonenzymatic Glucose Biosensors Based on Silver Nanoparticles Deposited on TiO_2 Nanotubes. *J. Nanotechnol.* **2016**, *2016*, 9454830.

(238) Ruth, C.; Loren, W. A.; Maria, G. M. P. Development of DNA Biosensor Based of Silver Nanoparticles UV-Vis Absorption Spectra for Escherichia Coli Detection. In *The 3rd International Conference on Biological Science*; 2013; pp 382–389.

(239) Mahmudin, L.; Suharyadi, E.; Utomo, A. B. S.; Abraha, K. Optical Properties of Silver Nanoparticles for Surface Plasmon Resonance (SPR)-Based Biosensor Applications. *J. Mod. Phys.* **2015**, *06* (08), 1071–1076.

(240) Sistani, P.; Sofimaryo, L.; Masoudi, Z. R.; Sayad, A.; Rahimzadeh, R.; Salehi, B. A Penicillin Biosensor by Using Silver Nanoparticles. *Int. J. Electrochem. Sci.* **2014**, *9* (11), 6201–6212.

(241) Tung, N. H.; Chikae, M.; Ukita, Y.; Viet, P. H.; Takamura, Y. Sensing Technique of Silver Nanoparticles as Labels for Immunoassay Using Liquid Electrode Plasma Atomic Emission Spectrometry. *Anal. Chem.* **2012**, *84* (3), 1210–1213.

(242) Wu, J. T.; Hsu, S. L. C. Preparation of Triethylamine Stabilized Silver Nanoparticles for Low-Temperature Sintering. *J. Nanoparticle Res.* **2011**, *13* (9), 3877–3883.

(243) Carbone, M.; Donia, D. T.; Sabbatella, G.; Antiochia, R. Silver Nanoparticles in Polymeric Matrices for Fresh Food Packaging. *J. King Saud Univ. - Sci.* **2016**, *28* (4), 273–279.

(244) Mahdi, S. S.; Vadood, R.; Nourdahr, R. Study on the Antimicrobial Effect of Nanosilver Tray Packaging of Minced Beef at Refrigerator Temperature. *Glob. Vet.* **2012**, *9* (3), 284–289.

(245) Emamifar, A.; Kadivar, M.; Shahedi, M.; Soleimanian-Zad, S. Evaluation of Nanocomposite Packaging Containing Ag and ZnO on Shelf Life of Fresh Orange Juice. *Innov. Food Sci. Emerg. Technol.* **2010**, *11* (4), 742–748.

(246) Fernández, A.; Picouet, P.; Lloret, E. Cellulose-Silver Nanoparticle Hybrid Materials to Control Spoilage-Related Microflora in Absorbent Pads Located in Trays of Fresh-Cut Melon. *Int. J. Food Microbiol.* **2010**, *142* (1), 222–228.

(247) Fernández, A.; Picouet, P.; Lloret, E. Reduction of the Spoilage-Related Microflora in Absorbent Pads by Silver Nanotechnology during Modified Atmosphere Packaging of Beef Meat. *J. Food Prot.* **2010**, *73* (12), 2263–2269.

(248) Khalaf, H. H.; Sharoba, A. M.; El-Tanahi, H. H.; Morsy, M. K. Stability of

Antimicrobial Activity of Pullulan Edible Films Incorporated with Nanoparticles and Essential Oils with Impact on Turkey Deli Meat Quality. *J. Food Dairy Sci.* **2013**, *4* (11), 557–573.

(249) Abreu, A. S.; Oliveira, M.; de Sá, A.; Rodrigues, R. M.; Cerqueira, M. A.; Vicente, A. A.; Machado, A. V. Antimicrobial Nanostructured Starch Based Films for Packaging. *Carbohydr. Polym.* **2015**, *129*, 127–134.

(250) Incoronato, A. L.; Conte, A.; Buonocore, G. G.; Del Nobile, M. A. Agar Hydrogel with Silver Nanoparticles to Prolong the Shelf Life of Fior Di Latte Cheese. *J. Dairy Sci.* **2011**, *94* (4), 1697–1704.

(251) de Moura, M. R.; Mattoso, L. H. C.; Zucolotto, V. Development of Cellulose-Based Bactericidal Nanocomposites Containing Silver Nanoparticles and Their Use as Active Food Packaging. *J. Food Eng.* **2012**, *109* (3), 520–524.

(252) Morsy, M. K.; Khalaf, H. H.; Sharoba, A. M.; El-Tanahi, H. H.; Cutter, C. N. Incorporation of Essential Oils and Nanoparticles in Pullulan Films to Control Foodborne Pathogens on Meat and Poultry Products. *J. Food Sci.* **2014**, *79* (4), M675–M684.

(253) Mohammed Fayaz, A.; Balaji, K.; Girilal, M.; Kalaichelvan, P. T.; Venkatesan, R. Mycobased Synthesis of Silver Nanoparticles and Their Incorporation into Sodium Alginate Films for Vegetable and Fruit Preservation. *J. Agric. Food Chem.* **2009**, *57* (14), 6246–6252.

(254) Echegoyen, Y.; Nerín, C. Nanoparticle Release from Nano-Silver Antimicrobial Food Containers. *Food Chem. Toxicol.* **2013**, *62*, 16–22.

(255) Kah, M.; Tufenkji, N.; White, J. C. Nano-Enabled Strategies to Enhance Crop Nutrition and Protection. *Nat. Nanotechnol.* **2019**, *14* (6), 532–540.

(256) Babu, M.; Devi, V.; Ramakritinan, C. M.; Umarani, R.; Taredahalli, N.; Kumaraguru, A. K. Application of Biosynthesized Silver Nanoparticles in Agricultural and Marine Pest Control. *Curr. Nanosci.* **2013**, *10* (3), 374–381.

(257) Kumar, A.; Vemula, P. K.; Ajayan, P. M.; John, G. Silver-Nanoparticle-Embedded Antimicrobial Paints Based on Vegetable Oil. *Nat. Mater.* **2008**, *7* (3), 236–241.

(258) Chen, D.; Qiao, X.; Qiu, X.; Chen, J. Synthesis and Electrical Properties of Uniform Silver Nanoparticles for Electronic Applications. *J. Mater. Sci.* **2009**, *44* (4), 1076–1081.

CHAPTER 2:

Synthesis of Silver Nanoparticles Using Bhimkol (*Musa Balbisiana*) Peel Extract as Biological Waste: Antibacterial Activity and Role of Ripen Stage of the Peels

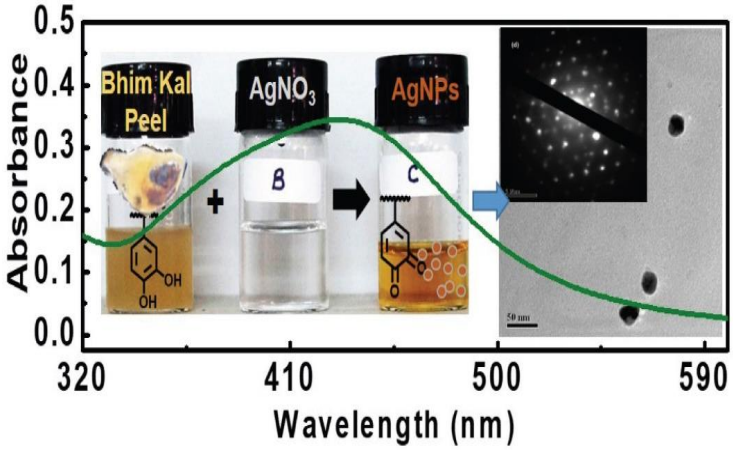

2.1. Introduction

Metallic silver with 1-100 nm size is identified as silver nanoparticle (AgNP), and its most common sources are inorganic salts. AgNPs are very beneficial for their antibacterial activities against many microbes. Their significant biological effectivity is much higher than their equivalent metal salt.[1] Thus, AgNPs have got major interest among all other metal nanoparticles due to their distinctive electrical, physical, optical and antimicrobial properties and a broad range of applications.[2,3] AgNPs have high conductivity, chemical stability, catalytic activity and localized surface plasmon resonance (LSPR), making AgNPs even more user-friendly for many applications.[4] Reactive oxygen species(ROS), which forms at the AgNP surface or by the free Ag ions released under definite conditions, may cause cell death of microbial cells or mammalian cells. These properties demonstrate the antibacterial as well as antifungal properties of AgNPs. AgNPs illustrate lower toxicity to human health compared to other metal nanoparticles with the most effective antibacterial action.[5,6] Due to these effects, AgNPs find numerous applications in the biomedical field, such as in the prevention of wound inflammation and thus promoting wound healing, in scaffolds for water purification and agricultural uses. Nowadays, silver-containing agents are used in various clinical wound dressings (*e.g.*, silver sulfadiazine) as well as in biomedical material coatings (*e.g.*, silver-impregnated catheters).[7–9] Therefore, many research efforts led to the development of various synthetic methodologies, including physical methods and chemical methods.[10–12] Among these, green synthesis of AgNPs has got recent research attentions as it is non-toxic, eco-friendly and cost-effective. The green synthesis also provides stabilization to these particles by natural capping agents. Plant extracts are reported to contain abundant natural compounds such as flavonoids, saponins, tannins, alkaloids, steroids and other kinds of nutritional compounds. They provide the reducing components for bio-reduction as well as for the stabilization of the nanoparticles formed. Thus, it is clear that the utilization of plant extracts and agricultural waste significantly impacts the synthesis of AgNPs even over the production by a microorganism.[10,13]

2.2. Green Synthesis of Silver Nanoparticles (AgNPs)

Green synthesis is an emerging branch of nanotechnology in which metallic nanoparticles are synthesized using biological or environmentally benign materials. These materials can be plant extracts, whole cells or metabolites from microbes, biomass, fruit and vegetable extracts or agricultural wastes. Green synthesis is considered advantageous over the other chemical and

physical methods for the synthesis of metallic nanoparticles. It is very simple, cost-effective, and safer, resulting in stable and reproducible materials.[14,15] Green synthesis is used to synthesise metal and metal oxide nanoparticles of desirable morphology and size with improved properties. Toxic chemicals are not used in this synthesis as they can have adverse environmental effects.[16] Plants, varieties of plant parts and their potential secondary metabolites are used for green synthesis, as plants have rich biodiversity and easy availability.[17]

Naturally, plant extracts contain compounds such as flavonoids, saponins, steroids, tannins, alkaloids, etc., which can be obtained from the various parts of a plant such as seeds, roots, flowers, leaves, shoots, stems and barks. These compounds are responsible for the bioreduction reaction in the process of metallic nanoparticle synthesis. They act as both stabilizing as well as reducing agents for the green synthesis of various nanoparticles, including copper, gold, cobalt, palladium, silver, platinum, magnetite and zinc oxide.[18] Figure 2.1 illustrates the one-pot synthesis of silver nanoparticles by reducing silver nitrate via the addition of plant/agro waste extract.

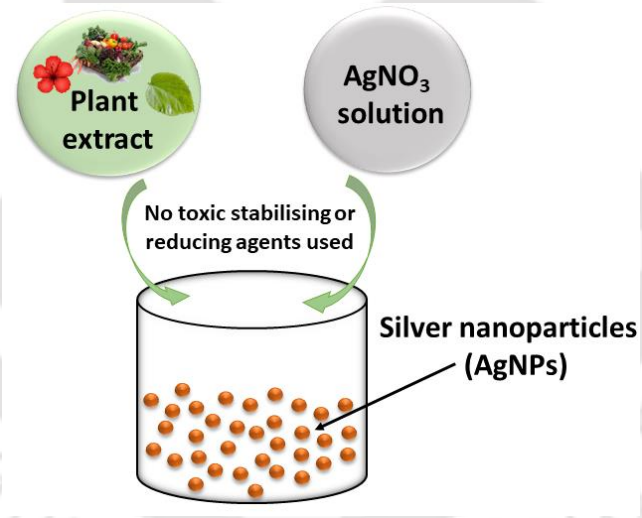

Figure 2.1. Green synthesis of silver nanoparticles using plant or agro-waste extract.

For green synthesis purposes, the consumption of commercially valued plant-based products might reduce the efficacy of the process as these plants are widely available and used as food materials or for other medicinal purposes. The waste generated after the use of the plants, plant parts or other agricultural wastes can be utilized as an excellent alternative for the synthesis of nanoparticles. Such processes would provide a sustainable and eco-friendly way for proper utilization and management of biomass and plant wastes.[19] Few of the green syntheses are highlighted below.

2.3. Green Synthesis Using Agricultural Waste

Nanoparticles have been successfully synthesized using various agricultural wastes rich in biomolecules such as phenolics, flavonoids and proteins. They act as the bioreductants for the synthesis of different types of metallic nanoparticles. The agricultural wastes mainly used for the green synthesis purpose include fruit seeds and peels,[20] rice bran,[21] wheat bran,[22] palm oil mill effluent,[23] *Cocos nucifera* coir[24] and corn cob, etc. Extracts of these wastes are used as reducing and stabilizing agents for the formed nanoparticles with various properties ranging from larvicidal, antioxidant, catalytic, antimicrobial and cytotoxic properties against cancer cells.

The processing of agricultural wastes produces a large number of agro-wastes which when released into the environment may cause pollution.[16] Thus, these waste need to be managed properly for environmental concern. One important way to manage such waste is to utilise them properly. Thus, a few biotechnological processes help utilising agro-wastes to enhance the nutritional qualities by solid state fermentation, treatment with enzymes/organic acids and using as renewable materials for biogas production.[25] The utilization of agricultural wastes as sources of biomolecules in green nanotechnology has also gained remarkable attention. A few agro-wastes have been listed for their significance in nanobiotechnology in table 2.1. Usually, extracts containing active biomolecules could be obtained through easy procedures that catalyze the formation of nanoparticles. The utilization of plant extracts and agricultural wastes as a means of eco-friendly synthesis of AgNPs has dramatically impacted the field of nanotechnology.

Table 2.1. Synthesis of nanoparticles by agro-wastes.

Sl No.	Extract	Types Of Nanoparticles Formed	Particle Size (Nm)	Application	References
1	Pomegranate fruit peel	Ag NPs	5 - 50 nm	Antibacterial	26
2	Rambutan peel	Ag NPs	132.6±42	Free radical scavenger	27
3	Rambutan peel	ZnO nanocrystal	-	Antibacterial	28
4	Rambutan peel	NiO nanocrystal	50	Antibacterial	29
5	Sugar apple*(Annona squamosa)* peel	Ag NPs	35±5	-	30

6	Oak fruit hull	Ag NPs	40	Cancer therapy	31
7	*Cocos nucifera* coir	Ag NPs	23±2	Larvicidal	24
8	*Punica granatum* peel	Pt NPs	16-23	Catalyst	32
9	Wheat bran xylan	Ag NPs	20-45	Antioxidant and fibrinolytic	22
10	*Citrus* peel	Ag NPs	5-20 nm	Biomedical	20
11	Grape waste	Au NPs	20-25	Medical	33
12	Lemon peel	Ag NPs	17.3-61.2	Antidermatophytic activity	34
13	Watermelon rinds	Fe_3O_4M NPs	2 - 20 nm	Catalyst	35
14	Watermelon rinds	Pd NPs	96	Catalytic activity	36
15	Groundnut peel	Ag NPs	20-50 nm	Larvicidal activity	37
16	*Jatropha* waste	Au NPs	14	-	38
17	*Moringa oleifera* flower	Au NPs	28	Antibacterial	39
18	Teak waste	Ag NPs	28	Antibacterial	19
19	*Cola nitida* seed shell	Ag NPs	5-40 nm	Antibacterial	40
20	*Cola nitida* pod	Ag NPs	12-80 nm	Antibacterial, antifungal, additive in paint and antioxidant	41
21	*Cola nitida* pod	Ag-Au NPs	12-91 nm	Antifungal, dye degradation, larvicidal, anticoagulant and thrombolytic	14
22	Cola nitida seed shell	Ag-Au NPs	10 -40 nm	Antifungal, dye degradation, larvicidal, anticoagulant and thrombolytic	42
23	Cocoa (*Theobroma cacao*) pod husk	Ag NPs	4-32 nm	Antibacterial, antifungal, synergistic, additive in paint, antioxidant and larvicidal	43
24	Egg shell membrane(ESM)	Ag NPs	25 ± 7	Biosensing	40
26	Egg shell membrane	Au NPs	< 20	Bioimaging and bio labelling	41

One example of widely available household waste is pomegranate fruit peels. These peels have potent antioxidant property. Thus, pomegranate peel extracts have been utilized to reduce

gold and silver ions to form gold and silver nanoparticles. The absorption peak was observed at 427 nm for the synthesized AgNPs, and the nanoparticles are polydispersed in nature and spherical in shape. A naturally occurring phenolic compound, ellagic acid, is abundantly present in the fruit peel responsible for forming nanoparticles. X-ray diffraction (XRD) study confirmed the particles to be face-centred cubic in symmetry with an average size of 5 to 10 nm.[42] The synthesis of spherical AgNPs of average size 5-50 nm showing UV-Visible absorption at 371 nm has also been demonstrated using pomegranate fruit peel extract. The Fourier transform infrared spectroscopy (FTIR) showed the association of primary and secondary amines and other aromatic groups, which might help in the synthesis of AgNPs. The particles show remarkable antibacterial activity at a concentration of 2 mg/L against *Staphylococcus aureus* ATCC 25923.[26] *Punica granatum* peel extract has been used to synthesize AgNPs. The formation of AgNPs shows brownish-yellow colouration with surface plasmon resonance (SPR) at 432 nm. Colouration of the nanoparticles is due to the surface plasmon resonance effect. Surface plasmon resonance is the resonance of the outer electron bands of the particles with light wavelengths. The particle size for such nanoparticles has been reportedas about 30 nm with a distorted spherical shape with highly negative zeta potential values revealing their high stability. Thus the magnitude of the zeta potential gives an indication of the potential stability of the colloidal system. The synthesized AgNPs in combination with sodium borohydride effectively catalyzed the instantaneous reduction of 4-nitrophenol (4-NP), an anthropogenic pollutant.[43]

Peel extract of *Nephelium lappaceum L*. (Rambutan) has been utilised for AgNPs synthesis. The particles showed two peaks on the UV-vis spectra at 370 and 495 nm. The formation of a truncated triangle, and hexagonal shape has been demonstrated with the particle size of 132.6 ± 42 nm. The particles are reported to be crystalline in nature with face-centered cubic symmetry as analysed with selected area electron diffraction (SAED) and XRD. Free radical scavenging activity of such nanoparticles against 2, 2-diphenyl-1- picrylhydrazyl (DPPH) is remarkable indicating their relevance in biomedicine.[27] AgNPs are also successfully synthesized using citrus peels such as orange, tangelo, grapefruits, lemon, and lime. Aqueous extract of orange peel extract shows the efficient synthesis of AgNPs within 15 min inside microwave at 90°C and 15 psi pressure indicated from absorbance at about 402-428 nm. TEM analysis of such nanoparticles confirmed the particle size of 7.36 ± 8.06 nm. The GC-MS indicated the presence of aldehydes in the peels, which are mainly responsible for reducing and capping the synthesized AgNPs.[44] The synthesis of AgNPs of average size 5-20 nm with

maximum absorbance at 440 nm has also been demonstrated using Satsuma mandarin (*Citrus unshiu*) peel extract.[20]

Biogenic AgNPs of 91 nm in size have been synthesized using fresh suspension of orange peel extract at room temperature. Silver nanoparticles formation is facilitated by the flavonoids present in the extract. UV-vis spectroscopy has shown the maximum absorbance at 466 nm. The synthesized particles displays significant antibacterial activities against gram-negative bacterial strains.[45] The biosynthesized AgNPs using lemon peel extract particles exhibits good antidermatophytic activity against multidrug-resistant *Candida albicans* and *Trichophyton mentagrophytes* to the tune of 11-12 mm.[34]

Acetone precipitated banana peel extract (*Musa paradisiaca*) has also been utilized to reduce silver nitrate to form AgNPs. These particles possessed appreciable antimicrobial activity.[46] Similarly, spherical and monodispersed AgNPs using banana(*Musa paradisiaca*) peel extract had maximum absorbance at 433 nm. The particles with an average size of 23.7 nm were formed due to the activities of pectin, cellulose, hemicelluloses and proteins present in the extract, as evidenced from FTIR data. Thus, the AgNPs produced shows growth inhibitions of 12-20 mm against strains of *Bacillus subtilis, Escherichia coli, Staphylococcus aureus*, and *Pseudomonas aeruginosa*. It also enhances the activities of an antibiotic, levofloxacin, in a synergistic manner producing 1.16-1.32 fold improvement in antibacterial activities against the tested bacteria.[47]

Therefore, it is clear that the plants have made an enormous contribution since a very early period for assisting human health as well as in the advancement of scientific discoveries. The maturity stage in the plants affects the concentrations of nutrients in them significantly. Most common plants are broadly studied for their medicinal prospects, collected and compiled as they lack knowledge of these plants, making them highly underutilized.[48] A series of developmental changes occur during the process of growth and development of plant fruits and vegetables. So many catabolic and anabolic reactions changes ensue in these processes, leading to the degradation or synthesis of a wide variety of bioactive compounds. So, fruits at different maturity levels possess bioactive compounds, which are to be studied for use as a resource of medicine or food.[49] Compounds that derive ethnobotanical has bioactive compounds and provide a better perspective for product development.[50] Phytochemicals are chemical compounds that occur naturally and are biologically active in plants. These chemicals act as a natural defense system for host plants and offer flavour, aroma and colour. They are bioactive

substances that are responsible for protecting the plants from adverse environmental conditions, insects, microbial attacks and other exterior aggression. These phytochemicals, such as flavonoids, saponins, alkaloids, anthraquinone, terpenoids and carotenoids, are also known as secondary metabolites that help in the treatment and other therapeutic benefits public health.[51] Another major bioactive constituent includes antioxidants demonstrating the oxidation process. This process involves free radical production. In a living system, food and drug, these free radicals are associated with most human diseases like ageing, diabetics, atherosclerosis, cancer, cardiovascular disorders etc.[52] Therefore, the use of plants, plants parts, agricultural wastes with potent phytochemicals can be of great value for utilising properly, such as for the synthesis of nanoparticles.

2.4. Background: Banana Peels as Agricultural waste

The consumption of bananas all over the world is very high due to their high food value. However, in general, banana peels are discarded after the pulp is being consumed. Literature study showed the utilization of the discarded banana peels in several ways. Mainly for medicinal use,[53] fermentation of ethanol,[54] fungal biomass generation,[55] laccase production[56] and as biosorbent for heavy metal removal.[57] In addition, banana peels are naturally loaded with polymers such as lignin, cellulose, hemicellulose, as well as pectin.[58]

Figure 2.2. *Musa balbisiana* Colla or locally called Bhimkol.

Musa balbisiana Colla is a banana variety of Musaceae family commonly cultivated in Assam, India.[59] It is considered as one of the parent plants with *Musa acuminate* Colla for the evolution of the indigenous cultivars of *Musa L*. The wild plants are no longer considered wild as this variety has been cultivated and domesticated for a long time in Assam. The local name of this banana variety is *Bhimkol* or *Athiyakol*. Bhimkol is a dietary supplement and is used for nutrition. Almost all parts of this banana variety are used in various ways in rituals and

food. As such are different traditional uses of Bhimkol as medicine and food in the northeastern part of India. The wide consumption of Bhimkol, availability of their peels around the household and biochemicals present in it, may be useful for the synthesis of AgNPs.

2.5. AIM AND OBJECTIVES

With this above literature background, attractive phytochemicals present and the availability of 'Bhimkol' (*Musa balbisiana Colla*) peel waste in this region, the following objectives are summarized below:

a) Study of the qualitative and quantitative phytochemical compositions of bhimkol (*Musa balbisiana*) peels at ripe, unripe and blacken stages of development. Both phytochemical tests were conducted to observed, which was the best stage for application in the synthesis of AgNPs.
b) Synthesis of AgNPs via the green route using 'Bhimkol' (*Musa balbisiana Colla*) peel extracts as bioreductant and stabilizing agent. It was carried out using the various concentration of the peel extract and $AgNO_3$ solutions.
c) These AgNPs were optimized under various conditions. For the standardization, effect of concentration of Peel Extract, effect of pH , effect of $AgNO_3$ concentration and the effect of reaction time were studied thoroughly.
d) Characterization of the AgNPs were carried out using by X-ray diffraction (XRD) method, DLS, TEM and FESEM techniques.
e) Study of the antibacterial activities of both bhimkol peel extract and green synthesized AgNPs were carried out using the disc diffusion method against both gram-positve and gram-negative bacteria respectively.

2.6. RESULTS AND DISCUSSION

2.6.1. Study of the Qualitative and Quantitative Phytochemical Compositions of Bhimkol (*Musa balbisiana*) Peels

There is no report of phytochemical tests on this variety of banana peels. Therefore, to know the various phytochemical constituents present in the three stages of development of bhimkol (*Musa balbisiana)* peels, the different phytochemical assays are performed. Secondary metabolites of plants are responsible for many therapeutic activities. Thus, the preliminary phytochemical analysis (Table 2.2) of the bhimkol peels showed that in all the three stages,

peels contained secondary metabolites such as glycosides, saponins, alkaloids, phenols, tannins and flavonoids. The presence of such phytochemicals confirms the medicinal value of the bhimkol peels. These are non-nutritive plant chemicals having some disease preventive properties. The presence of phenols in the peels indicated the richness in antioxidant properties. Also, due to the antimicrobial activity of phenolic compounds, it can be an active ingredient in antiseptics and disinfectants. The presence of phenol compounds contributes to the sensory, antioxidant properties and colouration of the food. In the test for phlobatannins, the red precipitate was more in the ripe and blacken stage of banana peels than the unripe stage of the peels. For flavonoid test, the yellowish colouration was observed to be in all the stage which indicated that the flavonoid is abundantly present in all the stage of peels. As flavonoids are naturally occurring phenols, the presence of flavonoids is considered to have antimicrobial activities. It also has good hydroxyl radicals, lipid peroxy-radicals, and oxide anions scavenging activities. The presence of alkaloids indicated the therapeutic and antimicrobial nature of the peels. These compounds can intercalate with the DNA of the microorganisms. Again, the presence of tannin showed the wound healing properties or its stringent properties of the peels. Therefore, though it is qualitative, the phytochemical tests suggested the presence of more components in the ripen state of banana peels than the other two stages (unripe and blacken). The reducing ability and the stabilizing property of ripen peels would be more compared to the other two stages.

Next, the quantitative phytochemical analysis of three different stages of development of Bhimkol(*Musa balbisiana*) peels was evaluated using the methods described. From the different phytochemical tests, it was observed that this variety of bananas has a high quantity of phytochemicals in its peels. As such, its potential utility is in the formation and stabilization of silver nanoparticles. The results of the quantitative analysis were presented in Table 2.3. From data in table 2.3, it was clear that all the three stages of development of bhimkol peel contained almost a similar quantity of alkaloids, saponin and tannin. There was a significant difference in flavonoids content among the three different stages of development. Moreover, the phenol content was found to be highest in the ripe stage compared to its unripe and black stage of the peels(Table 2.3). The antioxidants capacity of plants is firmly associated with phenol compounds. A major active ingredient in antiseptics and disinfectants is phenol due to its antimicrobial activity. In short, phytochemical analysis of bhimkol peels aqueous extract revealed the presence of alkaloids, flavonoids, and phenols, which are mainly responsible for the reduction of Ag^{+} to generate AgNPs. Moreover, the presence of phenols in the highest

quantity in the ripe stage of peels was expected to be more efficient in the generation of AgNPs by reducing more quantity of Ag^+ compared to the other two stages of development.

Table 2.2. Qualitative phytochemicals constituents of Bhimkol (*Musa balbisiana*) peels.

Phytochemicals	**Three Stages of Development of Bhimkol (*Musa balbisiana*) Peel**		
	Ripe Stage	**Unripe Stage**	**Blacken Stage**
Glycosides	+	+	+
Flavonoids	+	+	+
Saponins	+	+	+
Anthraquinone	-	-	-
Phlobatannins	+	+	+
Tannins	+	+	+
Phenols	+	+	+
Alkaloids	+	+	+

+ = Presence - = Absence

Table 2.3. Quantitative phytochemicals constituents of Bhimkol (*Musa balbisiana*) peels.

Peel Samples	**% Alkaloid**	**% Saponin**	**% Tannin**	**Phenol (mgGAE/g)[a]**	**Flavanoid (mgRE/g) [b]**
Unripe peels	2.83 ± 0.74*	5.11 ± 0.05*	0.14 ± 0.01*	8.12 ± 0.07*	33.33 ± 0.63*
Ripe peels	1.35 ± 0.33*	5.45 ± 0.11*	0.52 ± 0.02*	42.54 ± 0.02*	12.78 ± 0.48*
Black peels	1.27 ± 0.37*	6.06 ± 0.17*	1.23 ± 0.02*	23.64 ± 0.03*	97.33 ± 0.42*

[a]GAE = Gallic acid equivalent; [b] RE = Rutin equivalent; *mean total phytochemical content ± % standard deviation. All the values are represented in '% weight'.

2.6.2. Comparative Efficiency of Three Stages of Development of Bhimkol Peels for the Green Synthesis of AgNPs

The detailed study of the green synthesis of AgNPs was next carried out using BPE of all three stages. This variety of banana is available only in Assam, which is loaded with nutrients and phytochemicals. Thus, it could act as an excellent reducing as well as a stabilising agent for the formation and stabilization of AgNPs. Therefore, at first, a comparative analysis of the

synthesis of AgNPs was executed using unripe peel extract, ripe peel extract and blacken peel extracts. Thus, freshly prepared Bhimkol peels aqueous extracts, as mentioned under the section, material and methods were used as a reducing agent for the reduction of $AgNO_3$ to produce AgNPs. The formation of AgNPs was first visually observed by the colour change of the reaction (Fig. 2.3(i)) from yellow to yellowish-brown and then looking at the surface plasmon resonance (SPR) band of the Ag-NPs at 431 nm in the UV-visible spectra. Figure 2.3(ii) represents the UV-visible spectra of the synthesized AgNPs using unripe, ripe, and blacken bhimkol peel extracts. Ripe peel extract showed a very good SPR band at around 431 nm, which indicated the formation of more small-sized AgNPs. In the case of unripe peel extract, there was formation of AgNPs, but as the SPR band is low, there is the formation of lesser and large-sized AgNPs. Again in the case of blacken peel extract, no appearance of AgNPs was observed, which was confirmed by the UV-visible spectra. Therefore, it was observed that the ripe peel extract is the best among the other two stages of peels for the synthesis and stabilization of AgNPs as was evident from a stronger SPR band in the UV-visible spectra. The greater efficiency of the ripening stage is may be due to the presence of a high amount of phytochemicals, mainly phenolic compounds. These compounds can cause the dark colouration in plants. Most possibly, the mechanism of formation of AgNPs might be explained as follows. The Ag^+ ions could easily form phenolate complexes with phenols/polyphenols present in the aqueous extract of the peel and get reduced to Ag^0 leaving quinones as the oxidized products of phenols.

2.6.3. Green Synthesis of AgNPs

After establishing the fact that the ripening stage of banana peel extract is efficient most for the synthesis of AgNPs, the detailed study of the green synthesis of AgNPs using ripen Bhimkol peels aqueous extract was performed. Thus, the optimization of the synthetic route for the development of AgNPs was tested first. The amount of banana peel extract (BPE) varied from 1-50% v/v of a total solution of 100 mL. The concentration of $AgNO_3$ solution was varied from 0.25 to 2 mM. Further, the pH and the reaction times were also varied to test the maximum AgNPs formation. The reduction of Ag^+ ion, *i.e.*, the formation of AgNPs was monitored by the colour change of the solution from yellow to yellowish-brown using UV-visible spectroscopy. Figure 2.3(i) shows the physical change, *i.e.*, colour of the synthesized silver nanoparticles in the colloidal form. The silver ion from the silver nitrate salt was reduced into metallic silver by banana peel extract. Banana peels contain mainly cellulose, phenols, alkaloids, glycosides, pectin, lignin and proteinaceous matter, which was evident from the

phytochemical test especially involved in silver ion reduction to afford AgNPs. For the standardization, we sequentially tested the (a) effect of concentration of BPE, (b) effect of pH, (c) effect of $AgNO_3$ concentration and (d) the effect of reaction time.

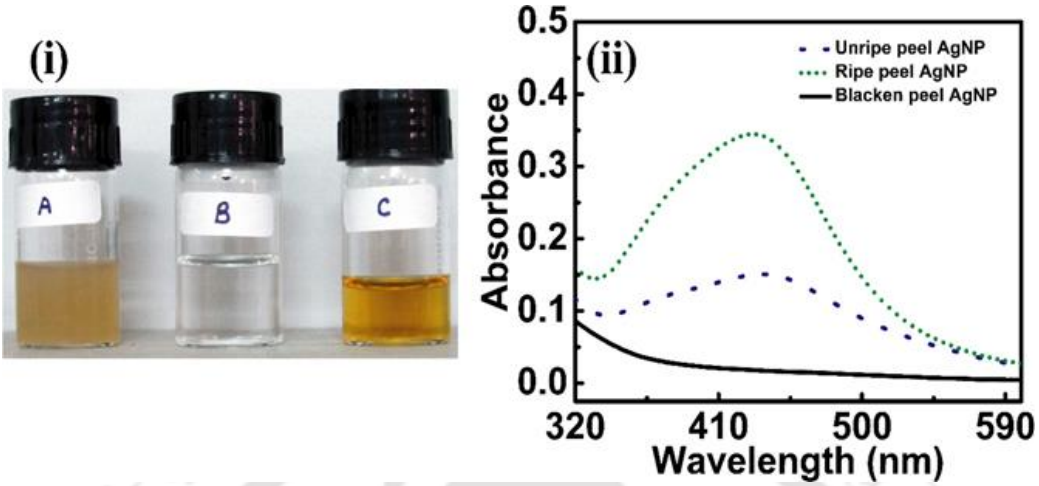

Figure. 2.3. (i) Vials containing samples of (A) only banana peel (ripen stage) extract, (B) only silver nitrate solution (1 mM), and (C) produced AgNPs in colloidal form (transparent yellowish-brown). (ii) UV-visible spectra of AgNPs synthesized using unripe, ripe, and blacken bhimkol peel extracts.

2.6.3.1. Effect of Concentration of BPE

The effect of concentration of BPE on the synthesis of AgNPs formation was studied first. Thus, firstly reduction of 1 mM $AgNO_3$ solution with BPE varying the overall concentration of the reaction mixture from 1-50% was carried out. The formation of AgNPs was monitored using a UV-visible spectrophotometer (Perkin Elmer Lambda-45), monitoring the characteristic surface plasmon absorption band at around 435- 441 nm. Figure 2.4(a) represents the UV-visible absorption spectra for reducing 1mM AgNO3 solution in the presence of 1-50% v/v of banana peel extract (BPE), keeping the total volume of the reaction mixture 100 ml.

From the graph in figure. 2.4(a), it is clear that the formation of AgNPs is better in 9% BPE, which showed the highest intensity in UV-visible spectra amongst all other reaction mixtures studied. The intensity in UV-visible spectra was directly proportional to the formation of AgNPs. SPR band intensity was found to increase from 1 to 9% and then it started decreasing to 50% BPE. The increase in SPR band intensity from 1 to 9% BPE is due to the formation of more and more AgNPs because of the high initial concentration of Ag^+ ions. The regular decrease in SPR band intensity with peak broadening from 10 to 50% supported the formation of large-sized AgNPs. According to Mie's theory, only a single SPR band was expected in the absorption spectra of spherical metal nanoparticles. A single SPR band at 438 nm was

observed, which suggested spherical shaped AgNPs formation. Thus, from this experiment, it can be considered that the optimum formation of spherical shaped AgNPs is when BPE concentration was 9% of the total volume of the reaction solution (100 mL). For all other studies, 9% BPE concentration was considered as the optimum.

2.6.3.2. Effect of pH

Next, the effect of pH on the formation of AgNPs was studied with the help of UV-visible absorption spectra taking 1mM $AgNO_3$ and 9% BPE for a total reaction volume of 100 ml. From figure. 2.4(b), it can be concluded that the formation of Ag-NPs is optimum when the pH was 6.24; the absorption peak was observed between 435-441. In a strongly acidic medium (pH 3), the reaction mixture does not show a prominent absorption band when analyzed even after 1 hour of reaction. Thus, there was no or negligible formation of AgNPs in a strongly acidic medium (pH 3). The slow rate of formation and aggregation of AgNPs at pH 3 could be related to the electrostatic repulsion of anions present in the solution. On the other hand, in basic medium (pH 8), the reaction was immediate and the color of the reaction mixture became black. It did not show the absorption in the range of 400 to 450nm. This is maybe because of the precipitation of Ag^+ ions as AgOH in strongly alkaline pH. Therefore, the $AgNO_3$ solution in MQ water (pH 6.24) was considered as the best for the formation of optimum AgNPs.

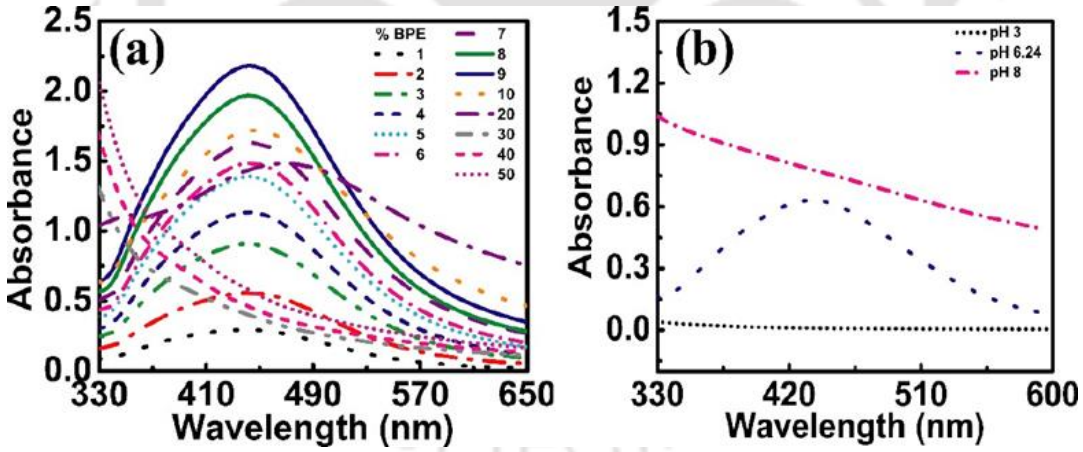

Figure. 2.4. (a) UV-visible absorption spectra for the formation of Ag-NPs from 1mM $AgNO_3$ with varying concentrations of BPE (1-50% of the total volume of reaction mixture 100 ml) in neutral double-distilled water. (b) UV-Vis spectra for the formation of AgNPs 1mM $AgNO_3$ and 9 % BPE solution under three different pH.

2.6.3.3. Effect of $AgNO_3$ Concentration

To know whether the concentration of initial $AgNO_3$ has any role in optimum formation of spherical shaped AgNPs, the effect of concentration of $AgNO_3$ was evaluated using UV-visible

spectroscopic studies. As the concentration of $AgNO_3$ solution increases, the formation of AgNPs also increases. From figure 2.5(a), it is clear that the formation of AgNPs was high in 1.5-2 mM, moderate in 1 mM and less in 0.25 mM concentration of $AgNO_3$ using 9% BPE. However, the size and shape of the AgNPs formed were higher in the case of a high concentration of $AgNO_3$ (1.5-2 mM) compared to the case of 1mM $AgNO_3$ solution, as was initially indicated by the absorption spectra in fig. 2.5(a). The UV-visible spectra revealed that the spherical shape of AgNPs of fair particle size was formed while using a 1mM $AgNO_3$ solution. There was the least formation of AgNPs in 0.25mM concentration might be due to the very less concentration of $AgNO_3$ solution used for the reaction. Therefore, the concentration of 1 mM $AgNO_3$ was utilized for further preparation of AgNPs and considered as optimum concentration.

2.6.3.4. Effect of Reaction Time

The optimum reaction time for the formation of AgNPs of fair size and shape was studied using 1 mM $AgNO_3$, 9% BPE in neutral pH (MQ water) and by monitoring the reaction under UV-visible spectroscopy. The reaction mixture was incubated at 25°C and UV-visible spectra were recorded from time to time. The intensity of the colour change was directly proportional to the incubation time of the reaction mixture. From figure 2.5(b), it is clear that the rate of reduction of Ag^+ by the BPE, *i.e.*, the formation of AgNPs was increased slowly as the incubation time was increased from 30 minutes to 198 hours. The increase in absorbance monitored at 431 nm, also deepness of colour was observed from yellow to yellowish-brown. Maximum reduction was obtained between 126-198 hours, which was considered the optimum time for the optimum formation of spherical shaped AgNPs of fair size.

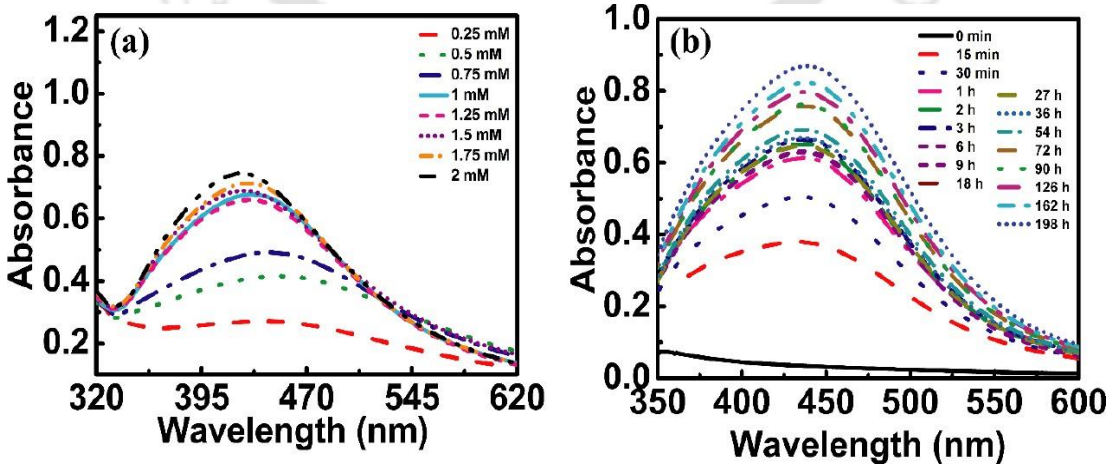

Figure 2.5. UV-Vis spectra for the formation of AgNPs showing (a) the effect of concentration of $AgNO_3$ solution and (b) the effect of reaction time.

However, for practical purposes, 1 hr is regarded as the standard time for the synthesis of AgNPs. The above study concluded that under the condition of 9% v/v BPE in a 100 ml solution of 1 mM $AgNO_3$ under neutral aqueous pH and at about 168 hours incubation time at 37°C, the maximum formation of AgNPs of fair size and spherical was accomplished. Therefore, under neutral aqueous media, this was considered an optimized condition for the synthesis of AgNPs. Using this optimized reaction condition, the AgNPs were synthesized, characterized, and utilized for further studies.

2.6.4. Characterisation of AgNPs

2.6.4.1. Fourier Transform Infrared (FTIR) Analysis

Fourier Transform Infrared (FT-IR) spectra were recorded in a Perkin Elmer FT-IR Spectrophotometer (Model no: Perkin Elmer Spectrum 2, USA) to determine the functional group present in the Bhimkol peel extract alone and in the as-synthesized AgNPs. Band intensities in different regions of the spectrum for the BPE and AgNPs were analyzed and are shown in figure 2.6**.** FT-IR data of banana peel extract showed carbonyl, -OH, - phenolic-OH, -COOH and amide functional groups. We observed the bands at 3443, 2075.71, 1633 and 667 cm-1 in the peel extract in the FT-IR. These bands shifted to 3436, 2075.99, 1633.89 and 598 cm^{-1}, respectively. The strong and broad absorption peak at around 3443 cm^{-1} corresponds to the N-H stretching vibrations of amines. This peak also corresponds to the O-H (H-bonded) stretching vibrations of phenols and carboxylic acids. The shift from 3443 to 3436 cm^{-1} indicated the involvement of the O-H functional group in the synthesis of AgNPs.

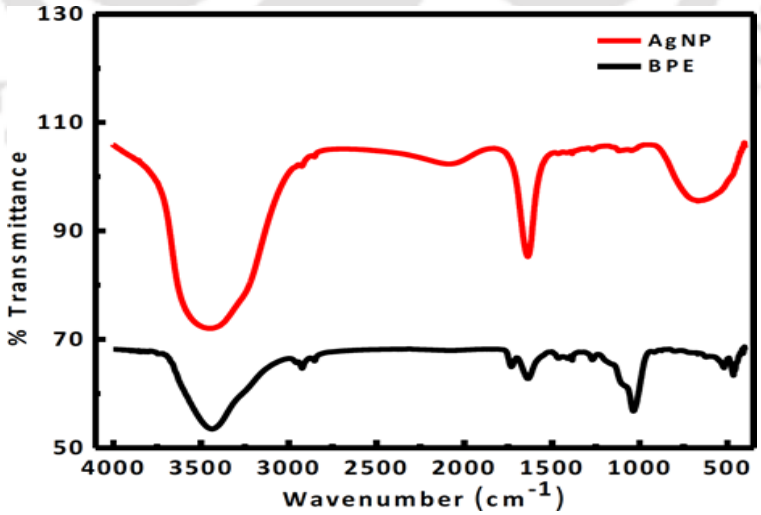

Figure. 2.6. FTIR spectrum of Banana peel extract (BPE) and AgNPs bio-reduced by BPE.

The peak located at around 2075 cm^{-1} corresponded to the C-O stretching vibrations. The peak shift from 2075.71 to 2075.99 cm^{-1} showed that the functional groups are involved in

synthesizing and stabilizing nanoparticles. The peak at 1633 cm^{-1} was attributed to the C=O stretching in carboxyl or C=N bending vibration in the amide group. The peak at 667 and 598 cm^{-1} corresponds to the C-H stretching of the aromatic group. The shifts in the peak highlighted the involvement of functional groups of BPE in the reduction of silver salt (Ag^{+}) to metallic silver (Ag^{0}) and involved in stabilization. Thus, the amide groups and COOH groups and the phenols act as ligands to synthesis and stabilzing the nanoparticles.[60,61]

2.6.4.2. Field Emission Electron Scanning Microscopy (FESEM) Analysis

Next, the FESEM analysis was carried out to understand the microstructure of synthesized AgNPs, which is shown in figure. 2.7. The analysis was carried out in ZEISS GEMINI OXFORD Instruments X-MAX^{N} with a data acceleration voltage of 0.02 to 30 kV. All the particles were spherical in morphology and the diameter of mostly monodispersed AgNPs was in the range of 30-70 nm with an average size of 44.24 nm. Image J software was used for measuring the diameter of the nanoparticles. There was a homogenous distribution of nanoparticles, but slight agglomeration was also observed as few bigger nanoparticles were present.

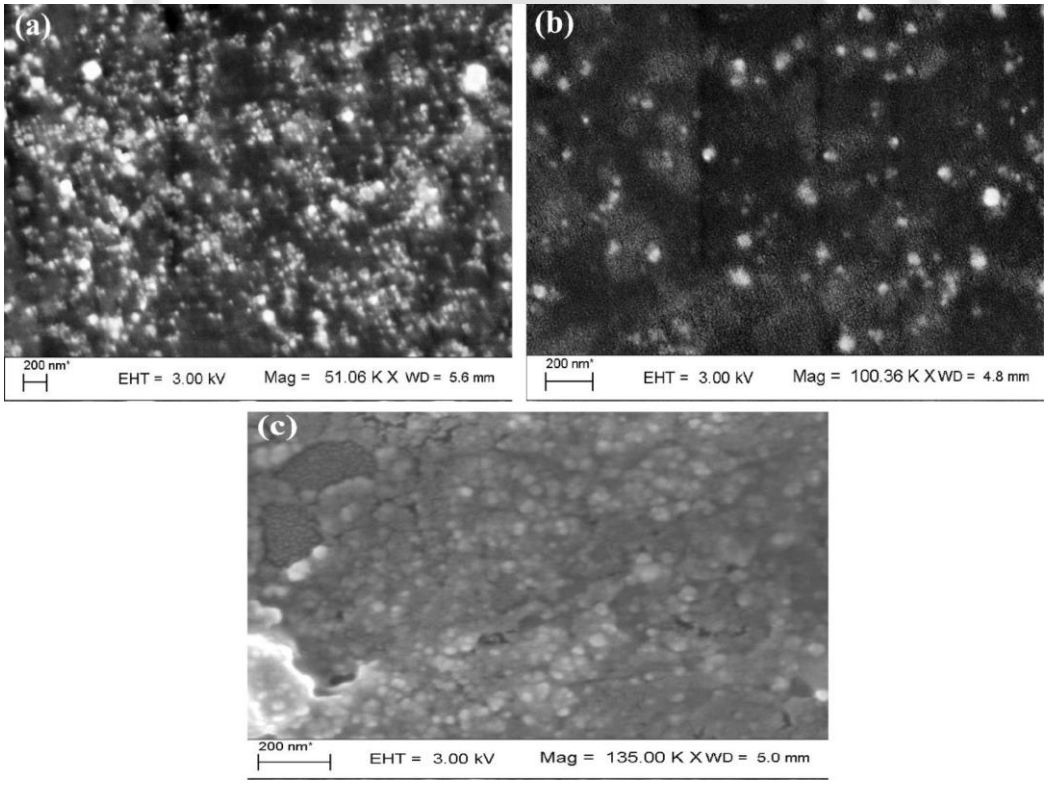

Figure. 2.7. Microstructures of synthesized AgNPs (9% reaction mixture of BPE and 1mM $AgNO_3$ solution at pH 6), (a) magnified 51,000x inset bar represented at 200nm resolution, (b) magnified 100,000x inset bar represented at 200 nm resolution and (c) magnified 135,000x inset bar represented at 200nm resolution.

2.6.4.3. Transmission Electron Microscopy (TEM) Analysis

The size and shape of the synthesized AgNPs were illuminated with the use of transmission electron microscopy. Diluted aliquots of AgNPs solution were put on a carbon-coated copper grid and dried under ambient conditions for TEM analysis. TEM micrographs revealed that the particles were monodispersed in nature with a size of around 40-50 nm. The shape of AgNPs mainly was spherical, supporting the results obtained from FESEM. The crystalline structure of the AgNPs was marked by the selected area electron diffraction (SAED) patterns with circular bright dots (Figure. 2.8).

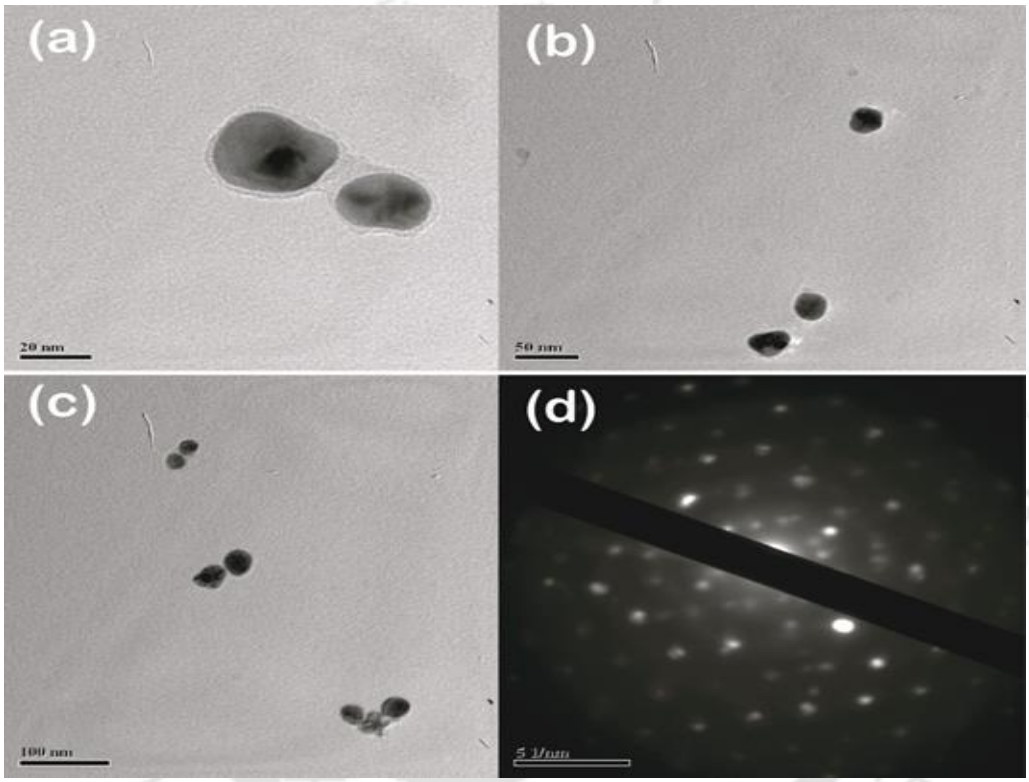

Figure. 2.8. Micrographs of TEM images of green synthesized silver nanoparticles using the Bhimkol peel extract. Transmission electron microscopy images of AgNPs (a) at 20 nm resolution, (b) at 50 nm resolution, and (c) at 100 nm resolution, (d) SAED pattern of the crystalline structure of silver nanoparticles.

2.6.4.4. X-ray Diffraction Analysis

X-ray diffraction (XRD) was used to illustrate the crystallographic structure, grain size, and orientation in polycrystalline or powder samples. Thus, the crystalline nature of AgNPs was confirmed by XRD analysis. Figure. 2.9(a) showed the patterns observed by XRD of synthesized AgNPs. Thus, the synthesized AgNPs showed Bragg's reflection peaks at 2θ range- 38.12°, 44.24°, 64.44°and 77.38°. These peaks are assigned to (111), (200), (220) and (311) planes respectively of a face-centered cubic (fcc) lattice of silver. These diffraction peaks

are compared to the standard diffraction pattern of JCPDS No 04-0783 and observed that synthesized AgNPs were composed of pure crystalline silver. The peak at (111) plane was more intense than other planes indicating the crystalline nature of the nanoparticles and its predominant orientation.

2.6.4.5. Particle Size Distribution

The particle size distribution of AgNPs was measured by dynamic light scattering (DLS) experiments. DLS instrument measures the shell thickness of a stabilizing or capping agent, enclosing the particles with the actual core size. The size (diameter) *vs*. intensity graph was shown in figure 2.9(b). The particle size distribution curve reveals the average size of AgNPs obtained from *Delsa*^{tm} *Nano C Particle Analyzer* was 53.4 nm from the cumulative result and 88.9 nm from the distribution result. The measured size of the particles using DLS was moderately bigger than that found from the FESEM and TEM measurement, which is probably due to the hydrodynamic radius of particles measured in the DLS method. The larger particle size observed was possibly due to the size of the bio-organic compounds inclosing the core of the AgNPs. DLS measurement indicated the polydisperse nature of the particles, which is due to the green synthetic process using biomaterials. For this reason, the poly-dispersity index (P.I.) of the green synthesized AgNPs was found to be 0.312 *i.e.*, the DLS measurement showed 31.2 % poly-dispersity of the particles (Fig. 2.9(b)) which is in good agreement with FESEM and TEM results.

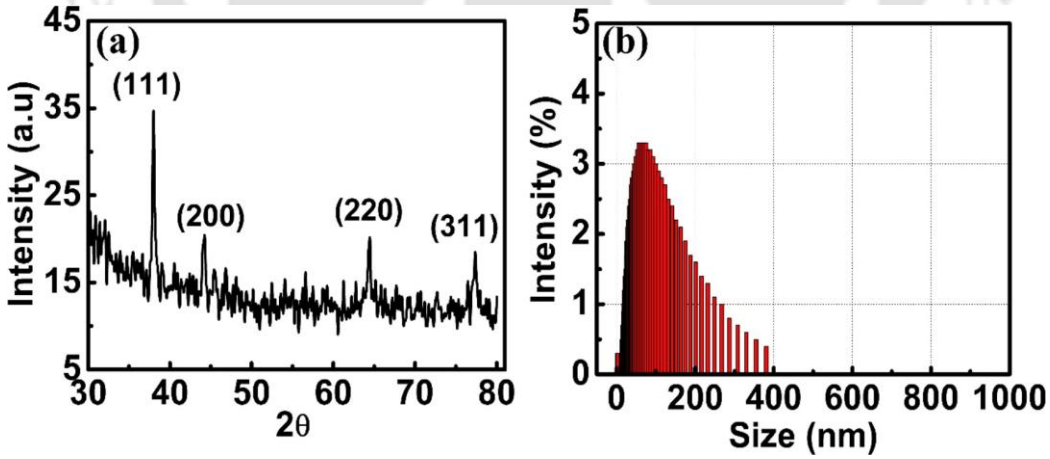

Figure. 2.9. (a) X-ray diffraction pattern and (b) DLS measurement of the biosynthesized silver nanoparticles.

2.6.4.6. Energy Dispersive X-ray (EDX) Analysis

In the formation of AgNPs, EDX analysis detects the quantitative and qualitative status of elements present. The formation of AgNPs was confirmed by the elemental profiling of these

nanoparticles and represented in figure 2.10(a). At 3 keV, the counts showed highest due to silver, and it indicated the formation of AgNPs. Metallic silver nanocrystals showed the optical absorption peak at 3 keV, which may be due to the surface plasmon resonance (SPR). The elemental analysis of AgNPs showed the highest proportion of silver followed by Cl, C and O.

2.6.4.7. Zeta Potential (ZP) Measurement

Zeta potential is considered as an essential parameter to determine the particle surface charge and its stability. The zeta potential value of the prepared AgNPs was found to be –30.86 mV and displayed in figure 2.10(b), indicating a strong negative charge on the surface of these nanoparticles and the nanoparticles were dispersed in the medium. The negatively charged particles exert a robust repulsive interaction among the particles, prevent potential aggregation of the particles, and offer them long-term stability. Zeta potential of the nanoparticles, thus, supported the reasonable stability of the nanoparticles. The negative potential value shown by biosynthesized AgNPs could be due to the presence of bio-organic components in the extract.

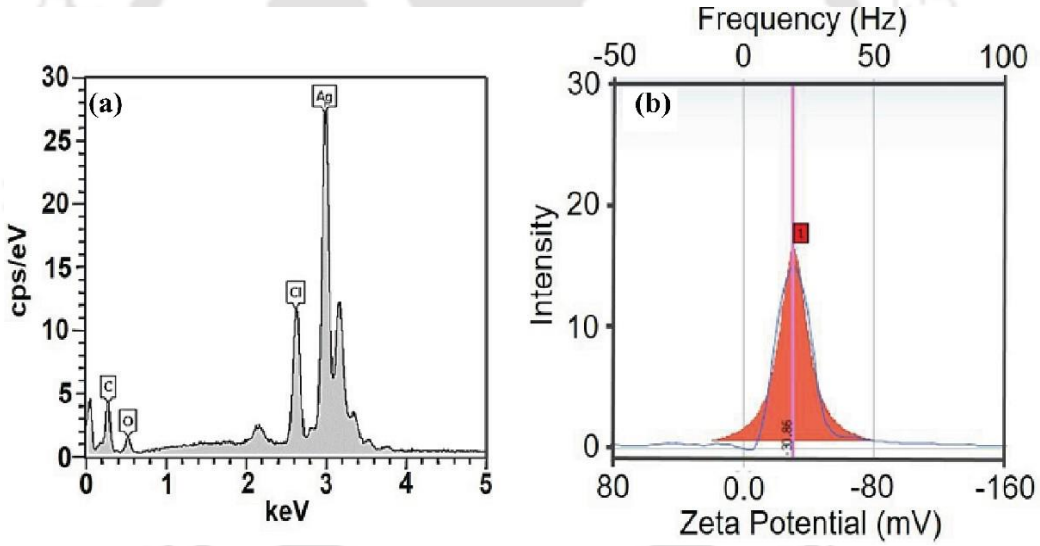

Figure 2.10. (a) EDX elemental profile and (b) Zeta potential of silver nanoparticles.

2.6.5. Study of the Antibacterial Activity of Both Bhimkol Peel Extract and AgNPs Synthesized by Using Bhimkol Peels

2.6.5.1. Zone of Inhibition Assay

The antibacterial activity of the Bhimkol peel extract, as well as the AgNPs synthesized from Bhimkol peel extract, were tested against Gram-negative bacteria (*Escherichia coli)* (MTCC strain no. 1696) and gram-positive bacteria (*Bacillus subtilis*)(MTCC strain no.441). The mean inhibitory zone of diameter was measured and tabulated (Table 2.4). In both Gram-

negative and gram-positive bacteria, no zone of inhibition was observed in the case of the peel extract samples. In contrast, a clear zone of inhibition was observed for the AgNPs synthesized from the peel extract (Fig. 2.11(a-b**)**). The zone of inhibitions was represented in mm in Table 2.4. The high antibacterial activity was mainly due to the silver cations released from Ag nanoparticles that act as reservoirs for the Ag^+ antibacterial agent. The change in the membrane structure of bacteria appears due to the interaction with silver cations leading to increased membrane permeability. From the results, it was found that the 50 µL of AgNPs offered a higher antibacterial effect compared to others (Table 2.4, Fig. 2.11(c-d)). Table 2.5 represents the zone of inhibitions by multi antibiotic discs against *E.coli* and *B.subtilis* for comparative study with the zone of inhibition formed by using AgNPs (Table 2.5, Fig. 2.11(e-f)). Overall, the AgNPs showed moderate antibacterial activity against gram-negative and gram-positive bacteria but less than multi antibiotic discs.

Table 2.4. The different zone of inhibition of AgNPs against *E. coli* and *B. subtilis*.

Green Synthesized Silver Nanoparticles (AgNPs)	**Zone of Inhibition (Diameter in mm)**	
	E. coli	***B. subtilis***
10 µL	8	7.5
50 µL	17	15
Dipped in AgNP solution	16	10

Table 2.5. Multi antibiotic disc representing the zone of inhibitions against respective microorganisms.

Multi Antibiotic Disc (Hexa G Negative-29 Against *E. coli*)	**Zone of Inhibition (Dia. mm)**	**Multi Antibiotic Disc (Hexa G Positive-6 Against *B. subtilis*)**	**Zone of Inhibition (Dia. mm)**
GEN 10	25	C 25	32
TE 30	24	P 1	22
CIP 5	30	S 10	-
CN 30	29	S3 300	33
COT 25	30	TE 25	32
AMP 10	20	AMP 10	16

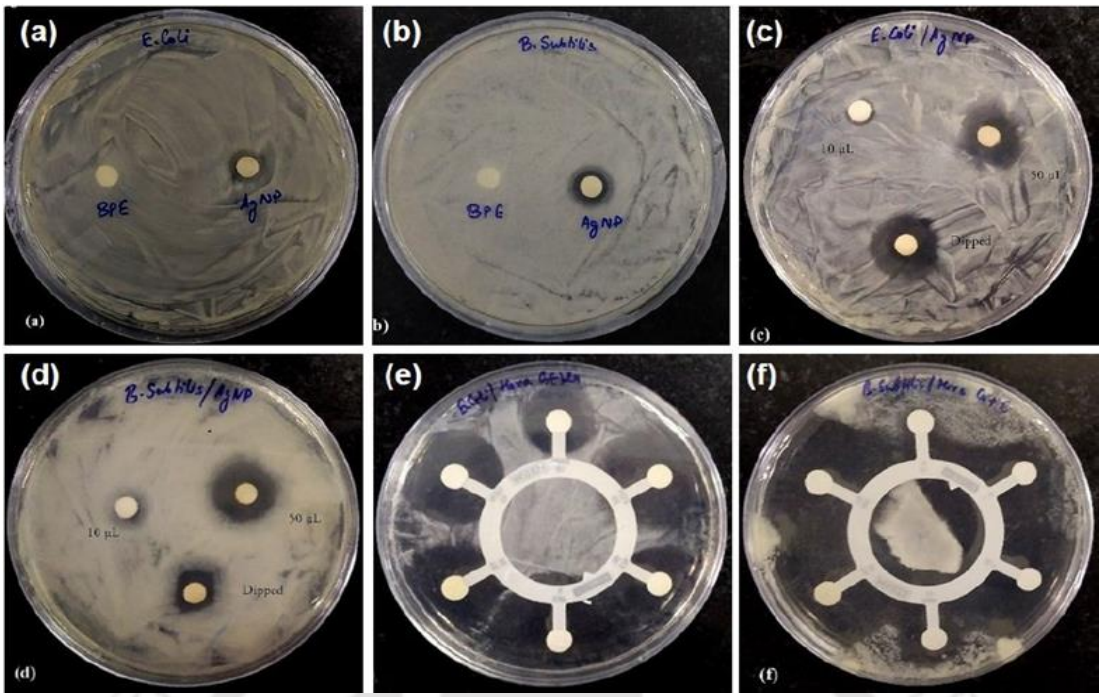

Figure 2.11. Antibacterial activity of Bhimkol peel extract (BPE) and AgNP(10 µL) against (a) *E. coli* and (b) *B. subtilis*. Zone of inhibition was observed against (c) *E.coli* and (d) *B. subtilis* using 10 µL AgNP, 50 µL AgNP, and dipping the discs in AgNP solution. (e) Zone of inhibition was observed against *E.coli* by Hexa G-negative 29 multi antibiotic discs, (f) Zone of inhibition were observed against *B.subtilis* by Hexa G- positive six multi antibiotic discs.

2.7. CONCLUSION

Silver nanoparticles were synthesized using waste bhimkol peel extract *via* the green route. A qualitative and quantitative analysis of phytochemical composition was also carried out for the three different stages of development of the peels, for the first time. Synthesis of AgNPs was also carried out using all three stages (ripe, unripe, and blacken) of the development of peels. The ripe peels were best for the consideration of the AgNPs synthesis in high yield because of the presence of the highest amount of phenolic components. Various spectroscopic and imaging techniques were used for the characterizations. The average size of the nanoparticles formed was around 44 nm, as indicated by TEM and FESEM images. The synthesized AgNPs showed moderate antibacterial activity against both gram-negative bacteria and gram-positive bacteria. The advantage of our method lies in the fact that waste peels material can be utilized both for the generation and stabilization of AgNPs. The banana peel-mediated synthesised AgNPs are utilized further for the preparation of wound healing gel in this thesis.

2.8. EXPERIMENTAL SECTION

2.8.1. Materials and Methods

2.8.1.1. Materials

The banana peel extract (BPE) was prepared using locally available banana variety, i.e., Bhimkol (*Musa balbisiana*) peels obtained from Amingaon Market, Guwahati, Assam. Initially, ripe banana peels were used to prepare the extract and this extract was used for further experiments. Three stages of peels such as ripe, unripe and rotten peels, were also collected and tested, compared the formation of AgNPs in each stage. Silver nitrate ($AgNO_3$) used as a precursor of AgNPs was purchased from Sigma-Aldrich, India. Luria-Bertini(LB) broth, Luria Berini agar, Nutrient agar, Nutrient broth, Protease peptone, and Agar required for antimicrobial testing were purchased either from Himedia, India. Double distilled water was used for all experimental purposes. All the glassware was properly washed and dried in an oven before use. Representative microorganisms of Gram-negative bacteria (*Pseudomonas aeruginosa and Escherichia coli)* and a gram-positive bacteria (*Bacillus subtilis*) were used to evaluate the antibacterial activity of synthesized AgNPs. Bacterial strains were maintained on LB broth and LB agar plates at 4°C.

2.8.1.2. Preparation of Banana Peel Extract (BPE)

Fresh bananas (*Musa balbisiana*) were washed repeatedly with distilled water to remove dust particles and impurities present on the peels. Peels were then removed, air-dried, and then cut into small pieces. About 5 g of peels were taken in a conical flask containing 100 mL double distilled water and then this solution was kept in a shaking water bath at 80°C for 1 hour at 90 rpm. The resultant solution was filtered through muslin cloth then with Whatman No. 1 filter paper twice. The resultant filtrate was stored at 4°C and used as a reducing as well as a stabilizing agent for further experiments.

2.8.1.3. Synthesis of AgNPs

AgNPs were synthesized *via* the green route using BPE. Thus, the biological reduction of $AgNO_3$ was carried out initially as follows: To optimize the synthesis route for the development of AgNPs, the reaction solution concentrations varied from 1-50%. The varying amount of BPE (1 mL-50 mL) was added to 99 mL-50 mL of 1mM aqueous $AgNO_3$ solution to make the volume of reaction solution 100 mL respectively. The reaction mixture was kept in the dark at 25°C to avoid any photo-activation of $AgNO_3$ under inert conditions. BPE and $AgNO_3$ solution (1 mM) was used as control. The reduction of silver ions started within 15 minutes, which was

physically observed with the colour change of the solution. The yellowish-brown color was observed after 30 minutes, indicating the formation of AgNPs. Optimization for the development of AgNPs under different conditions such as variation in $AgNO_3$ concentration, time and pH was also reported.

2.8.1.4. Preparation of Buffers

The acidic buffer (pH 3) was prepared using citric acid and disodium hydrogen phosphate. Thus, 39.8 mL of 0.1M aqueous citric acid solution and 10.2 mL of 0.2M aqueous Na_2HPO_4 solution were taken in 100 mL volumetric flask and diluted up to the mark with distilled water. The mixture was mixed well, and the resultant solution's pH was verified using a pH meter showing the pH of the solution as 3. This solution was further used in the optimization part of the experiment as an acidic buffer of pH 3.

Basic sodium phosphate buffer (pH 8) was prepared using Na_2HPO_4 and NaH_2PO_4. Thus, 93.2 mL aqueous Na_2HPO_4 solution (1M) and 6.8 mL aqueous NaH_2PO_4 solution (1M) was taken in 1000 mL standard volumetric flask and diluted the mark with distilled water. The mixture was mixed well, and the pH of the resultant solution was checked on a pH meter showing the pH of the solution as 8. This solution was further used in the optimization part of the experiment as a basic buffer of pH 8.

2.8.2. Characterizations of AgNPs

2.8.2.1. UV–visible Spectroscopy

The reduction of pure silver ions into AgNPs was monitored using UV–visible spectroscopy at regular intervals. The nanoparticles were primarily characterized by UV-visible spectroscopy, which is a very useful technique for the analysis of nanoparticles. The spectra were obtained using a Perkin Elmer precisely Lambda 45 UV-visible spectrophotometer using Tungsten-halogen and Deuterium interface with a 1 cm path length cell. The measurements were done in absorbance mode using 10 mm Quartz cuvette. 3 mL of sample was used for the experiments. The sample solutions' absorbance values were measured in the wavelength range of 200–700 nm. All the sample solutions were prepared freshly just before doing the experiment.

2.8.2.2. FT-IR Spectroscopy

FTIR is carried out using FT-IR Spectrophotometer (PerkinElmer Spectrum 2, USA) and a ATR (attenuated total reflection) sampling instrument. ATR can directly observe solid or liquid samples without additional preparation. The FT-IR spectra of the BPE and green synthesized

AgNPs were collected at a resolution of 4 cm^{-1} in the transmission mode from 4000 cm^{-1} - 400 cm^{-1} wavenumbers. Only a drop of the colloidal sample is casted in the sample holder. The functional groups present in the peel extract, which are responsible for the reduction of silver ions as well as a stabilizer of formed nanoparticles was identified with the help of FT-IR spectroscopy.

2.8.2.3. Field Emission Scanning Electron Microscopy (FESEM)

Field emission scanning electron microscopy(FESEM) analysis was carried out in Zeiss Gemini Oxford Instruments X-MAXN^{N}. This system has an accelerating voltage of 0.02 to 30 kV and a high magnification range of up to 200kx. Field Emission Scanning Electron Microscopy (FESEM) was used for the microstructural analysis of the synthesized AgNPs. The shape and diameter of the synthesized nanoparticles were studied with the help of FESEM data.

2.8.2.4. Transmission Electron Microscopy (TEM)

Transmission electron microscopy(TEM) analysis was carried out using the JEOL model JEM2100 Field Emission Transmission Electron Microscope. Electron microscopy parameters were set at a 1.4 Å (lattice) resolution and 1.94 Å (point to point). All images and analyses were obtained at 200 kV accelerating voltage. In the process, three magnification modes (at 200 kV) were maintained at: Standard magnification mode: 2,000× to 1,500,000×; Selected area magnification mode: 2,000× to 1,500,000×; Low magnification mode (LOW MAG): 50× to 1,000×. SAED camera length was controlled at 8 to 20 cm. The HR-TEM images were obtained by selecting ultra-high resolution (URH) pole pieces in the objective lens. The objective aperture sizes are 20, 40, 60 and 120 µm in diameter. SAD aperture sizes are 10, 20, 50 and 100 µm in diameter. In Low-Mag mode, the objective lens was turned off, and the objective mini-lens were made active. TEM is an imaging technique in which the electron beam is focused on a sample specimen, which enlarges the image of the sample in a fluorescent screen of photographic film. Transmission electron microscopy (TEM) was used to know the size and structure of AgNPs precisely and support the results obtained by FESEM.

2.8.2.5. Electron Diffraction X-ray (EDX) Analysis

Energy dispersive X-Ray(EDX) analysis is measured using Zeiss Gemini 300 made of Carl Zeiss. This system images at a very high resolution, *i.e.*, 0.8 nm at 15 kV and 1.4 nm at 1 kV. Electron Diffraction X-ray (EDX) analysis in-situ in the FESEM machine was utilized to know the status of elements involved in the formation of nanoparticles.

2.8.2.6 Dynamic Light Scattering (DLS)

Particle size distribution was measured by dynamic light scattering(DLS) in a Delsa^{tm} Nano C Particle Analyzer from Beckman Coulter. Delsa^{tm} Nano is used to measure the zeta potential and the submicron size analysis from about 0.6nm to 7.0 micron with forward 15° and backscatter 165°. The average size of AgNPs in an aqueous medium was used to determine the hydrodynamic diameter using Dynamic Light Scattering (DLS) technique. Zeta potential analysis was carried out to measure the polydispersity index and stability of synthesized AgNPs.

2.8.2.7. X-ray Diffraction (XRD) Analysis

Crystallinity and phase of the synthesized nanoparticles were studied through X-ray Diffraction. The instrument used for this analysis was Rigaku make Micromax-007HF diffractometer. The XRD patterns were measured at 50 kV and 100 mA using Cu Kα radiation with x-ray wavelength λ = 1.5406 Å. An R-AXIS IV++ x-ray detector was used to detect the diffracted x-rays. The scanning velocity was fixed at 2^{o}/min, and the diffraction pattern was recorded in the angular 2θ range 30°-80°. It provides details of the lattice structures of crystalline substances. X-Ray Diffraction results showed the crystalline/amorphous nature of the nanoparticles under study.

2.8.2.8. Study of Antibacterial Activity

The antibacterial activity of synthesized AgNPs and BPE was tested against gram-negative (*Escherichia coli)* (MTCC strain no. 1696) and gram-positive (*Bacillus subtilis*)(MTCC strain no. 441) bacteria using agar disc diffusion method. Approximately, 15 mL of autoclaved LB agar media was poured into each of the sterilized Petri dishes in a laminar airflow system. The plates were then sealed with paraffin strips, allowed to dry, and left overnight at 4°C temperature. The LB agar plates were precisely spread with the respective bacteria, and the discs containing the solution of AgNPs and BPE were put into the plates. The agar plates were then incubated at 37°C for 12-24 hrs. After the incubation period, the zone of inhibition (in mm diameter) was observed and tabulated.

2.8.3. Qualitative/Quantitative Phytochemical Analysis of Bhimkol (*Musa balbisiana*) Peels

The bhimkol (Musa balbisiana) samples were both analyzed for tannins, phenols, glycosides, flavonoids, saponins, anthraquinone, alkaloids, and phlorotannins qualitatively and quantitatively using standard literature procedures.

2.8.3.1. Test for Saponin

Bhimkol peel samples of 20 mg were boiled in 20 mL of distilled water in a water bath for 5 minutes and filtered. 10 mL of the filtrate was mixed with 5 mL of distilled water and shaken vigorously for froth formation. The emulsion test is a screening test for checking the ability of the formation of emulsion with oil due to the presence of saponin. Thus, 3-5 drops of olive oil were mixed with froth, shaken vigorously and observed for emulsion development. The formation of a stable emulsion indicates the presence of saponin.

2.8.3.2. Estimation of Saponin

Saponin was quantified using the process as described below. 20 g of the peel sample was crushed, then 20% aqueous ethanol (100 mL) added. The sample solution was allowed to stir continuously and heated at around 55°C on a hot water bath for about 4 hours. Then the sample mixture was filtered and the residue was extracted again with 20% ethanol (200 mL). The total extracted solutions were reduced to about 40 mL over a water bath at about 90°C. 20 mL of diethyl ether was added to the concentrated sample solution and vigorously shaken in a separating funnel. The aqueous layer was discarded, 20 mL of diethyl ether was added for the purification process. Then about 60 mL of n-butanol was added to the purified sample solution in a separating funnel and shaken again. The bottom layer was discarded and the upper layer recovered. The total n-butanol sample extracts were washed twice with 5% aqueous sodium chloride (10 mL). The excess sodium chloride containing layer was discarded and the residual solution was heated. Samples were dried in the oven to obtain a constant weight, and the saponin content was calculated as percentage weight using the formulae below and tabulated. The experiment was repeated thrice with three varieties of peel samples.[48]

$$\% \text{ Saponin} = \frac{W_2 - W_1}{Weight\ of\ the\ sample} \times 100$$

W_2 = weight of crucible + Sample after oven drying.

W_1 = weight of empty crucible,

Weight of peel sample = 20g

2.8.3.3. Test for Flavonoids

50 mg of filtrate peel extract was suspended in 100 mL of distilled water. Diluted ammonia solution of 5 mL was added to 10 mL of filtrate then a few drops of concentrated H_2SO_4 were added. Yellow colouration in the solution indicated the presence of flavonoids.

2.8.3.4. Estimation of Flavonoids

Total flavonoid content was quantified using the method described by Payum *et al.*, with slight modification.[62] About 50 mg of peel sample was dissolved in 80% aqueous methanol (10 ml) and filtered using Whatman filter paper No. 42. Then 0.3ml of methanolic peel extract was added to 3.4 mL of 30% methanol. Again 0.5 M sodium nitrite (0.15 mL) and 0.3 M aluminium chloride hexahydrate (0.15 mL) solutions were added later and thoroughly mixed. The total mixture was allowed to stand for 5 minutes and then 1 M sodium hydroxide (1 mL) solution was added. The absorbance of the solution mixtures was measured at 510 nm using a UV-Vis spectrophotometer. The values were described as Rutin equivalent antioxidant capacity. Linear calibration curves of rutin were produced with $R^2 = 0.9919$ and the values were tabulated. The experiment was repeated thrice with three varieties of peel samples.

2.8.3.5. Test for Glycosides

Few drops of 5% ferric chloride and few drops of concentrated sulphuric acid were added to a solution of the BPE (2 mL) in 2 mL of glacial acetic acid. The colour change was observed. Bluish-green colouration at the top junction and a reddish-brown coloration at the lower junction of two layers was an indication of the presence of glycosides.

2.8.3.6. Test for Alkaloids

To 3 ml of the peel extract, 1ml of 1% HCL was added. Then few drops of Meyer's reagent were added to the resultant mixture. The appearance of a precipitate of creamy white colouration indicated the presence of alkaloids.

2.8.3.7. Estimation of Alkaloids

The alkaloid quantification was done as below. About 5g of the peel sample was weighed, and 10% HCL in ethanol (200 mL) was added. It was then covered and allowed to stand for 4 h. The sample was then filtered using Whatman filter paper 1 and the sample extract was reduced to less than half of the original volume on a water bath. 100 mL chloroform was added to the concentrated sample to remove pigments and unwanted materials along with distilled water and allowed to shake in a separating funnel. The lower layer was collected. To precipitate

free ammonia, an excess amount of ammonia was added to the lower layer. The total amount of the solution was filtered using Whatman filter paper 42. The filtrate was evaporated in an oven and weighed to constant weight for measuring the percentage of alkaloids present in the three varieties of peel samples. The alkaloid content was calculated as percentage weight using the formulae below and tabulated. The experiment was repeated thrice with three types of peel samples.

$$\% \text{ Alkaloids} = = \frac{(W_2 - W_1)}{Weight\ of\ sample} \times 100$$

W_2 = weight of filter paper + Residue after oven drying.

W_1 = weight of filter paper

Weight of peel sample = 5g.

2.8.3.8. Test for Anthraquinones

Bhimkol peel samples of 100 mg were boiled with 3 mL of 1% HCl and filtered. 2.5 mL of benzene was added to the filtrate and shaken and filtered again. About 1 mL of 10% ammonia solution was added to the filtrate. After shaking the mixture, colouration in the ammonical phase appeared. Appearance of violet, red or pink colour indicated the presence of free hydroxyl anthraquinones.

2.8.3.9. Test for Tannin

To 1 mL of the peel extract, 2 drops of 5% $FeCl_3$ were added. The appearance of a dull-green precipitate indicated the presence of tannin. This test was also carried out by boiling 50 mg of the peel samples in 20 mL of distilled water and filtered. In the filtrate, a few drops of 0.1% $FeCl_3$ were added to the filtrate and a change of colour was observed. The colouration of brownish-green or a blue-black indicated the presence of tannins.

2.8.3.10. Estimation of Tannin

The total tannin was estimated using the following method. About 0.5 g of the peel sample was crushed and then weighed and 50 mL of distilled water was added. The solution was allowed to stir continuously for 1 hour on a magnetic stirrer. The mixture was filtered, 5 ml of the filtrate was mixed with 2 mL of 0.1M $FeCl_3$ in 0.1N HCl and 0.008 M $K_4Fe(CN)_6$ (potassium ferrocyanide). For the standard solution preparation, about 0.1g of tannic acid was dissolved in 100 mL of distilled water to form a tannic acid solution. 5 mL was used to prepare the standard solution from this tannic acid solution, and 5 mL of distilled water was used to

prepare a blank sample solution. All the prepared solutions were then incubated for one and half an hour at ambient temperature. Later, the solutions were made up to the 50 mL mark using distilled water. The absorbance was measured at 760 nm for all the standard and sample solutions using a UV-Vis Spectrophotometer. The total tannin content was calculated as percentage weight using the formulae below and tabulated. The experiment was repeated thrice with three varieties of peel samples.

$$\text{Tannin in mg/100} = \frac{(X-Z)}{(Y-Z)}$$

Absorbance of 5 mL of extract = X

Absorbance of tannic acid solution = Y Absorbance of Blank = Z

2.8.3.11. Test for Phenolic Compounds

Ferric Chloride test: Peel samples of 50 mg were dissolved in 5 mL of distilled water. Few drops of neutral 5% ferric chloride solution were added to the mixture. The colouration of dark green indicated the presence of phenolic compounds.

Gelatin test: Peel samples of 50 mg were dissolved in 5 mL of distilled water. 2 mL of 1% gelatin solution containing 10% NaCl was added to the mixture. The appearance of white precipitate indicated phenolic compounds.

Lead acetate test: 50 mg of peel sample was dissolved in 5 mL of distilled water. Again, 3 mL of 10% lead acetate solution was added to the mixture. The appearance of bulky white precipitate demonstrated the presence of phenolic compounds.

2.8.3.12. Estimation of Phenolic compounds

The Folin-Ciocalteu method was used for the total phenol determination described by Barimah *et al.* with slight modification.[63] It is based on determining the colour change from yellow to blue-black due to reducing the Tungstate-molybdate mixture, which is present in the Folin-Ciocalteu reagent in the solution. Thus, the detection of phenol was concluded.

2.8.3.13. Preparation of Gallic Acid Stock

Dry Gallic acid (0.5 g) was dissolved in 10 mL ethanol. This was diluted, and volume was made up to 100 mL with distilled water.

2.8.3.14. Standard Calibration Curve for Phenol Analysis

For the standard curve preparation of gallic acid, a stock solution of 1000 ppm (mg/l) of the Gallic acid was prepared. Various gallic acid solutions of different concentrations were prepared by dilution with distilled water. The standard Gallic acid solutions prepared were 1,

10, 50, 100, 250, and 1000 mg/L, respectively. An amount of 0.1 mL of each standard Gallic acid was added to 6.0 mL distilled water. Folin-Ciocalteu reagent of about 0.5 mL was also added. The solutions were mixed thoroughly and allowed to stand for about 5-10 minutes. Then 20 % sodium carbonate (1.5 mL) solution was added to each solution and the solutions were made up to 10 mL mark with distilled water and mixed. The subsequent solutions were then incubated for 90 minutes in the dark at ambient temperature. The absorbance was measured at 765 nm using a UV-VIS spectrophotometer. Distilled water was used as blank in the experiment.

2.8.3.15. Estimation of Total Phenol Content

The peel sample extraction was initially started by crushing about 0.5 g peels in a mortar and pastel and weighed. Then about 50% methanol (10 mL) was added to the crushed peel sample and mixed thoroughly and allowed to stand for 24 hours. The sample extracts were then obtained by sieving and filtrated using Whatman filter paper 1. Next, about 0.1 mL sample was added to 6.0 mL of distilled water followed by the addition of 0.5 mL of Folin-Ciocalteu reagent and mixed well. It was then allowed to stand for 5-10 mins. Afterward, 20% sodium carbonate (1.5 mL) solution was added. The solutions were made up to the 10 mL mark with distilled water and mixed well. The subsequent solutions were then incubated for 90 min in the dark at ambient temperature. Later, the absorbance readings were measured at 765 nm. Absorbance readings were measured for triplicate samples for each variety of peels. Distilled water was used as blank in this experiment. Finally, the total phenolic contents of each fraction were converted into milligram Gallic acid equivalents per gram dry weight of bhimkol peel samples. Linear calibration curves of gallic acid were produced with R^2 = 0.9995. The data were tabulated. The experiment was repeated thrice with three varieties of peel samples.

2.8.3.16. Test for Phlobatannins

Peel samples of 100 mg boiled for 5-10 minutes in 3 mL of 1% aqueous hydrochloric acid. There may be the presence of red colouration at the bottom. The deposition of red precipitate indicated the presence of phlobatannins.

2.8. REFERENCES

(1) Korani, M.; Ghazizadeh, E.; Korani, S.; Hami, Z.; Mohammadi-Bardbori, A. Effects of Silver Nanoparticles on Human Health. *Eur. J. Nanomedicine* **2015**, *7* (1), 51–62.

(2) Ankanna, S.; Prasad, T. N. V. K. V.; Elumalai, E. K.; Savithramma, N. Production of Biogenic Silver Nanoparticles Using *Boswellia ovalifoliolata* Stem Bark. *Dig. J. Nanomater. Biostructures* **2010**, *5* (2), 369–372.

(3) Nurani, S. J.; Saha, K. C.; Rahman Khan, M. A.; Sunny, S. M. H. Silver Nanoparticles Synthesis, Properties, Applications and Future Perspectives: A Short Review. *IOSR J. Electr. Electron. Eng. Ver. I* **2015**, *10* (6), 117–126.

(4) Wang, M.; Marepally, S. K.; Vemula, P. K.; Xu, C. Chapter 5 - Inorganic Nanoparticles for Transdermal Drug Delivery and Topical Application; Hamblin, M. R., Avci, P., Prow, T. W. B. T.-N. in D., Eds.; Academic Press: Boston, 2016; pp 57–72.

(5) Samberg, M. E.; Oldenburg, S. J.; Monteiro-Riviere, N. A. Evaluation of Silver Nanoparticle Toxicity in Skin in Vivo and Keratinocytes in Vitro. *Environ. Health Perspect.* **2010**, *118* (3), 407–413.

(6) Sintubin, L.; De Gusseme, B.; Van der Meeren, P.; Pycke, B. F. G.; Verstraete, W.; Boon, N. The Antibacterial Activity of Biogenic Silver and Its Mode of Action. *Appl. Microbiol. Biotechnol.* **2011**, *91* (1), 153–162.

(7) Jain, J.; Arora, S.; Rajwade, J. M.; Omray, P.; Khandelwal, S.; Paknikar, K. M. Silver Nanoparticles in Therapeutics: Development of an Antimicrobial Gel Formulation for Topical Use. *Mol. Pharm.* **2009**, *6* (5), 1388–1401.

(8) Dastjerdi, R.; Montazer, M. A Review on the Application of Inorganic Nano-Structured Materials in the Modification of Textiles: Focus on Anti-Microbial Properties. *Colloids Surf. B. Biointerfaces* **2010**, *79* (1), 5–18.

(9) Harrasser, N.; Jüssen, S.; Obermeir, A.; Kmeth, R.; Stritzker, B.; Gollwitzer, H.; Burgkart, R. Antibacterial Potency of Different Deposition Methods of Silver and Copper Containing Diamond-like Carbon Coated Polyethylene. *Biomater. Res.* **2016**, *20*, 17.

(10) Bag, S. S.; Banerjee, A.; Singh, A.; Goldar, A.; Bora, A. Green Synthesis of Silver Nanoparticle Using *Sechium edule* Aqueous Extract and Study of Antimicrobial and Catalytic Activity. *Curr. Nanomater.* **2018**, *3* (3), 140–146.

(11) Liz-Marzán, L. M.; Lado-Touriño, I. Reduction and Stabilization of Silver Nanoparticles in Ethanol by Nonionic Surfactants. *Langmuir* **1996**, *12* (15), 3585–3589.

(12) Prabhu, S.; Poulose, E. K. Silver Nanoparticles: Mechanism of Antimicrobial Action, Synthesis, Medical Applications, and Toxicity Effects. *Int. Nano Lett.* **2012**, *2* (1), 32.

(13) Ahmed, S.; Ahmad, M.; Swami, B. L.; Ikram, S. A Review on Plants Extract Mediated Synthesis of Silver Nanoparticles for Antimicrobial Applications: A Green Expertise. *J. Adv. Res.* **2016**, *7* (1), 17–28.

(14) Lateef, A.; Ojo, S. A.; Akinwale, A. S.; Azeez, L.; Gueguim-Kana, E. B.; Beukes, L. S. Biogenic Synthesis of Silver Nanoparticles Using Cell-Free Extract of *Bacillus safensis* LAU 13: Antimicrobial, Free Radical Scavenging and Larvicidal Activities. *Biologia (Bratisl).* **2015**, *70* (10), 1295–1306.

(15) Thunugunta, T.; Reddy, A. C.; Reddy D.C., L. Green Synthesis of Nanoparticles: Current Prospectus. *Nanotechnol. Rev.* **2015**, *4* (4), 303–323.

(16) Adelere, I. A.; Lateef, A. A Novel Approach to the Green Synthesis of Metallic Nanoparticles: The Use of Agro-Wastes, Enzymes, and Pigments. *Nanotechnol. Rev.* **2016**, *5* (6), 567–587.

(17) Madhumitha, G.; Roopan, S. M. Devastated Crops: Multifunctional Efficacy for the Production of Nanoparticles. *J. Nanomater.* **2013**, *2013*, 1–12.

(18) Kuppusamy, P.; Yusoff, M. M.; Maniam, G. P.; Govindan, N. Biosynthesis of Metallic Nanoparticles Using Plant Derivatives and Their New Avenues in Pharmacological Applications – An Updated Report. *Saudi Pharm. J.* **2016**, *24* (4), 473–484.

(19) Devadiga, A.; Shetty, K. V.; Saidutta, M. B. Timber Industry Waste-Teak (*Tectona grandis* Linn.) Leaf Extract Mediated Synthesis of Antibacterial Silver Nanoparticles. *Int. Nano Lett.* **2015**, *5* (4), 205–214.

(20) Basavegowda, N.; Rok Lee, Y. Synthesis of Silver Nanoparticles Using Satsuma Mandarin (*Citrus unshiu*) Peel Extract: A Novel Approach towards Waste Utilization. *Mater. Lett.* **2013**, *109*, 31–33.

(21) Malhotra, A.; Sharma, N.; Navdezda; Kumar, N.; Dolma, K.; Sharma, D.; Nandanwar, H. S.; Choudhury, A. R. Multi-Analytical Approach to Understand Biomineralization of Gold Using Rice Bran: A Novel and Economical Route. *RSC Adv.* **2014**, *4* (74), 39484–39490.

(22) Harish, B. S.; Uppuluri, K. B.; Anbazhagan, V. Synthesis of Fibrinolytic Active Silver Nanoparticle Using Wheat Bran Xylan as a Reducing and Stabilizing Agent. *Carbohydr. Polym.* **2015**, *132*, 104–110.

(23) Gan, P. P.; Ng, S. H.; Huang, Y.; Li, S. F. Y. Green Synthesis of Gold Nanoparticles Using Palm Oil Mill Effluent (POME): A Low-Cost and Eco-Friendly Viable Approach.

Bioresour. Technol. **2012**, *113*, 132–135.

(24) Roopan, S.; Thakur, R.; Rahuman, A.; Kamaraj, D. C.; Annadurai, B.; Tammineni, S. Low-Cost and Eco-Friendly Phyto-Synthesis of Silver Nanoparticles Using *Cocos nucifera* Coir Extract and Its Larvicidal Activity. *Ind. Crop. Prod.* **2013**, *43*, 631–635.

(25) Lateef, A.; Oloke, J. K.; Gueguim Kana, E. B.; Oyeniyi, S. O.; Onifade, O. R.; Oyeleye, A. O.; Oladosu, O. C.; Oyelami, A. O. Improving the Quality of Agro-Wastes by Solid-State Fermentation: Enhanced Antioxidant Activities and Nutritional Qualities. *World J. Microbiol. Biotechnol.* **2008**, *24* (10), 2369–2374.

(26) Shanmugavadivu, M.; Kuppusamy, S.; Ranjithkumar, R. Synthesis of Pomegranate Peel Extract Mediated Silver Nanoparticles and Its Antibacterial Activity. *Am. J. Adv. Drug Deliv.* **2014**, *2* (2), 174–182.

(27) Kumar, B.; Smita, K.; Cumbal, L.; Angulo, Y. Fabrication of Silver Nanoplates Using *Nephelium lappaceum* (Rambutan) Peel: A Sustainable Approach. *J. Mol. Liq.* **2015**, *211*, 476–480.

(28) Yuvakkumar, R.; Suresh, J.; Nathanael, A. J.; Sundrarajan, M.; Hong, S. I. Novel Green Synthetic Strategy to Prepare ZnO Nanocrystals Using Rambutan (*Nephelium lappaceum* L.) Peel Extract and Its Antibacterial Applications. *Mater. Sci. Eng. C. Mater. Biol. Appl.* **2014**, *41*, 17–27.

(29) Yuvakkumar, R.; Suresh, J.; Nathanael, A. J.; Sundrarajan, M.; Hong, S. I. Rambutan (*Nephelium lappaceum* L.) Peel Extract Assisted Biomimetic Synthesis of Nickel Oxide Nanocrystals. *Mater. Lett.* **2014**, *128*, 170–174.

(30) Kumar, R.; Roopan, S. M.; Prabhakarn, A.; Khanna, V. G.; Chakroborty, S. Agricultural Waste Annona Squamosa Peel Extract: Biosynthesis of Silver Nanoparticles. *Spectrochim. Acta. A. Mol. Biomol. Spectrosc.* **2012**, *90*, 173–176.

(31) Heydari, R.; Rashidipour, M. Green Synthesis of Silver Nanoparticles Using Extract of Oak Fruit Hull (Jaft): Synthesis and In Vitro Cytotoxic Effect on MCF-7 Cells. *Int. J. Breast Cancer* **2015**, 846743.

(32) Dauthal, P.; Mukhopadhyay, M. Biofabrication, Characterization, and Possible Bio-Reduction Mechanism of Platinum Nanoparticles Mediated by Agro-Industrial Waste and Their Catalytic Activity. *J. Ind. Eng. Chem.* **2015**, *22*, 185–191.

(33) Krishnaswamy, K.; Vali, H.; Orsat, V. Value-Adding to Grape Waste: Green Synthesis of Gold Nanoparticles. *J. Food Eng.* **2014**, *142*, 210–220.

(34) Najimu Nisha, S.; Aysha, O. S.; Syed Nasar Rahaman, J.; Vinoth Kumar, P.; Valli, S.; Nirmala, P.; Reena, A. Lemon Peels Mediated Synthesis of Silver Nanoparticles and Its

Antidermatophytic Activity. *Spectrochim. Acta. A. Mol. Biomol. Spectrosc.* **2014**, *124*, 194–198.

(35) Prasad, C.; Gangadhara, S.; Venkateswarlu, P. Bio-Inspired Green Synthesis of Fe_3O_4 Magnetic Nanoparticles Using Watermelon Rinds and Their Catalytic Activity. *Appl. Nanosci.* **2016**, *6* (6), 797–802.

(36) Lakshmipathy, R.; Palakshi Reddy, B.; Sarada, N. C.; Chidambaram, K.; Khadeer Pasha, S. Watermelon Rind-Mediated Green Synthesis of Noble Palladium Nanoparticles: Catalytic Application. *Appl. Nanosci.* **2015**, *5* (2), 223–228.

(37) Velu, K.; Elumalai, D.; Hemalatha, P.; Janaki, A.; Babu, M.; Hemavathi, M.; Kaleena, P. K. Evaluation of Silver Nanoparticles Toxicity of *Arachis hypogaea* Peel Extracts and Its Larvicidal Activity against Malaria and Dengue Vectors. *Environ. Sci. Pollut. Res. Int.* **2015**, *22* (22), 17769–17779.

(38) Kanchi, S.; Kumar, G.; Lo, A.-Y.; Tseng, C.-M.; Chen, S.-K.; Lin, C.-Y.; Chin, T.-S. Exploitation of De-Oiled Jatropha Waste for Gold Nanoparticles Synthesis: A Green Approach. *Arab. J. Chem.* **2018**, *11* (2), 247–255.

(39) Anand, K.; Gengan, R. M.; Phulukdaree, A.; Chuturgoon, A. Agroforestry Waste *Moringa oleifera* Petals Mediated Green Synthesis of Gold Nanoparticles and Their Anti-Cancer and Catalytic Activity. *J. Ind. Eng. Chem.* **2015**, *21*, 1105–1111.

(40) Zheng, B.; Qian, L.; Yuan, H.; Xiao, D.; Yang, X.; Paau, M. C.; Choi, M. M. F. Preparation of Gold Nanoparticles on Eggshell Membrane and Their Biosensing Application. *Talanta* **2010**, *82* (1), 177–183.

(41) Devi, P. S.; Banerjee, S.; Chowdhury, S. R.; Kumar, G. S. Eggshell Membrane: A Natural Biotemplate to Synthesize Fluorescent Gold Nanoparticles. *RSC Adv.* **2012**, *2* (30), 11578–11585.

(42) Ahmad, N.; Sharma, S.; Rai, R. Rapid Green Synthesis of Silver and Gold Nanoparticles Using Peels of *Punica granatum*. **2012**, *3* (5), 376–380.

(43) Edison, T. J. I.; Sethuraman, M. G. Biogenic Robust Synthesis of Silver Nanoparticles Using *Punica granatum* Peel and Its Application as a Green Catalyst for the Reduction of an Anthropogenic Pollutant 4-Nitrophenol. *Spectrochim. Acta. A. Mol. Biomol. Spectrosc.* **2013**, *104*, 262–264.

(44) Kahrilas, G. A.; Wally, L. M.; Fredrick, S. J.; Hiskey, M.; Prieto, A. L.; Owens, J. E. Microwave-Assisted Green Synthesis of Silver Nanoparticles Using Orange Peel Extract. *ACS Sustain. Chem. Eng.* **2014**, *2* (3), 367–376.

(45) Awad, M. A.; Hendi, A. A.; Ortashi, K. M. O.; Elradi, D. F. A.; Eisa, N. E.; Al-Lahieb,

L. A.; Al-Otiby, S. M.; Merghani, N. M.; Awad, A. A. G. Silver Nanoparticles Biogenic Synthesized Using an Orange Peel Extract and Their Use as an Anti-Bacterial Agent. *Int. J. Phys. Sci.* **2014**, *9* (3), 34–40.

(46) Bankar, A.; Joshi, B.; Kumar, A. R.; Zinjarde, S. Banana Peel Extract Mediated Novel Route for the Synthesis of Silver Nanoparticles. *Colloids Surfaces A Physicochem. Eng. Asp.* **2010**, *368* (1–3), 58–63.

(47) Ibrahim, H. M. M. Green Synthesis and Characterization of Silver Nanoparticles Using Banana Peel Extract and Their Antimicrobial Activity against Representative Microorganisms. *J. Radiat. Res. Appl. Sci.* **2015**, *8* (3), 265–275.

(48) A, O. O.; Izundu, A. I.; Helen, O. N.; Pauline, I. A. Phytochemical Compositions of Fruits of Three Musa Species at Three Stages of Development. *IOSR J. Dntal amd Med. Sci.* **2016**, *11* (3), 48–59.

(49) Duhan, A.; Chauhan, B. M.; Punia, D. Nutritional Value of Some Non-Conventional Plant Foods of India. *Plant Foods Hum. Nutr.* **1992**, *42* (3), 193–200.

(50) Chandra, S.; Kaneria, M.; Nair, R. Antibacterial Activity of *Psoralea corylifolia* L. Seed and Aerial Parts with Various Extraction Methods. *Res. J. Microbiol.* **2011**, *6* (2), 124–131.

(51) Trease, G.; Evans, W. *Pharmacognosy, 15th Ed. Harcourt Publishers, Edinburg, UK*; 2002.

(52) Lobo, V.; Patil, A.; Phatak, A.; Chandra, N. Free Radicals, Antioxidants and Functional Foods: Impact on Human Health. *Pharmacogn. Rev.* **2010**, *4* (8), 118–126.

(53) Parmar, H. S.; Kar, A. Medicinal Values of Fruit Peels from *Citrus sinensis*, *Punica granatum*, and *Musa paradisiaca* with Respect to Alterations in Tissue Lipid Peroxidation and Serum Concentration of Glucose, Insulin, and Thyroid Hormones. *J. Med. Food* **2008**, *11* (2), 376–381.

(54) Tewari, H. K.; Marwaha, S. S.; Rupal, K. Ethanol from Banana Peels. *Agric. Wastes* **1986**, *16* (2), 135–146.

(55) Essien, J. P.; Akpan, E. J.; Essien, E. P. Studies on Mould Growth and Biomass Production Using Waste Banana Peel. *Bioresour. Technol.* **2005**, *96* (13), 1451–1456.

(56) Osma, J. F.; Toca Herrera, J. L.; Rodríguez Couto, S. Banana Skin: A Novel Waste for Laccase Production by *Trametes pubescens* under Solid-State Conditions. Application to Synthetic Dye Decolouration. *Dye. Pigment.* **2007**, *75* (1), 32–37.

(57) Annadural, G.; Juang, R. S.; Lee, D. J. Adsorption of Heavy Metals from Water Using Banana and Orange Peels. *Water Sci. Technol. a J. Int. Assoc. Water Pollut. Res.* **2003**,

47 (1), 185–190.

(58) Happi Emaga, T.; Andrianaivo, R. H.; Wathelet, B.; Tchango, J. T.; Paquot, M. Effects of the Stage of Maturation and Varieties on the Chemical Composition of Banana and Plantain Peels. *Food Chem.* **2007**, *103* (2), 590–600.

(59) Borborah, K.; Borthakur, S. K.; Tanti, B. *Musa balbisiana* Colla-Taxonomy, Traditional Knowledge and Economic Potentialities of the Plant in Assam, India. *Indian J. Tradit. Knowl.* **2016**, *15* (1), 116–120.

(60) Eby, D. M.; Schaeublin, N. M.; Farrington, K. E.; Hussain, S. M.; Johnson, G. R. Lysozyme Catalyzes the Formation of Antimicrobial Silver Nanoparticles. *ACS Nano* **2009**, *3* (4), 984–994.

(61) Furno, F.; Morley, K. S.; Wong, B.; Sharp, B. L.; Arnold, P. L.; Howdle, S. M.; Bayston, R.; Brown, P. D.; Winship, P. D.; Reid, H. J. Silver Nanoparticles and Polymeric Medical Devices: A New Approach to Prevention of Infection? *J. Antimicrob. Chemother.* **2004**, *54* (6), 1019–1024.

(62) Payum, T.; Das, A. K.; Shankar, R.; Tamuly, C.; Hazarika, M. Antioxidant Potential of *Solanum spirale* Shoot and Berry : A Medicinal Food Plant Used in Arunachal Pradesh. *Am. J. Pharmtech Res.* **2015**, *5* (July), 307–314.

(63) Barimah, J.; Yanney, P.; Laryea, D.; Quarcoo, C. Effect of Drying Methods on Phytochemicals, Antioxidant Activity and Total Phenolic Content of Dandelion Leaves. *Am. J. Food Nutr.* **2021**, *5* (4), 136–141.

CHAPTER 3:

Green Synthesis of Silver Nanoparticle Using *Sechium Edule* Aqueous Extract and Study of Antimicrobial and Catalytic Activity

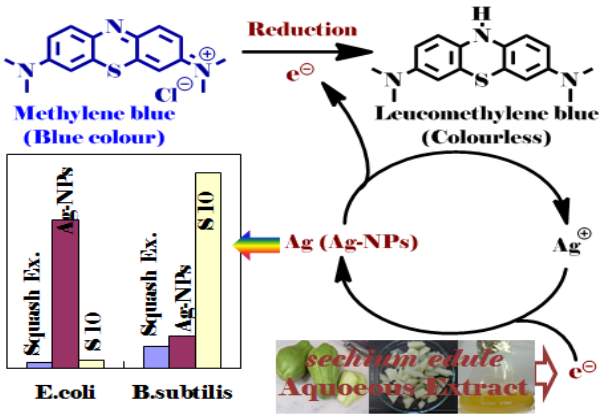

3.1. Introduction

Among all the noble metal nanoparticles, silver nanoparticles(AgNPs) have got special interest because of their small sizes and large surface areas with unique photophysical and chemical properties. AgNPs are also known to exhibit antibacterial, antiviral, antifungal and anti-inflammatory activities.[1] Thus, a vast majority of research involves the synthesis of AgNPs due to their potential applications ranging from chemistry, physics, material science, biology to medical science and nanobiotechnology. Therefore, many synthetic techniques for AgNPs, such as chemical reduction, radiation, and photochemical methods, are available[2] and many more are under research. Most of these methods are not cost-effective, not environment friendly and do not meet the current research trend or the market demand.

To meet the current industrial demand and overcome the challenges faced by the living organisms in the environment during the synthesis of AgNPs, the environment-friendly synthesis of AgNPs is highly desirable and considered a widely accepted technology. Thus, in the race of synthesis of AgNPs via biomimetic green synthetic route, several methodologies have been adopted, such as synthesis using microorganisms,[3,4] fungus,[5] enzymes,[6] plant extracts,[2,7] etc. These methodologies are considered environment-friendly and are alternatives to physicochemical methods. Among these biological approaches, the less time-consuming, cost-effective, and less tedious approach, such as using plants or plant extracts, are advantageous over other eco-friendly synthetic methods. Therefore, such cost-effective and environment-friendly green synthetic methods of silver nanoparticles (AgNPs), using cheap and widely available plant extracts such as vegetable extract, are highly demanding.

3.2. Green synthesis of AgNPs using Plant Extracts

The use of plant extracts for the synthesis of AgNPs is potentially advantageous over microorganisms due to its simple process, less time consumption by averting the elaborate process of cell culture maintenance in the case of microbe-mediated synthesis. Due to the requirement of high aseptic conditions, the microbe-mediated synthesis is not industrial feasibility. So, green synthesis provides the best platform for nanoparticle synthesis as it is free from toxic chemicals, and plant extracts provide natural capping agents for AgNPs stabilization. Additionally, the use of plant extracts reduces the cost of isolation of microbes and their culture media, which helps enhance cost-competitive feasibility over AgNPs synthesis by microbes. Due to the amalgamation of biomolecules with silver ions, the reduction and stabilization of the formed nanoparticles can easily be established using plant extracts with

medicinal values. Thus, these processes are environment-friendly beneficial for environmental applications. The biomolecules involved in the process of synthesis and stabilization of nanoparticles are the secondary metabolites present in the plant extracts such as proteins, enzymes, alkaloids, tannins, phenolic compounds, polysaccharides, saponins, vitamins, terpenoids, etc.[8] A large number of plants facilitate AgNPs synthesis, some of these are reported in table 3.1.[2]

Table 3.1. Green synthesis of silver nanoparticles using various plant extracts.

Sl.No.	Plant Extract	Plant parts used	Nanoparticle size (nm)	References
1	Little ruby (*Alternanthera dentate*)	Leaves	50-100	9
2.	Sweet flag (*Acorus calamus*)	Rhizome	31.83	10
3.	Tea (*Camellia sinensis*)	Leaves	20-90	11
4.	Punarnava (*Boerhaavia diffusa*)	Whole plant	25	12
5.	*Tribulus terrestris*	Fruit	16-28	13
6.	Cyprus turpentine tree (*Pistacia atlantica*)	Seeds	10-50	14
7.	Coconut (*Cocous nucifera*)	Inflorescence	22	15
8.	Indian mallow (*Abutilon indicum*)	Leaves	7-17	16
9.	*Ziziphora tenuior*	Leaves	8-40	17
10.	Common fig (*Ficus carica*)	Leaves	13	18
11.	Indian mercury (*Acalypha indica*)	Leaves	0.5, 20-30	19,20
12.	Lemon grass (*Cymbopogan citratus*)	Leaves	32	21
13.	Stemless Premna (*Premna herbacea*)	Leaves	10-30	22
14.	Rubber Tree (*Calotropis procera*)	Plant	19-45	23

15.	Asiatic pennywort (*Centella asiatica*)	Leaves	30-50	24
16.	Woolly morning glory (*Argyreia nervosa*)	Seeds	20-50	25
17.	Field mustard (*Brassica rapa*)	Leaves	16.4	26
18.	Babchi (*Psoralea corylifolia*)	Seeds	100-110	14
19.	Scarlet gourds (*Coccinia indica*)	Leaves	10-20	27
20.	Chinese chaste tree (*Vitex negundo*)	Leaves	5, 10-30	28
21.	*Melia dubia*	Leaves	35	29
22.	Pursley (*Portulaca oleracea*)	Leaves	<60	30
23.	Yellow oleander (*Thevetia peruviana*)	Latex	10-30	31
24.	Shrub-Mint (*Pogostemon benghalensis*)	Leaves	>80	32
25.	Ajwain (*Trachyspermum ammi*)	Seeds	87,99	33
26.	West Indian mahogany (*Swietenia mahogany*)	Leaves	50	34
27.	French plantain banana (*Musa paradisiacal*)	Peels	20	35
28.	Drumstick tree (*Moringa oleifera*)	Leaves	57	36
29.	Lotus (*Nelumbo nucifera*)	Leaves	25-80	37
30.	Bhringraj (*Eclipta prostrate*)	Leaves	35-60	38
31.	Garlic (*Allium sativum*)	Cloves	4-22	39
32.	*Aloe vera*	Leaves	50-350	40
33.	Navel orange (*Citrus sinensis*)	Peels	10-35	41

34.	Eucalyptus tree (*Eucalyptus hybrid*)	Peels	50-150	42
35.	Nemaaru tree (*Memecylon edule*)	Leaves	20-50	43
36.	Indian Thornappe (*Datura metel*)	Leaves	16-40	44
37.	European wine grape (*Vitis vinifera*)	Fruits	30-40	45
38.	Papaya (*Carica papaya*)	Leaves	25-50	46
39.	Mangosteen (*Garcinia mangostana*)	Leaves	35	47

Thus, it is clear that the different plants and their various parts have been utilized to synthesize AgNPs. These nanoparticles are mainly spherical in shape with 10-100 nm average dimensions. The synthesis of nanoparticles involves collecting the plants from the available sites and washing thoroughly to remove dust or any impurities. Then the extract is prepared either by dissolving freshly cut plant parts in distilled water or by using dried powders of the respective plant's parts in an appropriate quantity, and the mixture is boiled. After cooling down, the solution is filtered thoroughly until no more insoluble material appears in the broth. Some definite concentration of silver nitrate ($AgNO_3$) is added to the plant extract, which results in the reduction of pure Ag(I) ions to metallic Ag(0). The formation of AgNPs can be monitored using UV-Visible spectroscopy by observing the absorbance at regular intervals.[2]

The secondary metabolites present in plants or plant parts, such as steroids, sapogenins, carbohydrates, phenolics and flavonoids at high levels, act as reducing agents for the bioreduction of silver ions during the synthesis of AgNPs. These phytochemicals also act as capping agents that provide stability to the AgNPs. The extracellular AgNPs synthesized using the aqueous plant extracts prove more straightforward, economical, and quicker than chemical and microbial methods. The AgNPs also exhibit antibacterial activities against pathogenic bacteria such as *Pseudomonos aeruginosa*, *Escherichia coli*, *Klebsiella pneumonia*, etc.[9] Due to the antibacterial properties of AgNPs, these are widely used in the health industry, food storage and various environmental applications. AgNPs and their composites also show superior catalytic activities in dye reduction and removal. Also, the application of AgNPs as an antimicrobial agent is known.[48,49] Several reports exist addressing the AgNPs synthesis ssing plant extracts. However, there is a need for economic and a commercially viable methodology

for finding the natural phytochemicals or the reducing agents, which help in the eco-friendly synthesis of AgNPs. There are differences in the chemical compositions of the same species of plant extract from different places, leading to different outcomes. As such, identifying the biomolecules present in the plant responsible for the synthesis of AgNPs and developing a faster and efficient protocol can aid in solving this problem.

Chayote (squash) or *sechium edule* is an underutilized vegetable crop consisting of an adequate amount of nutritionally important amino acids and other phytochemicals. These fruits are used as therapeutic applications to control high blood pressure and renal diseases.[50] Therefore, wide availability and phytochemical constituents of chayote (squash) may be a good opportunity for the synthesis of AgNPs using chayote (squash) or *sechium edule* aqueous extract.

3.3. AIM AND OBJECTIVES

Following the background literature, we have concentrated ourselves for the first time to use a vegetable, Chayote (*Sechium edule*) known as 'Squash' which is widely available, cheap and has antioxidant properties for framing the following research objectives for this chapter.

a) Synthesis of stable silver nanoparticles(AgNPs) with the bioreduction method using chayote squash, or *Sechium edule* aqueous extract.
b) Characterization and determination of the crystalline phase of synthesized AgNPs from X-ray diffraction (XRD) method.
c) Evaluation of the antimicrobial effect of biologically synthesized Ag-NPs by disc diffusion method against gram positive and gram negative bacteria.
d) Study of the catalytic activity of synthesized Ag-NPs toward the reduction of methylene blue using UV–visible spectrophotometer.

3.4. RESULTS AND DISCUSSION

3.4.1. Preparation of the Chayote Squash Aqueous Extract

Chayote squash was purchased from the local market. Its peel was removed and appropriately washed with water and cut into small pieces. 150 g squash was taken in 200 ml distilled water and boiled for 24 hrs. The cold extract was filtered through Whatman 42 filter paper and was preserved in a refrigerator (10^{o}C).[51] The filtrate (aqueous extract) was used for the phytochemical test as well as for the preparation of AgNPs from $AgNO_3$.

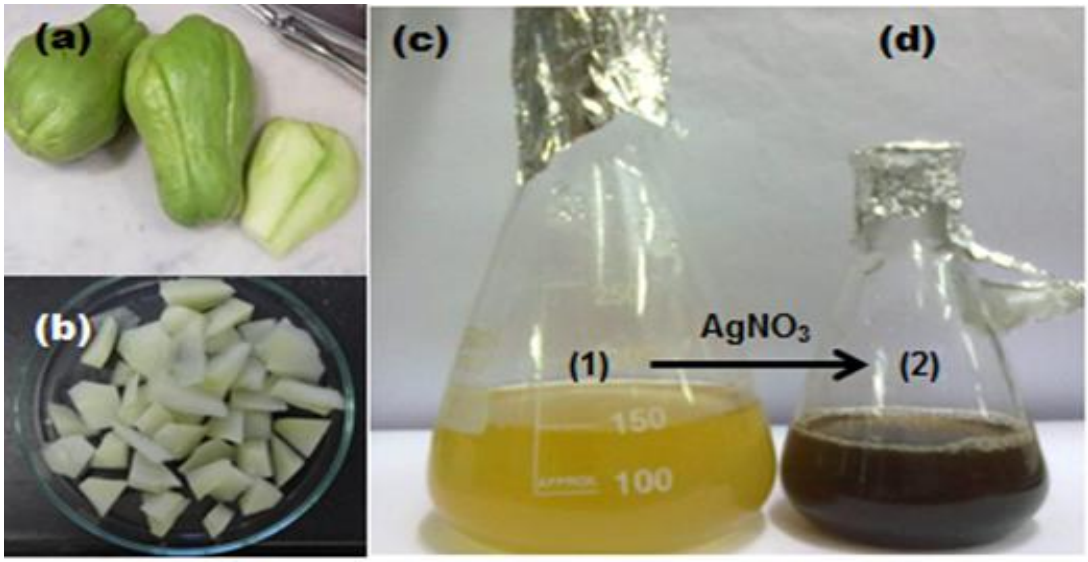

Figure 3.1. Chayote Squash (*Sechium edule)* (a) fruits; (b) pulp pieces and (c-d) aqueous extract and the synthesis of Ag-NPs with *Sechium edule* aqueous extract. Change in colour of *Sechium edule* aqueous extract upon addition of $AgNO_3$ is an indication of the reduction of Ag^+ to Ag^0.

3.4.2. Study of the Qualitative Phytochemical Compositions of the Chayote (*Sechium edule*) squash

The aqueous and organic extracts of chayote squash were used for the phytochemical tests. Thus, the aqueous extract responded to all the tests except for the presence of tannins, while organic extracts showed negative tests against tannins and terpenoids. The chloroform and ethyl acetate extracts responded only to steroids/flavonoids and flavonoids tests, respectively (table 3.2). Table 3.2 represents all the various qualitative tests of the Sechium edule extracts indicating the presence and absence of the phytochemicals.

As such, the aqueous extract contains most of the secondary metabolites, which helps in the synthesis of AgNPs. The presence of phenols and flavonoids indicates the richness of antioxidant properties, which results in antimicrobial properties. The presence of alkaloids also contributes to the therapeutic and antimicrobial properties. The presence of tannin indicates healing properties in the plant extract. From the various qualitative phytochemical analysis, it is observed that the chayote vegetable is rich in all the secondary metabolites, which may act as an excellent stabilizing as well as a reducing agent for the formation of stable AgNPs.

Table 3.2. Qualitative phytochemical evaluation of the *sechium edule* extracts

Phytoconstituents	**Test performed/ reagents used**	**Aqueous extract**	**Methanol extract**	**Chloroform extract**	**Ethyl acetate extract**
Alkaloids	Meyers test	+	+	-	-
	Dragendorffís test	+	+	-	-
	Wangers test	+	+	-	-
Steroids	Libermann-Burchard test	+	+	+	-
Flavonoids	Shinoda test	+	+	+	+
Tannins	Ferric chloride	-	-	-	-
	Lead acetate	-	-	-	-
Saponin	Test for stable foam	+	+	-	-
Glycosides	Borntager test	+	+	-	-
Proteins and amino acids	Ninhydrin test	+	+	-	-
Reducing sugar	Benedict test	+	+	-	-
	Fehling's test	+	+	-	-
Terpinoids		+	-	-	-
Phenols	Ferric chloride test	+	+	-	-

+ = Presence - = Absence

3.4.3. Synthesis of Silver nanoparticles(AgNPs)

After performing the qualitative phytochemical test with an aqueous extract of squash, it was used for the preparation of AgNPs. Thus, when silver nitrate was added to the aqueous extract, the colour of the solution changed from light yellow to brown, indicating the reduction of Ag^{+} to Ag^{0} (Fig. 3.2). The colour change is indicative of the formation of AgNPs, which was confirmed by the appearance of an absorption peak at 450 nm in the UV-visible spectra (Fig. 3.2A).

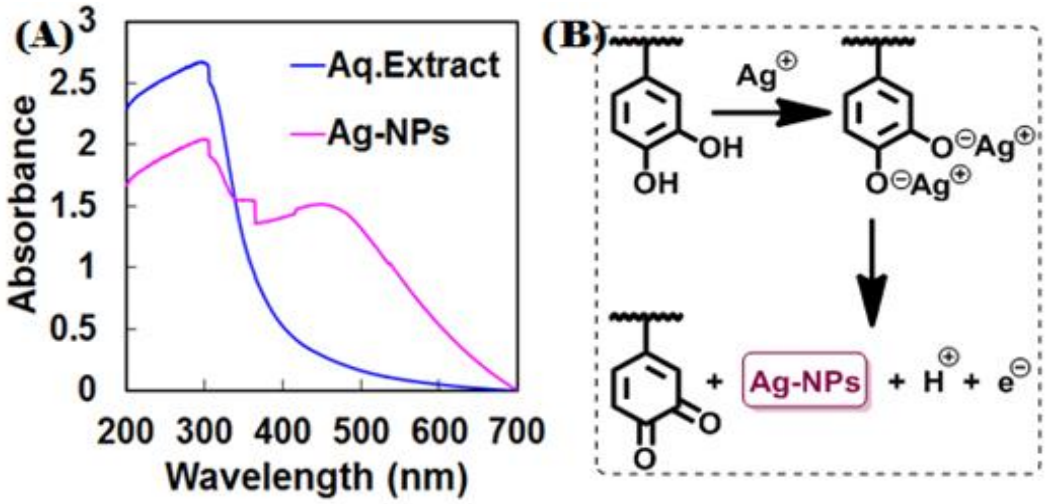

Figure 3.2. (A) UV-visible absorption spectra of *Sechium edule* aqueous extract and AgNPs. (B) Mechanism of formation of Ag-NPs. Ag^{+} ions form phenolate complexes with polyphenols present in aqueous extract and get reduced to Ag^{0} leaving quinones as the oxidized products of phenols.

3.4.4. Characterizations of AgNPs

Phytochemical analysis of *Sechium edule* aqueous extract revealed alkaloids, flavonoids, and phenols, which are mainly responsible for reducing Ag^{+} to generate Ag-NPs. Thus, FTIR spectra of *Sechium edule* extract as well as of AgNPs have been analyzed. The appearance of FTIR peaks at 3450.14 cm^{-1}, 2086.21 cm^{-1}, 1636.95 cm^{-1} and at around 680 cm^{-1} in *Sechium edule* aqueous extract indicated the presence of functional group -OH, -COOH, -NH-amides and phenyl ring substitution, respectively. On the other hand, a shift in peak position of all the peaks was observed in the case of AgNPs. This observation indicated that the AgNPs were attached with phenols with aromatic ring, acid and amide group. Thus, the amide groups and COOH groups and the phenols act as a ligand for the synthesis and stabilizing the nanoparticles. A possible mechanism of formation of AgNPs was demonstrated in figure 3.2(B).

Further evidence of the formation of crystalline AgNPs comes from the X-ray diffraction (XRD) analysis. The crystalline nature of AgNPs was confirmed from X-ray diffraction (XRD) analysis (Fig. 3.3A). Two intense peaks in the spectrum of 2θ value ranging from 10 to 50 were observed in the XRD pattern indicating the formation of AgNPs. From the XRD, the crystalline size of the nanoparticles was found to be 9.3 nm. The transmission electron microscopic study revealed the average particle size to be 12-15 nm size. The nanoparticles were spherical with

diffused ring patterns indicating the short-range crystalline nature of silver nanoparticles (Fig. 3.3B).

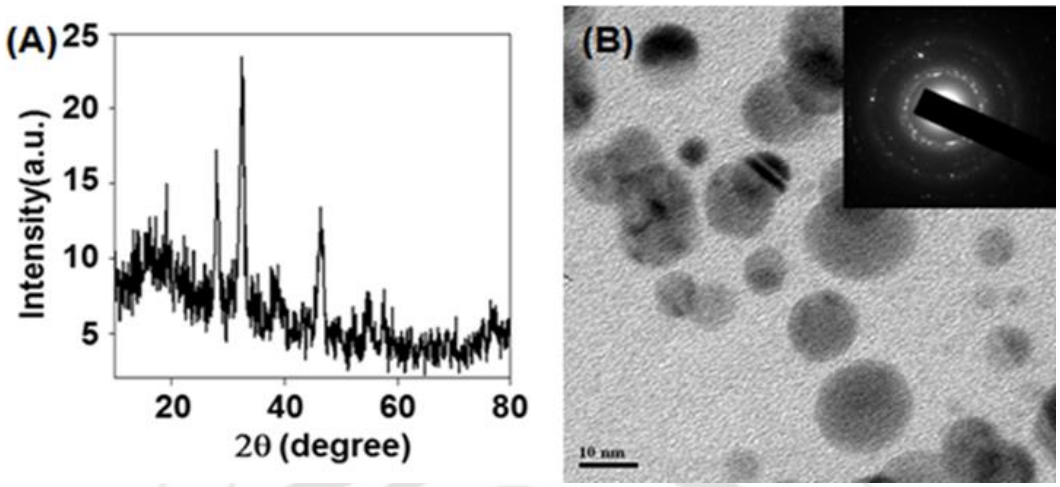

Figure 3.3. (A) XRD pattern of synthesized Ag-NPs. (B) Transmission electron microscopic image of as-synthesized silver nanoparticles, showing spherical features. Inset shows SAED patterns of silver nanoparticles. The diffused ring pattern is indicative of the short-range crystalline nature of silver nanoparticles.

3.4.5. Study of Antibacterial/Antifungal Activity

After characterizing, the AgNPs were tested for their antibacterial activity and compared with that of the aqueous extract of *Sechium edule* against gram-positive *B. subtilis*(MTCC strain no. 441) and gram-negative *E. coli*(MTCC strain no. 1696). The individual activities of AgNPs and aqueous extract of *Sechium edule* were compared with the control antibiotics, streptomycin (S10) and ampicillin (Amp) (Fig. 3.4). The nanoparticle solution was tested against the pathogens by placing 5 µl of the solution on a disc in a disc diffusion method. Then the zone around the disc was compared separately with inhibition zones of two standard antibiotics (Fig. 3.4A).

The results showed that the synthesized AgNPs had better antibacterial activity on both gram-positive and gram-negative bacteria than only the *Sechium edule* aqueous extract. In particular, AgNPs are almost 8 times more effective against gram-negative *E. coli* compared to both the control and the aqueous extract of *Sechium edule*. However, both the Ag-NPs and the aqueous extract of *Sechium edule* were found to be less effective compared to the control streptomycin (S 10) (Fig. 3.4B).

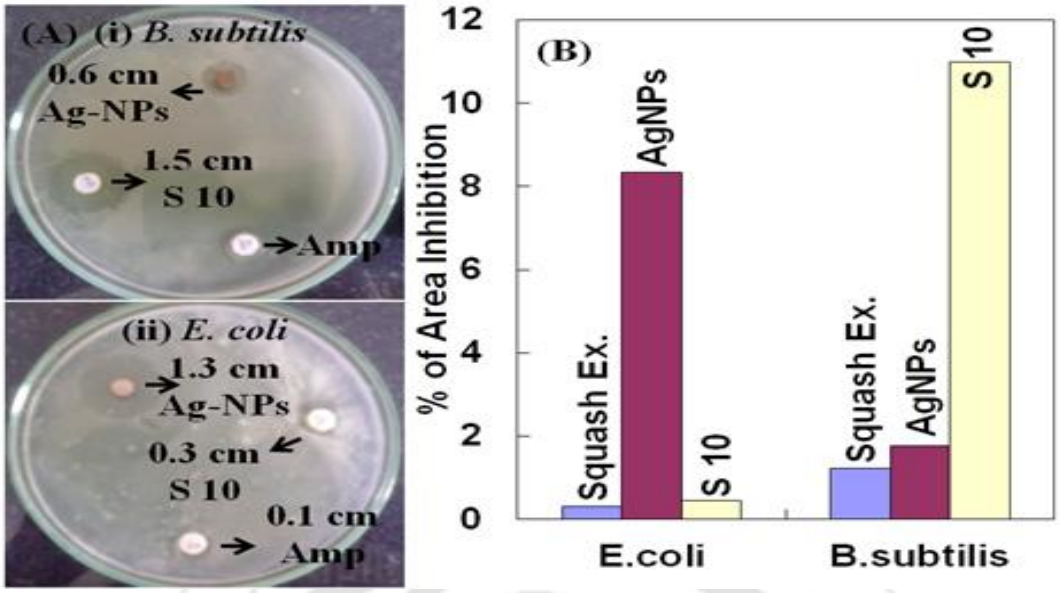

Figure 3.4. (A) Antibacterial activity of silver nanoparticle against (i) *B. subtilis and* (ii) *E. coli*. (B) Comparison of antibacterial activity of squash aqueous extract and Ag-NPs with control S10.

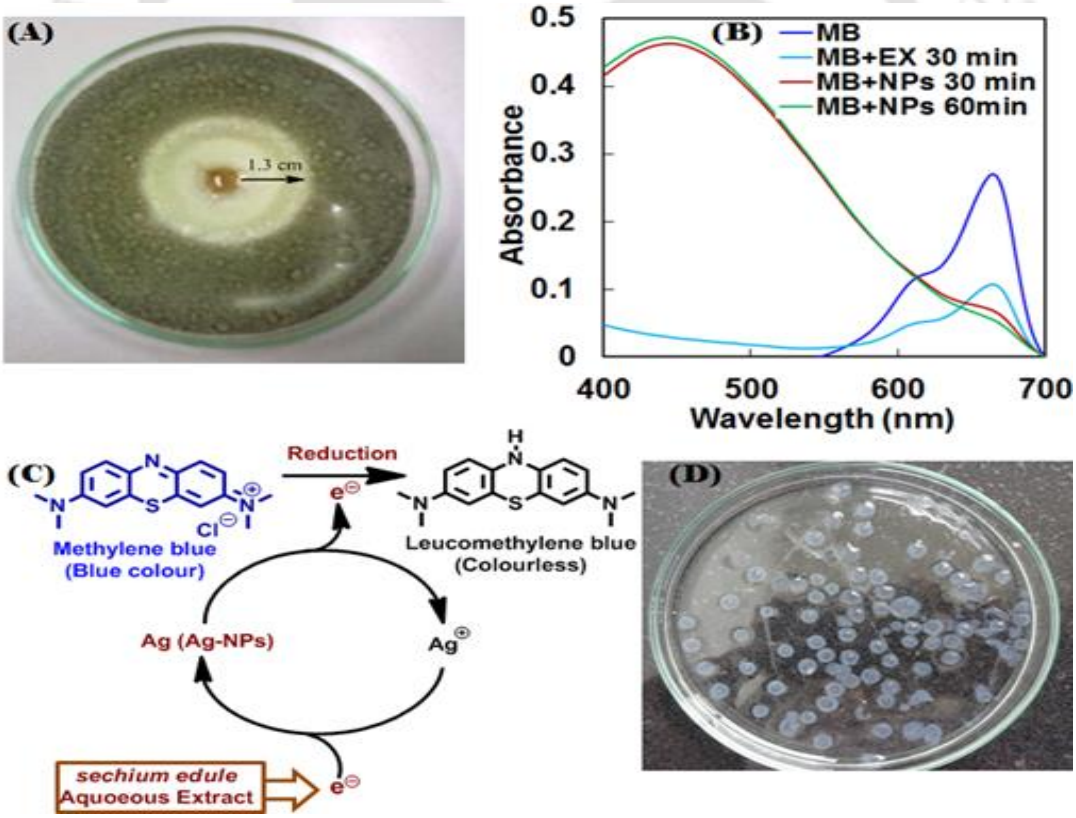

Figure 3.5. (A) Antifungal activity of *Sechium edule* and Ag-NPs against *Aspergillus thermomutans.* (B) UV–visible spectra of methylene blue reduction by *Sechium edule* aqueous extract and Ag-NPs. (C) Electron relay effect in the catalytic action of Ag-NPs between s*echium edule* aqueous extract and methylene blue. (D) Immobilized AgNPs.

Next, the antifungal activity of AgNPs was tested against pathogenic fungi, *Aspergillus thermomutans* and compared the result in respect of the *Sechium edule* aqueous extract. Thus, 5 µl of the solution of AgNPs and *Sechium edule* aqueous extract were placed in two separate wells and the plates were examined for evidence of zone of inhibition. The diameter of such zones of inhibition was examined and found that upon adding AgNPs the diameter of the inhibition zone increased to 1.3 cm compared to that observed with *Sechium edule* aqueous extract. Therefore, a repeated experimental result revealed that the antifungal activity of Ag-NPs is much more compared to that of only aqueous extract (Fig. 3.5A).

3.4.6. Study of Catalytic Activity

AgNPs are known to show catalytic activity. Therefore, the reduction of methylene blue was evaluated next by the synthesized AgNPs. Methylene blue (MB) absorbs (λ_{max}) at 664 nm. A gradual decrease in absorbance and a redshift in the absorption wavelength of MB were noticed upon the addition of *Sechium edule* aqueous extract into the MB dye within 30 minutes. The decrease of absorbance showed the ability of phyto-extract to degrade methylene blue. A sample containing MB dye, Ag-NPs and the *Sechium edule* aqueous extract showed a marked decrease in the absorbance of MB and increased absorbance of AgNPs at the end of 30 min time interval. After 60 minutes, the absorbance of Ag-NPs increased with almost disappearance of the absorbance of MB dye (Fig. 3.5B). This observation showed that AgNPs act as electron transfer mediator between the *Sechium edule* aqueous extract and methylene blue. Therefore, AgNPs acted as a redox catalyst with an electron relay effect in reducing methylene blue by *Sechium edule* aqueous extract (Fig. 3.5C). Finally, the synthesized AgNPs were immobilized using sodium alginate and calcium chloride (Fig. 3.5D). These immobilized nanoparticles might find widespread applications in various fields such as in clinics for the production of antiseptic bandage material, in water treatment and many other biotechnological and clinical applications.

3.5. CONCLUSION

The ability of *Sechium edule* fruit aqueous extract to synthesize silver nanoparticles has been demonstrated. The phytoconstituents such as polyphenols, the amide groups, and COOH groups might act as ligands for synthesizing and stabilizing the AgNPs, as evident from FT-IR studies. From our study in chapter 2 and chapter 3, we have observed the aqueous extract of the banana peels and the chayote squash contains the similar phytochemicals such as flavonoids, saponins, phenols, alkaloids and glycosides. Only tannins were absent in case of

the chayote squash extract. Synthesized silver nanoparticles were characterized by UV-Visible, FTIR and XRD. The antimicrobial results state that the silver nanoparticles have a strong antibacterial effect on gram-negative bacteria. Moreover, the synthesized AgNPs show catalytic activity that influences the reduction of methylene blue in the presence of *Sechium edule* aqueous extract attributed to the electron relay effect. The catalytic effect of AgNPs in organic transformations under reducing environment can be further explored.

3.6. EXPERIMENTAL SECTION

3.6.1. Materials and Methods

3.6.1.1. Chemicals and squash

Chayote squash was purchased from the local market of Amingaon, Guwahati, Assam, India. $AgNO_3$ was purchased from E-Merck Germany and used as a silver precursor as supplied. Millipore water was used for extraction process. Methylene blue was purchased from E-Merck Germany. Potato dextrose agar (PDA) was purchased from Himedia and used as supplied. All reagents were of analytical grade and were used as received without further purification. All solutions were freshly prepared using Millipore water and kept in the dark to avoid any photochemical reactions. All glassware used in experimental procedures was cleaned and dried before use.

2.6.1.2. Preparation of the chayote squash aqueous extract

Chayote squash purchased and cleaned properly, then its peels were removed and cut into small pieces. The methodology is already described and same is followed.[51] The aqueous extract was used for the phytochemical test and for synthesis of AgNPs.

3.6.1.3. Synthesis of silver nanoparticles

30 ml of chayote squash aqueous extract was added to 30 ml of an aqueous solution of 20 mM silver nitrate to reduce Ag^+ ions and incubated at room temperature for 48 hrs. The AgNPs were purified by repeated centrifugation of brown suspension at 10,000 rpm for 20 min. Then, redispersion of the pellet of AgNPs in deionized water and again centrifugation in the same way. Thus produced AgNPs were characterized and studied for their antimicrobial activity and catalytic activities.[52,53]

3.6.2. Characterization of AgNPs

3.6.2.1. UV-Visible spectroscopy

The reduction of Ag^+ ions into AgNPs was monitored by measuring the absorption of the reaction medium in a range of 400-450 nm wavelength using a Shimadzu UV-2550 UV-Visible spectrophotometer with a cell of 1 cm path length. The nanoparticles were primarily characterized by UV-visible spectroscopy, which is a very useful technique for the nanoparticles analysis. The measurements were done in absorbance mode. All the sample solutions were prepared freshly just before doing the experiment.

3.6.2.2. XRD measurement

The freeze-dried pellet nanoparticles were analyzed by X-ray diffraction. The instrument used was Bruker X-ray powder diffractometer. X-ray Diffraction is mainly used to measure crystallinity and phase of syhtnesized nanoparticles. The XRD patterns were measured at 50 kV and 100 mA using Cu Kα radiation with x-ray wavelength λ = 1.5406 Å. An R-AXIS IV++ x-ray detector was used to detect the diffracted X-rays. The scanning velocity was fixed at 2^o/min, and the diffraction pattern was recorded in the angular 2θ range 30°-80°. It provides details of the lattice structures of crystalline substances. Crystalline or amorphous nature of the nanoparticles are revealed under X-Ray Diffraction.

3.6.3.3. FTIR Measurements

The AgNPs were purified and dried, after that FTIR spectrum was recorded on a Perkin Elmer Spectrum One FT-IR spectrometer. The FT-IR spectra of the green synthesized AgNPs were collected at a resolution of 4 cm^{-1} in the transmission mode from 4000 cm^{-1} - 400 cm^{-1} wavenumbers. The functional groups present in the aqueous extract, which are responsible for the reduction of silver ions as well as a stabilizer of formed nanoparticles was identified with the help of FT-IR spectroscopy.

3.6.3.4. Transmission Electron Microscopy (TEM)

Transmission electron microscopy(TEM) analysis was carried out using the JEOL model JEM2100 Field Emission Transmission Electron Microscope. Electron microscopy parameters were set at a 1.4 Å (lattice) resolution and 1.94 Å (point to point). All images and analyses were obtained at 200 kV accelerating voltage. In the process, three magnification modes (at 200 kV) were maintained at: Standard magnification mode: 2,000× to 1,500,000×; Selected area magnification mode: 2,000× to 1,500,000×; Low magnification mode (LOW MAG): 50× to 1,000×. SAED camera length was controlled at 8 to 20 cm. TEM is an imaging technique in

which the electron beam is focused on a sample specimen, which enlarges the image of the sample in a fluorescent screen of photographic film. Transmission electron microscopy (TEM) was used to know the size and structure of AgNPs precisely and support the results obtained by FESEM.

3.6.4. Application of AgNPs

3.6.4.1. Antibacterial assay

The silver nanoparticles synthesized by the aqueous extract of s*echium edule* were tested for antimicrobial activity by disc diffusion method against gram-positive and gram-negative bacteria and compared with the control (S10, Amp). Approximately, 15 mL of autoclaved LB agar media was poured into each of the sterilized Petri dishes in a laminar airflow system. The plates were then sealed with paraffin strips, allowed to dry, and left overnight at 4°C temperature. The LB agar plates were precisely spread with the respective bacteria, and the discs containing the solution of AgNPs, aqueous extract and the antibiotics were put into the plates. The agar plates were then incubated at 37°C for 24 hrs. After incubation, the zone of inhibition (in mm diameter) was observed and tabulated.

3.6.4.2. Antifungal assay

The antifungal assay was carried out in petri plates containing 10 ml potato dextrose agar (PDA) as a culture medium supplemented with silver nanoparticles. *Aspergillus thermomutans* was point inoculated in above medium and incubated at 28 ºC for 72 hrs. The diameter of mycelial colonies developed was compared with the control plates.

3.6.4.3. Effect of AgNPs on the reduction of methylene blue (MB)

The catalytic activity of synthesized AgNPs was evaluated from a study of the reduction of methylene blue monitored using a UV–visible spectrophotometer. Thus, 1.5 ml of methylene blue (1×10^{-3} M) was mixed with 0.1 ml of aqueous fruit extract and 1.4 ml of water and the reaction was monitored after 30 min. In a separate tube, 1.5 ml of methylene blue (1×10^{-3} M) was mixed with 0.1 ml aqueous fruit extract and 1.4 ml of synthesized Ag-NPs and the reaction was monitored at three different time intervals viz., 30 min, 45 min and 60 min. The values of absorptions were compared with that of methylene blue.

3.7. REFERENCES

(1) Khalil, K. A.; Fouad, H.; Elsarnagawy, T.; Almajhdi, F. N. Preparation and Characterization of Electrospun PLGA / Silver Composite Nanofibers for Biomedical

Applications. *Int. J. Electrochem. Sci.* **2013**, *8*, 3483–3493.

(2) Ahmed, S.; Ahmad, M.; Swami, B. L.; Ikram, S. A Review on Plants Extract Mediated Synthesis of Silver Nanoparticles for Antimicrobial Applications: A Green Expertise. *J. Adv. Res.* **2016**, *7* (1), 17–28.

(3) Klaus-Joerger, T.; Joerger, R.; Olsson, E.; Granqvist, C. G. Bacteria as Workers in the Living Factory: Metal-Accumulating Bacteria and Their Potential for Materials Science. *Trends Biotechnol.* **2001**, *19* (1), 15–20.

(4) Shahverdi, A. R.; Minaeian, S.; Shahverdi, H. R.; Jamalifar, H.; Nohi, A.-A. Rapid Synthesis of Silver Nanoparticles Using Culture Supernatants of Enterobacteria: A Novel Biological Approach. *Process Biochem.* **2007**, *42* (5), 919–923.

(5) Mukherjee, P.; Ahmad, A.; Mandal, D.; Senapati, S.; Sainkar, S. R.; Khan, M. I.; Parishcha, R.; Ajaykumar, P. V; Alam, M.; Kumar, R.; Sastry, M. Fungus-Mediated Synthesis of Silver Nanoparticles and Their Immobilization in the Mycelial Matrix: A Novel Biological Approach to Nanoparticle Synthesis. *Nano Lett.* **2001**, *1* (10), 515–519.

(6) Willner, I.; Baron, R.; Willner, B. Growing Metal Nanoparticles by Enzymes. *Adv. Mater.* **2006**, *18* (9), 1109–1120.

(7) Kuppusamy, P.; Yusoff, M. M.; Maniam, G. P.; Govindan, N. Biosynthesis of Metallic Nanoparticles Using Plant Derivatives and Their New Avenues in Pharmacological Applications – An Updated Report. *Saudi Pharm. J.* **2016**, *24* (4), 473–484.

(8) Kulkarni, N.; Muddapur, U. Biosynthesis of Metal Nanoparticles: A Review. *J. Nanotechnol.* **2014**, *2014*, 510246.

(9) Kumar, D. A.; Palanichamy, V.; Roopan, S. M. Green Synthesis of Silver Nanoparticles Using *Alternanthera dentata* Leaf Extract at Room Temperature and Their Antimicrobial Activity. *Spectrochim. Acta Part A Mol. Biomol. Spectrosc.* **2014**, *127*, 168–171.

(10) Nakkala, J. R.; Mata, R.; Gupta, A. K.; Sadras, S. R. Biological Activities of Green Silver Nanoparticles Synthesized with *Acorous calamus* Rhizome Extract. *Eur. J. Med. Chem.* **2014**, *85*, 784–794.

(11) Sun, Q.; Cai, X.; Li, J.; Zheng, M.; Chen, Z.; Yu, C.-P. Green Synthesis of Silver Nanoparticles Using Tea Leaf Extract and Evaluation of Their Stability and Antibacterial Activity. *Colloids Surfaces A Physicochem. Eng. Asp.* **2014**, *444* (C), 226–231.

(12) Vijay Kumar, P. P. N.; Satyanarayana, K. V. V; Kollu, P.; Pammi, S. V. N.; Shameem,

U. Green Synthesis and Characterization of Silver Nanoparticles Using *Boerhaavia diffusa* Plant Extract and Their Anti Bacterial Activity. *Ind. Crop. Prod.* **2014**, *52*, 562–566.

(13) Gopinath, V.; MubarakAli, D.; Priyadarshini, S.; Priyadharsshini, N. M.; Thajuddin, N.; Velusamy, P. Biosynthesis of Silver Nanoparticles from *Tribulus terrestris* and Its Antimicrobial Activity: A Novel Biological Approach. *Colloids Surf. B. Biointerfaces* **2012**, *96*, 69–74.

(14) Sadeghi, B.; Rostami, A.; Momeni, S. S. Facile Green Synthesis of Silver Nanoparticles Using Seed Aqueous Extract of *Pistacia atlantica* and Its Antibacterial Activity. *Spectrochim. Acta. A. Mol. Biomol. Spectrosc.* **2015**, *134*, 326–332.

(15) Mariselvam, R.; Ranjitsingh, A. J. A.; Usha Raja Nanthini, A.; Kalirajan, K.; Padmalatha, C.; Mosae Selvakumar, P. Green Synthesis of Silver Nanoparticles from the Extract of the Inflorescence of *Cocos nucifera* (Family: Arecaceae) for Enhanced Antibacterial Activity. *Spectrochim. Acta Part A Mol. Biomol. Spectrosc.* **2014**, *129*, 537–541.

(16) Ashokkumar, S.; Ravi, S.; Kathiravan, V.; Velmurugan, S. Synthesis of Silver Nanoparticles Using *A. indicum* Leaf Extract and Their Antibacterial Activity. *Spectrochim. Acta. A. Mol. Biomol. Spectrosc.* **2015**, *134*, 34–39.

(17) Sadeghi, B.; Gholamhoseinpoor, F. A Study on the Stability and Green Synthesis of Silver Nanoparticles Using *Ziziphora tenuior* (Zt) Extract at Room Temperature. *Spectrochim. Acta. A. Mol. Biomol. Spectrosc.* **2015**, *134*, 310–315.

(18) Ulug, B.; Haluk Turkdemir, M.; Cicek, A.; Mete, A. Role of Irradiation in the Green Synthesis of Silver Nanoparticles Mediated by Fig (*Ficus carica*) Leaf Extract. *Spectrochim. Acta. A. Mol. Biomol. Spectrosc.* **2015**, *135*, 153–161.

(19) Krishnaraj, C.; Jagan, E. G.; Rajasekar, S.; Selvakumar, P.; Kalaichelvan, P. T.; Mohan, N. Synthesis of Silver Nanoparticles Using *Acalypha indica* Leaf Extracts and Its Antibacterial Activity against Water Borne Pathogens. *Colloids Surf. B. Biointerfaces* **2010**, *76* (1), 50–56.

(20) Kumarasamyraja, D.; Jeganathan, N. S. Green Synthesis of Silver Nanoparticles Using Aqueous Extract of *Acalypha indica* and Its Antimicrobial Activity. *Int J Pharm Bio Sci* **2013**, *4* (3), 469–476.

(21) Geetha, N.; Geetha, T. S.; Manonmani, P.; Thiyagarajan, M. Green Synthesis of Silver Nanoparticles Using *Cymbopogan citratus* (Dc) Stapf. Extract and Its Antibacterial Activity. *Aust. J. Basic Appl. Sci.* **2014**, *8* (March), 324–331.

(22) Kumar, S.; Daimary, R. M.; Swargiary, M.; Brahma, A.; Kumar, S.; Singh, M. Biosynthesis of Silver Nanoparticles Using *Premna herbecea* Leaf Extract and Evaluation of Its Antibacterial Activity against Bacteria Causing Dysentary. *Int J Pharm Bio Sci* **2013**, *4* (4), 378–384.

(23) Gondwal, M.; Pant, G. J. N. Biological Evaluation and Green Synthesis of Silver Nanoparticles Using Aqueous Extract of *Calotropis procera*. *Int. J. Pharma Bio Sci.* **2013**, *4* (4), 635–643.

(24) Rout, A.; Jena, P.; Parida, U.; Bindhani, B. K. Green Synthesis of Silver Nanoparticles Using Leaves Extract of *Centella asiatica L*. for Studies against Human Pathogens. *Int. J. Pharma Bio Sci.* **2013**, *4* (4), 661–674.

(25) Thombre, R.; Parekh, F.; Patil, N. Green Synthesis of Silver Nanoparticles Using Seed Extract of *Argyreia nervosa*. *Int. J. Pharma Bio Sci.* **2014**, *5* (1), 114–119.

(26) Narayanan, K. B.; Park, H. H. Antifungal Activity of Silver Nanoparticles Synthesized Using Turnip Leaf Extract (*Brassica rapa L*.) against Wood Rotting Pathogens. *Eur. J. Plant Pathol.* **2014**, *140* (2), 185–192.

(27) Ashokkumar, S.; Ravi, S.; Kathiravan, V. Green Synthesis of Silver Nanoparticles and Their Structural and Optical Properties. *Int. J. Curr. Res.* **2013**, *5* (10), 3238–3240.

(28) Zargar, M.; Hamid, A. A.; Bakar, F. A.; Shamsudin, M. N.; Shameli, K.; Jahanshiri, F.; Farahani, F. Green Synthesis and Antibacterial Effect of Silver Nanoparticles Using *Vitex negundo L*. *Molecules* **2011**, *16* (8), 6667–6676.

(29) Kathiravan, V.; Ravi, S.; Ashokkumar, S. Synthesis of Silver Nanoparticles from *Melia dubia* Leaf Extract and Their in Vitro Anticancer Activity. *Spectrochim. Acta. A. Mol. Biomol. Spectrosc.* **2014**, *130*, 116–121.

(30) Jannathul, M.; Lalitha, P. Green Synthesis of Silver Nanoparticles Using the Aqueous Extract of *Portulaca oleracea* (L.). In *Asian Journal of Pharmaceutical and Clinical Research*; 2013; pp 92–94.

(31) Rupiasih, N. N.; Aher, A.; Gosavi, S.; Vidyasagar, P. B. Green Synthesis of Silver Nanoparticles Using Latex Extract of Thevetia Peruviana: A Novel Approach towards Poisonous Plant Utilization. In *Journal of Physics: Conference Series*; IOP Publishing, 2013; Vol. 423, p 12032.

(32) Gogoi, S. J. Green Synthesis of Silver Nanoparticles from Leaves Extract of Ethnomedicinal Plants-*Pogostemon benghalensis (B) O.Ktz*. *Pelagia Res. Libr. Adv. Appl. Sci. Res.* **2013**, *4* (4), 274–278.

(33) Vijayaraghavan, K.; Nalini, S. P. K.; Prakash, N. U.; Madhankumar, D. One Step Green

Synthesis of Silver Nano/Microparticles Using Extracts of *Trachyspermum ammi* and P*apaver somniferum*. *Colloids Surf. B. Biointerfaces* **2012**, *94*, 114–117.

(34) Mondal, S.; Roy, N.; Laskar, R. A.; Sk, I.; Basu, S.; Mandal, D.; Begum, N. A. Biogenic Synthesis of Ag, Au and Bimetallic Au/Ag Alloy Nanoparticles Using Aqueous Extract of Mahogany (*Swietenia mahogani JACQ*.) Leaves. *Colloids Surf. B. Biointerfaces* **2011**, *82* (2), 497–504.

(35) Bankar, A.; Joshi, B.; Kumar, A. R.; Zinjarde, S. Banana Peel Extract Mediated Novel Route for the Synthesis of Silver Nanoparticles. *Colloids Surfaces A Physicochem. Eng. Asp.* **2010**, *368* (1–3), 58–63.

(36) Prasad, T. N. V. K. V; Elumalai, E. K. Biofabrication of Ag Nanoparticles Using *Moringa oleifera* Leaf Extract and Their Antimicrobial Activity. *Asian Pac. J. Trop. Biomed.* **2011**, *1* (6), 439–442.

(37) Santhoshkumar, T.; Rahuman, A. A.; Rajakumar, G.; Marimuthu, S.; Bagavan, A.; Jayaseelan, C.; Zahir, A. A.; Elango, G.; Kamaraj, C. Synthesis of Silver Nanoparticles Using *Nelumbo nucifera* Leaf Extract and Its Larvicidal Activity against Malaria and Filariasis Vectors. *Parasitol. Res.* **2011**, *108* (3), 693–702.

(38) Rajakumar, G.; Abdul Rahuman, A. Larvicidal Activity of Synthesized Silver Nanoparticles Using *Eclipta prostrata* Leaf Extract against Filariasis and Malaria Vectors. *Acta Trop.* **2011**, *118* (3), 196–203.

(39) Ahamed, M.; Majeed Khan, M. A.; Siddiqui, M. K. J.; AlSalhi, M. S.; Alrokayan, S. A. Green Synthesis, Characterization and Evaluation of Biocompatibility of Silver Nanoparticles. *Phys. E Low-dimensional Syst. Nanostructures* **2011**, *43* (6), 1266–1271.

(40) Chandran, S. P.; Chaudhary, M.; Pasricha, R.; Ahmad, A.; Sastry, M. Synthesis of Gold Nanotriangles and Silver Nanoparticles Using *Aloe vera* Plant Extract. *Biotechnol. Prog.* **2006**, *22* (2), 577–583.

(41) Kaviya, S.; Santhanalakshmi, J.; Viswanathan, B.; Muthumary, J.; Srinivasan, K. Biosynthesis of Silver Nanoparticles Using *Citrus sinensis* Peel Extract and Its Antibacterial Activity. *Spectrochim. Acta. A. Mol. Biomol. Spectrosc.* **2011**, *79* (3), 594–598.

(42) Dubey, M.; Bhadauria, S.; Kushwah, B. Green Synthesis of Nanosilver Particles from Extract of *Eucalyptus hybrida* (Safeda) Leaf. *Dig J Nanomater Biostruct* **2009**, *4* (3), 537–543.

(43) Elavazhagan, T.; Arunachalam, K. D. Memecylon Edule Leaf Extract Mediated Green Synthesis of Silver and Gold Nanoparticles. *Int. J. Nanomedicine* **2011**, *6*, 1265–1278.

(44) Kesharwani, J.; Yoon, K.; Hwang, J.; Rai, M. Phytofabrication of Silver Nanoparticles by Leaf Extract of *Datura metel*: Hypothetical Mechanism Involved in Synthesis. *J. Bionanoscience* **2009**, *3* (1), 39–44.

(45) Gnanajobitha, G.; Paulkumar, K.; Vanaja, M.; Rajeshkumar, S.; Malarkodi, C.; Annadurai, G.; Kannan, C. Fruit-Mediated Synthesis of Silver Nanoparticles Using *Vitis vinifera* and Evaluation of Their Antimicrobial Efficacy. *J. Nanostructure Chem.* **2013**, *3* (1), 67.

(46) Lee, K. D.; Nagajyothi, P. C. Synthesis of Plant-Mediated Silver Nanoparticles Using *Dioscorea batatas* Rhizome Extract and Evaluation of Their Antimicrobial Activities. *J. Nanomater.* **2011**, *2011* (3), 557–563.

(47) Veerasamy, R.; Xin, T. Z.; Gunasagaran, S.; Xiang, T. F. W.; Yang, E. F. C.; Jeyakumar, N.; Dhanaraj, S. A. Photochemical Preparation of Silver Nanoparticles Supported on Zeolite Crystals. *J. Saudi Chem. Soc.* **2011**, *15* (2), 113–120.

(48) Kundu, S.; Ghosh, S. K.; Mandal, M.; Pal, T. Silver and Gold Nanocluster Catalyzed Reduction of Methylene Blue by Arsine in Micellar Medium. *Bull. Mater. Sci.* **2002**, *25* (6), 577–579.

(49) Sondi, I.; Salopek-Sondi, B. Silver Nanoparticles as Antimicrobial Agent: A Case Study on *E. coli* as a Model for Gram-Negative Bacteria. *J. Colloid Interface Sci.* **2004**, *275* (1), 177–182.

(50) Lokesh, M. K.; Puspita, D.; Angela, G. Quality Evaluation and Storage Studies of Legume Based Wadis (Traditional Delicacies) Formulated Using *Sechium edule* - An Underutilized Vegetable Crop of North East India. *Res. J. Biotechnol.* **2017**, *12* (6), 29–35.

(51) Tiwari, P.; Kumar, B.; Kaur, M.; Kaur, G.; Kaur, H. Phytochemical Screening and Extraction: A Review. *Int. Pharm. Sci.* **2011**, *1* (1), 98–106.

(52) Sivakumar, P.; Nethradevi, C.; Renganathan, S. Synthesis of Silver Nanoparticles Using *Lantana camara* Fruit Extract and Its Effect on Pathogens. *Asian J. Pharm. Clin. Res.* **2012**, *5* (3), 237–245.

(53) Edison, T. J. I.; Sethuraman, M. G. Instant Green Synthesis of Silver Nanoparticles Using *Terminalia chebula* Fruit Extract and Evaluation of Their Catalytic Activity on Reduction of Methylene Blue. *Process Biochem.* **2012**, *47* (9), 1351–1357.

CHAPTER 4:

Synthesis of Polystyrene Nanocomposites (PS-AgNPs) from Waste Thermocol and Green Synthesized Silver Nanoparticles for Water Disinfection Application

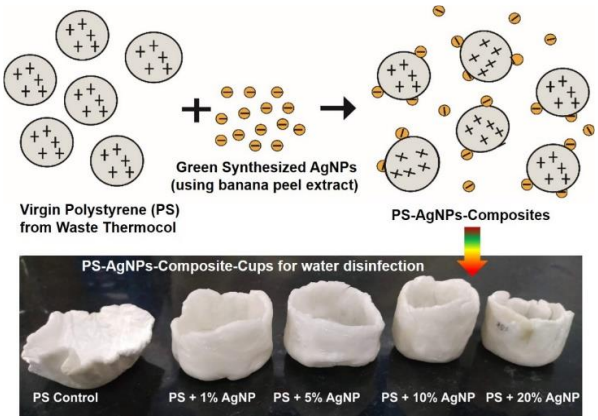

4.1. Introduction

Nanotechnology offers various treatment technologies for wastewater treatment. These technological processes include membrane processes, photocatalytic/elctrochemical oxidation or degradation, coagulation, adsorption, sedimentation, biological oxidation, flocculation, and other combined methodologies.[1] Nanomaterials offer opportunities to be used economically for expanding, restoring and cleaning the water systems. Nanomaterials or nanocomposites used for industrial waste treatment are extremely important and are used extensively. Figure 4.1 represents the significant applications of nanocomposites in wastewater treatment. The application of nanotechnology in wastewater treatment is advantageous as it can remove impurities and provide pure water with cost and time-effective way.[2]

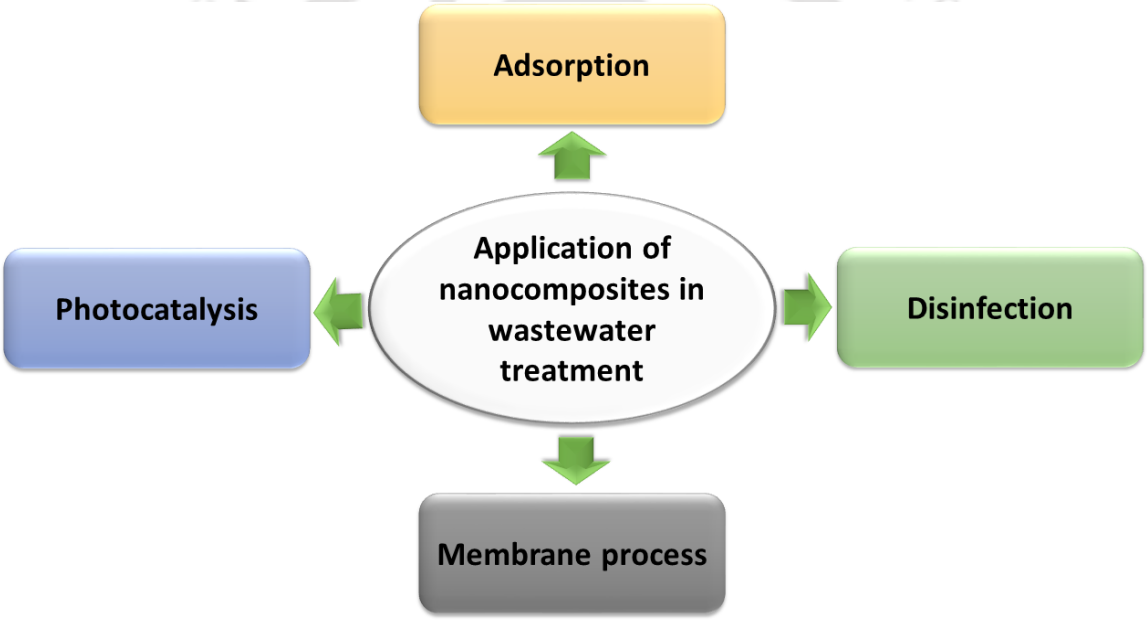

Figure 4.1. The various application of nanocomposites in wastewater treatment (Adapted from Naseem *et al.*, 2021).

Figure 4.1 represents four major applications of nanocomposites which include adsorption, membrane process, photocatalysis and disinfection.[1] Generally, physical forces cause adsorption, but sometimes poor chemical bonds can also cause adsorption. In removing the organic and inorganic impurities from water and wastewater, nano-adsorbents are used because they are ideal due to their exceptional properties such as smaller size, catalytic potential, easy separation, higher reactivity and high surface area.[3]

Nanotechnology also provides therapeutic aid with drug-resistant microbes. Numerous nanoparticles are extensively used as antibacterial agents in medical, agricultural, water resource, and environmental fields. Metal nanoparticles and metal oxide nanoparticles-based nanocomposites can overcome the conventional antibiotic drug limitations. The main mechanisms of the nanoparticle-based nanocomposites which involve antibacterial activity are reactive oxygen species generation, ion release and bacterial cell membrane impact. The physicochemical properties of nanocomposites, such as size, shape, solubility, orientation, surface area, crystallinity, and chemical composition, play a significant role in their antimicrobial activities.[4]

4.2. NANOCOMPOSITES

Nanocomposites are solid materials built up with numerous phases where one phase has either one, two or three dimensions in the nanometer range. These nanocomposites consist of nanomaterials which mainly include nanoparticles, nanofibers, and nanoclays.[5] Phase interfaces occur when the material dimensions go down to the nanometer level, one of the most critical factors for enhancing material properties.[6] These nanocomposite materials can be advantageous over conventional composites as they are composed of polymeric, metallic or non-metallic materials that help retain primary features for overcoming defects and enhancing new characteristics. Nanocomposites provide new alternative solutions for undergoing the existing limitations of micro composites and the monolithic.[5]

Nanocomposites have numerous advantages over conventional composite materials. They have a high surface-to-volume ratio, which aids small filler sizes; they have better mechanical properties, high ductility and scratch resistance. Nanocomposites also provide optical properties such as light transmission, which mainly depends on particle size. However, the toughness of the materials and impact on incorporating the nanoparticles into the bulk-matrix composite put several challenges for the applications of these materials. Also, there is not an adequate understanding of the formulation, the material properties, structure association. As such, more research on the complexity of the nanocomposite materials can provide better elucidations.[5]

4.2.1. Types of Nanocomposites

There are mainly three matrix groups of nanocomposite materials- ceramic matrix, metal matrix and polymer matrix nanocomposites-which are depicted in Figure 4.2. In ceramic

nanocomposite materials, one or more discrete ceramic phases are added mainly to boost resistivity, thermal and chemical stability. But these materials are brittle and have low toughness, and hence they have limited usage. Energy dissipating components such as fiber, particles, or platelets are incorporated in the ceramic matrix to lower the brittleness and enhance durability.[7,8] Ceramic nanocomposites have biomedical[9] and various photocurrent applications.[10] They are also used for acid fuchsin removal.[11]

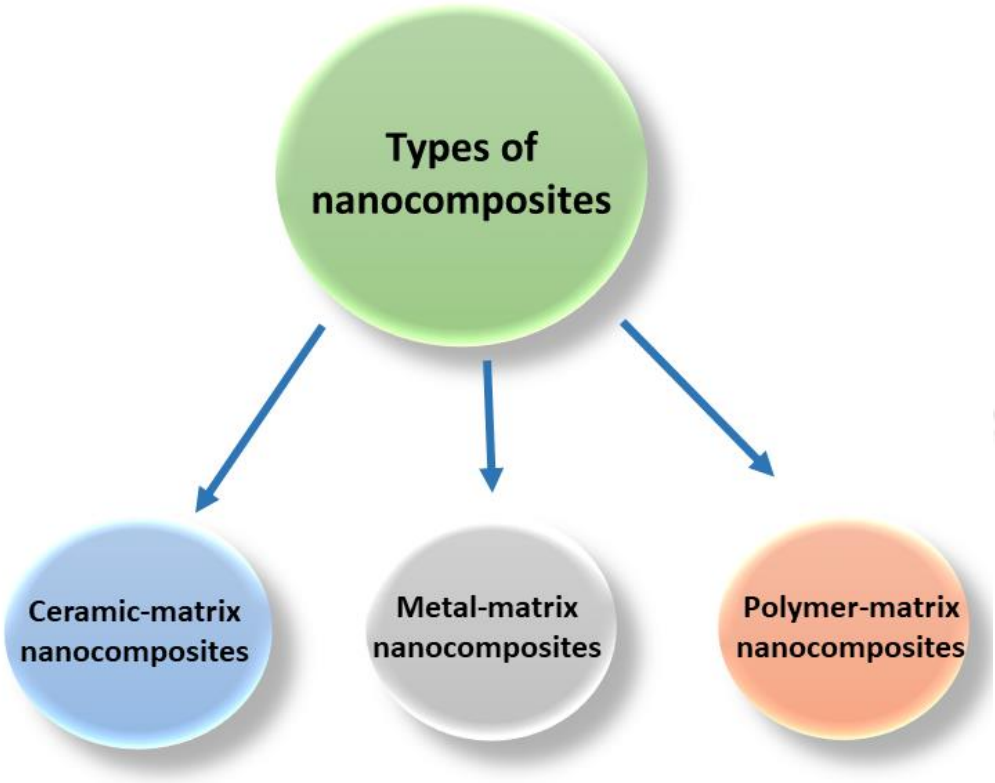

Figure 4.2. Schematic representation of the main types of nanocomposites.

The multiphase material in which ductile metal or alloy matrix is reinforced with nanosized materials is known as metal matrix nanocomposites. These types of nanocomposites find broad applications in aerospace, military, automotive and electronics. The polymer-metal nanocomposites mainly comprise of a polymer as matrix and metal nanoparticles as the nanofillers. These types of nanocomposites have huge applications in biomedical and medical devices. Further, The fillers in the polymer matrix nanocomposites are classified as 1D-linear, 1D-layered and 3D-powder, including carbon nanotubes(1D), montmorillonite(2D) and silver nanoparticles(AgNPs).[12] Polymer matrix and nanofillers interact on a molecular level which initiates the effect of attraction between nanocomposites. Nanofillers have a high surface area. A larger interface area means more significant interaction area, which determines the

magnitude of the effect produced by the presence of the filler. This interaction between the charge and polymer is a complex phenomenon involving several interaction mechanisms such as electrostatic interactions, diffusion, surface tension, mechanism interlocking, chemical bonding, surface tension, intermolecular bonding and surface wetting that are unique to the complex according to its type, size, shape and preparation. Thus, the addition of nanofiller to the polymer matrix with less than 100 nm dimension changes the properties of the nanocomposites. Polymer nanocomposites fundamentally have high thermal stability, low gas permeability and enhanced mechanical properties.[13]

4.2.2. Polymer Nanocomposites

Polymer nanocomposites are composite materials that include polymer as matrix and nanofillers as stable and uniform nanoparticles. Nanoparticles are well dispersed into the polymer matrix, resulting in improved properties in the nanocomposites compared to the conventional composites or neat polymers. Nanocomposites are materials in which polymer combines with the useful properties of metal nanoparticles such as electrical, catalytic, optical and magnetic properties and become functional in various commercial applications.[14–16] The main reason for choosing polymer nanocomposite technology is that it can prevent aggregation of particles which occurs due to the high surface energy of the added nanoparticles. To overcome this, alterations can be made to the surface of the particles, which enhances and modifies the polymer matrix and inorganic particles interfacial interactions.[17] Silver nanoparticles(AgNPs) are frequently used with polymers as nanofillers. They have a better catalytic and antimicrobial activity, better chemical stability, good conductivity, improved thermal and other properties of the polymer matrices.[16,18] Further, due to the addition of the proper size of AgNPs with the polymers, nanocomposites can achieve enhanced optical properties because of the stronger plasma resonance absorption of the materials.[19] For achieving this, polystyrene(PS) is one of the most effective polymers for AgNPs stabilization. These synthesized PS nanocomposites are utilized for designing numerous devices in which the PS properties are upgraded or retained.[20]

Polystyrene(PS) is commercially known as general-purpose or crystal polystyrene. PS is an aromatic hydrocarbon polymer made from styrene monomers. Figure 4.3 represents the structure of polystyrene. It is a vinyl polymer that is synthesized by free radical vinyl polymerization. It is a petroleum-based plastic that was first developed by distillation or pyrolyzing liquid storax. It is lightly weighted as it is composed of 95% of air and 5% PS.

Consumption of PS is highest in Asia, i.e., about 53% of the total world production and total consumption of about 47% respectively in the year 2010[21] There is a considerable environmental and health concern regarding the production of Styrofoam. They may cause health effects like irritation of the eyes and skin, gastrointestinal and upper respiratory tract issues. It can also affect the central nervous system or blood and kidney functioning.[22]

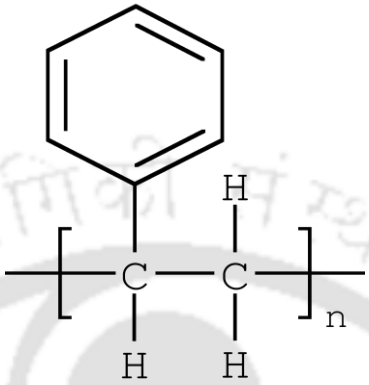

Figure 4.3. Structure of polystyrene formed after free radical vinyl polymerization.

PS has a considerable application in packaging industries, manufacturing items, medical equipment, craft items, construction, transportation, appliances, etc., due to its high insulation properties.[23] Increasing demand for PS-based materials for several household and commercial applications in developing countries has led to a drastic increase in the production of expanded polystyrene, known as thermocol, over the past two decades.[24] As a result, post-consumer waste polystyrene (WPS) accumulation has increased enormously in the environment causing disposal a severe concern. Current disposal practices, such as waste dump and open-burning, lead to environmental pollution via leakage of chemicals or release of genotoxic/carcinogenic PAHs, Cox, NOx, Sox, etc., gases into the environment.[25] Thus, it is causing a severe threat to the environment, especially in developing countries. This waste is dumped in the open and burnt, later on leading to air pollution[26]. In a few developing countries, limited oil resources are used to produce different kinds of products made from a range of plastics. Most of these plastic-made products are dumped into the open in non-sanitary dumps, which might cause grave environmental health issues.[27]

In many cases, plastic waste recovery is not feasible economically.[28] PS is a widely used plastic that is quite difficult to recycle for packaging purposes as its SPI (Society for Plastic Industries) code is 6. Different types of PS are used in industries, especially in the packaging industry. General-purpose polystyrene (GPPS), syndiotactic polystyrene (SPS), high impact polystyrene (HIPS) and expanded polystyrene (EPS) are the significant types of PS used in

industries.[25–27,29] These can also cause a nuisance in the environment as its density is low and dispersed. Therefore, proper disposal has become a severe problem. Incineration and landfilling are not the eventual solution for solving the problem of plastic waste. These methods are expensive and also lead to land and air pollution. Incineration causes the emission of greenhouse gases that lead to climate change and the release of carcinogenic gases.[25] Recycling and reusing waste polystyrene (WPS) is one of the best solutions to pollution problems and fulfils the increased demand for polystyrene-based materials for various applications. Thus, recycled plastics can be converted to value-added products requiring the low running cost of a recycling plant.

Silver has been used in food and beverage storage applications from a very ancient time. Storage of water and wine in silver vessels and keeping silver spoons at the bottom of milk or water bottles improves the shelf life. Silver is used for storing water for a long time as it acts as a sterilizing agent.[30] Silver has a wide-ranging antimicrobial activity and lowers expenditure, making it affordable for use in the food and water disinfection industry.[31] FDA permitted the reliable use of silver nitrate($AgNO_3$) as a disinfectant in 2009 in commercially bottled water at a low concentration of about 17 μg/kg.[32] AgNPs are found to be toxic to microorganisms; their mechanism is different from that of Ag^+ ions. The concentration of Ag^+ ions released from AgNPs is quite low to indicate the toxicity of AgNPs.[33] Also, AgNPs have controlled release properties, so AgNPs are advantageous as potential antimicrobial agents for a longer period. As such, AgNP/polymer nanocomposites are striking materials for use in food packaging and medical devices.[34] AgNP/polyethylene nanocomposite layer has been used in a layer of five (PE/ tie/PA-6/tie/PE; PA-6 = polyamide six and tie = maleic anhydride grafted polyethylene) plastic film. Antimicrobial activity against the fungus *A. niger*, a food contaminant, was observed.[35] AgNP/polymer nanocomposite materials are also tested in real food systems to establish the consequence of AgNP on food shelf-life. Sterilized pears and carrots, when dipped into solutions of alginate containing AgNPs, form edible antibacterial films. Water loss in the carrots and pears is less, and consumers' acceptability is also high based on the colour, taste, and texture even kept for ten days.[36] Other examples include an edible film preparation using AgNPs dispersed in glycogen. The glycogen biopolymer used was from bovine liver which is used as the stabilizing agent for the AgNPs growth. From the results it has been concluded that the method of preparation strongly influences the optical properties of the attained nanocomposite samples. Photoluminescence of the glycogen is quenched by AgNPs as such the samples which were prepared by microwave radiation showed narrow SPR peaks. Also, the

nanocomposites showed >99% of bacterial cell reduction when exposed for 2 hours depending upon the concentration of the Ag.[37]

4.2.5. Polystyrene-Ag-Nanocomposites

Polymer nanocomposites are functional materials used for various prospective applications in diverse fields. Mainly the antimicrobial property of silver nanoparticles (AgNPs) has been focused. AgNPs can adhere to the bacterial cell surface, degrading the lipopolysaccharides and formatting pits in the membranes, which increases permeability and penetration inside the bacterial cell. DNA damage occurs by releasing Ag^+ ions by the dissolution of AgNPs.[38–41] Polymer-Ag nanocomposites are studied for their antimicrobial efficacy by various researchers.[41] AgNPs easily form composites with different polymers like polyvinyl alcohol (PVA), chitosan, polypyrrole, cellulose and polyvinylidene fluoride. Controlled size and uniform distribution of nanoparticles within the polymer matrix are necessary to form polymer-Ag nanocomposites.[42] Ag-doped PS composite showed good antimicrobial features similar to the antimicrobial activities of pure Ag powder, whose Ag concentration is >30% by weight in the polymer.[43] PS-Ag nanocomposites also exhibit high antimicrobial activity against *B. circulens* BP2 culture type.[44] Again, AgNPs-PS nanocomposites with different concentrations of AgNPs have revealed that the addition of Ag in the PS matrix improved the thermal stability and the thermo-oxidative stability of PS.[45] There are two methods used for the development of PS-Ag nanocomposites. Firstly, incorporating pre-made nanoparticles into PS matrix, which is chemically produced with the organically passivated surface using a common solvent. Secondly, in solution, polymerization of styrene monomer occurs in the presence of pre-made nanoparticles or ions, which can be thermally or chemically reduced.[45–47,49] Figure 4.4. gives a graphical representation of the polystyrene-Ag nanocomposite complex.

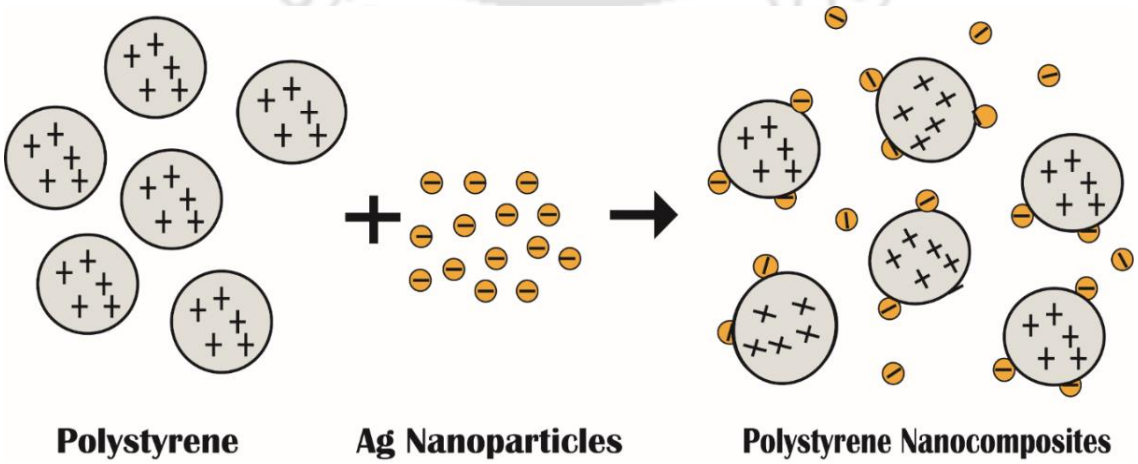

Figure 4.4. Graphical representation of the Polystyrene nanocomposite materials.

4.3. AIM AND OBJECTIVES

Scientists worldwide are keen to develop cost-effective, non-toxic and eco-friendly water disinfection systems to suffice the scarcity of clean water. Achieving proper disinfection without creating harmful byproducts for removing or inactivating waterborne pathogens is the main challenge. In this respect, polystyrene (PS) nanocomposites find wide applications in water storage, food packaging material, transportation, medicine, etc. The addition of nanoparticles such as silver nanoparticles(AgNPs) into PS enhances its mechanical properties, gas barrier properties, thermal stability, etc. This study reports the development of PS-AgNPs composite using green synthesized AgNPs and waste thermocol.

Motivated by the environmental issue related to waste management and with an aim of turning wastes into value-added materials, and following the background literature, we have concentrated ourselves on using our already synthesized AgNPs via green route for making composite with waste thermocol for water disinfection study. Thus we framed our objectives as below:

a) Green synthesis of AgNPs using Bhimkol (*Musa balbisiana*) peel extract (referring to chapter 2, section: 2.6.3. Green Synthesis of AgNPs).
b) Development of PS nanocomposites by directly mixing waste thermocol in acetone and addition of different amount of AgNPs.
c) Characterization of PS nanocomposites using UV-Vis spectrophotometry, Fourier transformation infrared(FT-IR) spectrometry, Energy-dispersive X-ray(EDX), Field Emission Transmission Electron Microscope(FESEM), Field Emission Transmission Electron Microscope(FETEM) and Thermogravimetric analysis(TGA) performed in nitrogen gas.
d) Water disinfection application of the nanocomposites.

4.4. RESULTS AND DISCUSSION

4.4.1. Synthesis of AgNPs

The preliminary detection of AgNP formation was carried out by visual observation of the reaction solutions' colour changes, as denoted in figure 4.5(a) (refer to chapter 2, section 2.6.3 and figure 2.3 for the relevant synthesis of AgNPs). These changes indicated the excitation of surface plasmon resonance (SPR) in the AgNPs. UV-Visible absorption was used to observe

the SPR. Figure 4.5 gives the visual observation of the formation of bhimkol synthesized by AgNPs by the colour change of the reaction solution from colourless to yellowish-brown.

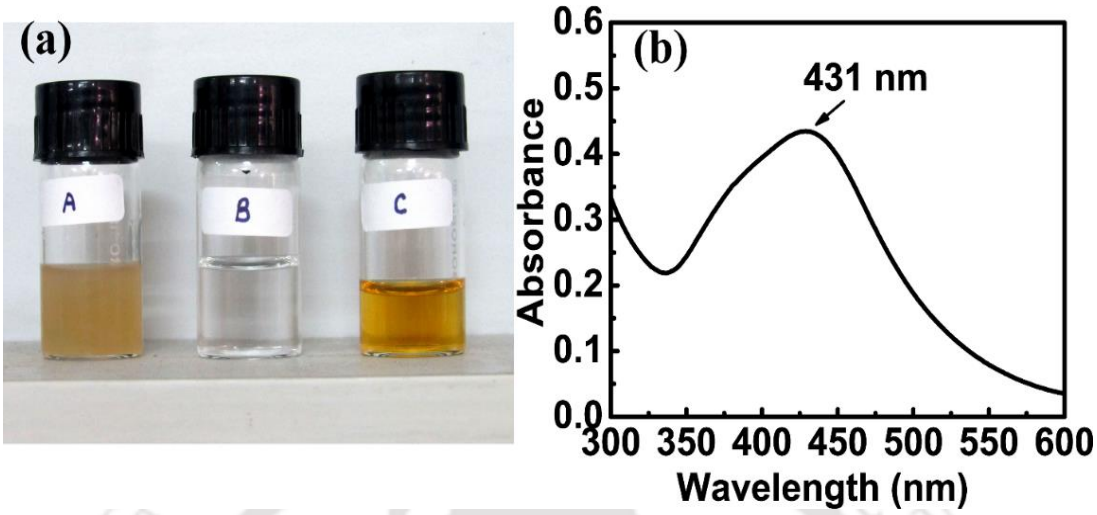

Figure 4.5. (a) Bhimkol peel extract(A), $AgNO_3$ solution(B), and Silver Nanoparticles(C), (b) UV-visible absorption spectrum of green synthesized AgNPs.

Figure 4.5(b) illustrates the UV-visible spectrum, which confirms the formation of AgNPs using Bhimkol peel extracts. It was recorded in a PerkinElmer Lambda/25/35/45 UV–vis spectrophotometer from 300 to 600 nm wavelength. Maximum peak absorbance was at 431 nm, which is detected as the characteristic surface plasmon resonance absorption band for the yellowish-brown coloured colloidal AgNPs.[50]

4.4.2. Development of Functional PS-Ag Nanocomposites

Packaging is one of the most widespread applications of PS among manufactured items, art and craft materials, transport and construction items. Extruded polystyrene, Styrofoam and expanded polystyrene are generally used for equipment, food and drink packaging. Apart from its use in a wide range of packaging applications, it is highly favourable in the development of polymer-based nanocomposites for various applications, such as water disinfection tanks. The polymer forms the base and the incorporation of nanoparticles get dispersed in the polymer matrix. In particular, AgNPs showed efficient antimicrobial properties.[29] PS-AgNPs composites could be used to prepare water containers and the antimicrobial property would enable disinfection of water. Thus, functional PS nanocomposite cups were developed and used to test for water storage (Figure 4.6). Bacteria colonization on water storage was studied and it was observed that the cups could prevent microbial growth on water.

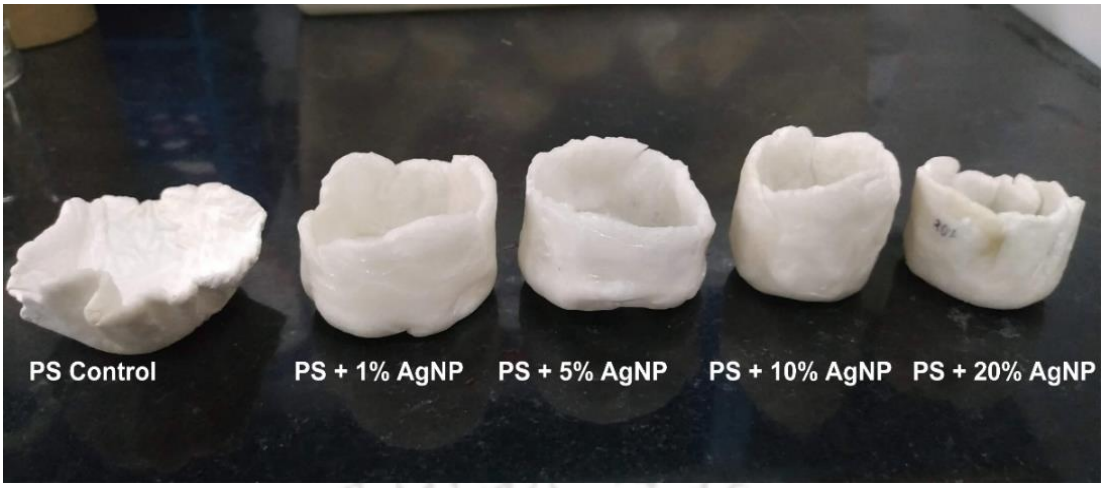

Figure 4.6. Polystyrene(PS) nanocomposite cups with varying concentrations of AgNPs for water disinfection application.

4.4.3. Characterization of the PS-Ag Nanocomposites

4.4.3.1. UV-Vis Spectroscopy of the PS nanocomposites

UV-Visible spectra confirm the formation and interaction of AgNPs with the polymer matrix. Figure 4.7(a) illustrated the absorption spectrum of the PS nanocomposite materials as a function of the wavelength of the incident light and was recorded using solid sample of the PS nanocomposites in a PerkinElmer Lambda/25/35/45 UV–visible spectrophotometer. From the figure, the absorbance of all the PS nanocomposites has a higher intensity peak at a wavelength between 200 nm to 300 nm and then gradually, the absorbance decreases with the increase of the wavelength. As such, the absorbance of the PS nanocomposites has a lower value in the visible and infrared regions. At 400 nm wavelength, absorbance of PS Control, PS +1 % AgNP, PS + 5% AgNPs, PS + 10% AgNPs, PS + 20% AgNPs were 0.1526, 0.1867, 0.1601, 0.193 and 0.207 respectively which decreased to 0.0864, 0.0728, 0.0663, 0.0852 and 0.0937 at 700 nm respectively. The incident photons at higher wavelength do not consist of enough energy to interact with atoms; thus, the photon is absorbed. Again when the wavelength decreases, the incident photon and material interaction occurs, leading to increased absorbance. Therefore, increasing the amount of AgNPs with the polymer, absorbance increases as the free electrons absorb the incident light.[51] The peak between 200-300 nm wavelength observed by all the PS composite materials indicates the interaction of the phenyl groups of the PS[52] with the AgNPs. Overall, there is a blue shift in absorption wavelength from the absorption of control PS and PS + 20% AgNP nanocomposite. This is because of the change in the dielectric constant of the two composites.

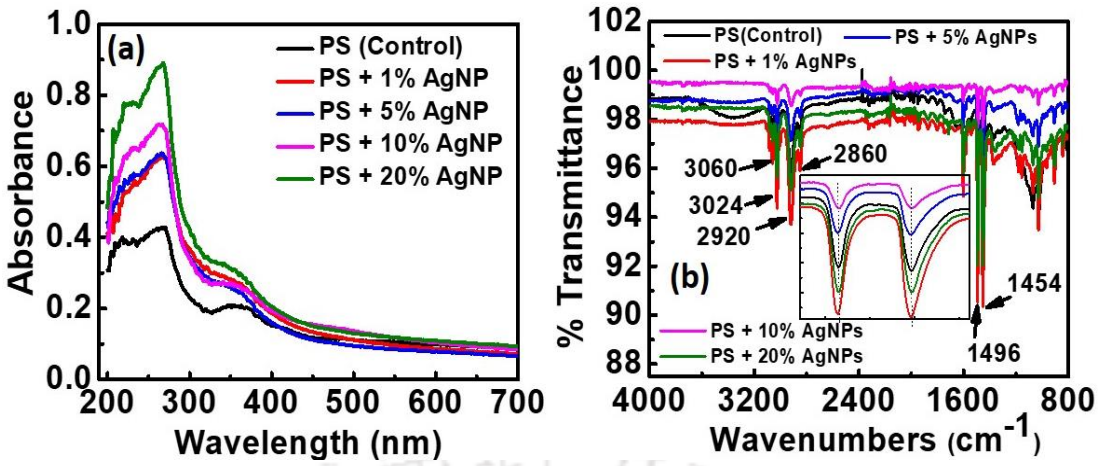

Figure 4.7. (a) UV-visible absorption and (b) FT-IR spectra of pure PS (PS control) and its various nanocomposites with different percentages of AgNPs.

4.4.3.2. FTIR Analysis

FTIR spectra of the control PS and PS nanocomposites illuminate interfacial interaction between AgNPs and PS matrix using solid sample in an FTIR-ATR spectrophotometer. Figure 4.7(b) represents the IR spectrum of the PS control and the PS nanocomposites containing the varying percentage of AgNPs. The vibrational stretching at 3060, 3024, 2920, and 2860 cm^{-1} corresponds to the C - H aromatic and aliphatic bands in the IR spectrum of pure PS. Vibrational C - H stretching band at 2924 cm^{-1} may be observed due to the presence of impurities. The peaks at 1026, 1188-1368, 1491-1599 and 1666-1945 cm^{-1} corresponds to aromatic C = C bond vibrations and range between 907-650 cm^{-1} corresponds to aromatic C – H bond vibrations. The infrared of the PS-AgNP nanocomposites spectra indicated all the characteristic bands as that of PS. All the spectra are almost similar, indicating that there may not be a very strong interaction between the functional groups of PS and the AgNPs. Though a distinctive shift in the IR spectra between PS (control) and the AgNPs-embedded PS is not present; however, detailed analysis showed that the aromatic C=C stretching at 1496 cm^{-1} and 1454 cm^{-1} for the AgNPs-embedded PS showed a minute shift towards the lower wavenumbers as compared to that of the control PS (Figure 4.7(b)).[53] This signifies that Ag-nanoparticles are embedded within the PS, resulting in a higher molecular mass as compared to virgin PS. Although the AgNPs remained dispersed into the PS matrix and its surfaces as observed from the FESEM(figure 4.8) and FETEM(figure 4.10) results, no new vibrational peaks appear in the PS-AgNPs nanocomposites' FT-IR spectra. The presence of AgNPs into the PS matrix can effectively cause the antimicrobial activity of the PS nanocomposites, as reported in this study in water disinfection analysis.[29,45,50]

4.4.3.3. Field Emission Scanning Electron Microscope (FESEM) Study

The morphology and size of the PS nanocomposite samples can be studied by analyzing the Field Emission Scanning Electron Microscopy (FESEM) images. Thus the FESEM technique was used for the microstructural analysis of the PS nanocomposites. Also, the interaction between the AgNPs and PS particles in the nanocomposites was studied. Both PS and AgNPs are predominately spherical; the AgNPs are embedded within the polymer matrix. Figure 3.8(a) confirms images of the PS without AgNPs, and figure 4.8 (b), (c) and (d)confirms PS matrix embedded with different percentages of AgNPs. The morphology of PS nanocomposites containing 1%, 5%, 10 %, and 20% AgNPs (% v/w w.r.t PS) were studied against neat PS (Figure 4.8 and SI). Although AgNPs are not seen to be evenly distributed in the PS nanocomposite matrix, the presence of AgNPs is evident. Nanoparticles are seen to be distributed on the surface of the PS particles. Also, aggregation of some nanoparticles was observed in the bright areas of the PS matrix. An increase in the % AgNPs might escalate the aggregation of nanoparticles inside the PS matrix. The shape and diameter of the synthesized nanoparticles and their aggregates are similar in all the different nanocomposites. Due to the addition of AgNPs in the PS, the polymer nanocomposites show some degree of toughness compared to the pure polystyrene and evident from tensile strength study.[45,50] Figure 4.8 represents the FESEM imaging of the PS nanocomposites at 25kx magnification of a particular area in each sample. The same PS nanocomposite samples are used for the elemental component analysis for each sample.

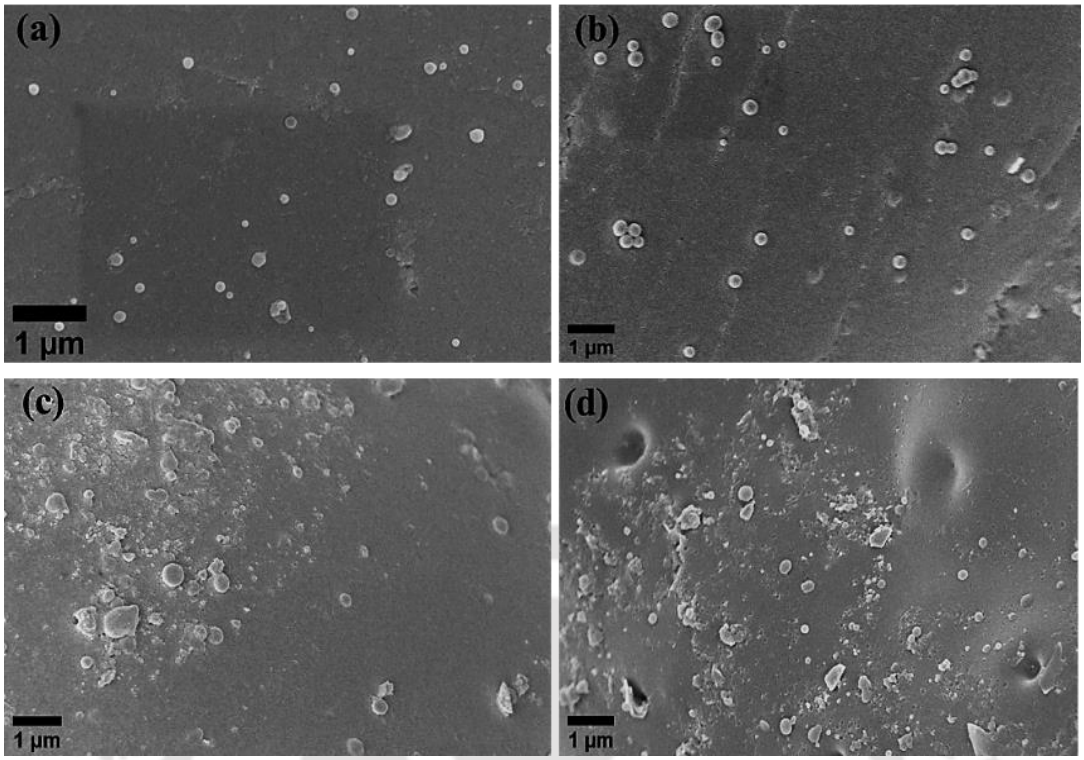

Figure 4.8. (a) PS, (b) PS + 1% AgNPs , (c) PS + 5% AgNPs and (d) PS + 10% AgNPs at 25,000 x magnification.

4.4.3.4. Energy-dispersive X-ray analysis(EDX)

EDX analysis detects the quantitative and qualitative status of elements present in the PS-AgNPs composites. Figure 4.9 gives the weight percentage of silver present in the different combinations of AgNPs with PS particles. Specific sites of the PS particles are selected for EDX profiling. Here, PS control contains no Ag whereas all the other PS nanocomposites consist of 0.1±0.5, 0.2±0.4, 0.3±0.5 and 0.9±0.5 wt%±error for PS + 1% AgNPs, PS + 5% AgNPs, PS + 10% AgNPs, and PS + 20% AgNPs respectively (Figure 3.9 and SI). At 3 keV, the count showed the presence of Ag and that indicated the presence of AgNPs. A signal in the silver region was observed at 3keV for AgNPs due to surface plasmon resonance. Other elements present apart from Ag are C and O. High percentage of carbon is detected as carbon tape is used to mount samples. An additional peak of Au is also detected in all the polymer complexes; this peak occurs due to gold coating during sample preparation for FESEM and EDX image analysis.

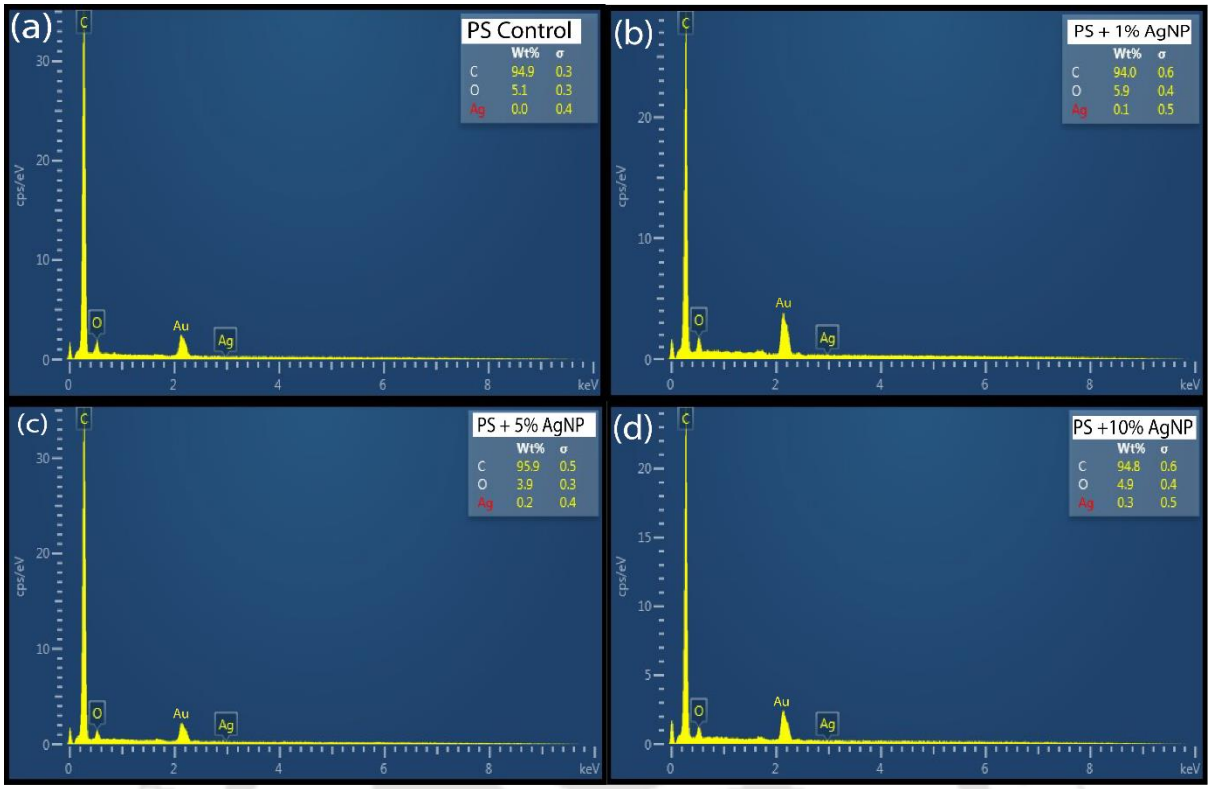

Figure 4.9. EDX elemental profiling of (a) PS control, (b) PS + 1% AgNPs, (c) PS + 5% AgNPs and (d) PS + 10% AgNPs.

4.4.3.5. Field Emission Transmission Electron Microscopy (FETEM) study

The shape and size distribution of the particles can be easily studied using field emission transmission electron microscopy (FETEM). Dispersion microstructures of the nanocomposites were investigated. The FETEM analysis confirms the presence of AgNPs embedded within the PS nanocomposites. Figure 4.10 (a) displays the FETEM image of the original structure of PS. It can be clearly seen that the formed PS particles are uniform in shape with smooth surfaces and having an average diameter of 300-500 nm. Figure 4.10 (b) and (c) display the FETEM images of the green synthesized AgNPs encapsulating PS particles. The AgNPs are attached to the surface of the PS particles and also embedded into the PS particles that form a complex polymer matrix. These FETEM images supported a good dispersion of the Ag nanoparticles within the polymer matrix and confirm the formation of nanocomposite materials.[50] The shape of the AgNPs is nearly spherical; its average diameter was found to be 44nm. Figure 4.10(d) represents the SAED pattern of the PS particles embedded with AgNPs. AgNPs have face cubic structure which provides some crystallinity to the PS nanocomposites. ImageJ software was used to measure the size of the PS as well as the AgNPs. AgNPs showed aggregation of the smaller particles due to drying for TEM sample preparations. FETEM

analysis gave a better visual understanding of the polymer complex and its attachment with the AgNPs.

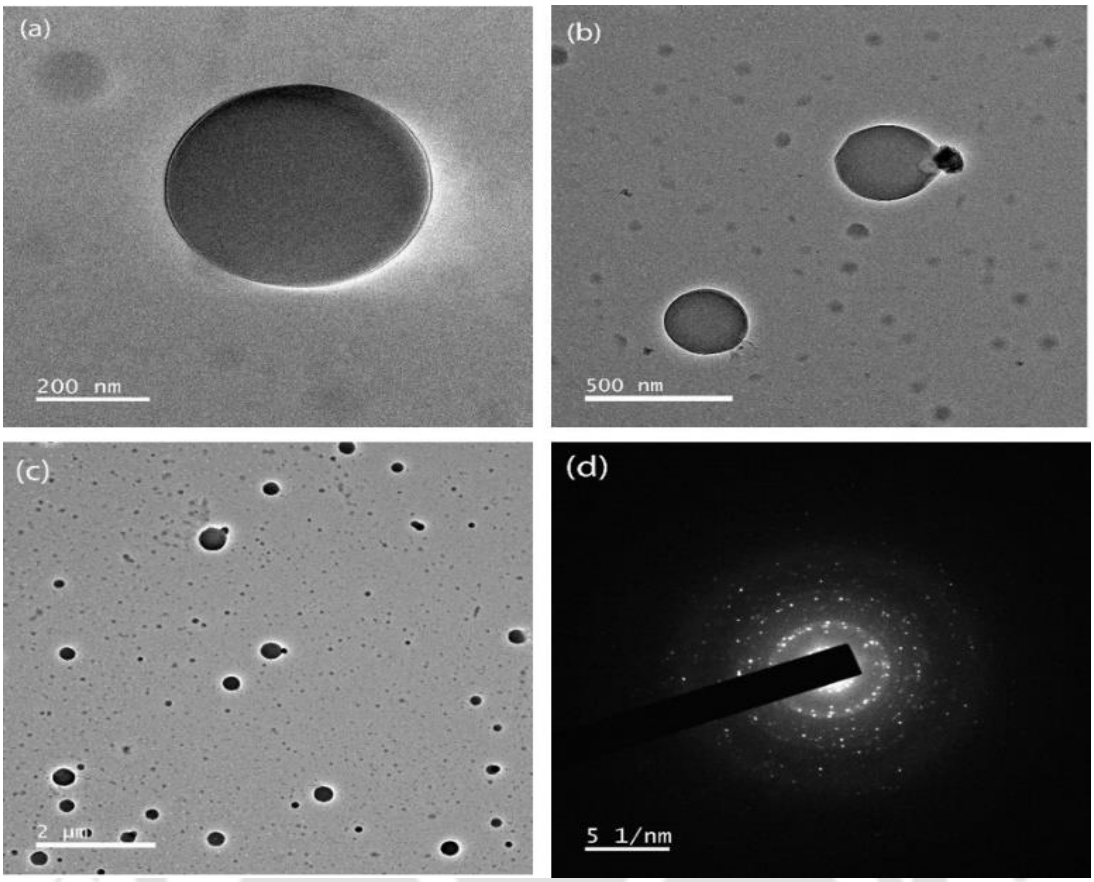

Figure 4.10. (a) FETEM image of PS without AgNPs (b) PS particles embeded with green synthesized AgNPs(500nm), (c) PS particles embeded with AgNPs(2µm) and (d) SAED image of PS nanocomposites.

4.4.4. Study of Thermal Stability of the PS-Ag Nanocomposite by Thermogravimetric Analysis (TGA)

The thermal stability of the pure PS and AgNPs incorporated PS nanocomposites were investigated using TGA. About 10 mg of the nanocomposite sample was placed in a ceramic crucible made of Al_2O_3 in a nitrogen atmosphere at a heating rate of 10°C min^{-1}. The temperature was raised from room temperature to 600°C during measurement. The thermal gravimetric curves are presented in figure 4.11. The virgin PS and PS-AgNPs composites showed similar weight loss pattern with accelerated temperature. The TGA indicated three prominent thermal degradation plateaus in the ranges of 100 to 600 ℃. The first degradation step at 100 - 350 ℃ showed a 2-3% weight decrease in the PS or PS-AgNPs-composites, probably due to the vaporization of residual solvents.

The second weight loss of approximately 50% mass loss in the range of 350-400 ℃ was attributed to the breaking of carbon-carbon bonds of PS matrix and decomposition of organic stabilizers of AgNPs. Our synthesized PS-Ag nanocomposites were found to decompose (100% decomposition) completely in between 430°C-450°C. Table 4.1 summarizes the characteristic temperatures of the thermal degradation at 2%, 25% and 50% of the residual mass of the virgin PS and the PS-AgNPs composites. There is a correlation between T_2, T_{25} and T_{50} values with the AgNPs weight (%). It can be observed that the degradation temperature difference between virgin PS and PS-Ag nanocomposite was not much significant. However, the boiling/degradation point temperature variations at T_2 cannot be solely correlated with the stability of the PS-Ag nanocomposite, as the chemical nature of the composite undergoes a complete transformation as it approaches its maximum kinetic energy due to heat. As seen from the data, the complete degradation of virgin PS at T_2 was 433°C which corresponds to the boiling point of PS.

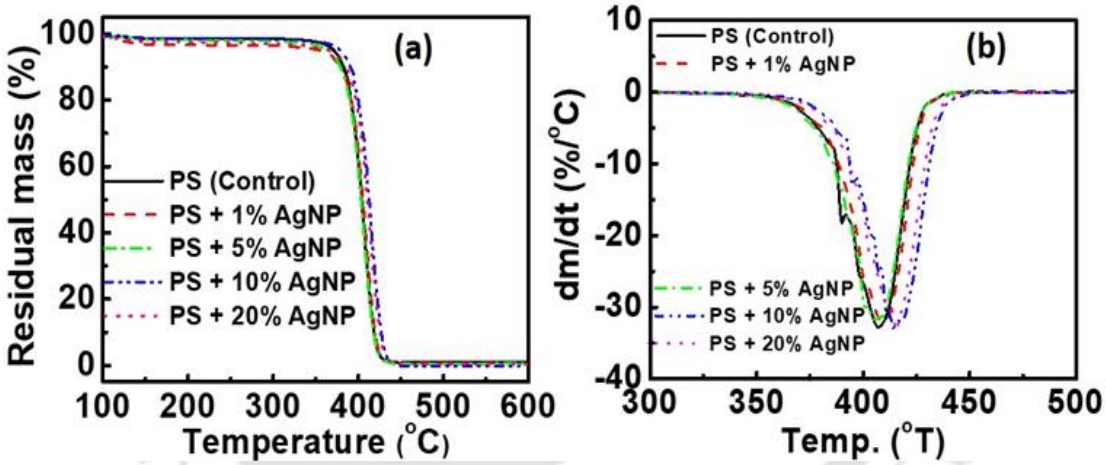

Figure 4.11. Thermogravimetric analysis - (a) TGA and (b) DTG curves of control PS(without AgNPs) and the PS-AgNP nanocomposites with 1% AgNPs, 5% AgNPs, 10% AgNPs and 20% AgNPs.

Similarly, at T_{25} and T_{50} the temperature recorded to be 410°C and 404°C for PS control. However, as compared to the PS-Ag composite, it can be observed that PS + 10% AgNPs show an elevated thermal temperature tolerance at 418°C and 413°C, respectively. Therefore, with an increase in Ag elemental percentage, the stability of the polymer nanocomposite increased. However, it was also observed that increasing the concentration of Ag elemental percentage to 20% of the stability of the polymer composite was affected. The same observation can be correlated with the tensile strength of the nanopolymer composite PS + 10% AgNPs showing better strength.

Table 4.1. The characteristic temperature of thermal degradation at 2, 25 and 50% of the residual mass (T_2, T_{25} and T_{50}, respectively)

Samples	Nitrogen atmospheric condition		
	T_2(°C)	T_{25}(°C)	T_{50}(°C)
PS Control	433	410	404
PS + 1% AgNPs	433	411	405
PS + 5% AgNPs	429	409	403
PS + 10% AgNPs	436	418	413
PS + 20% AgNPs	436	416	410

Compared to virgin PS, the thermal stability of the nanocomposites (PS-AgNPs) was consistently higher. The thermal stability increases as the % content of AgNPs increases, at least up to 10% AgNPs. This may be due to the introduction of the Ag-π bond between the aromatic rings of the PS matrix and AgNPs. This bonding interaction provided better reinforcement of thermal stability, increasing the PS-AgNPs composites' degradation temperature. For instance, the temperature [T_{50}(°C)] at 50% mass loss of 10% AgNPs-PS nanocomposite is about 9 °C higher than that of virgin PS which maybe because of the presence of well-dispersed AgNPs in the PS matrix.[44,45] In a nutshell, the thermal stability of the PS complex enhances with the incorporation of AgNPs, which influences the reduction of the chain transfer reactions of the PS complex during its thermal degradation.[45]

4.4.5. Study of Mechanical Properties of the PS-Ag Nanocomposites

Tensile strength of the various PS nanocomposites was measured using a 5 kN Universal Testing Machine(UTM). The specimen sizes were prepared according to ASTM standards. The tensile test was performed at 10 mm/min speed at atmospheric conditions (25°C). In this experiment, the samples were pulled at a constant rate that causes elongation and stress for deformation, quantified. Tensile strength (MPa) is mainly measured by a maximum load (Newton) divided by the cross-sectional area of the sample (mm^2).[54]

$$Tensile\ Strength = \frac{Load\ (N)}{Cross\ section\ area\ of\ sample\ (mm2)}$$

Again, percent elongation is measured by dividing by elongation at rapture by initial length and then multiplied with 100.

$$Elongation\ at\ Break\ (\%) = \frac{Elongation\ at\ rupture\ \times 100}{Initial\ length\ (mm)}$$

Table 4.2 represents the tensile strength and tensile elongation at break of the various PS nanocomposites. From table 4.3, it is seen that neat PS shows the least tensile strength (0.29 MPa), whereas the tensile elongation at break is highest (51.1%) among the others. Again, PS nanocomposites with 10% silver nanoparticles, i.e., PS+ 10% AgNPs show the highest tensile strength (3.73 MPa) and comparatively moderate tensile elongation at break (33.16%).

Table 4.2. Tensile strength and tensile elongation at break of the various PS nanocomposites.

Polystyrene Samples	Tensile strength (MPa)	Elongation at Break (%)
PS Control	0.29	51.1
PS + 1% AgNPs	0.72	25.52
PS + 5% AgNPs	1.04	27.75
PS + 10% AgNPs	3.73	33.16
PS + 20% AgNPs	1.98	23.87

As such, the tensile strength increases with the addition of AgNPs within the PS matrix. PS nanocomposite sample, PS + 20% AgNPs has relatively lower tensile strength than PS + 10% AgNPs this may be due to the increase in binding strength between the nanoparticles and the polymer matrix. Again, tensile strength decreases when the concentration of the AgNPs was much higher. It may be due to aggregation of the AgNPs, which influences the reduction of the strength of the polymer materials leading to the decrease in tensile strength in the PS nanocomposites with a much higher percentage of AgNPs. The tensile test clearly shows that the incorporation of AgNPs has increased the mechanical strength of the polymer nanocomposites compared to the pure polystyrene material.

Figure 4.12 represents the stress vs. strain curve for pure PS and the various percentage of PS nanocomposites. The stress-strain curve is considered the most consistent source for estimating the mechanical properties of any material. From the stress-strain plots of all the different PS nanocomposites, the nanocomposite materials have higher tensile strength than the virgin PS composite, proving that the PS nanocomposites provide better mechanical properties. PS nanocomposite with 10% AgNPs shows a high stress-strain ratio as well as tensile strength, proving it to be suitable for applications. The mechanical strength of the PS nanocomposites is affected by the nanoparticles' surface free energy, which influences the polymer and AgNPs interaction. This might cause variations in the aggregation of the nanoparticles in the nanocomposite materials as such influences the antibacterial activities of

the nanocomposite materials. The advantage of having better mechanical properties of the PS nanocomposites is high ductility and resistance from scratch.

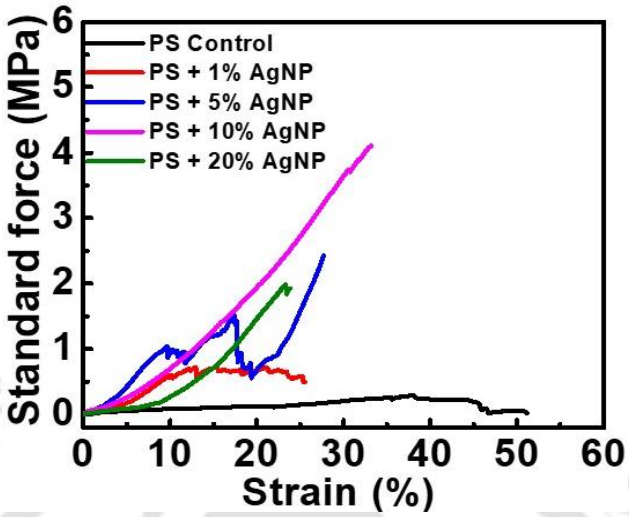

Figure 4.12. The stress vs strain plot of pure polystyrene (PS Control), PS+ 1% AgNPs, PS + 5% AgNPs, PS + 10% AgNPs and PS + 20% AgNPs.

4.4.6. Study of Water Disinfection Activity of the PS-Ag Nanocomposites

Water disinfection from *E. coli* bacteria is studied in this experiment by measuring the bacterial count in water-filled PS-AgNPs nanocomposite cups. *E. coli* is one of the most commonly found microorganisms in water, causing disease in humans. For this experiment, *E. coli* (MTCC strain no. 1696) is mixed with laboratory tap water taken in various cups developed of pure PS and PS-AgNPs composites, as shown in figure 4.13. In 5 cups, made up of pure PS, PS + 1% AgNPs, PS + 5% AgNPs, PS + 10% AgNPs and PS + 20% AgNPs, the water containing bacteria (10^7 cfu/ml) samples were prepared. Aliquots from each cup have been taken from time to time and the absorption was recorded. The absorbance recorded was 600 nm after every 60 minutes for 5 hours for each sample, reflecting the bacteria count (cfu/ml). The log number of bacterial cells (cfu/mL) *vs.* time (minutes) was plotted in figure 4.13. From here, it is clearly observed that water in all the PS-AgNPs cups showed a significant decrease in the bacterial cell count within 30 minutes, as was evident from the decreased optical density. Overall, a change in the log number of bacteria cells was observed. From 2.0×10^7 cfu/ml at 0 minute to 1.76×10^7 cfu/ml for PS cups containing 1% AgNPs, 1.68×10^7 cfu/ml for PS cups containing 5% AgNPs, 1.52×10^7 cfu/ml for PS cups containing 10% AgNPs and 1.44×10^7 cfu/ml for PS cups containing 20% AgNPs respectively. However, the cup made up of pure PS material (PS-cups) showed a slight increase in the bacterial cell count in 30 minutes, as

observed from increased optical density from 2.0×10^7 cfu/mL log number of bacteria cells to 2.16×10^7 cfu/ml. There was no increase in the bacterial count for all the PS nanocomposites after 120 minutes (3rd hour). Still, there was a slight increase in the bacterial cell count in pure PS material even after 120 minutes. As such, PS nanocomposite materials provide better antibacterial activity than virgin polystyrene for disinfection purposes.[55]

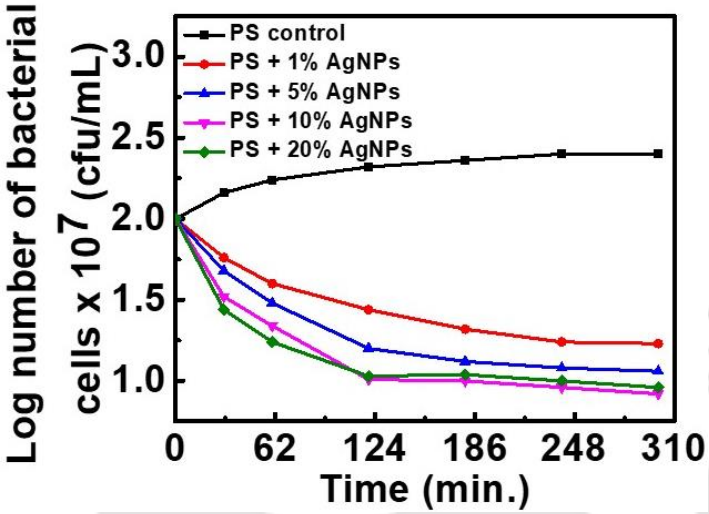

Figure 4.13. Log number of bacterial cells (cfu/ml) vs time (minutes) graph of the pure PS and different PS nanocomposites.

The log number of bacterial cells of the PS nanocomposites again decreases eventually with time and with the increases in the percentage of AgNPs in the cups of PS-AgNPs nanocomposite. Thus after 300 minutes, the log number of bacteria cells decreased from 2.0×10^7 cfu/ml at 0 minute to 1.23×10^7 cfu/ml in PS cups containing 1% AgNPs, 1.06×10^7 cfu/ml PS cups containing 5% AgNPs, 9.2×10^6 cfu/ml in PS cups containing 10% AgNPs and 9.6×10^6 cfu/ml in PS cups containing 20% AgNPs (5th hour). This pattern indicated the increase in the disinfection activity of the cups against the gram-negative bacteria *E. coli* present in water with an increase in the % of Ag content. Although all the PS-AgNPs cups showed no increase in the bacterial cell count, PS with 10% AgNPs showed the least log number of bacterial cells after 300 minutes. This may be because the antibacterial activity of the green synthesized AgNPs depends on the concentration of AgNPs and the formation of pits in the bacterial cell walls. At an increased concentration of AgNPs, the bacterial cell membrane might be disrupted, which ultimately may lead to bacterial cell death.[56] However, the better result on the disinfection property was shown by the PS-AgNPs cup containing 10% AgNPs compared to that contain 20% AgNPs. This may be because at very high concentrations (20%), the AgNPs tend to agglomerate, thus having less antibacterial properties. The agglomeration at 20%

concentration was supported from the FESEM image analysis (Fig. 4.8). In summary, all the PS nanocomposites showed a decrease in the bacterial count, which proves that all the nanocomposites are more effective in antibacterial activity than the PS control.

4.5. CONCLUSION

Waste thermocols and green synthesized AgNPs were used to develop low-cost, functional PS-AgNPs nanocomposites for water disinfection purposes. AgNPs were green synthesized using bhimkol (*Musa balbisiana*) peels, which act as reducing as well as a stabilizing agents. Different percentages of the green synthesized AgNPs were embedded in the PS matrix to produce PS-AgNPs nanocomposite materials. FESEM and EDX results confirm the quantitative and qualitative presence of AgNPs into the PS matrix. From FETEM imaging, the size and shape of PS and AgNPs in the nanocomposites were examined. Good dispersion of the AgNPs was observed in the polymer matrix. Due to the encapsulation of the AgNPs into the polymer matrix, undesirable polymer degradation was prevented, which ultimately increases the durability of the PS-AgNPs composites. The introduction of a small amount of AgNPs in the PS matrix considerably increases the thermal stability of the PS nanocomposites. Mechanical strength and the antibacterial activity of the PS nanocomposite cups are superior to that of the pure PS cup. 10% AgNPs content was found to be optimum as it has good mechanical strength as well as water disinfection properties against *E. coli*. This study may shed light on the development of PS-based functional materials as a part of turning wastes into value-added materials and thus, to find a solution to the disposal problem and make an effort to save the environment from plastic pollution.

4.6. EXPERIMENTAL SECTION

4.6.1. Material and Methods

4.6.1.1. Materials

Waste thermocols were collected from the laboratory waste and used for experimental purposes. Silver nitrate($AgNO_3$) was purchased from Sigma-Aldrich (India). Bhimkol (*Musa balbisiana*) banana variety was purchased from Amingaon Market, North Guwahati. Acetone was purchased from Merck (India). Double distilled water was used for all the experiments. All other chemicals used were of reagent grade.

4.6.1.2. Green synthesis of AgNPs

AgNPs were synthesized via the green route using Bhimkol (*Musa balbisiana*) peel extract with a slight modification of the work by Kokila et al., 2015. Biological reduction of $AgNO_3$ was carried out to optimize the synthesis of AgNPs. The reaction mixture, a solution of $AgNO_3$ and Bhimkol peel extract, was kept in the dark at 25°C to avoid any photoactivation of $AgNO_3$ under inert conditions. Different proportions of $AgNO_3$ and bhimkol peel extract (v/v ratio) were used. To observe the optimum formation of AgNPs of fair size and shape, 9% Bhimkol peel extract(v/v) and 1 mM $AgNO_3$ were mixed in neutral pH, incubated at 25°C and the UV-visible spectra were recorded after 30 mins.[57] The yellowish-brown colour was observed after 30 mins indicating the formation of silver nanoparticles. Optimized concentration of AgNPs was used in the synthesis of PS nanocomposites.[50,57]

4.6.1.3. Development of PS nanocomposites

Waste thermocols were collected and cleaned. About 10 g of the thermocol was cut into strips and slowly dissolved in 20 ml of acetone at room temperature (25°C). The green synthesized AgNPs were added to polystyrene (PS) in v/w ratio and expressed in percentage (%). The different combinations such as 1% AgNP, 5% AgNP, 10% AgNP, and 20% AgNPs were added into 10g of thermocol and mixed well in acetone. When the thermocol waste was dissolved totally in acetone, it converted into a clay-like substance, moldable into various shapes. The nanocomposite materials were later carefully molded into sheets and cups for various analyses. The AgNPs were added dropwise at the dissolving stage in acetone. The composite materials were then kept for drying at room temperature and stored in a desiccator for further use. Various combinations of PS and AgNPs are given in the table below. Table 4.3 represents the different combinations of AgNP:PS ratios of the PS-Ag nanocomposites.

Table 4.3: Different combinations of AgNP: PS in % (v/w) ratio

Samples	AgNP (v/mL)	PS (wt/g)	Sample code %(v/w)
Polystyrene (control)	-	10	PS (Control)
Polystyrene +1% AgNP	0.1	10	PS +1 % AgNPs
Polystyrene +5% AgNP	0.5	10	PS + 5% AgNP
Polystyrene +10%AgNP	1.0	10	PS + 10% AgNP
Polystyrene +20%AgNP	2.0	10	PS + 20% AgNP

4.6.2. Characterization of the PS nanocomposites

UV–visible spectra of the PS nanocomposites were recorded using a PerkinElmer Lambda/25/35/45 UV–vis spectrophotometer in the range of 200–700 nm using a solid sample

holder. The solid sample holder was filled with grounded PS control (polystyrene without AgNPs) and PS nanocomposites than attached to the removable chamber in the UV-Vis spectrophotometer. The FT-IR spectra of different PS nanocomposites and the control PS material were collected at a resolution of 4 cm^{-1} in the transmission mode from 4000 cm^{-1}-400 cm^{-1}. The UV-Vis and FT-IR spectra were measured using solid samples. For the FT-IR spectra measurement, an ATR mode was used. ATR stands for attenuated total reflection or transmission modes which permit analysis of a wide range of solids, powders, non-aqueous liquids and gases. Infrared spectra were recorded using an FT-IR spectrophotometer (Perkin Elmer Spectrum 2, USA) in an ATR. Nanostructures of the PS composites were elucidated by Field Emission Transmission Electron Microscope (FETEM) in JEOL-JEM 2100F(USA). For the FETEM analysis, 1-5 µL acetone is added to a small grounded portion of PS nanocomposite sample and mixed well. The sample along with acetone (before complete drying) is pipetted into a carbon grid and allowed to dry, later the carbon grid casted with the dried sample is used for FETEM analysis. Field emission scanning electron microscopy (FESEM) analysis was carried out in Zeiss Gemini Oxford Instruments X-MAXN^{N}(Germany). This system has an accelerating voltage of 0.02 to 30 kV and a high magnification range of 200 kx. FESEM was used for the microstructural analysis of the synthesized polymer nanocomposites. During the sample preparation for FESEM analysis, a small amount of 1-5 µL of acetone is added to a small grounded portion of the polystyrene nanocomposites, they are mixed and the final sample is allowed to dry before it is attached to the carbon tape. Thermal stability of the PS nanocomposites was analyzed by the Thermogravimetric analysis(TGA) technique using a DSC/TGA analyzer (NETZSCH, STA449F3A00, Germany). Thermogravimetric analysis(TGA) was used primarily to measure the change in physical and chemical properties as a function of increasing temperature, i.e., constant heating rate and as a function of time. It measured the residual mass percentage or weight change of the decomposition reactions when a particular amount of the nanocomposite was placed in a ceramic crucible in a nitrogen/argon atmosphere at a heating rate of 10°C min^{-1}. The tensile strength of the PS nanocomposites was measured by a tensile test using a 5kN Electromechanical Universal Testing Machine (UTM). The tensile test was performed on Zwick Roell: Z005TN UTM(Germany). The size of the specimen was prepared according to ASTM standards.

4.6.3. Water disinfection activity

E. coli (Gram-negative bacteria) is the most commonly found microorganism in water. Water disinfection study was tested against *E. coli* using a spectrophotometric procedure. The

original lyophilized *E. coli* strain (purchased from MTCC, strain-no: 1696) was revived in sterile Lysogeny (commonly known as Luria-Bertani, LB) broth incubating for 12-24 hours at 37°C at 180 rpm. Tap water was poured into each of the PS-AgNPs nanocomposite cups. Then fresh culture of *E. coli* was added to each cup equally. The absorbance of 1 mL of each sample(water mixed with bacteria) was recorded every hour for 5 hours using a UV-visible spectrophotometer. Absorbance (O.D) was measured at 600 nm wavelength, which gives an indirect measurement of the *E. coli* count. Increased turbidity in the samples reflects the bacterial growth and cell number(biomass) index in the samples. The amount of transmitted light decreases as the cell numbers increase with increased turbidity. Bacterial cell count vs. time graph was plotted in origin 8.5 software for the respective PS nanocomposites.[43]

4.7. REFERENCES

(1) Naseem, T.; Waseem, M. A Comprehensive Review on the Role of Some Important Nanocomposites for Antimicrobial and Wastewater Applications. *Int. J. Environ. Sci. Technol.* **2021**, No. 0123456789.

(2) Qu, X.; Alvarez, P. J. J.; Li, Q. Applications of Nanotechnology in Water and Wastewater Treatment. *Water Res.* **2013**, *47* (12), 3931–3946.

(3) Ali, I. New Generation Adsorbents for Water Treatment. *Chem. Rev.* **2012**, *112* (10), 5073–5091.

(4) Ghorbi, E.; Namavar, M.; Rashedi, V.; Farhadinejad, S.; Pilban Jahromi, S.; Zareian, M. Influence of Nano-Copper Oxide Concentration on Bactericidal Properties of Silver–Copper Oxide Nanocomposite. *Colloids Surfaces A Physicochem. Eng. Asp.* **2019**, *580*, 123732.

(5) Omanovi, E.; Badnjevi, A.; Kazlagi, A.; Hajlovac, M. Nanocomposites: A Brief Review. *Health Technol. (Berl).* **2020**, *10*, 51–59.

(6) Schmidt, D.; Shah, D.; Giannelis, E. P. New Advances in Polymer/Layered Silicate Nanocomposites. *Curr. Opin. Solid State Mater. Sci.* **2002**, *6* (3), 205–212.

(7) Lange, F. F. Effect of Microstructure on Strength of Si_3N_4-SiC Composite System. *J. Am. Ceram. Soc.* **1973**, *56* (9), 445–450.

(8) Harmer, M. P.; Chan, H. M.; Miller, G. A. Unique Opportunities for Microstructural Engineering with Duplex and Laminar Ceramic Composites. *J. Am. Ceram. Soc.* **1992**, *75* (7), 1715–1728.

(9) Gamal-Eldeen, A. M.; Abdel-Hameed, S. A. M.; El-Daly, S. M.; Abo-Zeid, M. A. M.;

Swellam, M. M. Cytotoxic Effect of Ferrimagnetic Glass-Ceramic Nanocomposites on Bone Osteosarcoma Cells. *Biomed. Pharmacother.* **2017**, *88* (April), 689–697.

(10) Dezfuly, R. F.; Yousefi, R.; Jamali-Sheini, F. Photocurrent Applications of Zn(1−x)CdxO/RGO Nanocomposites. *Ceram. Int.* **2016**, *42* (6), 7455–7461.

(11) Yu, Z.; Li, S.; Zhang, P.; Feng, Y.; Liu, X. Polymer-Derived Mesoporous Ni/SiOC(H) Ceramic Nanocomposites for Efficient Removal of Acid Fuchsin. *Ceram. Int.* **2017**, *43* (5), 4520–4526.

(12) Ogasawara, T.; Ishida, Y.; Ishikawa, T.; Yokota, R. Characterization of Multi-Walled Carbon Nanotube/Phenylethynyl Terminated Polyimide Composites. *Compos. Part A Appl. Sci. Manuf.* **2004**, *35* (1), 67–74.

(13) Alexandre, M.; Dubois, P. Polymer-Layered Silicate Nanocomposites: Preparation, Properties and Uses of a New Class of Materials. *Mater. Sci. Eng. R Reports* **2000**, *28* (1), 1–63.

(14) Croce, F.; Appetecchi, G. B.; Persi, L.; Scrosati, B. Nanocomposite Polymer Electrolytes for Lithium Batteries. *Nature* **1998**, *394* (6692), 456–458.

(15) Jancar, J.; Douglas, J. F.; Starr, F. W.; Kumar, S. K.; Cassagnau, P.; Lesser, A. J.; Sternstein, S. S.; Buehler, M. J. Current Issues in Research on Structure–Property Relationships in Polymer Nanocomposites. *Polymer (Guildf).* **2010**, *51* (15), 3321–3343.

(16) Vaia, R. A.; Maguire, J. F. Polymer Nanocomposites with Prescribed Morphology: Going beyond Nanoparticle-Filled Polymers. *Chem. Mater.* **2007**, *19* (11), 2736–2751.

(17) Kickelbick, G. Concepts for the Incorporation of Inorganic Building Blocks into Organic Polymers on a Nanoscale. *Prog. Polym. Sci.* **2003**, *28* (1), 83–114.

(18) Dallas, P.; Sharma, V. K.; Zboril, R. Silver Polymeric Nanocomposites as Advanced Antimicrobial Agents: Classification, Synthetic Paths, Applications, and Perspectives. *Adv. Colloid Interface Sci.* **2011**, *166* (1–2), 119–135.

(19) Farcau, C. A.; Astilean, S. Optical and Structural Characterization of Periodic Silver-Polystyrene Nanocomposites. *J. Optoelectron. Adv. Mater.* **2005**, *7* (5), 2721–2725.

(20) Wang, D.; An, J.; Luo, Q.; Li, X.; Li, M. A Convenient Approach to Synthesize Stable Silver Nanoparticles and Silver/Polystyrene Nanocomposite Particles. *J. Appl. Polym. Sci.* **2008**, *110* (5), 3038–3046.

(21) Mahmoud, M. E.; Abdou, A. E. .; Ahmed, S. B. Conversion of Waste Styrofoam into Engineered Adsorbents for Efficient Removal of Cadmium, Lead and Mercury from Water. *ACS Sustain. Chem. Eng.* **2016**, *4* (3), 819–827.

(22) NIM. Hazardous Substances Data Bank (HSDB, online database), 1993.

(23) Marsh, K.; Bugusu, B. Food Packaging—Roles, Materials, and Environmental Issues. *J. Food Sci.* **2007**, *72* (3), R39–R55.

(24) Mudgal, S.; Lyons, L.; Kong, M. A. *Study on an Increased Mechanical Recycling Target for Plastics*; 2013.

(25) Bekri-Abbes, I.; Bayoudh, S.; Baklouti, M. Converting Waste Polystyrene Intoadsorbent: Potential Use in the Removal of Lead and Cadmium Ions Fromaqueous Solution. *J. Polym. Environ.*, **2006**, *14*, 249–256.

(26) Ruziwa, D.; Chaukura, N.; Gwenzi, W.; Pumure, I. Removal of Zn^{2+} and Pb^{2+} Ions from Aqueous Solution Using Sulphonated Waste Polystyrene. *J. Environ. Chem. Eng.* **2015**, *3* (4, Part A), 2528–2537.

(27) Chaukura, N.; Gwenzi, W.; Bunhu, T.; Ruziwa, D. T.; Pumure, I. Potential Uses and Value-Added Products Derived from Waste Polystyrene in Developing Countries: A Review. *Resour. Conserv. Recycl.* **2016**, *107*, 157–165.

(28) Huysman, S.; Debaveye, S.; Schaubroeck, T.; Meester, S. De; Ardente, F.; Mathieux, F.; Dewulf, J. The Recyclability Benefit Rate of Closed-Loop and Open-Loop Systems: A Case Study on Plastic Recycling in Flanders. *Resour. Conserv. Recycl.* **2015**, *101*, 53–60.

(29) Lynwood, C. *Polystyrene: Synthesis, Characteristics and Applications*; Lynwood, C., Ed.; Nova publishers, New York, 2014.

(30) Silver, S. Bacterial Silver Resistance: Molecular Biology and Uses and Misuses of Silver Compounds. *FEMS Microbiol. Rev.* **2003**, *27* (2–3), 341–353.

(31) Solsona, F.; Méndez, J. P. Water Disinfection. *Water Disinfection*. 2011, pp 1–284.

(32) Federal Register. *Food Additives Permitted for Direct Addition to Food for Human Consumption; Silver Nitrate and Hydrogen Peroxide*; 2009; Vol. 74.

(33) Eby, D. M.; Schaeublin, N. M.; Farrington, K. E.; Hussain, S. M.; Johnson, G. R. Lysozyme Catalyzes the Formation of Antimicrobial Silver Nanoparticles. *ACS Nano* **2009**, *3* (4), 984–994.

(34) Furno, F.; Morley, K. S.; Wong, B.; Sharp, B. L.; Arnold, P. L.; Howdle, S. M.; Bayston, R.; Brown, P. D.; Winship, P. D.; Reid, H. J. Silver Nanoparticles and Polymeric Medical Devices: A New Approach to Prevention of Infection? *J. Antimicrob. Chemother.* **2004**, *54* (6), 1019–1024.

(35) Sánchez-Valdes, S.; Ortega-Ortiz, H.; Ramos-de Valle, L. F.; Medellín-Rodríguez, F. J.; Guedea-Miranda, R. Mechanical and Antimicrobial Properties of Multilayer Films

with a Polyethylene/Silver Nanocomposite Layer. *J. Appl. Polym. Sci.* **2009**, *111* (2), 953–962.

(36) Mohammed Fayaz, A.; Balaji, K.; Girilal, M.; Kalaichelvan, P. T.; Venkatesan, R. Mycobased Synthesis of Silver Nanoparticles and Their Incorporation into Sodium Alginate Films for Vegetable and Fruit Preservation. *J. Agric. Food Chem.* **2009**, *57* (14), 6246–6252.

(37) Božanić, D. K.; Dimitrijević-Branković, S.; Bibić, N.; Luyt, A. S.; Djoković, V. Silver Nanoparticles Encapsulated in Glycogen Biopolymer: Morphology, Optical and Antimicrobial Properties. *Carbohydr. Polym.* **2011**, *83* (2), 883–890.

(38) Li, Q.; Mahendra, S.; Lyon, D. Y.; Brunet, L.; Liga, M. V; Li, D.; Alvarez, P. J. J. Antimicrobial Nanomaterials for Water Disinfection and Microbial Control: Potential Applications and Implications. *Water Res.* **2008**, *42* (18), 4591–4602.

(39) Morones, J. R.; Elechiguerra, J. L.; Camacho, A.; Ramirez, J. T. The Bactericidal Effect of Silver Nanoparticles. *Nanotechnology* **2005**, *16* (2346), 53.

(40) Choi, O.; Deng, K. K.; Kim, N.-J.; Ross, L.; Surampalli, R. Y.; Hu, Z. The Inhibitory Effects of Silver Nanoparticles, Silver Ions, and Silver Chloride Colloids on Microbial Growth. *Water Res.* **2008**, *42* (12), 3066—3074.

(41) Damm, C.; Münstedt, H.; Rösch, A. The Antimicrobial Efficacy of Polyamide 6/Silver-Nano- and Microcomposites. *Mater. Chem. Phys.* **2008**, *108* (1), 61–66.

(42) Mohan, Y. M.; Premkumar, T.; Lee, K.; Geckeler, K. E. Fabrication of Silver Nanoparticles in Hydrogel Networks. *Macromol. Rapid Commun.* **2006**, *27* (16), 1346–1354.

(43) Palomba, M.; Carotenuto, G.; Cristino, L.; Di Grazia, M. A.; Nicolais, F.; De Nicola, S. Activity of Antimicrobial Silver Polystyrene Nanocomposites. *J. Nanomater.* **2012**, No. 185029, 1–7.

(44) Kamrupi, I. R.; Phukon, P.; Konwer, B. K.; Dolui, S. K. Synthesis of Silver–Polystyrene Nanocomposite Particles Using Water in Supercritical Carbon Dioxide Medium and Its Antimicrobial Activity. *J. Supercrit. Fluids* **2011**, *55* (3), 1089–1094.

(45) Vodnik, V.; Bozanic, D. K.; Dzunuzovic, J. V.; Vukoje, I.; Nedeljkovic, J. Silver/Polystyrene Nanocomposites: Optical and Thermal Properties. *Polym. Compos.* **2012**, *33* (5), 782–788.

(46) Wibawa, P. J.; Saim, H.; Agam, M. A.; Nur, H. Manufacturing and Morphological Analysis of Composite Material of Polystyrene Nanospheres/Cadmium Metal Nanoparticles. *Bull. Chem. React. Eng. Catal.* **2013**, *7* (3), 224–232.

(47) Kokila, T.; Ramesh, P. S.; Geetha, D. Biosynthesis of Silver Nanoparticles from Cavendish Banana Peel Extract and Its Antibacterial and Free Radical Scavenging Assay: A Novel Biological Approach. *Appl. Nanosci.* **2015**, *5* (8), 911–920.

(48) Tsuruoka, T.; Kumazaki, S.; Osaka, I.; Nawafune, H.; Akamatsu, K.; Department. Synthesis of Polystyrene-Based Nanocomposite Thin Films with Domain Structure Consisting of Au Nanoparticles Synthesis of Polystyrene-Based Nanocomposite Thin Films with Domain Structure Consisting of Au Nanoparticles. In *Journal of Physics: Conference Series*; 2013; Vol. 417, pp 12–20.

(49) Kim, J. K.; Ahn, H. Fabrication and Characterization of Polystyrene/Gold Nanoparticle Composite Nanofibers. *Macromol. Res.* **2008**, *16* (2), 163–168.

(50) Youssef, A. M.; Abdel-Aziz, M. S. Preparation of Polystyrene Nanocomposites Based on Silver Nanoparticles Using Marine Bacterium for Packaging. *Polym. - Plast. Technol. Eng.* **2013**, *52* (6), 607–613.

(51) Kan, C.; Wang, C.; Zhu, J.; Li, H. Journal of Solid State Chemistry Formation of Gold and Silver Nanostructures within Polyvinylpyrollidone (PVP) Gel. *J. Solid State Chem.* **2010**, *183* (4), 858–865.

(52) Li, T.; Zhou, C.; Jiang, M. Polymer Bulletin UV Absorption Spectra of Polystyrene. *Polym. Bull.* **1991**, *25*, 211–216.

(53) Awad, M. A.; Mekhamer, W. K.; Merghani, N. M.; Hendi, A. A.; Ortashi, K. M. O.; Al-abbas, F.; Eisa, N. E. Green Synthesis , Characterization , and Antibacterial Activity of Silver / Polystyrene Nanocomposite. *J. Nanomater.* **2015**, No. 943821, 1–6.

(54) Ahmad, S.; Alam, T.; Siddique, A.; Ansari, H. Tensile Strength of Synthesized Polystyrene Composites. *Int. J. Sci. Res. Eng. Technol.* **2015**, *4* (10), 1038–1044.

(55) Al-Hakami, S. M.; Khalil, A. B.; Laoui, T.; Atieh, M. A. Fast Disinfection of *Escherichia coli* Bacteria Using Carbon Nanotubes Interaction with Microwave Radiation. *Bioinorg. Chem. Appl.* **2013**, No. 458943, 1–10.

(56) Dragieva, I.; Stoeva, S.; Stoimenov, P.; Pavlikianov, E.; Klabunde, K. Complex Formation in Solutions for Chemical Synthesis of Nanoscaled Particles Prepared by Borohydride Reduction Process. *Nanostructured Mater.* **1999**, *12* (1), 267–270.

(57) Bag, S. S.; Bora, A.; Golder, A. Biomimetic Synthesis of Silver Nanoparticles Using Bhimkol (*Musa balbisiana*) Peel Extract as Biological Waste : Its Antibacterial Activity and Role of Ripen Stage of the Peel. *Curr. Nanomater.* **2020**, *5* (1), 47–65.

CHAPTER 5:

Development of PVA/Gelatin/AgNPs Based Polymer Hydrogel Nanocomposite for Wound Dressing Application

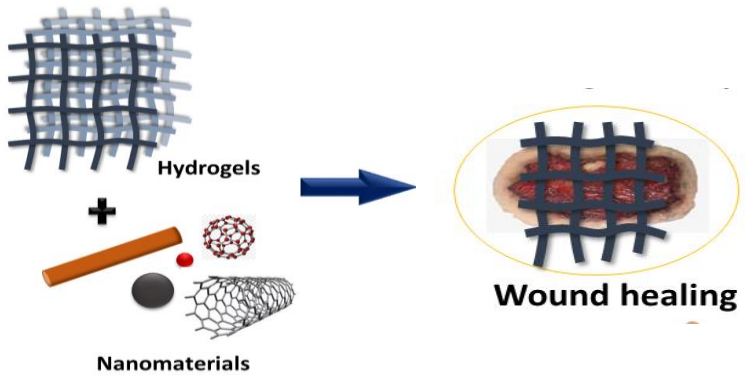

5.1. Introduction

Hydrogels are polymeric chains with hydrophilic properties and three-dimensional cross-linked networks. They are, in general, water-swollen cross-linked polymeric networks. Polymer hydrogels can also be defined as polymeric materials with the ability to swell and retain water as a significant fraction within its structure but never dissolve in water. Thus they behave like natural tissues with a similar degree of flexibility. While retaining water within it arises due to hydrophilic groups within the polymer backbone, resistance to dissolve in water is due to cross-links between polymeric networks. For the past half-century, polymer hydrogels have got considerable research interest due to their widespread applications. Hydrogels are of two kinds-natural and synthetic. Some naturally occurring hydrogels are Alginate, Guar gum, Gellan, Xyloglucan, Pectin etc. Polystyrene (PS), Polyethyleneglycol acrylate/methacrylate (PEGA/PEGMA), Polyvinylalcohol(PVA), Polyethyleneglycoldiacrylate/dimethacrylate (PEGDA/PEGDMA), Polyacrylic Acid (PAA), polymethacrylic acid (PMAA) etc. are few examples of widely used synthetic polymer hydrogels.[1]

Synthetic polymer hydrogels can have well-defined structures and can introduce broad functionality and stability toward strong temperature fluctuation. They can also be modified to achieve a long life with high gel strength and high water absorption capacity. Therefore, synthetic hydrogels are more advantageous compared to natural counterparts. Hence, natural hydrogels are often being replaced by synthetic or made composite hydrogel materials to meet the required property for their applications. These unique properties of polymer hydrogels, along with biocompatibility, made them attractive for applications such as wound dressing materials, bio-adhesive devices, control release devices, diagnostic/implantable/therapeutic devices and drug delivery systems.

Furthermore, several research efforts have reported that embedding metal, metal oxides or nanoparticles within the hydrogel's polymeric network offers the mixed hydrogel or nanocomposites polymer hydrogel with more advantageous properties, such as strong durability, high strength, and good water/biological fluid absorption. These nanocomposite polymer (NC) hydrogels can be applied in various fields such as biosensing, drug delivery, nanomedicine or environmental remediation.[2,3] The incorporation of nanoparticles results in an interactive enhancement of each constituent. This also results in diminished risks to the environment and human health. Thus, these pioneering combinations of the two different materials generate structural diversity and have the advantage of enrichment of properties, such

as the improved stimuli response and mechanical strength of the nanoparticle-hydrogel composite.[4]

5.2. Nanocomposite Hydrogels

The nanocomposite hydrogels (NC hydrogels) are nanomaterial-filled, hydrated, polymeric networks that exhibit higher elasticity and strength relative to traditionally made hydrogels. Various natural and synthetic polymers are used to design nanocomposite networks according to the need. Engineered NC hydrogels exhibit controlled interactions between nanoparticles and polymer chains, thus achieving a wide range of physical, chemical, and biological, electrical and swelling/de-swelling properties suitable for the desired applications. Organic polymers, synthetic/natural, embedded with inorganic nanomaterial, could provide NC hydrogels with improved properties that are not achievable by single material alone. Inspired by such properties with flexible tissue-like properties, scientists have synthesized hydrogels by incorporating polymeric/ceramic/carbon-based and/or metallic nanomaterials to achieve NC hydrogels useable for various material science and medical applications.[5]

Designing of such NC hydrogels with supramolecular architecture are of three kinds as below.

a. Nano or micro-gels stabilizing single or multi nanoparticles.
b. Nanoparticles immobilized in a hydrogel matrix non-covalently.
c. Nanoparticles immobilized in a hydrogel matrix covalently.

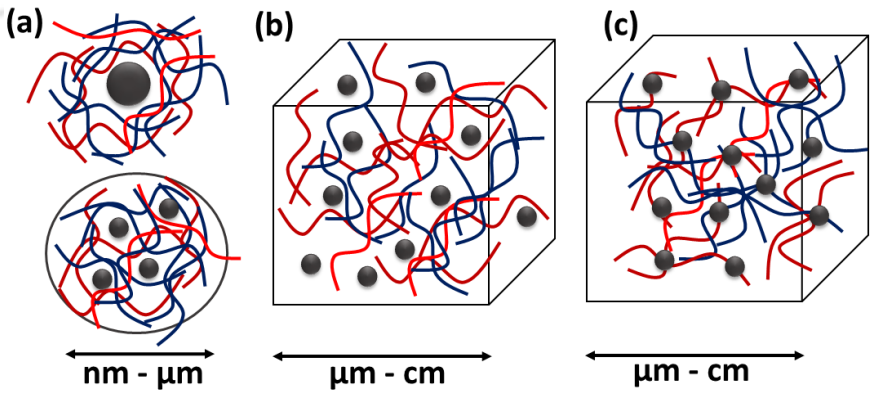

Figure 5.1. The three designs of the concept for the arrangement of hydrogel and nanoparticles in three designs. a) micro- or nano-sized hydrogel particles stabilizing polymer or inorganic nanoparticles, b) nanoparticles immobilized in a hydrogel matrix non-covalently, and c) nanoparticles immobilized in hydrogel matrix covalently(Graphical representation is adapted from Thoniyot *et al.*, 2015).

The NC hydrogels shown in figure 5.1(a), cover applications like biomedicine, electronics and catalysis.[5] On the other hand, figures 5.1 (b)-(c), which represent bulk hydrogel types, cover a few biomedical and pharmaceutical applications.[6,7]

Several hydrogel-nanoparticle composites are developed when different types of nanoparticles are embedded into hydrogel framework. The approach used mainly depends on the type of application of the hydrogel nanocomposites. The main five types of approach for the formation of the hydrogel-nanoparticle matrix are given below:

1. Hydrogel formation in a nanoparticle suspension.[8]
2. After gelation, Nanoparticles are physically embedded into hydrogel matrix.[9]
3. Reactive nanoparticle formation within a preformed gel.[10]
4. To form hydrogels cross-linking using nanoparticles.[11]
5. Nanoparticles used for gel formation, distinct gelator molecules and polymers.[12]

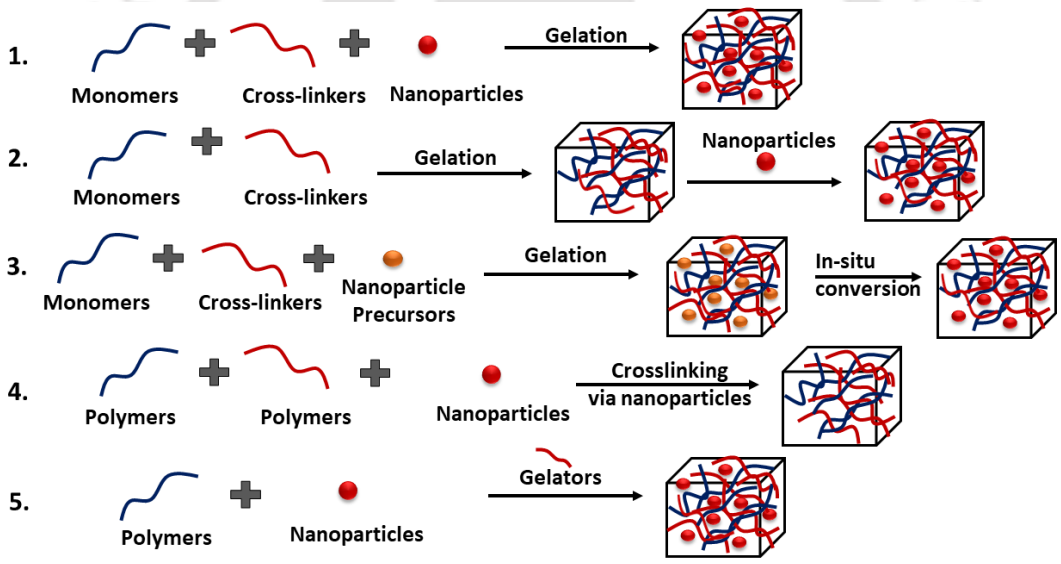

Figure 5.2. Schematic representation of the five approaches used to attain hydrogel-nanoparticle conjugates with even distribution.

5.3. Applications of Nanocomposite Hydrogels

Hydrogels find extensive applications in the biomedical industry due to their versatile biochemical and physical properties.[3,13] But hydrogels have poor mechanical strengths, so in order to improve their load-bearing properties and other properties, research has been in focus for the last few decades. Nanoparticles are used to improve the mechanical properties of the hydrogels mainly by link formation with the polymer chain, which desorbs under stress.[14,15]

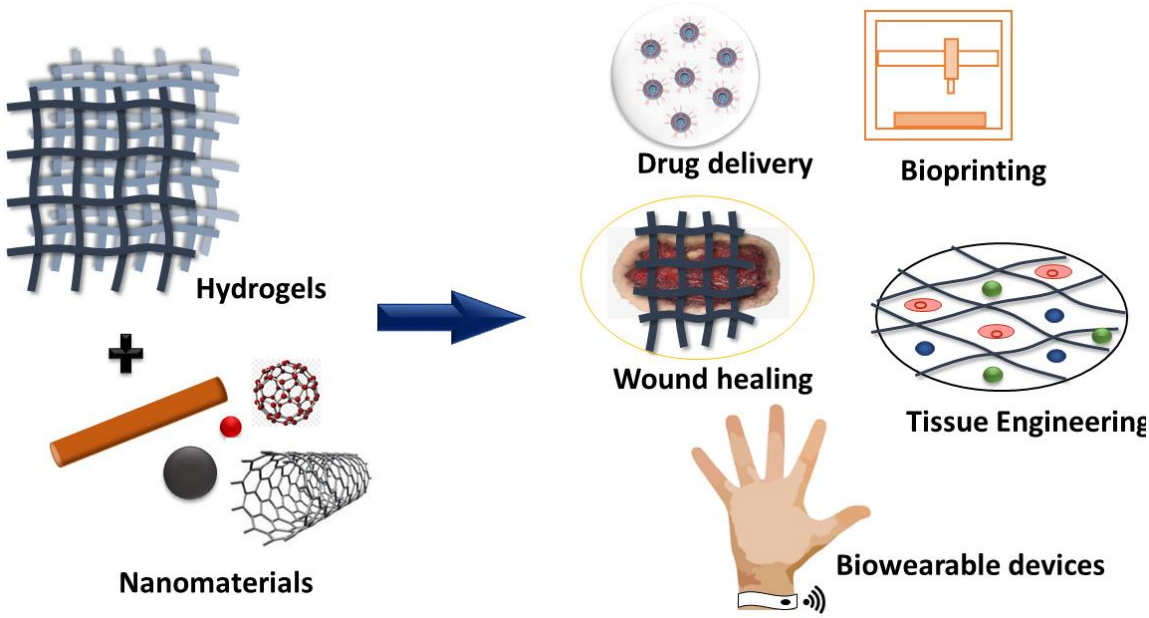

Figure 5.3. Schematic diagram representation of the broad applications of hydrogel nanocomposites in the biomedical sector.

Nanoparticles also contribute to the overall degree of crosslinking inside the polymer matrix, leading to improvements in the mechanical properties.[16,17] Hydrogel's stimuli sensitivity and bioactivity are important chemical properties of hydrogels that are essential for their use in the biomedical field.[18] Thus, incorporation of nanoparticles not only improves the mechanical strength, but also enhances the chemical properties of hydrogels making them versatile for use in various applications (Figure 4.3).[2,19,20] Figure 5.3 represents the various biomedical applications such as drug delivery, tissue engineering, adhesives, bioprinting and bio-wearable devices by hydrogels combined with nanomaterials. Among the various nanoparticles used for hydrogel preparations, silver nanoparticles(AgNPs) have grown to be quite advantageous due to their antibacterial properties, few of these are discussed in this chapter.

5.4. Silver Nanoparticle(AgNP)-Hydrogel Composites

AgNPs-hydrogel composites have been studied for their antimicrobial properties. They are primarily used in dental fillings and burn or wound dressings to avoid infections.[21] AgNPs bind non-specifically to bacterial membrane and cause structural changes such as damage of the intracellular structures (ribosomes, mitochondria, vacuoles, etc.) and biomolecules(lipids, DNA and protein), which enhances the permeability of membrane causing mitochondrial dysfunction.[22,23] To prolong the antimicrobial efficacy, the controlled release of these AgNPs

are essential. These nanocomposites may provide functional coatings for a large number of applications. Other properties like stimuli responsiveness, swelling ratio, mechanical toughness and degradability are to be studied for practical applications in such composites.[24] AgNPs-hydrogel composites show good functionality when used as antimicrobial coatings. For such purpose, AgNPs have been integrated into poly-acrylic acid (PAA),[25] NIPAAm,[26] PAAm,[27] polyvinyl alcohol (PVA)[28] based hydrogels. To produce biocompatible or degradable composites that have application as implantable dressings, naturally occurring materials like chitosan or carbohydrate polymers are utilized.[29] AgNPs consist of anti-inflammatory as well as antibacterial effects, which helps in assisting wound healing mechanism of action and causes resistance to bacteria. Also, the mechanism of action and impact of AgNPs in wound healing have been studied.[30]

From a very early time, due to the properties of silver, silver compounds were used in medicine[31]. There are various advantages of using AgNPs in medical, pharmaceuticals as well as in wound healing purposes. AgNPs are easy to synthesize via economical and safer routes;[32] these particles are very reactive as they have a negative charge on the surface, which helps modify the surface of AgNPs with numerous biomolecules. As a result, it causes a strong interface between thiol or amine-containing molecules with silver surface;[33] AgNPs possess a wide antibacterial spectrum. They are easily used in wound dressings without undesirable effects.[34] They also promote wound healing by reducing cytokine release declining lymphocyte and mast cell infiltration.[35] The three major components of the bacterial cells with which silver ions cooperate are peptidoglycan cell wall, bacterial proteins and DNA and the plasma membrane, and the electron transport chain.[36] Silver binds with the bacterial cell wall and cell membrane and stops the respiration process. Thus, the chemical energy of molecules is liberated and partially remains as ATP (adenosine triphosphate).[37] AgNPs inhibit replication of the bacteria when it interacts with sulfur-containing proteins of the membrane of bacteria and with phosphorus-containing compounds (DNA).[38] AgNPs can inactivate the most common pathway in bacteria, i.e., sugar catabolism, mainly by inactivating the enzyme phosphomannose isomerase.[39] Development of the free radicals and subsequent free radical-induced membrane damage is related to the mode of action of AgNPs.[40] The surface of these nanoparticles allows the development of free radicals, which are in charge of antimicrobial activity.[41] Different antibiotics in combination with AgNPs against *E. Coli* and *S. aureus* were studied. The antibacterial activities of the multi-antibiotic (penicillin G, Vancomycin, amoxicillin etc) discs with AgNPs increase against the two strains.[38]

5.4.1. Application of AgNPs Based Wound Dressings

For the healing process to be effective, the surface of the skin has to be covered for a sufficient amount of time. Wound dressings material should fulfil these following objectives: the diffusion of gases, maintaining a moist environment around the wound area, preventing saturation on the outer layer of the wound surface, mechanical protection of the wound, protection from microbes and other foreign particles, easily removable and changeable, non-toxic, cost-effective, and preventing desiccation of wound.[42]

Cotton is used as a better wound dressing material. Cotton fibres treated with chemicals can absorb moisture and are more susceptible to the growth of bacteria faster. AgNPs when used on clothes and sterile, can prevent infection. Metal-based dressings are quite suitable alternatives for wound healing such as burns, chronic ulcers or external wounds. Cotton fabrics were sterilized correctly, dried, dipped in nanoparticle solution then agitated for 24 hours at 600 rpm. Again, dried at 70°C and finally cured at 150°C.[43] Again, AgNPs can be infused into bacterial cellulose for antimicrobial wound healing[44]. Superior wound healing rates can be achieved by a chitosan-nanocrystalline silver dressing (89%) when compared with chitosan film (74%) and silver sulfadiazine dressings (68%). The use of this dressing caused less deposition of silver than conventional silver sulfadiazine, which indicates safer levels of silver[45]. *In vivo* experiments have been reported on the inflammatory response for wound repair and regeneration of tissue. Interleukin 10 (IL-10), a crucial mediator in this anti-inflammatory cascade, is produced by T lymphocytes, B lymphocytes, macrophages, and keratinocytes.[46]

The local and inflammatory response could be modulated by AgNPs and then cytokine modulation in burn wounds. Wound healing in diabetic mice is also reported by healing wounds in 16 ± 0.41 days after injury by treating with AgNPs, whereas control-treated mice recovered in 18.5 ± 0.65 days. The wound healing properties of AgNPs has been investigated in an animal model that reported that the healing is faster in a dose-dependent manner with improvement in surface appearance. Other studies such as proteomic, immunohistochemistry and quantitative PCR have shown that the use of AgNPs can reduce the inflammation of the wound and modulate fibrogenic cytokines. When wounds treated with AgNPs healed in about 25.2 ± 0.72 days after the injury, whereas wounds treated with antibiotics such as amoxicillin and metronidazole needed 28.6 ± 1.02 days to heal. This indicated that in this mechanism of action of AgNPs, other factors are also involved.[47] A decrease in inflammation in peritoneal adhesion without significant toxic effects by using AgNPs was also reported.[48] AgNPs could enhance

the rate of wound healing or wound closure by affecting the dermal contraction and epidermal re-epithelialization. AgNPs prevent infection in the wound surface by supporting the wound contraction by differentiating fibroblast/ myofibroblast, proliferation, and migration of keratinocytes. It also provides easy incorporation of nanosilver into cotton fabrics and drugs for a better therapeutic medication.[49]

5.4.2. Application of Polymer-Ag based Hydrogel Wound Dressings

Polymer-based wound dressings with antimicrobial properties have been gaining popularity in recent times in the field of biomaterials. Such materials are of much importance in medicine, especially with improved sterility and the longevity of the wound dressing materials reducing the frequent change of dressings in the wound sites.[50] Hydrogels are suitable wound dressing materials that offer a moist environment to the wound to avoid unnecessary sticking and quicker healing of the wound; they also absorb the excess exudates of the wound. Hydrogels are soft materials that can be synthesized using natural as well as synthetic polymers or composites. These are often helpful in biomedicine, including controlled drug and protein delivery, regenerative medicine, and tissue engineering.[51] Hydrogels are three-dimensional cross-linked networks of polymers that are generally hydrophilic and biocompatible. These types of polymeric materials are used in the manufacture of artificial corneas, catheters, contact lenses, wound dressings, etc. These materials have good swelling properties while do not get dissolved in water at physiological pH and temperature.[52]

Among the various wound dressing hydrogel materials used, poly (vinyl alcohol) acts as an excellent base for wound dressing. It has good elasticity and is a biocompatible synthetic polymer. The use of PVA avoids consuming other toxic chemical crosslinkers as it provides physical crosslinking of hydrogels. To improve biocompatibility and increase wound healing capacity, other natural polymers such as chitosan and its derivatives, starch, gelatin and alginate can be added with PVA.[50] Thus, PVA acts as a versatile polymeric material that has various properties such as nontoxicity, good biocompatibility, good elasticity, non-carcinogenicity, good swelling and other properties. The degree of hydrolysis, molecular weight, particle size distribution, its solubility in water influence the material's properties. PVA has an excellent water retention capacity as it is hydrophilic in nature.[52] The hydrogen bonding among the hydroxyl groups of PVA polymer influences the water solubility, crystallinity range and crystal modulus, which are known to be high. Semi-crystalline PVA has both crystalline and

amorphous regions, which causes the interfacial effect. PVA is usually low in electrical conductivity, and this property can be enhanced by blending it with other polymer.[53]

Gelatin is a natural polymer that is also used primarily in biomedical applications. Controlled hydrolysis of collagen protein forms gelatin which is the denatured form of collagen. It is highly recommended to use biomedicines in preparation of adhesives or plasma expander wound dressing or as absorbent hydrogel pads. It has high hemostatic properties and causes activation of microphages. It is used in a large number of wound dressings.[54,55] Gelatin forms very strong gels due to their triple helixes structure and a high level of pyrrolidines.[56] Other properties of gelatin are its compatibility with the body, its non-toxic and biodegradabile properties. It also forms promising hydrogel when blended with other components. Also, the properties of this blend and its mixing behavior are affected by the intermolecular interaction formation through hydrogen bonds of the polymers.[53]

The incorporation of an antibacterial agent is an excellent option to improve the hydrogel quality and its sterility. Use of antibiotics can cause resistance after use for a certain period. However, silver ions and AgNPs help improve the inhibitory effect against both gram-negative and gram-positive bacteria. The antimicrobial activities of AgNPs are associated with few distinct mechanisms. AgNPs Adhere onto the cell wall and cell membrane surfaces of bacteria or microbes, damaging the cytoplasmic membrane and other intracellular structures. It inhibits DNA replication and also may interrupt ATP production leading to respiratory disruption. AgNPs also induces the eeneration of reactive oxygen species(ROS) and free radical that causes oxidative stress and celluar toxicity. Also, AgNPs modulates the signal transduction pathways.[23] AgNPs over silver ion-based formulations is advantageous as they can be used in lower concentrations. AgNPs release Ag+ ions, causing induction of better antibacterial properties. Due to the high surface area of these AgNPs, there may be instability, but it can be overcomed by incorporating polymer blends that increase stability and functionality.[50,57] In recent times the use of AgNPs in the biomedical fields has grown tremendously. It is proven effective in wound healing by reducing infections caused by bacteria. It helps to heal wound faster, reduces scars and causes no inflammation when used in a dose-dependent manner. Also, it has no toxicity on the kidney and liver when uptake of AgNPs is dose, size and coating dependent. Again, AgNPs can be synthesized via the green route, providing better and enhanced biocompatibility and improved antibacterial properties.

Although studies have reported the green synthesis of AgNPs, its applications are not clearly documented.[58,59] Thus, it will be worthwhile to synthesise AgNPs via green route and utilise them to improve the polymer hydrogel quality and properties and explore the wound dressing application.

5.5. AIM AND OBJECTIVES

The effective wound-healing hydrogels should have the property to create a moist environment for wound healing, prevent the wound surface from microbial penetration and provide higher water vapour permeability. Toward this end, as part of our ongoing research on the synthesis of antibacterial AgNPs-based composite materials, we thought it would be worthwhile to utilize the green-synthesized AgNPs to develop low-cost composite polymer hydrogel for wound dressing application. Thus, the following are the objectives of this chapter:

a) Green synthesis of AgNPs by reducing silver nitrate($AgNO_3$) using Bhimkol (*Musa balbisiana*) peel extract.

b) Development of polymer based hydrogel nanocomposite films by adding PVA, gelatin and AgNPs by the casting method.

c) Swelling kinetics, mechanical strength, water transmission rate(WVTR) analysis and contact angle measurements analysis were performed for optimization of the polymer hydrogel nanocomposites,

d) Characterization of the PVA/gelatin/AgNPs hydrogel nanocomposite films using Fourier transformation infrared (FT-IR) spectrometry, Energy-dispersive X-ray(EDX), Field Emission Transmission Electron Microscope (FESEM), Field Emission Transmission Electron Microscope (FETEM) and Thermogravimetric analysis (TGA) performed in nitrogen gas and X-Ray Diffraction (XRD) Analysis.

e) Cell viability assay and *in vitro* scratch wound healing assay were performed to observe the cell toxicity and the wound healing efficacy of the hydrogel films.

5.6. RESULTS AND DISCUSSION

5.6.1. Preparation of the Polymer Nanocomposites Hydrogel

For preparation of AgNPs incorporated PVA/gelatin hydrogel films; initially hydrogels were prepared using PVA-gelatin blends and observing their swelling ratio and mechanical strength. Thus, polyvinyl alcohol (PVA) and PVA-gelatin hydrogel films with different concentrations of PVA and gelatin were prepared (% w/w ratio). The solution casting method was used to prepare PVA-gelatin films[53]. 4 grams of PVA was added slowly in 100 mL distilled water and stirred continuously for 2 hours in a magnetic stirrer at 60°C, which makes it 4% PVA(control) solution. After PVA dissolves completely in water, it is sonicated for 5 minutes to remove the air bubbles. The solution is then cast on clean and sterile Petri plates and kept in a hot air oven at 60°C for slow evaporation for a few hours. Similarly, 4 grams of gelatin was added slowly in 100 mL distilled water and stirred continuously at 60°C, which makes it a 4% gelatin(control) solution. The other combinations of PVA and gelatin films were prepared keeping the PVA amount constant at 3.5%, and the amount of gelatin was varied from 0.5% to 3.5% in w/w ratio. PVA was kept constant as a higher percentage of PVA was proven to be better for preparing homogenous and less porous hydrogel films than with a higher percentage of gelatin. 3.5 grams of PVA was added to 50 mL of Milli-Q water and allowed to stir at 60°C to get completely dissolved. Then the varying quantity of gelatin was added to the other 50 mL water, when the gelatin dissolves completely, it was then added to the polymeric solution with continuous stirring for esterification reaction to carry out between PVA and gelatin. The solution obtained was sonicated for 5 minutes and then cast into sterile Petri plates. The various combinations of the films were

i. 4% PVA (Control)
ii. 4% Gelatin(Control)
iii. 3.5% PVA + 0.5% gelatin
iv. 3.5% PVA + 1.0% gelatin
v. 3.5% PVA + 1.5% gelatin
vi. 3.5% PVA + 2.0% gelatin
vii. 3.5% PVA + 2.5% gelatin
viii. 3.5% PVA + 3.0% gelatin
ix. 3.5% PVA + 3.5% gelatin

Thin films of PVA, gelatin and PVA/gelatin hydrogels were prepared by the casting method. After drying the films in a hot air oven at 60°C for few hours, these films were peeled off and stored in a vacuum desiccator to further analysis.

After having the PVA/gelatin hydrogels in hand, we prepared the AgNPs following our green synthetic route as described in Chapter 2 and proceeded to synthesize NC hydrogels. Thus,1 mM concentration of green synthesized AgNPs was integrated slowly into the polymer hydrogels dropwise during solution casting method but continuously for even mixing the AgNPs and the polymers. PVA/gelatin ratio was maintained at 3.5% PVA + 0.5% Gelatin and at 3.5%PVA +1.0% Gelatin (% w/w ratio) and then 0.5%, 1.0%, 1.5% and 2.0% (% v/w ratio) of 1 mM of green synthesized AgNPs were incorporated in each hydrogel. The quantity of AgNPs was taken in mL, and the concentration of AgNPs was kept constant in each casting solution. After completely evaporating water when kept in a hot air oven, thin films of PVA/gelatin/AgNP hydrogel remained on the Petri dishes were peeled off and stored in a vacuum desiccator for further processing and characterizations.

5.6.2. Study of Swelling Properties of The NC Hydrogel Films

Blood contains about 90% of water in a body. As such excellent swelling behaviour of a hydrogel is considered one of the most important properties for the hydrogel to absorb a large quantity of water in the blood to help cease bleeding. Swelling behaviour is basically to maintain the state of the hydrogel when it absorbs water and the capacity to hold on to the water. Permeability to nutrients by the water present in the hydrogel and export of cellular products from the hydrogel is considered a desirable factor for choosing a dressing material[60]. This material should reach a swelling and de-swelling equilibrium in a short period. The swelling kinetics was carried out for 500 minutes, and the swelling behaviour of all the hydrogel film combinations was recorded at 30 minutes intervals each.

Figure 5.4(i) represents the swelling ratio of the 4% PVA control hydrogel, 4% gelatin control hydrogel and PVA/gelatin blend hydrogel films. The PVA control hydrogel film and PVA/gelatin hydrogel films showed good swelling behaviour since both gelatin and PVA are hydrophilic polymers. The hydrogel film 3.5% PVA + 0.5% gelatin achieved swelling equilibrium within 30 minutes and the water uptake capacity was found to be 587.28% at equilibrium, while other PVA/gelatin hydrogel films took about 30 minutes to achieved equilibrium. Still, their water uptake capacity was less than 500%. Again, 4% PVA (control) hydrogel film achieved equilibrium within 60 minutes with a water uptake capacity of

504.03%. The swelling behaviour of 4% gelatin (control) hydrogel film could not be recorded as it got dissolved within 60 minutes. The swelling behaviour of 3.5% PVA + 0.5% gelatin and 3.5% PVA + 1.0% gelatin hydrogel films showed better results than the other combinations, so these samples were considered for further characterization.

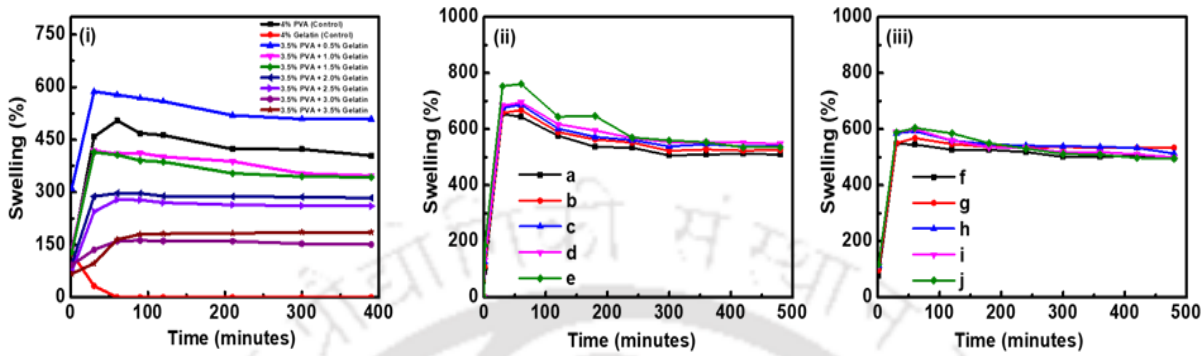

Figure 5.4: (i) Swelling kinetics of PVA (control), gelatin (control)and PVA-gelatin hydrogels in which PVA is kept constant and gelatin is varied. Swelling kinetics of (ii) (a) 3.5% PVA + 0.5% gelatin(Control), (b) 3.5% PVA + 0.5% gelatin + 0.5% AgNP, (c) 3.5% PVA + 0.5% gelatin + 1.0% AgNP, (d) 3.5% PVA + 0.5% gelatin + 1.5% AgNP and (e) 3.5% PVA + 0.5% gelatin + 2.0% AgNP hydrogel films and (iii) (f) 3.5% PVA + 1.0% gelatin(Control), (g) 3.5% PVA + 1.0% gelatin + 0.5% AgNP, (h) 3.5% PVA + 1.0% gelatin + 1.0% AgNP, (i) 3.5% PVA + 1.0% gelatin + 1.5% AgNP and (j) 3.5% PVA + 1.0% gelatin + 2.0% AgNPs hydrogel films respectively.

Figure 5.4(ii) and 5.4(iii) presents the swelling kinetics of 3.5% PVA + 0.5% gelatin and 3.5% PVA + 1.0% gelatin hydrogel films incorporated with green synthesized AgNPs in various ratios respectively. In figure 5.4(ii) all the PVA/gelatin/AgNP hydrogel films achieved swelling equilibrium within 30 minutes and the water uptake capacity was found to be 654.44% for (a) 3.5% PVA + 0.5% gelatin(Control), 657.4% for (b) 3.5% PVA + 0.5% gelatin + 0.5% AgNP, 675.45% for (c) 3.5% PVA + 0.5% gelatin + 1.0% AgNP, 683.73% for (d) 3.5% PVA + 0.5% gelatin + 1.5% AgNP and 753.29% for (e) 3.5% PVA + 0.5% gelatin + 2.0% AgNP respectively at equilibrium. Since 3.5% PVA + 0.5% gelatin + 2.0% AgNP hydrogel film had the highest water uptake capacity among the other which was more than 700% at swelling equilibrium. All the AgNPs incorporated hydrogel films had more water uptake capacity than that of the control polymer hydrogel film.

Again, from the figure 5.4(iii) it is clear that all the PVA/gelatin/AgNP hydrogel films achieved swelling equilibrium within 30 minutes and the water uptake capacity was found to

be 547.93% for (f) 3.5% PVA + 1.0% gelatin(Control), 550.29% for (g) 3.5% PVA + 1.0% gelatin + 0.5% AgNP, 585.62% for (h) 3.5% PVA + 1.0% gelatin + 1.0% AgNP, 588.23% for (i) 3.5% PVA + 1.0% gelatin + 1.5% AgNP and 588.30% for (j) 3.5% PVA + 1.0% gelatin + 2.0% AgNP respectively at equilibrium. Here, hydrogel film 3.5% PVA + 1.0% gelatin + 2.0% AgNP showed the highest swelling equilibrium with water uptake capacity of 588.30% but it is not more than 700% at swelling equilibrium. In this case also, all the polymer hydrogel nanocomposite films had more water uptake capacity than that of the control polymer hydrogel film. The table 5.1 represents the swelling ratio or the water uptake capacity after 30 minutes of swelling by the combinations of 3.5% PVA + 0.5% gelatin and 3.5% PVA + 1.0% gelatin hydrogel films after incorporating AgNPs in various concentrations.

Table 5.1: Swelling ratio of the hydrogel films after 30 minutes.

Sample no.	PVA/gelatin/AgNP hydrogel films	Water uptake capacity or Swelling ratio(%)
(a)	3.5% PVA + 0.5% gelatin(Control)	654.44%
(b)	3.5% PVA + 0.5% gelatin + 0.5% AgNP	657.4%
(c)	3.5% PVA + 0.5% gelatin + 1.0% AgNP	675.45%
(d)	3.5% PVA + 0.5% gelatin + 1.5% AgNP	683.73%
(e)	3.5% PVA + 0.5% gelatin + 2.0% AgNP	753.29%
(f)	3.5% PVA + 1.0% gelatin(Control)	547.93%
(g)	3.5% PVA + 1.0% gelatin + 0.5% AgNP	550.29%
(h)	3.5% PVA + 1.0% gelatin + 1.0% AgNP	585.62%
(i)	3.5% PVA + 1.0% gelatin + 1.5% AgNP	588.23%
(j)	3.5% PVA + 1.0% gelatin + 2.0% AgNP	588.30%

This kinetic study shows that all the polymer hydrogel nancomposite films with low gelatin and high PVA ratio showed faster absorption rates, which helps provide a wet environment for faster recovery of wounds[53,61]. The results revealed that especially 3.5% PVA + 0.5% gelatin + 2.0% AgNP hydrogel film could absorb a large amount of wound exudate also hold water in the hydrogel for a longer time.

5.6.3. Study of Mechanical Properties of The NC Hydrogel Films

The mechanical properties of a dressing material are considered one of the most important factors for its use to protect wounds. In the experiment, the mechanical strength of the hydrogel

films was recorded by analyzing the tensile strength and elongation at break value of the prepared wound dressings. Figure 5.5 presents the stress vs strain curves of 3.5% PVA + 0.5% gelatin and 3.5% PVA + 1.0 % gelatin hydrogel films incorporated with green synthesized AgNPs in various ratios respectively. It was observed that the mechanical strength of 3.5% PVA + 0.5% gelatin + 2.0% AgNP hydrogel film showed highest among all the other hydrogel films with a tensile strength of 112.32 MPa and elongation at break was observed to be 7.5%(figure 5.5(i)). The mechanical strength of the 3.5% PVA + 1.0% gelatin + 1.0% AgNP hydrogel film showed highest among all the other hydrogel films with a tensile strength of 99.44 MPa and elongation at break was observed to be 4.98%(figure 5.5(ii)). In both the cases, the polymer hydrogel films incorporated with green synthesized AgNPs showed enhanced mechanical properties than the control polymeric hydrogel films. Table 5.2 records the tensile strength and elongation at break values for all the combinations of polymeric hydrogel films incorporated with and without AgNPs.

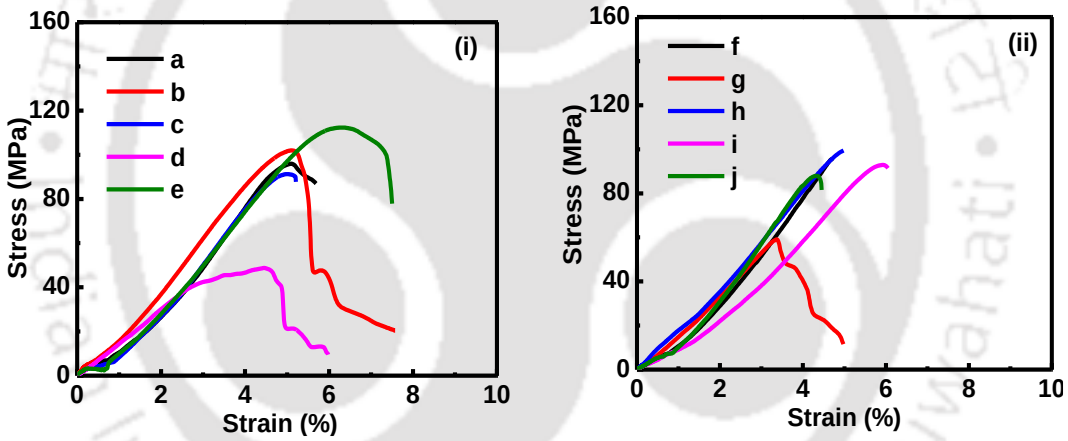

Figure 5.5: Tensile strength of (i) 3.5% PVA+ 0.5% gelatin (Control) and its other combinations with 0.5-2.0 % AgNPs(a-e) hydrogel films respectively; (ii) 3.5% PVA + 1.0% gelatin(Control) and its combinations with 0.5-2.0% AgNP(f-j) hydrogel films respectively.

Table 5.2: Tensile strength and Elongation at break of the the PVA/gelatin/AgNP hydrogel films.

Sample no.	PVA/gelatin/AgNP hydrogel films	Tensile strength (MPa)	Tensile Elongation at Break (%)
(a)	3.5% PVA + 0.5% gelatin(Control)	95.92	5.69
(b)	3.5% PVA + 0.5% gelatin + 0.5% AgNP	101.95	7.57
(c)	3.5% PVA + 0.5% gelatin + 1.0% AgNP	91.22	5.21
(d)	3.5% PVA + 0.5% gelatin + 1.5% AgNP	48.77	5.98

(e)	3.5% PVA + 0.5% gelatin + 2.0% AgNP	112.32	7.5
(f)	3.5% PVA + 1.0% gelatin(Control)	95.77	4.72
(g)	3.5% PVA + 1.0% gelatin + 0.5% AgNP	59.05	4.97
(h)	3.5% PVA + 1.0% gelatin + 1.0% AgNP	99.44	4.98
(i)	3.5% PVA + 1.0% gelatin + 1.5% AgNP	92.88	6.05
(j)	3.5% PVA + 1.0% gelatin + 2.0% AgNP	87.93	4.45

5.6.4. Study of Fourier Transform Infrared (FT-IR) Spectroscopic Character of the NC Hydrogel Films

FT-IR spectra study provides benefits to study precisely the molecular structure of a material. The position of the peaks as well as the intensity and width of the bands might be subjected to change due to environmental change and also due to conformation of macromolecules on molecular level. When different polymers are compatible, intermolecular interactions may occur. Thus, it is advantageous for studying polymer compatibility under FTIR spectrum. The FTIR spectrum for the blends of polymers appears different from that of pure polymers[53]. Figure 5.6(i) gives the FTIR spectrum of (a) 3.5% PVA+ 0.5% gelatin (Control), (b) 3.5% PVA + 0.5% gelatin + 0.5% AgNP, (c) 3.5% PVA + 0.5% gelatin + 1.0% AgNP, (d) 3.5% PVA + 0.5% gelatin + 1.5% AgNP and (e) 3.5% PVA + 0.5% gelatin + 2.0% AgNP hydrogel films respectively. And figure 5.6(ii) represents the FT-IR spectrum of (f) 3.5% PVA + 1.0% gelatin(Control), (g) 3.5% PVA + 1.0% gelatin + 0.5% AgNP, (h) 3.5% PVA + 1.0% gelatin + 1.0% AgNP, (i) 3.5% PVA + 1.0% gelatin + 1.5% AgNP and (j) 3.5% PVA + 1.0% gelatin + 2.0% AgNP hydrogel films respectively. In the FTIR spectra of both the figures 5.6(i) and 5.6(ii) in the PVA/Gelatin hydrogel films, bands at 916 and 850 cm^{-1} confirm the presence of PVA skeletal vibration. The band at 1096 cm^{-1} represents C-O stretching and O-H bending. Also, C-C and C-O stretching vibration occur at 1144 $cm^{-1,}$ and the small bands at 1438 and 1378 cm^{-1} correspond to the bending and wagging of CH_2 and C-H vibrations. There occurs a broad peak around 3279 cm^{-1}, which indicates hydroxyl group stretching vibration. Also, the smaller peaks around 2923 cm^{-1} and around 2850 cm^{-1} indicate C-H asymmetric stretching vibrations. The band at around 1640 cm^{-1} corresponds to the acetyl C=O stretching vibrations. Again, due to the presence of gelatin, the region between 3000-3600 cm^{-1} and between 1100-1700 cm^{-1} gives potential peaks, which indicates as N-H stretching vibrations which are hydrogen-bonded. The peak around 3286 cm^{-1} corresponds to a hydroxyl group with the polymeric association and a secondary amide. Again C-O stretching of secondary alcoholic

groups is indicated by the peak at 1088 $cm^{-1,}$ and the peak at 1635 cm^{-1} corresponds to the presence of the secondary amide group. The peak at 2932 cm^{-1} corresponds to the occurrence of a hydrocarbon chromophore in the esterified product. So this esterified product has a secondary alcoholic group and secondary amide groups along with the hydrocarbon chromophore. Thus good interaction between the two polymers i.e., gelatin and PVA was observed.[52,53,62]

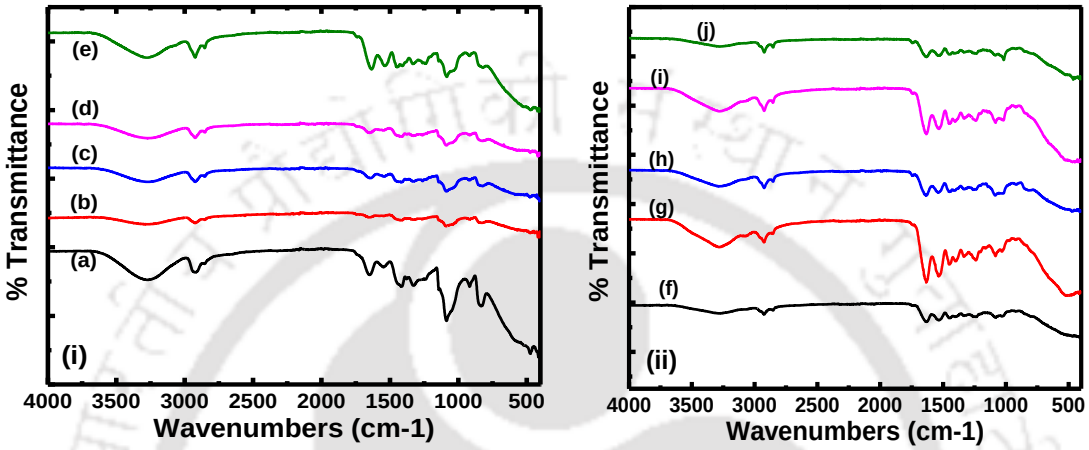

Figure 5.6: FT-IR spectrum of (i) 3.5% PVA+ 0.5% gelatin (Control) and its other combinations with 0.5-2.0 % AgNPs(a-e) hydrogel films respectively; (ii) 3.5% PVA + 1.0% gelatin(Control) and its combinations with 0.5-2.0% AgNP(f-j) hydrogel films respectively.

In the FTIR spectrums of both the combinations, PVA-gelatin hydrogel nanocomposite films, the strong and broad absorption peak at around 3284-3443 cm^{-1} corresponds to the N-H stretching vibrations of amines. This peak also corresponds to the O-H (H-bonded) stretching vibrations of phenols and carboxylic acids. Again, the peak observed at 1633 cm^{-1} attributes to the C=O stretching in carboxyl or C=N bending vibration in the amide group. The peak at 667-598 cm^{-1} corresponds to C-H stretching of aromatic group. The shifts in the peak highlight the involvement of functional groups of bhimkol (*Musa balbisiana*) peels in the reduction of silver salt(Ag^{+}) to metallic silver (Ag^{0}). There are major peak highlights in the FTIR spectrum of the polymer hydrogel films incorporated with silver nanoparticles than the polymer hydrogel films without incorporation of AgNPs. The chemical structures were well preserved without forming any new chemical bonds during the hydrogel forming process indicating that these hydrogel films are formed by cross-linking.[63,64]

5.6.5. Study of Water Vapour Transmission Rate (WVTR)

In the process of wound healing, the water vapour transmission rate (WVTR) of the uppermost surface of a membrane determines the wound's moist environment, which is one of the most important criteria. Lower WVTR of a membrane or hydrogel film material causes retention of the exudate builds up the back pressure, which might lead to softening of the surrounding healthy tissues of the wound area, triggering pain to the wounded area of the patient. This condition also increases the bacterial growth in the wounded area. On the contrary, higher WVTR of a membrane or material leads to excessive water loss, then dehydrates the wound, which ultimately initiates the formation of scar or dressing attachment to the wounded skin.[65] The water vapour transmission for skin without any injury, skin with first degree burn and skin with granulated injury was about 200, 300 and 5000 g/m^2.day, respectively. An ideal wound dressing material should prevent much loss of water and dryness. Also, it should be able to avoid the formation of exudates in the injury site. An ideal wound healing dressing material must have WVTR of about 2000-2500 g/m^2.day.[65,66] Table 5.3 represents the WVTR of the hydrogel samples after 24 hours duration.

Table 5.3. WVTR of the hydrogel films after 24 hours.

Sample no.	PVA/gelatin/AgNP hydrogel films	Water Vapour Transmission Rate ($g.m^{-2}$.24 hr) (WVTR±S.D)
(a)	3.5% PVA + 0.5% gelatin(Control)	1248.75±90.015
(b)	3.5% PVA + 0.5% gelatin + 0.5% AgNP	1426.45±75.873
(c)	3.5% PVA + 0.5% gelatin + 1.0% AgNP	1824.1±139.159
(d)	3.5% PVA + 0.5% gelatin + 1.5% AgNP	2095.9±126.855
(e)	3.5% PVA + 0.5% gelatin + 2.0% AgNP	2239±98.571
(f)	3.5% PVA + 1.0% gelatin(Control)	1072.9±48.507
(g)	3.5% PVA + 1.0% gelatin + 0.5% AgNP	1567.8±77.216
(h)	3.5% PVA + 1.0% gelatin + 1.0% AgNP	1909.8±79.196
(i)	3.5% PVA + 1.0% gelatin + 1.5% AgNP	2010.95±32.598
(j)	3.5% PVA + 1.0% gelatin + 2.0% AgNP	2232.15±74.034
PVA: Poly (vinyl alcohol), AgNP: Green synthesized Silver Nanoparticles, WVTR: Water vapour transmission rate, S.D: Standard deviation, where *p-value* <0.05 respectively.		

The water vapour transmission rate of 3.5% PVA + 0.5% gelatin + 2.0% AgNP is 2239 $g.m^{-2}.d^{-1}$ and 3.5% PVA + 1.0% gelatin + 2.0% AgNP is 2232.15 $g.m^{-2}.d^{-1}$ which showed much greater improvement when compared with the 3.5% PVA + 0.5% gelatin(Control) and 3.5% PVA + 1.0% gelatin(Control) which were 1248.75 $g.m^{-2}.d^{-1}$ and 1072.9 $g.m^{-2}.d^{-1}$ respectively(Table 5.3).

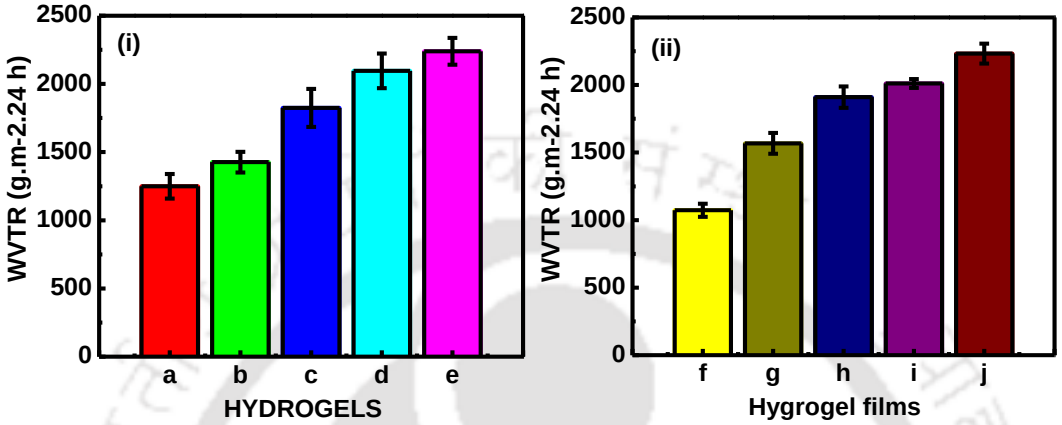

Figure 5.7: Water vapour transmission rate(WVTR) (i) of 3.5% PVA+ 0.5% gelatin (Control) and its other combinations with 0.5-2.0% AgNPs(a-e) hydrogel films, respectively; (ii) 3.5% PVA + 1.0% gelatin(Control) and its combinations with 0.5-2.0% AgNPs(f-j) hydrogel films respectively.

Figure 5.7(i) and (ii) showed a graphical representation of the comparative WVTR values of all the hydrogel films. In figure 5.7(i) 3.5% PVA + 0.5% gelatin(Control) hydrogel film and other formulations of 3.5% PVA + 0.5% gelatin hydrogel films after addition of silver nanoparticles are compared whereas in figure 5.7(ii) 3.5% PVA + 1.0% gelatin(Control) hydrogel film and other formulations of 3.5% PVA + 1.0% gelatin hydrogel films after addition of AgNPs are compared. From both the figures, it can be observed that WVTR of all the polymer nanocomposite hydrogel films increased with an increase in the AgNP content. So the ideal wound dressing material is the hydrogel film with 2.0% AgNP, which has a WVTR of 2239 $g.m^{-2}.d^{-1}$. This WVTR range is ideal for maintaining optimum moisture content at the times of the wound healing process.[67]

5.6.6. Study of Hydrophilicity and Wettability by Contact Angle Measurement

Hydrophilicity and wettability analysis of biomaterials is a significant study in biomedical applications as they come in contact with the blood and exudates. So water contact angle measurements are used to study the membrane surface hydrophilicity.[68] An ideal wound dressing material generally should have contact angle < 90° with a good ability to absorb excessive exudates from the wound sites.[66]

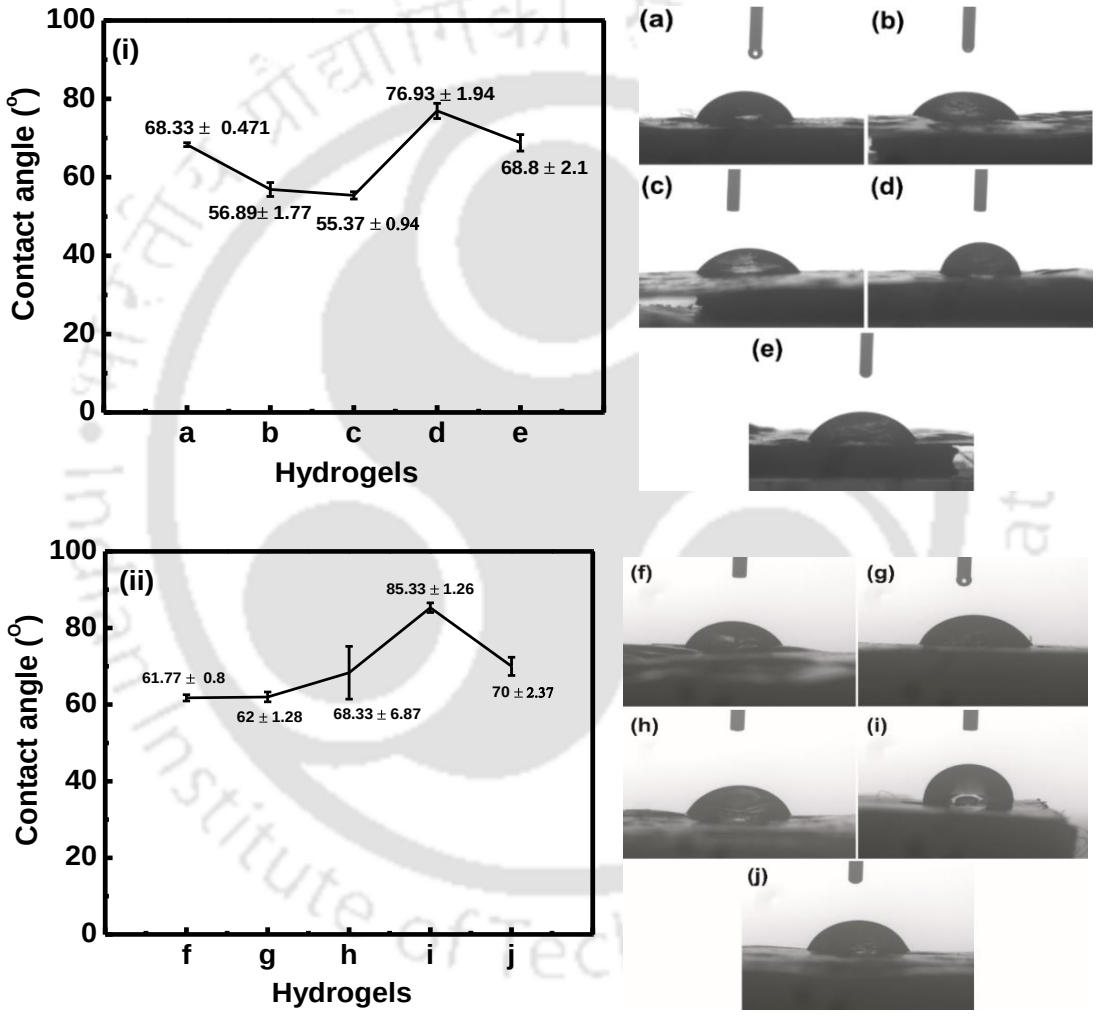

Figure 5.8: Graphical representation of the contact angles of (i) 3.5% PVA+0.5% gelatin+ AgNP(vary) hydrogel film formulations along with their contact angle measurement images; and (ii) 3.5% PVA+1.0% gelatin+AgNPs(vary) hydrogel film formulations along with their contact angle measurement images.

Figure 5.8(i) and (ii) represent the contact angle measurements and images of the various PVA/gelatin/AgNPs hydrogel film formulations. The addition of AgNPs has influenced the

contact angle measurements in both the combinations of PVA/gelatin hydrogel films. In the experiment, the concentration of PVA is kept constant, and gelatin concentration varies. AgNPs concentration was gradually increased. The contact angle measurements of the AgNP incorporated PVA/gelatin hydrogels are comparatively similar to that of the original hydrogel film without incorporation of AgNPs. From figure 5.8(i), it was clear that initially, there was a slight decrease in the contact angle. At a later stage, no further decrease in the contact angle was observed. This may be due to AgNPs aggregation in the hydrogel at higher concentration.[68] Figure 5.8(ii) shows no substantial contact angle decrease after adding AgNPs into the polymer hydrogel films. The contact angle measurements are in-between 55.37-85.33°, with a good ability to absorb water or exudates.

5.6.7. Study of Morphology of NC Hydrogel Films by FESEM

The FESEM micrographs of PVA-gelatin hydrogel films and PVA/gelatin/AgNP hydrogel films, shown in figure 5.9(i-viii). The FESEM technique can easily study the surface morphology of the hydrogels. From figure 5.9(i), (ii) and (v), (vi), the microstructure of the control polymeric hydrogel film can be analyzed easily. It is observed that the surface of the polymeric PVA/gelatin hydrogel, i.e., 3.5% PVA + 0.5% gelatin and 3.5% PVA +1.0% gelatin blend without AgNPs, showed clear or plain surface without much irregularities, which confirms in homogenous mixing of the polymers. The hydrogels were transparent and mostly amorphous in nature. Figure 5.9(iii) and (iv) displays 3.5% PVA + 0.5% gelatin + 2% AgNP hydrogel films whereas figure 5.9(vii) and (viii) displays 3.5% PVA + 1.0% gelatin + 2% AgNP hydrogel films. After adding 2% AgNPs in both the combinations, the structure changed to be rough but showed a homogenous surface of the polymeric hydrogel film matrix with silver nanoparticles distributed evenly.[69] These micrographs confirm the incorporation of AgNPs with dimensions smaller than 100 nm within the polymeric matrix. It seems that at higher concentrations of AgNPs, aggregations are observed in the polymeric hydrogel matrix. Agglomeration of AgNPs might have occurred as the images show the poly disperse nature of AgNPs originally synthesized using Bhimkol (*Musa balbisiana*) peel extract. The average nanoparticle size was around 44.24 nm, which was embedded into the PVA and gelatin hydrogel film.[70]

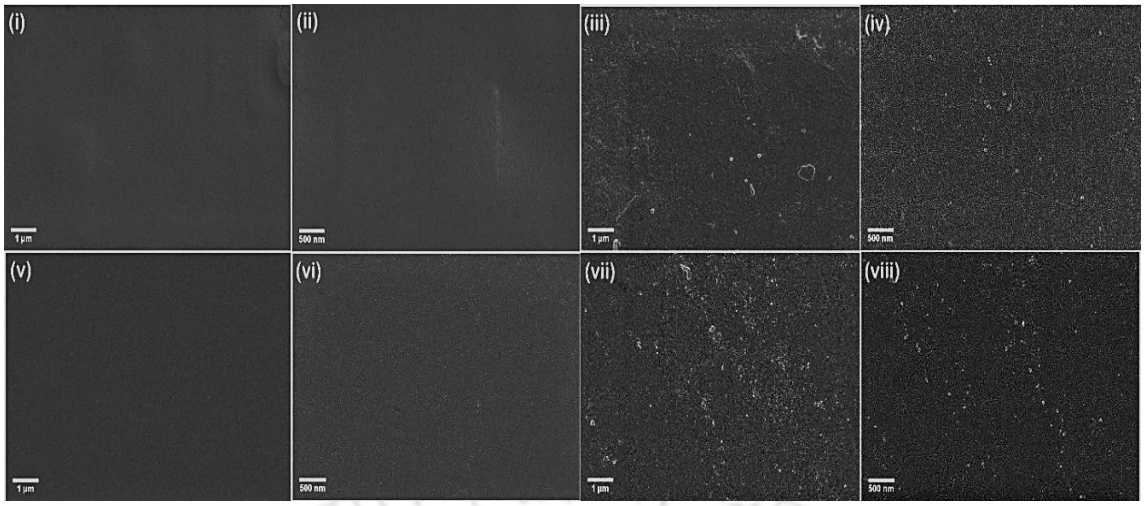

Figure 5.9: FESEM images of (i-iv) 3.5% PVA+0.5% gelatin hydrogel films and 3.5%PVA+0.5% Gelatin+ 2% AgNPs hydrogel films at 1µm scale (25kx magnification) and 500 nm scale(50kx magnification); and (v-viii) 3.5% PVA+1.0% gelatin hydrogel films and 3.5%PVA+ 1.0% gelatin+ 2% AgNPs hydrogel films at 1µm scale(25kx magnification) and 500 nm scale(50kx magnification) respectively.

5.6.8. Study of Morphology of NC Hydrogel Films by Field Emission Transmission Electron Microscopy (FETEM) Analysis

The FETEM analysis can efficiently study the PVA and gelatin hydrogel blend's surface morphology. The SAED pattern determines the amorphous or crystalline nature of the polymeric hydrogel film. The existence and distribution of AgNPs within the polymer matrics was investigated by FETEM analysis. Figure 5.10 represents the FETEM images of PVA/gelatin polymeric hydrogel and PVA/gelatin/AgNPs polymeric hydrogels, providing the size and shape of the AgNPs, which are clearly observed in the polymeric hydrogels.

Figures 5.10(i) and (iv) show the hydrogel matrix formation was visible between PVA and gelatin without much irregularities. Both the control hydrogel films i.e., 3.5% PVA + 0.5% gelatin and 3.5% PVA + 1.0% gelatin are smooth. Again, figure 5.10(ii) and (v) i.e., in hydrogel films 3.5% PVA + 0.5% gelatin + 2%AgNPs and 3.5% PVA + 1.0% gelatin + 2%AgNPs, presence of AgNPs was quite evident. Figure 5.10(iii) and (vi) represents the SAED pattern of 3.5% PVA + 0.5% gelatin + 2%AgNPs and 3.5% PVA + 1.0% gelatin + 2%AgNPs hydrogel films. This study reveals that AgNPs are almost polydispersed in nature with mostly spherical shape. The nanoparticles are randomly distributed within the polymeric matrices of PVA and gelatin. AgNPs had an average particle size of around 12-66 nm when analyzed using ImageJ

software. In figure 5.10(ii) and (v), due to the addition of a high concentration of AgNPs(2% v/v), there was nanoparticle agglomeration which makes it difficult to measure the exact particle size and separate the AgNPs.[71] But still, the nanoparticles are visibly seen integrated within the hydrogel matrix and some smaller sized AgNPs are found to be scattered. This may be during the time of sonication in the process of hydrogel preparation, some nanoparticles might have come out of the swollen hydrogel matrix. The AgNPs have face cubic structure and its pattern was studied in the SAED pattern of the polymer/AgNP hydrogel film, which provides some crystallinity to the hydrogel film.[66,68] So it can be concluded that in situ AgNP formation within a well-defined crosslinking hydrogel network can produce controlled as well as smaller sized nanoparticles. Further the presence of elemental silver was confirmed by energy-dispersive X-Ray analysis.

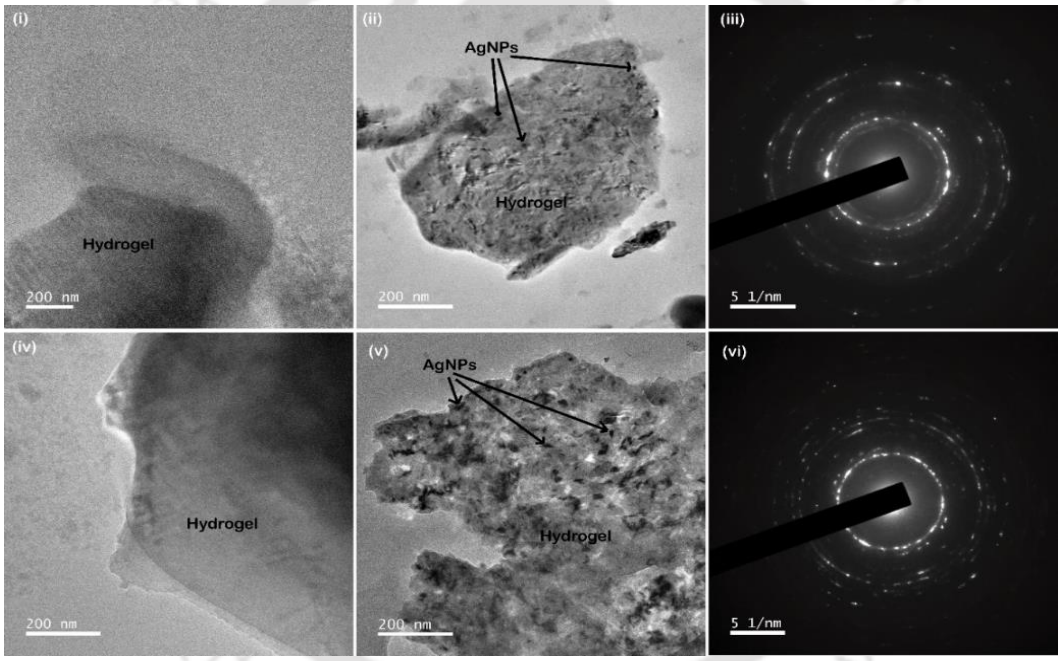

Figure 5.10: FETEM images of (i) 3.5% PVA + 0.5% gelatin hydrogel film(control), (ii) 3.5% PVA + 0.5% gelatin + 2% AgNPs, (iii) SAED pattern of the 3.5% PVA + 0.5% gelatin + 2% AgNPs hydrogel film. (iv) FETEM images of 3.5% PVA + 1.0% gelatin hydrogel film(control), (v) 3.5% PVA + 1.0% gelatin + 2% AgNPs and (v) SAED pattern of .5% PVA + 1.0% gelatin + 2% AgNP hydrogel film.

5.6.9. Study of X-Ray Diffraction of the NC Hydrogel

The microstructures of the PVA-gelatin hydrogel film with and without incorporation of AgNPs were investigated by the wide-angle X-Ray Diffraction. The X-ray diffraction spectrum for PVA/gelatin hydrogel films and PVA/gelatin/AgNPs hydrogel film are shown in figure

5.11. The XRD pattern of both PVA/Gelatin hydrogel film without AgNP and with 2% AgNP showed a sharp and prominent peak at around 19.6° 2θ having high intensities of 5670 and 4858, respectively. This peak indicates that the crystallinity of the hydrogel films are mainly influenced by gelatin more than PVA.[52] Also, it specifies the semi crystalline nature of PVA, which comprises both amorphous and crystalline regions. Small crystallites are distributed arbitrarily in the amorphous matrix which is considered as the crystalline phase.[72] Also, a much broader hump was observed at around 40º 2θ at much lower intensities for both the hydrogel films. This peak confirms the presence of PVA in the composite hydrogels.

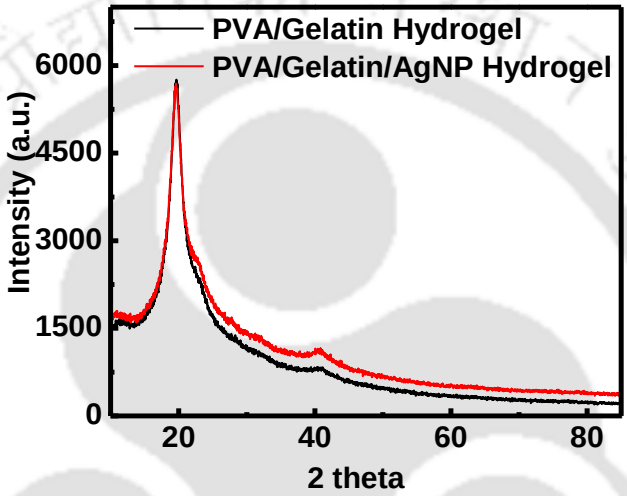

Figure 5.11: X-Ray Diffraction patterns of PVA/Gelatin hydrogel and PVA/gelatin/AgNP hydrogel films.

Table 5.4: Crystalline sizes and percentage crystallinity of the hydrogel films.

Hydrogel samples	Crystalline size(d) nm	Crystallinity (%)
PVA/Gelatin Hydrogel	2.16	79.87
PVA/Gelatin/AgNP Hydrogel	0.27	72.02

For the X-Ray diffraction, d-spacing and crystallinity percentages can be obtained from the 2θ values. The percentage crystallinity decreases from 79.87% to 72.02% after addition of AgNPs into the polymer hydrogel, this may be due to the interaction of Ag ions with the polymer chain, mainly with the hydroxyl groups present in the hydrogel matrix. From figure 5.11, it can be concluded that there is good miscibility between the two polymers which may be due to strong interaction among the intermolecular hydrogen bonds.

5.6.10. Study of Elemental Analysis of the NC Hydrogel via EDX

EDX method mainly focuses on the elemental identification of Ag in the polymer hydrogel matrix. To confirm the presence of AgNPs in the polymer hydrogel system, the EDX analysis was conducted on the PVA/Gelatin nanocomposite hydrogel films. Figure 5.12 represents the elemental distribution of the PVA/gelatin/AgNP hydrogel films. In figure 5.12(i) and (ii) the control (without AgNPs) PVA/Gelatin hydrogel films i.e., 3.5% PVA + 0.5% Gelatin and 3.5% PVA + 1.0% Gelatin comprises of C and O whereas in figure 5.12(ii) and (iv) which represents PVA/Gelatin hydrogel films after addition of 2% AgNPs i.e., 3.5% PVA + 0.5% Gelatin + 2% AgNPs and 3.5% PVA + 1.0% Gelatin + 2% AgNPs comprising of C, O and Ag. Carbon tape was used for mounting the hydrogel films and it justifies the presence of carbon in the elemental analysis. Presence of Ag in the composite hydrogel films was clearly observed from EDX analysis.

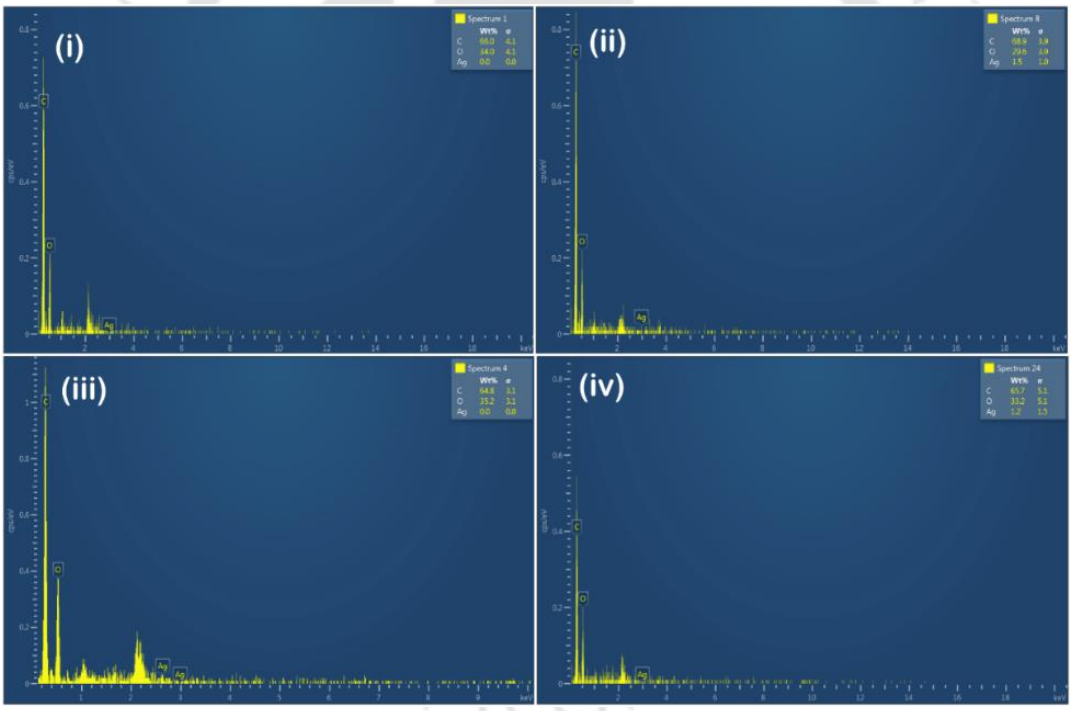

Figure 5.12: EDX analysis of the PVA/Gelatin hydrogel films (i) 3.5% PVA+ 0.5% gelatin (ii) 3.5% PVA + 0.5% gelatin + 2.0% AgNP, (iii) 3.5% PVA+ 1.0% gelatin and (iv) 3.5% PVA + 1.0%gelatin+ 2.0% AgNP

5.6.11. Study of Thermal Property of NC Hydrogel Films

The property of thermal stability is very important in material used for application in biomedical and packaging fields. The thermal analysis of the PVA-gelatin polymeric hydrogel

film and the PVA-gelatin hydrogel nanocomposite films were investigated using a Differential scanning calorimeter (DSC/TGA Analyser). The thermogravimetric analysis TGA includes the measurement of changes in the sample weights over a range of temperatures. The dry hydrogel films were evaluated in a temperature range of 20-600°C and the thermal stabilities of these hydrogels were affected by their molecular weights and a number of different components. Figure 5.13(i) and (ii) show the TG and DSC thermograms for the PVA/gelatin hydrogel film and PVA/gelatin incorporated with AgNPs. Figure 5.13(i) gives the thermo gravimetric analyses of the PVA/gelatin and PVA/gelatin/AgNP hydrogel films. In the hydrogels, two main decomposition steps take place, among them, the initial decomposition temperature was from 100°C to 200°C. Both the hydrogels exhibited small weight loss (3-6%) initially which may be due to water molecule evaporation. PVA/gelation hydrogel showed lesser weight loss at this temperature that may be due to the hydrophobic nature of PVA, and its weight loss started at around 150°C that may be due to the partial bond scission but later recovered at higher temperature by reformation of bonds. TGA curve of the PVA/gelatin/AgNP hydrogel shifted towards a higher temperature compared to the polymer hydrogel blend. Degradation at 270°C (higher temperature) may be due to the intermolecular disintegration and partial breaking of molecular structure. Again, above 380°C the polymeric hydrogel blend decomposes completely to residues, whereas the silver nanoparticle incorporated film showed better thermal stability. Weight loss above 480°C indicated delay of the thermal degradation process. And above 500°C the residual mass was around 8.98% and 9.95% for PVA/gelatin hydrogel and PVA/gelatin/AgNP hydrogel films which is the weight value of carbon and ash after decomposition.

In the DSC thermograms in figure 5.13(ii), the endothermic peaks corresponding to the melting point of PVA was obtained at around 200-230°C. Also, the endothermic peaks corresponding to the glass transition of gelatin was observed in the same range of the melting temperature of PVA. As such, the endothermic peaks of PVA/gelatin hydrogels are considered as the melting temperature of PVA. There are two significant endothermic peaks at around 220°C which is the melting transition peak, and at 330°C indicating the degradation temperature of PVA. The melting transition peaks in the hydrogel films of PVA-gelatin incorporated with AgNPs were observed to be of the intermediate value of the two polymers (PVA and gelatin). The transition width of the AgNP incorporated polymeric hydrogels was similar to that of the PVA and gelatin components.

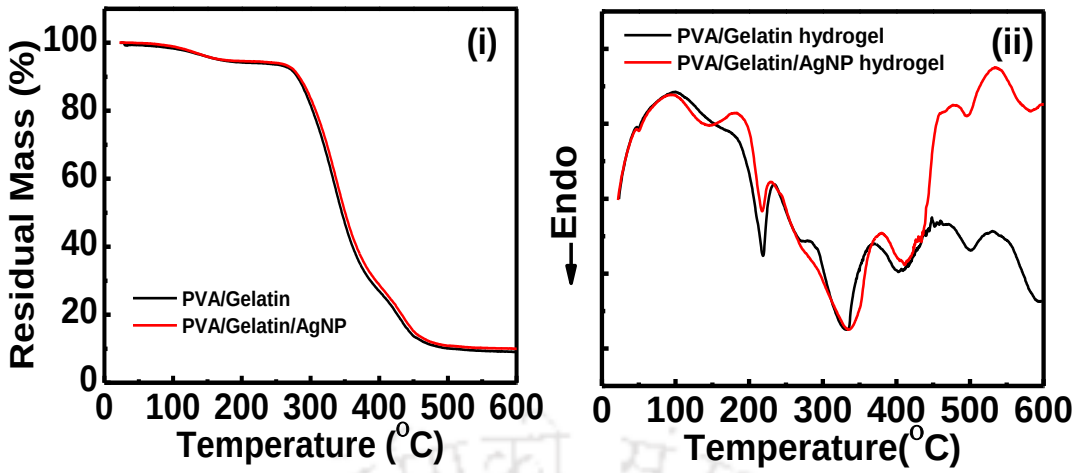

Figure 5.13: (i) Thermal Gravimetric Analysis (TGA) curves of the PVA/Gelatin hydrogel film and silver nanoparticle incorporated PVA/Gelatin hydrogel films. (ii) DSC thermograms for the PVA/Gelatin hydrogel film and silver nanoparticle incorporated PVA/Gelatin hydrogel films.

Incorporation of AgNPs has little significance in the peak shifting, which might indicate higher stability of the PVA-gelatin hydrogel films. Again the addition of AgNPs in the PVA/gelatin hydrogel lowers the melting temperature slightly. The melting endotherm for the PVA/gelatin hydrogel was around 220°C and PVA/gelatin/AgNPs hydrogels was 217°C. There was slight change or lowering of the melting temperature of the AgNPs added polymer hydrogel than the PVA/gelatin control hydrogel but both appears in the region of 200-230°C. This lowering of melting temperature is may be due to the mixing of the three components. The degradation temperature also changes due to the incorporation of AgNPs into the polymeric matrics. The miscibility of both the polymers with AgNPs might be the reason for the depression of the melting temperature and the degradation temperature changes. The decrease of the melting temperature interprets the interaction of the PVA, gelatin and AgNPs, causing strong compatibility among the components and forming a better polymeric hydrogel nanocomposite material.[53,60,72]

5.6.12. Applications of the NC Hydrogel Films

5.6.12.1. Study of Antibacterial Activity of NC Hydrogel Films

The antibacterial activity of the hydrogel films developed using PVA, gelatin and AgNPs were evaluated by the zone of inhibition study by the disc diffusion method. Gram positive, *E. coli* (MTCC strain no. 1696) and gram negative, *S. aureus* (ATCC strain no. 33592) are the

most common bacteria causing a severe infection on the skin and other body soft tissues, which results in the delay of the wound healing process. The zone of inhibitions caused by the hydrogel films against *E. coli* and *S. aureus* after 12 hours are shown in figure 5.14(A). Here, two combinations of the polymer hydrogels i.e., 3.5% PVA + 0.5% gelatin and 3.5% PVA + 1.0 % gelatin hydrogel films were studied. In both cases, the control PVA/gelatin hydrogel films (without AgNPs) showed no zone of inhibition in both E. coli and S. aureus, which means no antibacterial activity was observed in the control hydrogel film combination. The AgNPs loaded hydrogel films showed antibacterial activity against both *E. coli* and *S. aureus* except for hydrogel films with 0.5% AgNP. This may be due to the presence of a low concentration of Ag in the polymer hydrogel.

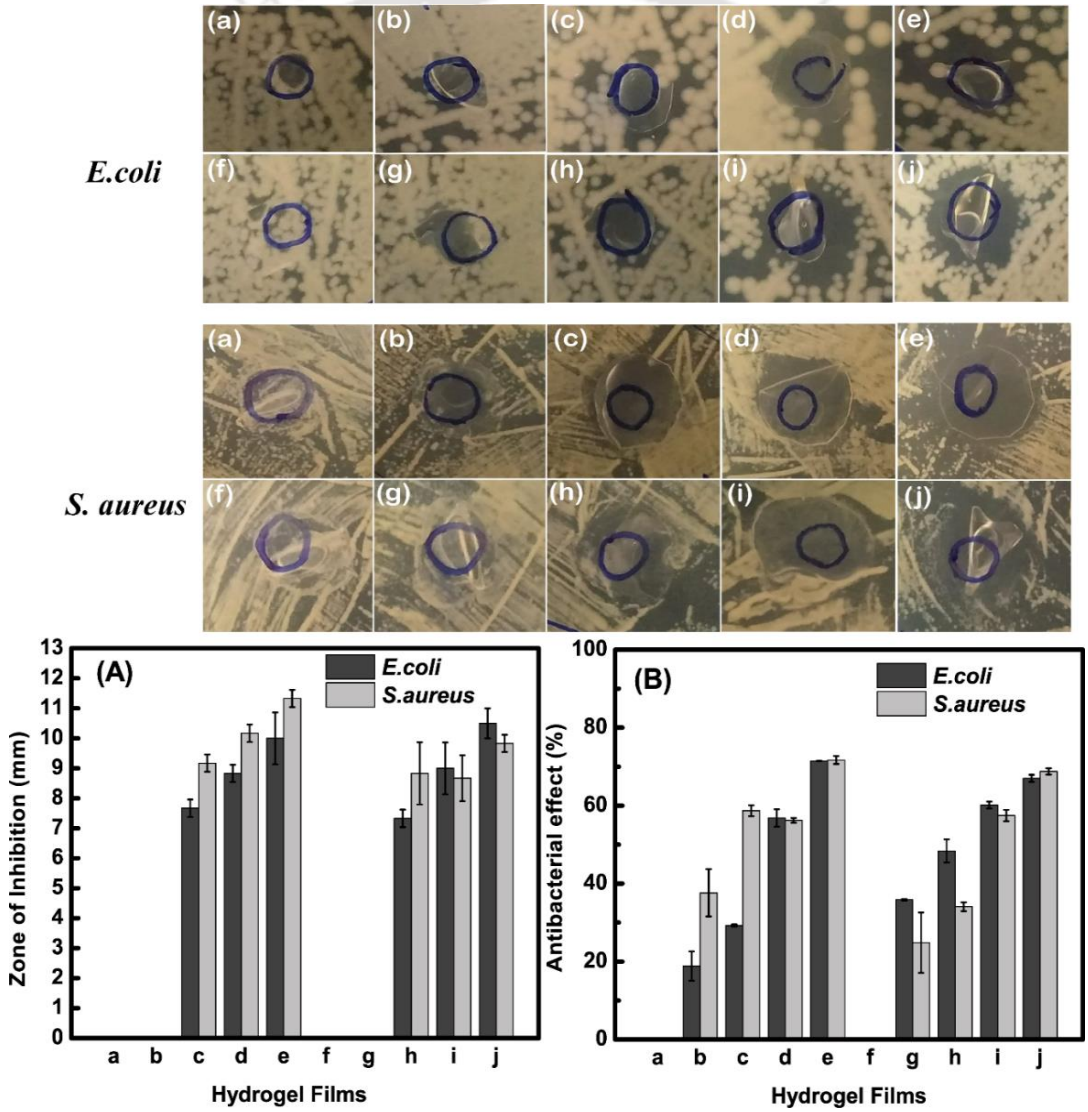

Figure 5.14: Antibacterial activity of the PVA/Gelatin/AgNP hydrogel films(a-j) against *E. coli* and *S. aureus.* (A) Zone of inhibition diameters (mm) of all the combinations(a-j) and (B)

Antibacterial effect (%) of the hydrogel films(a-j). Film no. (e) 3.5% PVA + 0.5% Gelatin + 2% AgNP hydrogel film showed >70 % of antibacterial effect against both *E. coli* and *S. aureus* bacteria.

The PVA/gelatin hydrogel films with 2% AgNPs showed the highest zone of inhibition against both *E.coli* and *S.aureus* among all the other combinations. The 3.5% PVA + 0.5% gelatin + 2% AgNP hydrogel film showed highest zone of inhibition, indicating a good antibacterial activity against *E. coli* as well as *S. aureus*. The inhibition zone basically occurs due to the Ag^+ ions which are released from silver (Ag) particle oxidation in the hydrogel.[73] Bacterial cell division and bacterial respiratory chain damages after moisture contact, which leads to bacterial cell death. PVA/gelatin hydrogel with 2% AgNP can be selected for wound dressings purposes. It showed good antibacterial activity against both *E. coli* and *S. aureus*, among the other hydrogel combinations. Also evaluating the antibacterial effect, 3.5% PVA + 0.5% Gelatin + 2% AgNP hydrogel film showed >70 % of antibacterial effect against both *E. coli* and *S. aureus* bacteria(figure 5.14(B)).

5.6.12.2. Study of Cell Viability of NC Hydrogel Films

To determine the biocompatibility of these AgNPs incorporated PVA/gelatin hydrogel film, the morphology of the BJ human foreskin fibroblast cells was first examined, subjected to exposure with the control polymer hydrogel film and AgNP incorporated hydrogel films. As shown in figure 5.15(A), no significant changes in the morphology of BJ fibroblasts were observed on exposure to these films. Next, its effect on the viability of human cells using MTT assay were analysed. The absorbance was measured at 540 nm, and then a bar graph was plotted (n=3). The BJ fibroblasts were thus exposed with PVA/Gelatin hydrogel film and PVA/Gelatin/AgNP hydrogel film for 24 and 48 hours. Relative to untreated BJ cells, the viability of BJ cells with PVA/Gelatin hydrogel and PVA/Gelatin/AgNP hydrogel films were calculated. There was a slight significant difference after 48 hours in the viability of BJ cells treated with AgNP incorporated hydrogel film (cell viability>67%) than that of the PVA/gelatin hydrogel film (cell viability>59% keeping untreated BJ cells as 100% (Figure 5.15(B)). There is not much difference between the hydrogels with and without AgNPs(60-70% viability levels), and the cell morphology is unchanged from the control untreated cells. The lower MTT measured metabolic level may just mean that the cells are growing slower on the PVA-gelatin matrix hydrogels, which is probably the case because cells generally spread better on stiffer, more hydrophobic culture surfaces. The cells multipled from 24 hours till 48

hours duration, they appeared elongated fibroblast like morphology were seen. Results further confirmed that the AgNP incorporated hydrogel film is non-toxic. Thus, the MTT assay demonstrated the biocompatibility of the AgNP incorporated PVA/Gelatin hydrogel film, which can be used for various biological applications.[60]

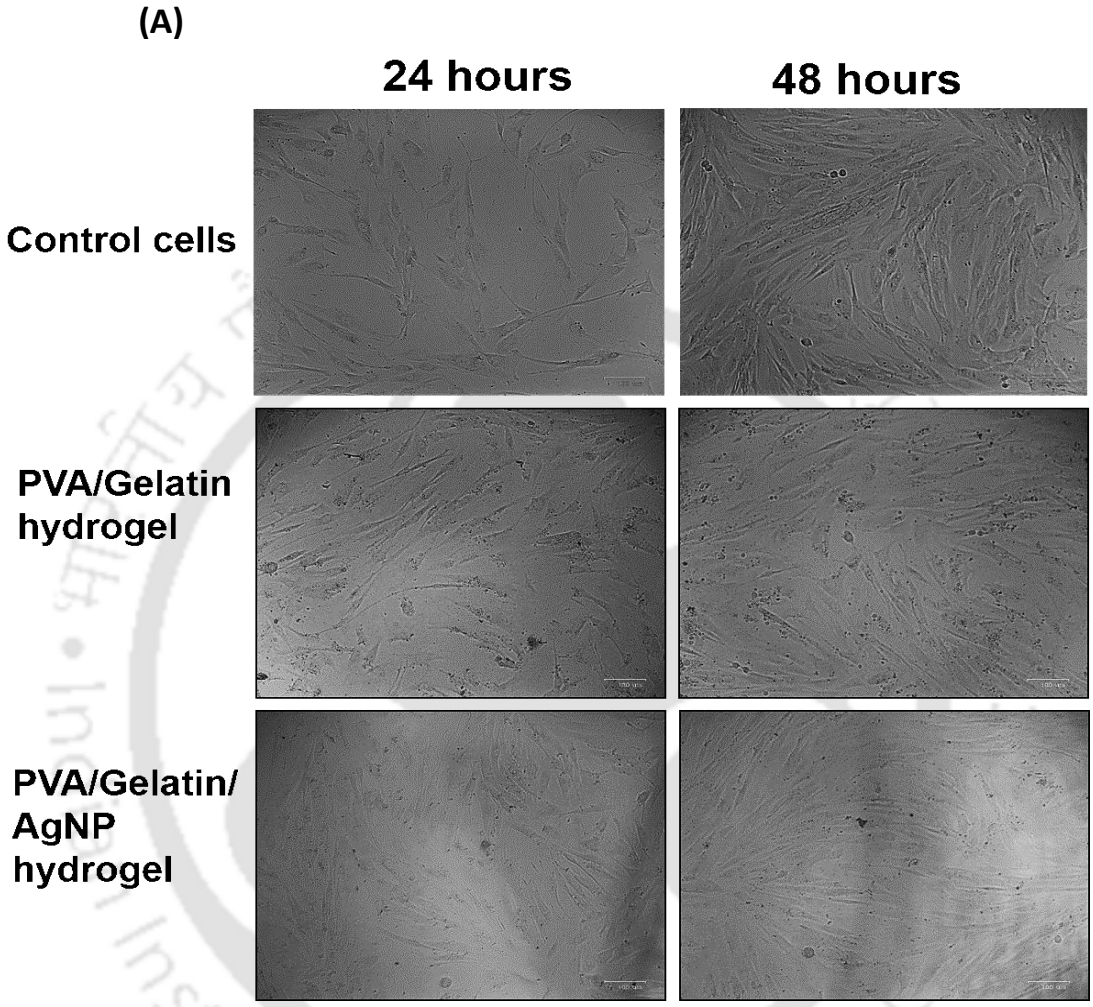

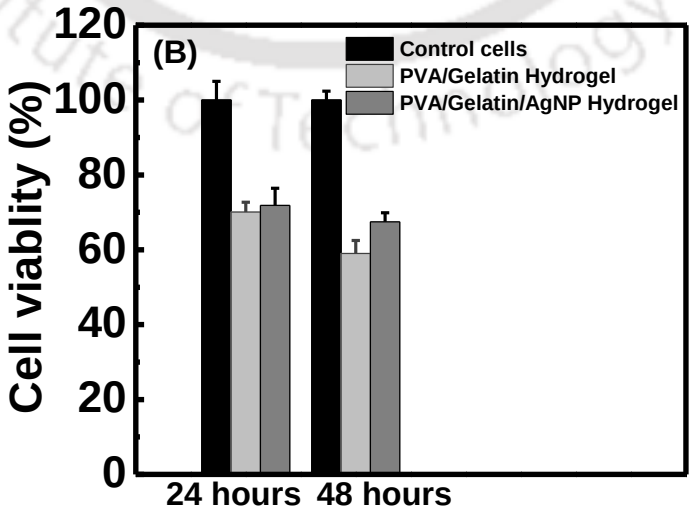

Figure 5.15 (A): Morphology of the BJ fibroblast cells on exposure with the polymer hydrogel films at 24 and 48 hours using an inverted brightfield microscope at 20x magnification. (B) Percentage cell viability of PVA/Gelatin and PVA/Gelatin/AgNP hydrogel film after 24 and 48 hours (keeping control sample at 100%).

5.6.12.3. Study of Wound Healing Property of NC Hydrogel Films *via In vitro* Scratch Wound Healing Analysis

The wound healing property of the biocompatible PVA/Gelatin/AgNP hydrogel film on a monolayer of BJ fibroblast cells was studied by the *in vitro* scratch assay. For this analysis, BJ human foreskin fibroblast cells were used due to their crucial role in cell migration, one of the essential characteristics of scar formation and skin wound healing.[74–76] Also, the synthesis of extracellular matrix and different growth factors occurs, which later contributes to wound healing development.[77] As such, BJ fibroblast cells were used to evaluate the wound closure effects of the PVA/Gelatin/AgNP hydrogel film using *in vitro* scratch assay method. Migration of BJ cells was observed within 6 hours of exposure. The cells migrated towards the centre of the wound area with the PVA/Gelatin/AgNP hydrogel film. For the cells with the PVA/Gelatin hydrogel film(control), no migration was observed even after 6 hours of exposure (Figure 5.16(A)). For both control and AgNPs incorporated hydrogel films, more than 90% of wound closure was seen after 48 hours of exposure and 60-70% after 24 hours. However, we observed a significant difference in the rate of wound closure at 6 and 12 hours between PVA/Gelatin/AgNP hydrogel film and the PVA/Gelatin hydrogel film. PVA/Gelatin/AgNP hydrogel film showed 21.62% wound closure at 6 hours and 47.17% wound closure at 12 hours whereas PVA/Gelatin hydrogel film showed only 4.03% wound closure at 6 hours and 25.17% wound closure at 12 hours(figure 5.16(B)). The wound closure (%) was calculated using Image J software, and a bar graph was plotted (n=2). These results signify that PVA/Gelatin/AgNP hydrogel film has efficient wound healing potential than its counterpart (Figure 5.16(B)).

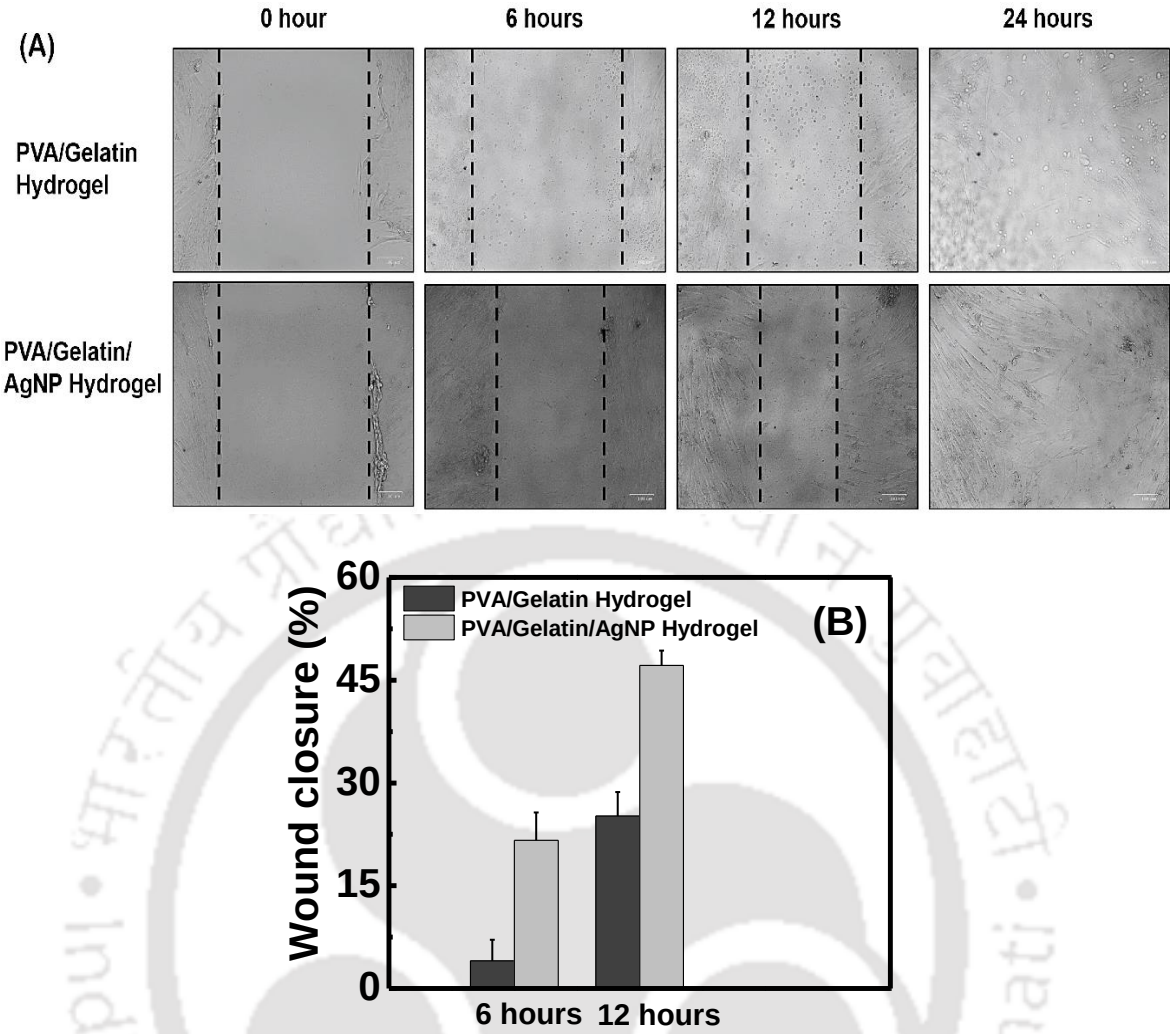

Figure 5.16: (A) Illustrative micrographs of the human cells migrating into a scratch area over 24 hours in PVA/Gelatin(control) and PVA/Gelatin/AgNP hydrogel. (B) The percentage wound closure or the migration rate of the cells in PVA/Gelatin and PVA/Gelatin/AgNP hydrogel films.

5.7. CONCLUSION

A cost-effective and easily usable functional wound dressing nanocomposite-polymer hydrogel-triad was developed by combining polyvinyl alcohol (PVA), gelatin and silver nanoparticles (AgNP). Bhimkol (*Musa balbisiana*) peel extract was used for green synthesis of AgNPs, which acted as the reducing agent and were incorporated into the various combinations of PVA-gelatin hydrogel and developed into hydrogel dressing material for wound healing. The polymer hydrogels have superior crosslinking within their matrices. The incorporation of AgNPs provided better swelling behaviour, mechanical strength and thermal stability to the prepared polymer hydrogel films. Toxicity and antimicrobial assays

demonstrated that the prepared PVA/Gelatin/AgNP hydrogels were non-toxic to human skin cells and exhibited an appropriate antibacterial activity against *E. coli* and *S. aureus*, respectively. The cell viability was more than 90% after 24 and 48 hours for the PVA/Gelatin/AgNP hydrogel. The antibacterial effect was >70% for the PVA/Gelatin hydrogel with 2% AgNP. Wound closure was more than 90% in both control and AgNP incorporated hydrogel films after 24 hours of exposure when evaluated by the scratch assay. PVA/Gelatin/AgNP hydrogel film has a faster cell migration rate than PVA/Gelatin hydrogel film. So, the prepared PVA/Gelatin/AgNP hydrogel film can accelerate the wound healing procedure and have the potential to efficiently protect the wounded skin surface against exudate accumulation, dehydration and prevent bacterial growth and infection.

5.8. EXPERIMENTAL SECTION

5.8.1. Materials and Methods

5.8.1.1. Materials

Poly (vinyl) alcohol i.e., PVA powder was purchased from LOBA Chemicals, India. Its molecular weight is 111,000 g/mol. Gelatin purchased from SRL Pvt. Ltd, India, which could be used without any further purification. Silver nitrate($AgNO_3$) was purchased from Sigma-Aldrich, India. Milli-Q water was used for all the experimental works. Other chemicals, equipments and glassware used were hot plate, magnetic stirrer, magnetic bead, weighing machine, glass beakers, hot air oven, petri dishes, marker pen, acetone, mortar and pestle, hydraulic press, Laminar hood (for antimicrobial works), Bunsen burner, sterile L-spreader, ethanol, tissue paper, incubator, pipette, Eppendorf tube, tweezer, scissor, centrifuge, falcon tubes, micropipette tips, copper-coated TEM grid, carbon tape.

5.8.1.2. Green Synthesis of AgNPs

AgNPs were synthesized via the green route using Bhimkol (*Musa balbisiana*) peel extract with slight modification.[78] Biological reduction of $AgNO_3$ was carried out initially: To optimize the synthesis route for the development of silver nanoparticles (AgNPs), the reaction solution concentrations 1-50% v:v ratio of Banana peel extract: $AgNO_3$ Solution were varied. The reaction mixture was kept in the dark at room temperature to avoid any photoactivation of silver nitrate under inert conditions. Yellowish-brown color was observed after 30 mins indicating the formation of silver nanoparticles. Optimization for the development of AgNPs for different parameters like variation in AgNO3 concentration, time, pH was also reported.[70]

5.8.1.3. Preparation of the Polymer hydrogel nanocomposites

Poly (vinyl) alcohol (PVA) and PVA-gelatin hydrogel films with different concentrations of PVA and gelatin were prepared (% w/w ratio). Solution casting method was used to prepare PVA-gelatin films which is already described above.[53]

5.8.2. Characterizations of the NC Hydrogel Films

5.8.2.1. Swelling Kinetics

The dry hydrogel films were submerged in deionized water and incubated in a water bath at 37°C; then the hydrogel was taken out at regular intervals (after every 30 mins). The hydrogel was dabbed in a tissue cloth to remove excess surface water and then wet hydrogels were weighed until equilibrium was reached.

The water uptake capacity (Wu) was determined by the formula given below:

$$Wu = \frac{Mt - Mg}{Mg} \times 100\%$$

Here, Wu represents the water uptake capacity.

Mt is the weight of the hydrogel at regular time intervals

Mg is the initial weight of the hydrogel.

The water holding performance of these hydrogels was determined by placing the swollen hydrogels at room temperature until they attain a constant weight. Then the hydrogels were weighed at regular intervals of time.[60]

5.8.2.2. Mechanical Properties

Tensile strength of the polymer hydrogel films (control) and the green synthesized AgNPs incorporated polymer hydrogels films were measured by tensile test using a 5kN Electromechanical Universal Testing Machine (UTM). Tensile test was performed on Zwick Roell: Z005TN UTM. The size of the specimen was prepared according to ASTM standards. The hydrogel films were cut into 10 mm×60 mm×1 mm (Width × Height × Thickness) pieces and placed under 5kN load cell, the stretching speed was kept at 10 mm/min at room temperature to measure the tensile strength and the elongation at break.

5.8.2.3. FT-IR Spectroscopy

Fourier Transform Infrared (FT-IR) spectroscopy of the different compositions of the PVA/gelatin/AgNPs hydrogels were verified by ATR-FTIR spectrophotometer in the range of 400-4000 cm^{-1} wavenumbers and with a resolution of 4 cm^{-1}. The mode of spectrum was taken in transmittance mode. FTIR spectroscopy basically characterizes the occurrence of specific functional chemical groups and their interactions. PVA-gelatin cross-linking is easily detected by FTIR analysis.

5.8.2.4. Water Vapour Transmission Rate(WVTR) Analysis

Water vapour transmission rate(WVTR) of the hydrogel films were measured using the ASTM E 96-95 standard method. The device for this experiment was prepared in the laboratory itself. Measuring dishes which were corrosion resistant, airtight and water-resistant was taken. The gap between the liquid level(water) and the specimen (hydrogel films) was about 5±1 mm. The hydrogel film samples were cut into square pieces with a thickness of 1.5 mm approx. and sealed over the opening of dishes making square cut of 20 mm×20 mm in the aluminium foils which were used to cover the dishes. The dishes were filled with 20 mL of distilled water each. The hydrogel films were fastened tightly using tape with aluminum foil to prevent any moisture loss from the sides of the hydrogel films. The initial total weight of the dish, hydrogel film, distilled water was weighed and recorded as W1. This experiment was carried out in an incubator kept at 37°C. After 18 hours and 24 hours intervals, the W2 (final weight) was recorded. The water vapour transmission rate(WVTR) is also called as moisture vapour transmission rate(MVTR), it is be calculated by the following formula:

$$WVTR = \frac{W1 - W2}{T} \times 1000 \times 24$$

Where,

WVTR represents water vapour transmission rate,

W1 represents the initial weight of the dish, hydrogel film and water(g),

W2 represents the final weight of the dish, hydrogel film and water(g) and

T represents the time (hours).[60,79]

5.8.2.5. Contact Angle Measurements Analysis

Quantitative measurement of wetting of a solid by a liquid is referred to as the contact angle (θ, theta) measurement. Angle formed at the three-phase boundary where a liquid, gas or a solid interconnect by the liquid is the contact angle. Wound dressing material of surface having <90° of contact angle is considered ideal as it has a good ability to absorb the wound exudates.[65] Contact angle was measured using a drop shape analyser made by Kruss Company, Germany. The hydrogel films were cut into 10 × 10 mm pieces and placed on the sample holder of the contact angle measurement apparatus. A small drop of distilled water <5 µL was injected into the hydrogel surface by using a micro-syringe. The contact angle was measured at room temperature and three replicates were measured for each hydrogel composition.[66,69]

5.8.2.6. FESEM and EDX Analysis

To obtain the surface morphology of the prepared polymeric hydrogels and the polymeric hydrogel nanocomposite films in higher resolution of imaging Field Emission Scanning Electron Microscopy(FESEM) can be used. Gemini 300 FESEM from CARL ZEISS company was used for both the FESEM and EDX analysis. The FESEM imaging was carried out at resolution of 200 nm and 1 µm scale at 3-4 kV accelerating voltage and at 25 kx - 50kx magnification. Elemental analysis of the hydrogels was also conducted using energy dispersive X-ray spectroscopy. Both qualitative as well as quantitative analysis were performed.

5.8.2.7. FETEM Analysis

Field Emission Transmission Electron Microscopy (FETEM-JEOL 2100F) technique is used for higher resolution imaging of the PVA/gelatin/Ag nanoparticles hydrogel complex. Morphology, size and shape of the nanoparticles, and the polymer blend formation can be easily determined.

5.8.2.8. Thermogravimetric(TG) Analysis

The thermal analysis was performed using a differential scanning calorimeter DSC/TGA analyzer (NETZSCH, STA449F3A00). Around 5.8 mg of the hydrogel film sample was placed into the ceramic crucible and the heating rate was kept at 10°C/min under Argon atmosphere in a temperature range of 20°C-600°C. The thermogravimetric analyser was mainly used for analyzing the chemical structure of the polymer hydrogel film samples.[60]

5.8.2.9. X-Ray Diffraction Analysis

X-Ray Diffraction of the hydrogel films were recorded by using Bruker D8 Advance X-ray diffraction meter (Netherlands) with "Ni-filtered" Cu anode Kα radiation of wavelength λ = 1.54060 Å. The scan was taken at room temperature, in the range of 10-85° of 2θ at a scanning speed of 1°/mm and with step size of 0.05° respectively. The crystalline size is calculated using the following Scherrer equation:

$$D = \frac{k\lambda}{\beta \cos\theta}$$

Where, D is the crystal dimensions, λ is the X-ray wavelength, k is scherrer constant(0.9 rad), β is FWHM (full width at half maximum) and θ is the bragg angle.[53,66]

5.8.2.10. Statistical Analysis

The data were collected in a Microsoft Excel 2016 database and Origin 8.5 software is used for the data analysis and graph preparation. All the experiments were carried out in triplicate and the results are expressed as mean ± standard deviation (SD). Two-way ANOVA was applied to determine whether the results have significant variations and a P-value ≤ 0.05 was considered acceptable or statistically significant.

5.8.3. Applications of the NC Hydrogel Films

5.8.3.1. Antibacterial Properties

Antibacterial activity of the polymer nanocomposite hydrogels prepared from PVA, gelatin and AgNPs was evaluated by the disc diffusion method against a gram-negative bacteria, *E.coli* (1969) and gram-positive bacteria, *S.aureus* (ATCC33592). Initially, 100 µL of the bacterial (*E.coli* and *S.aureus*) suspension(10^8 CFU/mL) was spread on LB(Luria-Bertini) agar plates. The hydrogel film samples were evenly punched into circular discs of 5 mm diameter and placed on the surface of the LB agar plates. Then the plates were incubated at 37°C for 12 hours, the diameter of zone of inhibition formed around the samples were measured.[73] 100 mg of the hydrogel films were added to 2 ml of bacterial culture suspensions (*E. coli* and *S. aureus*) each and incubated for 12 hours at 37°C in a shaker incubator (180 rpm). Then, optical density (O.D) was measured at 600 nm and CFU/mL was counted for all the samples. The antibacterial effect was evaluated by using the following equation:

$$\% \text{ AE} = ((C-H)/C) \times 100$$

Where, AE is the antibacterial effect, C is the number of bacteria on the surface of the control sample and H is the number of bacteria on the surface of the hydrogel film samples.[66]

5.8.3.2. Cell Viability Assay

BJ normal human foreskin fibroblasts (ATCC catalog CRL-2522) were cultured in Dulbecco's Modified Eagle Medium (DMEM, GIBCO) supplemented with 10% Fetal Bovine Serum (FBS, GIBCO), 1% non-essential amino acids (NEAA; GIBCO) and Penicillin-Streptomycin solution (GIBCO; 100 U/ml penicillin and 100 µg/ml streptomycin). Cells were maintained in a humidified atmosphere of 5% CO_2 at 37°C in a CO_2 incubator (Eppendorf). In all experiments, the medium was changed every second day with complete media.

Cell viability assay was performed using 3-(4,5-dimethylthiazol-2-yl)-2,5-diphenyl-2H-tetrazolium bromide (MTT) as described previously.[80] Briefly, BJ human foreskin fibroblast cells were seeded in a 96-well flat-bottomed plate at a density of 4×10^4 cells per well and incubated for 24 hours in complete media in a CO_2 incubator. Thereafter, cells were incubated with PVA/Gelatin(Control) and PVA/Gelatin/AgNP hydrogel film of 5 mm diameter(circular) for 24 and 48 hours. The medium was discarded after the treatment and cells were treated with MTT (0.5 mg/ml) for 2 hours at 37°C in a CO_2 incubator. Purple-colored formazan crystals were formed, which were then dissolved in dimethyl sulfoxide. Cell viability (%) was finally measured using a multi-plate reader (Multiscan GO, Thermo Scientific) at 540 nm.

5.8.3.3. *In Vitro* Scratch Wound Healing Assay

To study in vitro collective cell migration, the scratch assay, also known as wound healing assay, is one of the most used technique.[81] BJ normal human foreskin cells were seeded in a 12-well plate at a density of 1×10^5 cells/well in the complete growth medium and then grown to full confluency. The fully confluent monolayers were scratched with a 20µL sterile pipette tip and the media was aspirated out, followed by a rinse with PBS. Scratched monolayers were incubated in standard cell culture conditions with circular PVA/Gelatin(Control) and PVA/Gelatin/AgNP hydrogel films (about 17 mm diameter) in complete growth medium for 24 hours. Images were captured at different time intervals using an inverted brightfield microscope (ZOE Fluorescent Cell Imager, Bio-Rad) at 20x magnification. The migration efficiency was analyzed using ImageJ (1.48v) software.

5.9. REFERENCES

(1) Saini, K. Preparation Method, Properties and Crosslinking of Hydrogel: A Review. *PharmaTutor* **2017**, *5* (1), 27–36.

(2) Barrett-Catton, E.; Ross, M. L.; Asuri, P. Multifunctional Hydrogel Nanocomposites for Biomedical Applications. *Polymers (Basel).* **2021**, *13* (6), 856.

(3) Biondi, M.; Borzacchiello, A.; Mayol, L.; Ambrosio, L. Nanoparticle-Integrated Hydrogels as Multifunctional Composite Materials for Biomedical Applications. *Gels* **2015**, *1* (2), 162–178.

(4) Thoniyot, P.; Tan, M. J.; Karim, A. A.; Young, D. J.; Loh, X. J. Nanoparticle-Hydrogel Composites: Concept, Design, and Applications of These Promising, Multi-Functional Materials. *Adv. Sci.* **2015**, *2* (1–2), 1–13.

(5) Satarkar, N. S.; Biswal, D.; Hilt, J. Z. Hydrogel Nanocomposites: A Review of Applications as Remote Controlled Biomaterials. *Soft Matter* **2010**, *6* (11), 2364–2371.

(6) Schexnailder, P.; Schmidt, G. Nanocomposite Polymer Hydrogels. *Colloid Polym. Sci.* **2009**, *287* (1), 1–11.

(7) Gaharwar, A. K.; Peppas, N. A.; Khademhosseini, A. Nanocomposite Hydrogels for Biomedical Applications. *Biotechnol. Bioeng.* **2014**, *111* (3), 441–453.

(8) Sershen, S. R.; Westcott, S. L.; Halas, N. J.; West, J. L. Independent Optically Addressable Nanoparticle-Polymer Optomechanical Composites. *Appl. Phys. Lett.* **2002**, *80* (24), 4609–4611.

(9) Pardo-Yissar, V.; Gabai, R.; Shipway, A. N.; Bourenko, T.; Willner, I. Gold Nanoparticle/Hydrogel Composites with Solvent-Switchable Electronic Properties. *Adv. Mater.* **2001**, *13* (17), 1320–1323.

(10) Wang, C.; Flynn, N. T.; Langer, R. Controlled Structure and Properties of Thermoresponsive Nanoparticle–Hydrogel Composites. *Adv. Mater.* **2004**, *16* (13), 1074–1079.

(11) Castaneda, L.; Valle, J.; Yang, N.; Pluskat, S.; Slowinska, K. Collagen Cross-Linking with Au Nanoparticles. *Biomacromolecules* **2008**, *9* (12), 3383–3388.

(12) Wu, H.; Yu, G.; Pan, L.; Liu, N.; McDowell, M. T.; Bao, Z.; Cui, Y. Stable Li-Ion Battery Anodes by in-Situ Polymerization of Conducting Hydrogel to Conformally Coat Silicon Nanoparticles. *Nat. Commun.* **2013**, *4* (1), 1943.

(13) Caló, E.; Khutoryanskiy, V. V. Biomedical Applications of Hydrogels: A Review of Patents and Commercial Products. *Eur. Polym. J.* **2015**, *65*, 252–267.

(14) Haraguchi, K.; Li, H.-J. Mechanical Properties and Structure of Polymer−Clay Nanocomposite Gels with High Clay Content. *Macromolecules* **2006**, *39* (5), 1898–1905.

(15) Haraguchi, K.; Song, L. Microstructures Formed in Co-Cross-Linked Networks and Their Relationships to the Optical and Mechanical Properties of PNIPA/Clay Nanocomposite Gels. *Macromolecules* **2007**, *40* (15), 5526–5536.

(16) Zaragoza, J.; Babhadiashar, N.; O'Brien, V.; Chang, A.; Blanco, M.; Zabalegui, A.; Lee, H.; Asuri, P. Experimental Investigation of Mechanical and Thermal Properties of Silica Nanoparticle-Reinforced Poly(Acrylamide) Nanocomposite Hydrogels. *PLoS One* **2015**, *10* (8), e0136293.

(17) Zaragoza, J.; Fukuoka, S.; Kraus, M.; Thomin, J.; Asuri, P. Exploring the Role of Nanoparticles in Enhancing Mechanical Properties of Hydrogel Nanocomposites. *Nanomaterials(Basel)* **2018**, *8* (11), 882.

(18) Betsch, M.; Cristian, C.; Lin, Y.-Y.; Blaeser, A.; Schöneberg, J.; Vogt, M.; Buhl, E. M.; Fischer, H.; Duarte Campos, D. F. Incorporating 4D into Bioprinting: Real-Time Magnetically Directed Collagen Fiber Alignment for Generating Complex Multilayered Tissues. *Adv. Healthc. Mater.* **2018**, *7* (21), 1800894.

(19) Haraguchi, K.; Murata, K.; Takehisa, T. Stimuli-Responsive Nanocomposite Gels and Soft Nanocomposites Consisting of Inorganic Clays and Copolymers with Different Chemical Affinities. *Macromolecules* **2012**, *45* (1), 385–391.

(20) Oh, Y.; Islam, M. F. Preformed Nanoporous Carbon Nanotube Scaffold-Based Multifunctional Polymer Composites. *ACS Nano* **2015**, *9* (4), 4103–4110.

(21) Nair, L. S.; Laurencin, C. T. Silver Nanoparticles: Synthesis and Therapeutic Applications. *J. Biomed. Nanotechnol.* **2007**, *3* (4), 301–316.

(22) Barani, H.; Montazer, M.; Samadi, N.; Toliyat, T. In Situ Synthesis of Nano Silver/Lecithin on Wool: Enhancing Nanoparticles Diffusion. *Colloids Surf. B. Biointerfaces* **2012**, *92*, 9–15.

(23) Dakal, T. C.; Kumar, A.; Majumdar, R. S.; Yadav, V. Mechanistic Basis of Antimicrobial Actions of Silver Nanoparticles. *Front. Microbiol.* **2016**, *7* (NOV), 1–17.

(24) Moritz, M.; Geszke-Moritz, M. The Newest Achievements in Synthesis, Immobilization and Practical Applications of Antibacterial Nanoparticles. *Chem. Eng. J.* **2013**, *228*, 596–613.

(25) Bardajee, G. R.; Hooshyar, Z.; Rezanezhad, H. A Novel and Green Biomaterial Based Silver Nanocomposite Hydrogel: Synthesis, Characterization and Antibacterial Effect.

J. Inorg. Biochem. **2012**, *117*, 367–373.

(26) Murali Mohan, Y.; Lee, K.; Premkumar, T.; Geckeler, K. E. Hydrogel Networks as Nanoreactors: A Novel Approach to Silver Nanoparticles for Antibacterial Applications. *Polymer (Guildf).* **2007**, *48* (1), 158–164.

(27) Vimala, K.; Samba Sivudu, K.; Murali Mohan, Y.; Sreedhar, B.; Mohana Raju, K. Controlled Silver Nanoparticles Synthesis in Semi-Hydrogel Networks of Poly(Acrylamide) and Carbohydrates: A Rational Methodology for Antibacterial Application. *Carbohydr. Polym.* **2009**, *75* (3), 463–471.

(28) Juby, K. A.; Dwivedi, C.; Kumar, M.; Kota, S.; Misra, H. S.; Bajaj, P. N. Silver Nanoparticle-Loaded PVA/Gum Acacia Hydrogel: Synthesis, Characterization and Antibacterial Study. *Carbohydr. Polym.* **2012**, *89* (3), 906–913.

(29) Luo, R.-C.; Lim, Z. H.; Li, W.; Shi, P.; Chen, C.-H. Near-Infrared Light Triggerable Deformation-Free Polysaccharide Double Network Hydrogels. *Chem. Commun.* **2014**, *50* (53), 7052–7055.

(30) Gunasekaran, T.; Nigusse, T.; Dhanaraju, M. D. Silver Nanoparticles as Real Topical Bullets for Wound Healing. *J. Am. Coll. Clin. Wound Spec.* **2011**, *3* (4), 82–96.

(31) Klasen, H. J. A Historical Review of the Use of Silver in the Treatment of Burns. II. Renewed Interest for Silver. *Burns* **2000**, *26* (2), 131–138.

(32) Patra, C. R.; Bhattacharya, R.; Wang, E.; Katarya, A.; Lau, J. S.; Dutta, S.; Muders, M.; Wang, S.; Buhrow, S. A.; Safgren, S. L.; Yaszemski, M. J.; Reid, J. M.; Ames, M. M.; Mukherjee, P.; Mukhopadhyay, D. Targeted Delivery of Gemcitabine to Pancreatic Adenocarcinoma Using Cetuximab as a Targeting Agent. *Cancer Res.* **2008**, *68* (6), 1970–1978.

(33) Parmar, H. S.; Kar, A. Medicinal Values of Fruit Peels from *Citrus sinensis*, *Punica granatum*, and *Musa paradisiaca* with Respect to Alterations in Tissue Lipid Peroxidation and Serum Concentration of Glucose, Insulin, and Thyroid Hormones. *J. Med. Food* **2008**, *11* (2), 376–381.

(34) Castillo, P. M.; Herrera, J. L.; Fernandez-Montesinos, R.; Caro, C.; Zaderenko, A. P.; Mejías, J. A.; Pozo, D. Tiopronin Monolayer-Protected Silver Nanoparticles Modulate IL-6 Secretion Mediated by Toll-like Receptor Ligands. *Nanomedicine (Lond).* **2008**, *3* (5), 627–635.

(35) Boucher, W.; Stern, J. M.; Kotsinyan, V.; Kempuraj, D.; Papaliodis, D.; Cohen, M. S.; Theoharides, T. C. Intravesical Nanocrystalline Silver Decreases Experimental Bladder Inflammation. *J. Urol.* **2008**, *179* (4), 1598–1602.

(36) Yang, W.; Shen, C.; Ji, Q.; An, H.; Wang, J.; Liu, Q.; Zhang, Z. Food Storage Material Silver Nanoparticles Interfere with DNA Replication Fidelity and Bind with DNA. *Nanotechnology* **2009**, *20* (8), 85102.

(37) Lansdown, A. B. G. Silver. I: Its Antibacterial Properties and Mechanism of Action. *J. Wound Care* **2002**, *11* (4), 125–130.

(38) Shrivastava, S.; Bera, T.; Roy, A.; Singh, G.; Ramachandrarao, P.; Dash, D. Characterization of Enhanced Antibacterial Effects of Novel Silver Nanoparticles. *Nanotechnology* **2007**, *18* (22), 225103.

(39) Beddy, D.; Watson, R. W. G.; Fitzpatrick, J. M.; O'Connell, P. R. Increased Vascular Endothelial Growth Factor Production in Fibroblasts Isolated from Strictures in Patients with Crohn's Disease. *Br. J. Surg.* **2004**, *91* (1), 72–77.

(40) Kim, J. S.; Kuk, E.; Yu, K. N.; Kim, J.-H.; Park, S. J.; Lee, H. J.; Kim, S. H.; Park, Y. K.; Park, Y. H.; Hwang, C.-Y.; Kim, Y.-K.; Lee, Y.-S.; Jeong, D. H.; Cho, M.-H. Antimicrobial Effects of Silver Nanoparticles. *Nanomedicine* **2007**, *3* (1), 95–101.

(41) Pissuwan, D.; Valenzuela, S. M.; Miller, C. M.; Cortie, M. B. A Golden Bullet? Selective Targeting of *Toxoplasma gondii* Tachyzoites Using Antibody-Functionalized Gold Nanorods. *Nano Lett.* **2007**, *7* (12), 3808–3812.

(42) Kokabi, M.; Sirousazar, M.; Hassan, Z. PV-Clay Nanocomposite Hydrogels for Wound Dressing. *Eur. Polym. J.* **2007**, *43*, 773–781.

(43) Lansdown, A. B. G. Silver. 2: Toxicity in Mammals and How Its Products Aid Wound Repair. *J. Wound Care* **2002**, *11* (5), 173–177.

(44) Maneerung, T.; Tokura, S.; Rujiravanit, R. Impregnation of Silver Nanoparticles into Bacterial Cellulose for Antimicrobial Wound Dressing. *Carbohydr. Polym.* **2008**, *72* (1), 43–51.

(45) Lu, S.; Gao, W.; Gu, H. Y. Construction, Application and Biosafety of Silver Nanocrystalline Chitosan Wound Dressing. *Burns* **2008**, *34* (5), 623–628.

(46) Moore, K. W.; O'Garra, A.; Malefyt, R. W.; Vieira, P.; Mosmann, T. R. Interleukin-10. *Annual Review of Immunology*. Annual Reviews April 1, 1993, pp 165–190.

(47) Tian, J.; Wong, K. K. Y.; Ho, C. M.; Lok, C. N.; Yu, W. Y.; Che, C. M.; Chiu, J. F.; Tam, P. K. H. Topical Delivery of Silver Nanoparticles Promotes Wound Healing. *ChemMedChem* **2007**, *2* (1), 129–136.

(48) Wong, K. K. Y.; Cheung, S. O. F.; Huang, L.; Niu, J.; Tao, C.; Ho, C.-M.; Che, C.-M.; Tam, P. K. H. Further Evidence of the Anti-Inflammatory Effects of Silver Nanoparticles. *ChemMedChem* **2009**, *4* (7), 1129–1135.

(49) Liu, X.; Lee, P.-Y.; Ho, C.-M.; Lui, V. C. H.; Chen, Y.; Che, C.-M.; Tam, P. K. H.; Wong, K. K. Y. Silver Nanoparticles Mediate Differential Responses in Keratinocytes and Fibroblasts during Skin Wound Healing. *ChemMedChem* **2010**, *5* (3), 468–475.

(50) Nešović, K.; Janković, A.; Kojić, V.; Vukašinović-Sekulić, M.; Perić-Grujić, A.; Rhee, K. Y.; Mišković-Stanković, V. Silver/Poly(Vinyl Alcohol)/Chitosan/Graphene Hydrogels – Synthesis, Biological and Physicochemical Properties and Silver Release Kinetics. *Compos. Part B Eng.* **2018**, *154* (July), 175–185.

(51) Koehler, J.; Brandl, F. P.; Goepferich, A. M. Hydrogel Wound Dressings for Bioactive Treatment of Acute and Chronic Wounds. *Eur. Polym. J.* **2018**, *100* (January), 1–11.

(52) Pal, K.; Banthia, A.; Majumdar, D. K. Preparation and Characterization of Polyvinyl Alcohol – Gelatin Hydrogel Membranes for Biomedical Applications. *AAPS PharmSciTech* **2007**, *8* (1), 142–146.

(53) Pawde, S. M.; Deshmukh, K. Characterization of Polyvinyl Alcohol / Gelatin Blend Hydrogel Films for Biomedical Applications. *J. Appl. Polym. Sci.* **2008**, *109* (March), 3431–3437.

(54) Neumann, P. M.; Zur, B.; Ehrenreich, Y. Gelatin-Based Sprayable Foam as a Skin Substitute. *J. Biomed. Mater. Res.* **1981**, *15* (1), 9–18.

(55) Takahashi, H.; Miyoshi, T.; Boki, K. Study on Hydrophilic Properties of Gelatin as a Clinical Wound Dressing. II. Water-Absorbing Property and Hemostatic Effect of Gelatin. *Tokushima J. Exp. Med.* **1993**, *40* (3–4), 169–175.

(56) Oakenfull, D.; Scott, A. Gelatin Gels in Deuterium Oxide. *Food Hydrocoll.* **2003**, *17* (2), 207–210.

(57) Morones, J. R.; Elechiguerra, J. L.; Camacho, A.; Ramirez, J. T. The Bactericidal Effect of Silver Nanoparticles. *Nanotechnology* **2005**, *16* (2346), 53.

(58) Shankar, S.; Jaiswal, L.; Aparna, R. S. L.; Vara Prasad, R. G. S.; Kumar, G. P.; Manohara, C. M. Wound Healing Potential of Green Synthesized Silver Nanoparticles Prepared from *Lansium domesticum* Fruit Peel Extract. *Mater. Express* **2015**, *5* (2), 159–164.

(59) Shankar, S.; Rhim, J.-W. Amino Acid Mediated Synthesis of Silver Nanoparticles and Preparation of Antimicrobial Agar/Silver Nanoparticles Composite Films. *Carbohydr. Polym.* **2015**, *130*, 353–363.

(60) Pan, H.; Fan, D.; Cao, W.; Zhu, C.; Duan, Z.; Fu, R. Preparation and Characterization of Breathable Hemostatic Hydrogel Dressings and Determination of Their Effects on Full-Thickness Defects. *Polymer(Basel)* **2017**, *9* (12), 727.

(61) Imtiaz, N.; Niazi, M. B. K.; Fasim, F.; Khan, B. A.; Bano, S. A.; Shah, G. M.; Badshah, M.; Menaa, F.; Uzair, B. Fabrication of an Original Transparent PVA/Gelatin Hydrogel: In Vitro Antimicrobial Activity against Skin Pathogens. *Int. J. Polym. Sci.* **2019**, *2019* (7651810), 1–11.

(62) Fan, L.; Yang, H.; Yang, J.; Peng, M.; Hu, J. Preparation and Characterization of Chitosan/Gelatin/PVA Hydrogel for Wound Dressings. *Carbohydr. Polym.* **2016**, *146*, 427–434.

(63) Sarwar, M. S.; Bilal, M.; Niazi, K.; Jahan, Z.; Ahmad, T.; Hussain, A. Preparation and Characterization of PVA/Nanocellulose/Ag Nanocomposite Films for Antimicrobial Food Packaging. *Carbohydr. Polym.* **2018**, *184* (March), 453–464.

(64) Li, R.; Fei, J.; Cai, Y.; Li, Y.; Feng, J.; Yao, J. Cellulose Whiskers Extracted from Mulberry: A Novel Biomass Production. *Carbohydr. Polym.* **2009**, *76* (1), 94–99.

(65) Morgado, P. I.; Aguiar-Ricardo, A.; Correia, I. J. Asymmetric Membranes as Ideal Wound Dressings: An Overview on Production Methods, Structure, Properties and Performance Relationship. *J. Memb. Sci.* **2015**, *490*, 139–151.

(66) Khorasani, M. T.; Joorabloo, A.; Moghaddam, A.; Shamsi, H.; MansooriMoghadam, Z. Incorporation of ZnO Nanoparticles into Heparinised Polyvinyl Alcohol/Chitosan Hydrogels for Wound Dressing Application. *Int. J. Biol. Macromol.* **2018**, *114* (October), 1203–1215.

(67) Masood, N.; Ahmed, R.; Tariq, M.; Ahmed, Z.; Masoud, M. S.; Ali, I.; Asghar, R.; Andleeb, A.; Hasan, A. Silver Nanoparticle Impregnated Chitosan-PEG Hydrogel Enhances Wound Healing in Diabetes Induced Rabbits. *Int. J. Pharm.* **2019**, *559* (August 2018), 23–36.

(68) Dubey, P.; Bhushan, B.; Sachdev, A.; Matai, I.; Uday Kumar, S.; Gopinath, P. Silver-Nanoparticle-Incorporated Composite Nanofibers for Potential Wound-Dressing Applications. *J. Appl. Polym. Sci.* **2015**, *132* (35), 1–12.

(69) Noshirvani, N.; Ghanbarzadeh, B.; Mokarram, R. R.; Hashemi, M.; Coma, V. Preparation and Characterization of Active Emulsified Films Based on Chitosan-Carboxymethyl Cellulose Containing Zinc Oxide Nano Particles. *Int. J. Biol. Macromol.* **2017**, *99*, 530–538.

(70) Bag, S. S.; Bora, A.; Golder, A. Biomimetic Synthesis of Silver Nanoparticles Using Bhimkol (*Musa balbisiana*) Peel Extract as Biological Waste : Its Antibacterial Activity and Role of Ripen Stage of the Peel. *Curr. Nanomater.* **2020**, *5* (1), 47–65.

(71) Nguyen, T. D.; Nguyen, T. T.; Ly, K. L.; Tran, A. H.; Nguyen, T. T. N.; Vo, M. T.; Ho,

H. M.; Dang, N. T. N.; Vo, V. T.; Nguyen, D. H.; Nguyen, T. T. H.; Nguyen, T. H. In Vivo Study of the Antibacterial Chitosan/Polyvinyl Alcohol Loaded with Silver Nanoparticle Hydrogel for Wound Healing Applications. *International Journal of Polymer Science*. 2019, p 7382717.

(72) Pawde, S. M.; Deshmukh, K.; Parab, S. Preparation and Characterization of Poly(Vinyl Alcohol) and Gelatin Blend Films. *J. Appl. Polym. Sci.* **2008**, *109*, 1328–1337.

(73) Chalitangkoon, J.; Wongkittisin, M.; Monvisade, P. Silver Loaded Hydroxyethylacryl Chitosan/Sodium Alginate Hydrogel Films for Controlled Drug Release Wound Dressings. *Int. J. Biol. Macromol.* **2020**, *159*, 194–203.

(74) Vittorazzi, C.; Endringer, D. C.; Andrade, T. U. de; Scherer, R.; Fronza, M. Antioxidant, Antimicrobial and Wound Healing Properties of Struthanthus Vulgaris. *Pharm. Biol.* **2016**, *54* (2), 331–337.

(75) Reinke, J. M.; Sorg, H. Wound Repair and Regeneration. *Eur. Surg. Res. Eur. Chir. Forschung. Rech. Chir. Eur.* **2012**, *49* (1), 35–43.

(76) Eming, S. A.; Martin, P.; Tomic-Canic, M. Wound Repair and Regeneration: Mechanisms, Signaling, and Translation. *Sci. Transl. Med.* **2014**, *6* (265), 265sr6.

(77) Barrientos, S.; Stojadinovic, O.; Golinko, M. S.; Brem, H.; Tomic-Canic, M. Growth Factors and Cytokines in Wound Healing. *Wound repair Regen. Off. Publ. Wound Heal. Soc. Eur. Tissue Repair Soc.* **2008**, *16* (5), 585–601.

(78) Kokila, T.; Ramesh, P. S.; Geetha, D. Biosynthesis of Silver Nanoparticles from Cavendish Banana Peel Extract and Its Antibacterial and Free Radical Scavenging Assay: A Novel Biological Approach. *Appl. Nanosci.* **2015**, *5* (8), 911–920.

(79) Jiang, Y.; Hou, Y.; Fang, J.; Liu, W.; Zhao, Y.; Huang, T.; Cui, J.; Yang, Y.; Zhou, Z. Preparation and Characterization of PVA/SA/HA Composite Hydrogels for Wound Dressing. *Int. J. Polym. Anal. Charact.* **2019**, *24* (2), 132–141.

(80) Haridhasapavalan, K. K.; Sundaravadivelu, P. K.; Bhattacharyya, S.; Ranjan, S. H.; Raina, K.; Thummer, R. P. Generation of Cell - Permeant Recombinant Human Transcription Factor GATA4 from *E coli*. *Bioprocess Biosyst. Eng.* **2021**, *137* (2), e11-e16.

(81) Alavarse, A. C.; de Oliveira Silva, F. W.; Colque, J. T.; da Silva, V. M.; Prieto, T.; Venancio, E. C.; Bonvent, J. J. Tetracycline Hydrochloride-Loaded Electrospun Nanofibers Mats Based on PVA and Chitosan for Wound Dressing. *Mater. Sci. Eng. C* **2017**, *77*, 271–281.

SUMMARY AND OUTLOOK

Summary and Thesis Outlook

This dissertation entitled, "**Studies on the Green Synthesis of Silver Nanoparticles and their Utilization on the Development of Polymer Nanocomposites for Water Disinfection and Wound Healing Applications,"** contains a total of 5 chapters, including one Introduction Chapter (Chapter 1). Each chapter has its individual introduction, objectives, results and discussion and reference sections. **Chapter 1** is a review chapter that contains a general overview of nanotechnology, nanomaterials and a concise history of nanoparticles. This chapter also provides an overview of the various methods, including conventional and environmentally friendly (green) synthesis of silver nanoparticles (AgNPs). It briefly discusses the multiple diverse applications of AgNPs, which are impactful in various sectors. Although there are a lot of applications of AgNPs, mostly those AgNPs have been synthesized using chemical reduction or other conventional methods. So, to counter the expense of various stabilizing and reducing agents and toxic chemicals, more emphasis has to be provided on the use of green synthesis to develop multiple applications. Bio-renewable sources like plant extracts and agro-waste are used instead of the conventional chemicals and reagents, making the synthesis process much simple and easy.

Chapter 2 elaborates an environment-friendly and cost-effective synthesis of silver nanoparticles (AgNPs) using widely available agro waste, the peels of Bhimkol, an indigenous banana variety of Assam, Northeast India. Aqueous extract of Bhimkol (*Musa balbisiana*) peels acts as bioreductant and stabilizing agent for the preparation of AgNPs from silver nitrate. Apart from the synthesis of AgNPs, the phytochemicals properties of the three-stage development of the bhimkol peels are also studied. The synthesized AgNPs shows good antibacterial activities for further applications in healthcare, packaging or water treatment.

Chapter 3 also describes a cost-effective green synthesis method for silver nanoparticles (AgNPs) using Chayote squash (*Sechium edule*) vegetable aqueous extract. Squash or chayote is widely available and has medicinal properties. It acts as both reducing and stabilizing agents for AgNP synthesis. AgNPs generated showed good antibacterial and antifungal activities as was observed in the disc diffusion method. Furthermore, the green synthesized AgNPs showed good catalytic activity towards the reduction of methylene blue dye through an electron relay process.

DIAGRAMMATIC REPRESENTATION OF THESIS WORK

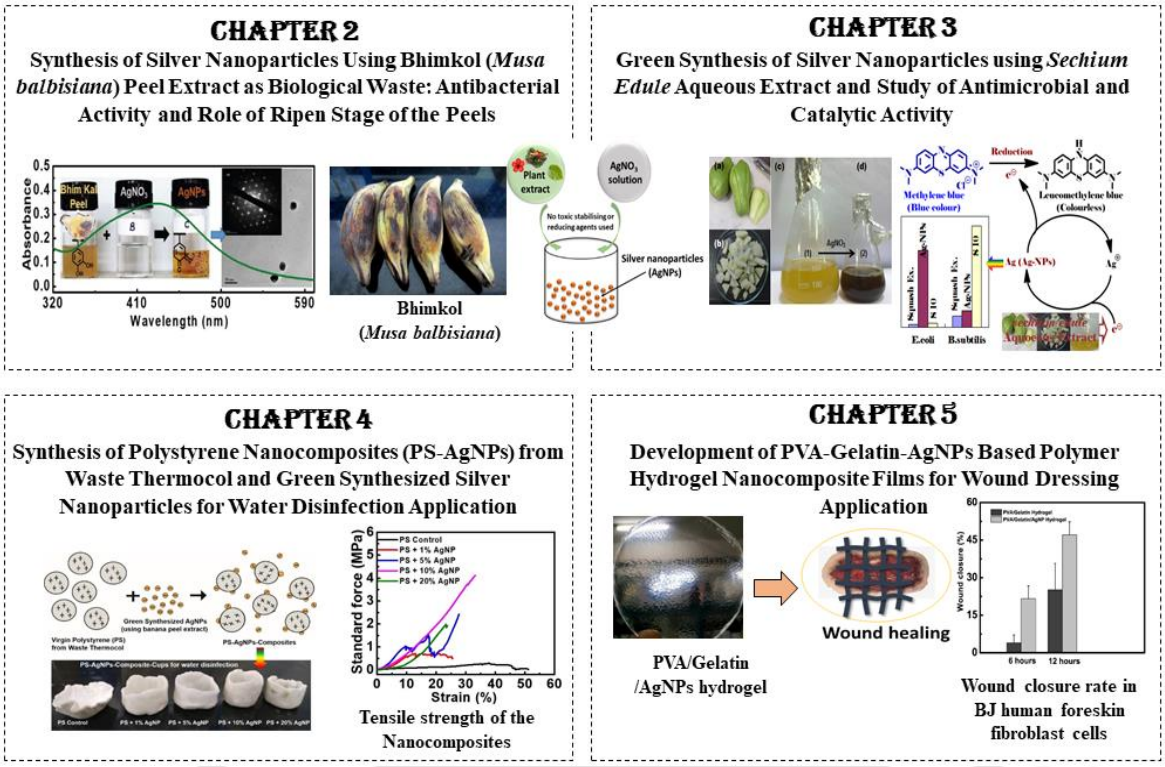

Chapter 4 deals with developing polystyrene nanocomposites (PS-AgNPs) using waste thermocol and incorporating it with green synthesized AgNPs. The developed PS-AgNPs composite material was utilized to prepare cups as a water tank model to study water storage disinfection properties. The green synthesized AgNPs were prepared using bhimkol peel extract then embedded into the PS matrix in different combinations with respect to PS. The developed PS-Ag nanocomposites were characterized using various instruments. PS-AgNPs cups showed optimum tensile strength and bacteria disinfection properties.

Chapter 5 focuses on developing a low-cost nanocomposite polymer hydrogel composed of triads materials- polyvinyl alcohol(PVA), gelatin, and green-synthesized silver nanoparticles (AgNPs) for wound dressing application. AgNPs were synthesized using peels of *Musa balbisiana* (Bhimkol) and incorporated into the PVA-Gelatin blend. The hydrogel films showed no toxicity against the BJ normal human foreskin fibroblasts cells. This triad polymeric nanocomposite hydrogel was found to accelerate wound healing, efficiently protect the wounded skin surface against exudate accumulation/dehydration and prevent bacterial growth and infection. All the properties made our PVA-gelatin-AgNPs triad nanocomposite hydrogel ideal for wound dressing applications.

In conclusion, the thesis contains embodiment of research aimed towards (a) Synthesis, optimization and characterization of silver nanoparticles (AgNPs) via the green route using 'Bhimkol' (*Musa balbisiana Colla*) peel extracts; (b) Study of the phytochemical properties of Bhimkol *(Musa balbisiana Colla)* peels and the antibacterial activities of both bhimkol peel extract and green synthesized AgNPs; (c) Synthesis and characterization of Silver Nanoparticle via green route using *Sechium edule* Aqueous Extract, study of their antimicrobial as well as catalytic activity; (d) Characterization and development of polystyrene nanocomposites (PS-AgNPs) from waste thermocol and green synthesized AgNPs for water disinfection application and (e) Characterization and development of PVA/gelatin/AgNPs based polymer nanocomposite hydrogel for wound dressing application.

The thesis opens up the opportunity to search for other waste materials of indigenous availability and utilise them as bioreductant for the large scale synthesis of nanomaterials of wide applications. The focus of the thesis is, though, limited to AgNPs, based on the phytochemical constituents of the studied banana peels or Chayote squash, we believe that other metallic nanoparticles can also be synthesised. Turning waste into value-added product, as is shown in Chapter 3, could also be further explored for practical application toward large scale production of tanks for storing water without bacterial growth/infection. The final chapter devoted to showcase the preparation of triad polymeric nanocomposite hydrogel for wound healing applications. Such materials would find immediate application for the production of wound healing bandages, which might be efficient and cost-effective. Finally, with the available facilities and limitations, the works presented in the thesis would find an opportunity for further exploration towards designing strategies, chemistry, and engineering models to develop efficient materials of clinical importance.

PUBLICATIONS

Received: 4 February 2021 | Revised: 17 May 2021 | Accepted: 22 August 2021

DOI: 10.1002/pc.26287

RESEARCH ARTICLE

Polymer COMPOSITES WILEY

Turning wastes into value-added materials: Polystyrene nanocomposites (PS-AgNPs) from waste thermocol and green synthesized silver nanoparticles for water disinfection application

Subhendu Sekhar Bag[1,2] | **Anupama Bora**[2] | **Animes Kr. Golder**[2,3]

[1]Chemical Biology/Genomics Laboratory, Department of Chemistry, Indian Institute of Technology Guwahati, Guwahati, India

[2]Centre for the Environment, Indian Institute of Technology Guwahati, Guwahati, India

[3]Department of Chemical Engineering, Indian Institute of Technology Guwahati, Guwahati, India

Correspondence
Subhendu Sekhar Bag, Chemical Biology/Genomics Laboratory, Department of Chemistry, Indian Institute of Technology Guwahati, Guwahati, Assam 781039, India.
Email: ssbag75@iitg.ac.in

Abstract

Due to the scarcity of clean water, scientists worldwide are keen to develop cost-effective, non-toxic and eco-friendly water disinfection systems. Achieving proper disinfection without creating harmful byproducts for removing or inactivating waterborne pathogens is the main challenge. In this respect, polystyrene (PS) nanocomposites find wide applications in water storage, food packaging material, transportation, medicine, and so forth. The addition of nanoparticles such as silver nanoparticles (AgNPs) into PS enhances its mechanical properties, gas barrier properties, thermal stability, and so forth. This study reports the development of PS-AgNPs composite using green synthesized AgNPs and waste thermocol. Firstly, the green synthesized AgNPs were prepared in different concentrations and embedded accordingly into the PS matrix. The morphology of PS-AgNPs nanocomposites was studied using Field Emission Transmission Scanning Microscopy (FESEM) and Field Emission Transmission Electron Microscopy (FETEM). Fourier transform infrared spectroscopy (FTIR) was used to evaluate the prepared nanocomposites' surface chemical bonding and surface composition. The thermal property of the nanocomposites was investigated by Thermogravimetric analysis (TGA). The tensile strength of the composites was also estimated. These PS-AgNPs nanocomposites showed an antibacterial effect against *Escherichia coli*, a disease-causing gram-negative bacteria commonly found in water. Among them, the PS-AgNPs cup encapsulating 10% AgNPs showed optimum tensile strength and bacteria disinfection property. These nanocomposites have been utilized to prepare cups as a model of water tank for water storage having disinfection properties.

KEYWORDS

green synthesis, polystyrene/Ag nanocomposites (PS-AgNPs), PS-AgNPs-based water container, silver nanoparticles (AgNPs), waste polystyrene (WPS), water disinfection

Send Orders for Reprints to reprints@benthamscience.net

Current Nanomaterials **2020**, *5*, 000-000

RESEARCH ARTICLE

Biomimetic Synthesis of Silver Nanoparticles Using Bhimkol (*Musa balbisiana*) Peel Extract as Biological Waste: Its Antibacterial Activity and Role of Ripen Stage of the Peel

Subhendu Sekhar Bag[1,2,*], Anupama Bora[2] and Animesh Golder[2,3]

[1]*Chemical Biology/Genomics Laboratory, Department of Chemistry, India;* [2]*Centre for the Environment;* [3]*Department of Chemical Engineering, Indian Institute of Technology Guwahati-781039, India*

ARTICLE HISTORY

Received: November 13, 2019
Revised: January 02, 2020
Accepted: January 31, 2020

DOI:
10.2174/2405461505666200228121003

Abstract: We report herein a cost-effective and environment-friendly biomimetic synthesis of silver nanoparticles using Bhimkol (Musa balbisiana) peel aqueous extract as biological waste. We have used the biological waste peels from the household, which is widely available, and cheap for the synthesis of stable silver nanoparticles. We monitored the formation of silver nanoparticles by various spectroscopic techniques. As is revealed from both FESEM and TEM, all the particles are almost spherical in morphology and the diameter of the mostly monodispersed AgNPs is in the range of 30-70 nm with an average size of 44.24 nm. We also perform both the qualitative and quantitative phytochemical analyses, for the first time, of the bhimkol peel. Among the three stages of development (unripe, ripe, and blacken), we have found the ripening stage as most efficient in the highest yielding of AgNPs because of the maximum presence of phenol containing biological macromolecules. The effect of concentration of peel extract, $AgNO_3$, the pH, and time is also studied. The advantage of our method lies in the fact that we utilize peels as biological waste material both for the generation and stabilization of silver nanoparticles. The stabilisation of the nanoparticles is mainly by the biological macromolecules present in the peel extract. The synthesized nanoparticles are found to show potent biological activity towards gram-positive and gram-negative bacteria.

Keywords: Biological waste, bhimkol peels, biological constituents, ripen stage, biomimetic synthesis, green synthesis, silver nanoparticles, antibacterial effect.

1. INTRODUCTION

Silver nanoparticles (AgNPs) are of major interest among all other metal nanoparticles due to their distinctive electrical, physical, optical and antimicrobial properties and a broad range of applications [1-4]. These nanoparticles illustrate lower toxicity to human health compared to other metal nanoparticles with the most effective antibacterial action [5, 6]. For this reason, AgNPs have a wide scope of antimicrobial applications such as in health care as a burn dressing, as scaffolds for water purification and also in agricultural uses. Nowadays, silver-containing agents are used in various clinical wound dressings (*e.g.*, silver sulfadiazine) as well as in biomedical material coatings (*e.g.*, silver-impregnated catheters) [7-9]. Therefore, a tremendous amount of research efforts led to the development of various synthetic methodologies, including physical methods and chemical methods [10-12]. Among these, green synthesis of AgNPs has got recent research attention as it is a non-toxic, eco-friendly and cost-effective. The green synthesis also provides stabilization to these particles by natural capping agents [10]. Utilization of plant extracts and agricultural waste thus has a great impact on the synthesis of AgNPs even over the production by a microorganism. This increases the cost-competitive feasibility of the synthesis of nanoparticles by microorganisms [10, 13].

Therefore, rich biodiversity of plants, their various parts and potential secondary metabolites have been well used in recent times in the synthesis of varieties of nanoparticles such as cobalt, silver, palladium, copper, platinum, gold, magnetite and zinc oxide [14, 15]. Plant extracts are reported to contain abundant natural compounds such as flavonoids, saponins, tannins, alkaloids, steroids and other kinds of nutritional compounds. They provide the reducing components for bioreduction as well as for the stabilisation to the nanoparticles formed. Thus, the exploitation of food and commercial valued plant products for nanoparticle synthesis reduces the overall efficacy of the biosynthetic process. Previously, we have also reported the green synthesis of silver nanoparticles using chayote squash, or *sechium edule* aqueous extract [10]. However, utilisation of abundant agro-waste resources such as biomass and plant wastes is a more eco-friendly and sustainable way for the synthesis of nanoparticles [16].

*Address correspondence to this author at the Chemical Biology/Genomics Laboratory, Department of Chemistry; and Centre for the Environment, India; Tel: +91-361-258-2324; Fax: +91-258-2349; E-mail: ssbag75@iitg.ac.in

2405-4615/20 $65.00+.00

Current Nanomaterials **2018**, *3*, 140-146

RESEARCH ARTICLE

Green Synthesis of Silver Nanoparticle using *Sechium edule* Aqueous Extract and Study of Antimicrobial and Catalytic Activity

Subhendu Sekhar Bag[1,2,*], Ankita Banerjee[1], Anu Singh[1], Animes Goldar[3] and Anupama Bora[2]

[1]*Bioorganic Chemistry Laboratory, Department of Chemistry, Indian Institute of Technology, Guwahati-781039, Assam, India;* [2]*Centre for the Environment, Indian Institute of Technology, Guwahati-781039, Assam, India;* [3]*Department of Chemical Engineering, Indian Institute of Technology, Guwahati-781039, Assam, India*

ARTICLE HISTORY

Received: March 03, 2018
Revised: August 25, 2018
Accepted: September 13, 2018

DOI:
10.2174/2405461503666181002115659

Abstract: ***Background and Objective*:** A cost effective and environment friendly biomimetic green synthesis of silver nanoparticles from the aqueous extract of Chayote squash is demonstrated. In north eastern region of India chayote is known as Squash and used for benefit for stomach.

***Method*:** Therefore, we have used the Squash vegetable extract which is widely available, cheap and has antioxidant properties for the synthesis of stable silver nanoparticles. The formation of silver nanoparticles is tested by various spectroscopic techniques like, UV-Vis, FTIR-spectroscopy and X-ray diffraction (XRD). The advantage of our method lies on the fact that squash acts both as a reducing agent and a stabilizer of silver nanoparticles. The carbohydrate and the fiber part most probably act as stabilizers.

***Results and Conclusion*:** The synthesized nanoparticles are found to show antimicrobial activity and catalytic activity toward the reduction of methylene blue. The reduction of methylene blue by Ag-NPs in the presence of *Sechium edule* aqueous extract is attributed to the electron relay effect.

Keywords: Biomimetic synthesis, *Sechium edule*, silver nanoparticles (Ag-NPs), antimicrobial activity, catalytic activity, reduction of methylene blue.

1. INTRODUCTION

The noble metal nanoparticles, because of their small sizes, large surface areas, and unique photophysical and chemical properties, have attracted much research interest in recent time [1]. Nanoparticles are now widely used in various research fields, such as catalysis [2-4], photonics [5, 6], optoelectronics [7, 8], magnetic [9], nanomedicines and many other nanobio applications [10-12]. In particular, a vast majority of research in recent time involves the synthesis of silver nanoparticles due to their potential applications [13] ranging from chemistry [14, 15], physics [16, 17], material science [18], biology to medical science and nanobiotechnology [19-22]. Therefore, a large numbers of synthetic techniques for silver nanoparticles, such as chemical reduction [23, 24], radiation [25, 26], and photochemical methods [27] are available in the literature. Most of these methods are not cost effective, not environment friendly and do not meet the current market demand. To meet the current industrial demand and to overcome the challenges affecting the living organisms and the environment during the course of synthesis, environment friendly synthesis of silver nanoparticle is considered as a widely acceptable technology. Thus, in the race of synthesis of silver nanoparticles *via* biomimetic green synthetic route, several methodologies have been adopted such as synthesis using microorganisms [28, 29], fungus [30], enzymes [31], plant extracts [32-35], *etc.* These methodologies are considered as environment friendly alternatives to phyco-chemicals methods. Among these biomimetic approaches, the less time consuming, cost effective, less tedious approach, such as using plants or plants extracts, are advantageous over other ecofriendly methods of synthesis. Toward this end we have concentrated ourselves to use a vegetable extract which is widely available, cheap and has antioxidant properties for the synthesis of stable silver nanoparticles.

Therefore, we report herein the synthesis of stable silver nanoparticles with the bioreduction method using chayote squash, or *Sechium edule* aqueous extract. Chayote is an edible fruit of a tropical perennial vine plant which is a member of the cucurbitaceae family having a large number of food values and antioxidant properties. In north eastern region of India it is known as Squash and used for the benefit for stomach [36a]. The advantage of our method, which we already showed [36b-d], lies on the fact that squash acts both as a reducing agent and a stabilizer of silver nanoparticles. The crystalline phase of synthesized silver nanoparticles was determined from X-ray diffraction (XRD) method. The antimicrobial effect of biologically synthesized silver nanoparticles (Ag-NPs) was evaluated by disc diffusion method against gram positive and gram negative bacteria. The catalytic activity of synthesized Ag-NPs towards the reduction of methylene blue was tested and monitored by UV-visible spectrophotometer.

*Address correspondence to this author at the Department of Chemistry, IIT Guwahati 781039, Assam, India; Tel: +91-361-258-2324; Fax: +91-361-258-2349; E-mail: ssbag75@iitg.ernet.in

2405-4623/18 $58.00+.00